IMPACTS OF AUTOMATED RESIDENTIAL ENERGY MANAGEMENT TECHNOLOGY ON PRIMARY ENERGY SOURCE UTILIZATION

A Dissertation
Presented to
The Academic Faculty

by

Curtis Aaron Roe

In Partial Fulfillment
of the Requirements for the Degree
Doctor of Philosophy in the
School of Electrical and Computer Engineering

Georgia Institute of Technology
December 2012

IMPACTS OF AUTOMATED RESIDENTIAL ENERGY MANAGEMENT TECHNOLOGY ON PRIMARY ENERGY SOURCE UTILIZATION

Approved by:

Dr. A. P. Sakis Meliopoulos, Advisor
School of Electrical and Computer Engineering
Georgia Institute of Technology

Dr. C. S. Santiago Grijalva
School of Electrical and Computer Engineering
Georgia Institute of Technology

Dr. Ronald Harley
School of Electrical and Computer Engineering
Georgia Institute of Technology

Dr. Sudhakar Yalamanchili
School of Electrical and Computer Engineering
Georgia Institute of Technology

Dr. Christos Alexopoulos
School of Industrial and Systems Engineering
Georgia Institute of Technology

Date Approved: [September 12, 2012]

I dedicate this dissertation to my wife, her love and encouragement has been and continues to be of marvelous importance in my life.

ACKNOWLEDGEMENTS

If a man will begin with certainties, he shall end in doubts; but if he will be content to begin with doubts, he shall end in certainty. - Francis Bacon

This quote provides insight into and also reflection of my experience at The Georgia Institute of Technology. My experience could be described as a meandering journey starting from doubt and ending with certainty. Each step I took forward has led to a surprising outcome.

Through this process I have received a vast amount of support from countless people. Identification of the people in this acknowledgment is an indication of profound support of my journey from doubt to certainty. Clearly, not everyone whom has influenced me in the past five years can be mentioned in these pages. Nevertheless everyone who imparted guidance has been deeply appreciated.

First and foremost, I would like to thank Professor Sakis Meliopoulos. His guidance, leadership, and support over the past five years have been of profound importance. All that I have achieved at The Georgia Institute of Technology has been in no small part due to Professor Meliopoulos. Starting from the initial interview, I have been motivated to contribute to Professor Meliopoulos' ongoing and tireless efforts.

Second, I would like to thank the dissertation committee members: Dr. Santiago Grijhalva, Dr. Ronald Harley, Dr. Sudhakar Yalamanchili, and Dr. Christos Alexopoulos. Their support and encouragement has helped guide me though my last challenge at the Georgia Institute of Technology. My gratitude goes out especially to Dr. Ronald Harley who provided significant feedback on my Master's thesis from which much was learned.

Third, I would like to thank the sponsors of my work. My work over the past five years has been sponsored by the Power Systems Engineering Research Consortium and the Electric Power Research Institute. Beyond the financial support of these two organizations, numerous individuals have immensely supported my education. Specifically, Dr. Robert Entriken and Dr. Sunil Chhaya, both with the Electric Power Research Institute; their ongoing and diligent efforts have been of vast importance to me.

Fourth, I would like to thank all of my colleagues in the electric power group at the Georgia Institute of Technology. The supportive and challenging atmosphere of the electric power group has challenged me to grow and develop personally and professionally. Within this community of colleagues my continued development has been improved and expanded beyond anything I had expected.

Last but not least, I would like to thank my parents. My parents started me in the right direction in life and have been supporting me throughout each step. Specifically, my mother Linda has instilled in me the idea that I can do anything I set my mind to. My father David has impressed upon me a love and drive for a lifelong pursuit of education. My current and future achievements speak to both my abilities and theirs, as well.

The scientific method has been of supreme importance to the continued development of human kind. The support of the people mentioned in these acknowledgements is of supreme importance during the most recent stage of my meandering journey. I have learned and grown through the support of each person mentioned in these acknowledgements. My education and personal development has been supported by many others whom I have crossed paths with in the past five years. Their support is also greatly appreciated.

TABLE OF CONTENTS

LIST OF TABLES

Page

LIST OF FIGURES

Page

LIST OF SYMBOLS AND ABBREVIATIONS

$\alpha(g)$	Constant heat rate coefficient for generator g
$\beta(g)$	Linear heat rate coefficient for generator g
$\gamma(g)$	Quadratic heat rate coefficient for generator g
$\delta(n, \varsigma)$	Confidence interval half-length for sample size n and confidence level ς
λ	Constant conditional failure rate
ς	Confidence level
υ	Relative error
υ'	Adjusted relative error
$\Lambda(d, a, s)$	Scaling factor for day d, power system area a, and market penetration s
μ	Constant conditional repair rate
μ_i	Mean number of times that appliance i is used in a daily simulation
ρ_{25}	25^{th} percentile of a set of simulation results
ρ_{75}	75^{th} percentile of a set of simulation results
σ_i	Standard deviation the times that appliance i is used in a daily simulation
ϑ_{max}	Maximum valid value
ϑ_{min}	Minimum valid value
φ_{max}	Maximum observed simulation result
φ_{min}	Minimum observed simulation result
$a_e(g)$	Constant emission rate coefficient for EAP e and generator g
A_i	Random variable representing the availability of block i
AC	Air conditioner
AEC	Average energy cost
Ave	Sample average

b	Average demand during the control period with no control
BC	Base case
$b_e(g)$	Linear emission rate coefficient EAP e and for generator g
$C(i)$	Generator block i output
CD	Clothes dryer
CO_2	Carbon dioxide
CW	Clothes washer
DADRP	Day-ahead demand response program
DLC	Direct load control
DR	Demand response
Dw	Dishwasher
E	Amount of energy that would have been used without direct load control
$E_c(g)$	Expected generator g fuel cost
$E_e(g)$	Expected generator g environmental air pollution e
$E_{ge}(g)$	Expected generator g generated energy
$E_{ot}(g)$	Expected generator g operation time
$E_{sim}(d)$	The energy in the PPRS day d
E_u	Expected unserviced energy
EAP	Environmental air pollution
ECAK	Power system area with climate characteristics of Versailles Kentucky
EPA	U.S. Environmental Protection Agency
FERC	Federal Energy Regulatory Commission
FOR	Forced outage rate
GE	Generated energy
GEAP	Generated environmental air pollution

HVAC	Heating, ventilation, and air conditioning
HVAC DLC	Heating, ventilation, and air conditioning direct load control
IPM	Integrated Planning Model
l	Specific load level
L	Random variable representing the electric load
$L(x)$	Functional representation of the normalized inverted load duration curve
$L_i(x)$	Functional representation of the NILDC in PPC algorithm step i
LOLP	Loss of load probability
Max	Maximum capacity
MER	Mercury
n	Number of iterations in the procedure to determine the number of iterations
n_0	Initial number of iterations in the procedure to determine the number of iterations
n_{off}	Number of minutes during each half hour period in the demand response period
NILDC	Normalized inverted load duration curve
NIST	National Institute of Standards and Technology
NO_x	Nitrogen oxide
p	Percentage of time that a generator is available
$p(i)$	Percentage of time that generator block i is available
$P(s)$	The percentage of REMS penetration in simulation s
$P_{ij}(t)$	Probability of transitioning from state i to state j at time t
P_i	Probability of being in state i as time approaches infinity
p_{lol}	Loss of load probability
PAPS	Proposed Aggregate Primary-Energy-Source-Utilization Simulation
PDF	Probability distribution function
PESU	Primary energy source utilization

PEV	Plug-in electric vehicle
PPC	Probabilistic Production Costing
PPRS	Proposed Physically-Based Residential-Energy-Management-System Simulation
PSE	Puget Sound Energy
PV	Photovoltaic
q	Percentage of time that a generator is unavailable, the forced outage rate
$q(i)$	The forced outage rate of generator block i
q_{ij}	Instantaneous transition rate from state i to state j
R	Controlled appliances load during the control period
$R(a)$	The percentage of residential load for power system area a
$R_i(x)$	Functional representation of the residual load in PPC algorithm step i
Ref	Refrigerator
REMS	Residential energy management system
S1	Pseudo random number generator arbitrary seed number one
S2	Pseudo random number generator arbitrary seed number two
S3	Pseudo random number generator arbitrary seed number three
S_i	Seasonal usage distribution for appliance i
SAS	Smart appliance scheduling
SASB	Smart appliance scheduling with a stationary battery
S_n^2	Generic sample variance
SNV	Power system area with climate characteristics of Mercury Nevada
SO_2	Sulfur dioxide
SPPS	Power system area with climate characteristics of Stillwater Oklahoma
ST	Smart thermostat
Sum	Summer

T	Simulation length
UEL	Uncontrollable electric load
UE	Unserviced energy
Var	Sample variance
WH	Water heater
WH DLC	Water heater direct load control
Win	Winter
WUMS	Power system area with climate characteristics of Necedah Wisconsin
$x_o(i)$	Original Integrated Planning Model data for result i
$x_s(i)$	Simulation data for result i
X_o	Total original Integrated Planning Model data
X_j	Generic data point j
$\bar{X}(n)$	Generic sample mean

SUMMARY

The potential impact of smart grid technology includes cleaner, cheaper, and more reliable electricity generation. There exists the opportunity for residential electric load to provide some portion of the benefits from smart grid technology. Residential demand-side management through demand response (DR) has the potential to provide significant system level benefits via increased controllability of residential electric load.

This dissertation compares the performance of direct load control (DLC), a traditional form of energy management, with the performance of smart grid enabled energy management functions. Specifically, this dissertation documents simulations of five energy management functions, by testing various levels of residential energy management system complexity. This results in a quantified indication of which technology (energy management functions) provides the most significant automated DR.

The quantified performance of residential energy management provides benefits to the homeowner and electric utility, with additional benefits from distributed energy resources: photovoltaic array, plug-in electric vehicle, and stationary battery energy storage. To achieve the increased controllability of residential electric load requires investment in additional infrastructure.

Two levels of system simulation provide quantified performance of residential energy management functions from both the residence owner and electric utility perspectives. The proposed system simulations provide a test bed for energy management functions, quantifying the effects of the changes in electric load. The existing literature includes a wide variety in the quantified performance of residential energy management. This underscores confusion surrounding the potential benefits of

residential energy management. By testing residential energy management options in a single analysis, equitable comparisons can be made.

The quantified impact of multiple residential energy management functions is compared with various levels of distributed energy resources for four areas of the United States. For example, the potential benefits of 10% market penetration of DLC produce cleaner (CO_2 production reduced from $4.0262 \cdot 10^{10}$ kg to $4.0139 \cdot 10^{10}$ kg), cheaper (average energy cost reduced from 1,275 $/MWh to 1,253 $/MWh), and more reliable (loss of load probability reduced from 4.24% to 3.06%) electricity generation.

Simulation analysis and production cost analysis relies on input models to provide realistic results. The input models used in this work are based on existing literature. The simulation results are validated, compared to other resources and the input data itself. This work represents a first attempt at developing models to provide an equitable comparison of residential energy management technology. The comparison of residential energy management technology is not affected by uncertainty and errors in input data since the input data were consistent in all simulations. The input model, process, and results provide intellectual contributions and operational considerations for residential energy management technology developers and electric utility residential program developers.

This dissertation describes three original contributions: (1) the development of a discrete-event simulation of the energy use in a residential premises, (2) the side by side analysis of multiple energy management functions, and (3) the investigation of residential energy storage in conjunction with energy management functions, distributed energy resources for multiple regions of the U.S. for the residence owner and utility provider.

1 INTRODUCTION

This dissertation compares the performance of direct load control, a traditional form of energy management, with smart grid enabled energy management functions. The various energy management functions are compared in their ability to provide automated demand response. This chapter introduces the National Institute of Standards and Technology conceptual model of the smart grid; introduces the traditional and smart grid energy management functions under consideration/study; introduces the research motivation and key contributions; and outlines the remainder of this dissertation.

1.1 Smart Grid

The National Institute of Standards and Technology (NIST) was assigned the responsibility to develop a framework for protocols and standards required to develop smart grid devices and systems by the Energy Independence and Security Act of 2007. The NIST Smart Grid Conceptual Model is shown in Figure 1.

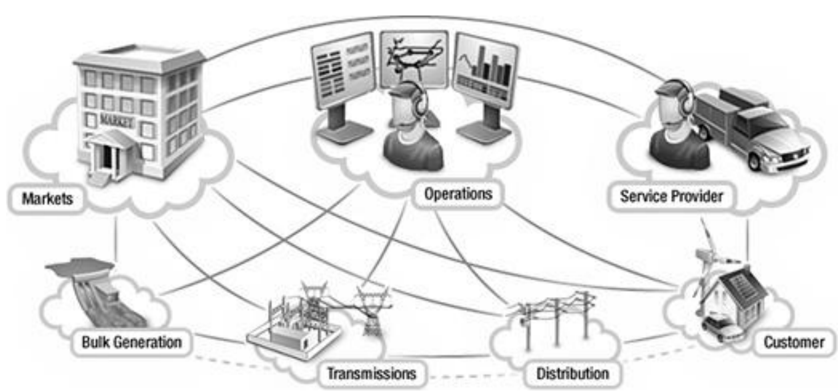

Figure 1: National Institute of Standards and Technology [NIST] Smart Grid Conceptual Model [1].

Figure 1 consists of seven domains: Bulk Generation, Transmission, Distribution, Customer, Operations, Markets and Service Provider; and interfaces between the seven domains. The interfaces between each domain shown in Figure 1 include pathways for communication (solid lines) and electric energy (dashed lines). Paramount to the current research is the Customer domain shown in the lower right hand corner of Figure 1.

The NIST Customer domain within the NIST Smart Grid Conceptual Model is shown in Figure 2.

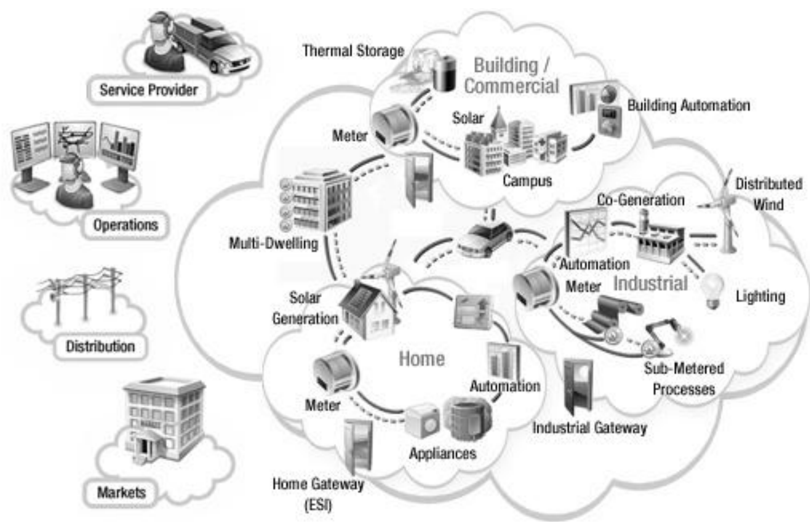

Figure 2: National Institute of Standards and Technology [NIST] Customer domain within the Smart Grid Conceptual Model [1].

The Customer domain consists of three segments: Building/Commercial, Industrial, and Home. Each segment in Figure 2 provides means to "generate, store and manage the use of energy" [1]. Similar to Figure 1, Figure 2 depicts communication (solid lines) and electric energy (dashed lines) interfaces within each Customer domain segment. The NIST Smart Grid Conceptual Model and Customer domain frames the current proposed research.

There is significant existing research, development, and demonstration work quantifying the capabilities of the smart grid. This dissertation documents simulations of residential energy management functions that provide automated demand response (DR). Through simulation, the ability of residential appliances to provide automated DR is quantified. Providing a quantified indication of what technology (energy management functions) provide the most significant automated DR.

1.2 Demand Response Services

The energy use in a typical single-family residence is quantified and compared under a variety of energy management functions in four climate regions of the United States. The energy use in a typical single-family is analyzed from the perspective of the residence owner and the electric utility. Further, the use of photovoltaic and plug-in electric vehicles is considered in conjunction with the energy management functions.

Residential energy management functions are not new [2] and [3]. A residential energy management system (REMS) is an amalgam of hardware and software that performs residential energy use monitoring, control, and planning. Monitoring functions include historical and (near) real-time energy use tracking. Control functions provide optional supervisory control of the energy use of residential appliances. Planning functions include the arrangement of energy use based on electric utility constraints.

Currently available REMS provide energy monitoring feedback via an in-home display, website, or handheld device; using whole residence energy use monitoring or individual circuit energy use monitoring, control, and planning. Heating, ventilation, and air-conditioning; water heater; and pool heater appliances are currently available.

The REMS provides an interface between multiple smart appliances within a home area network (suitable communication network) and two external actors: the residence owner and the electric utility. The controllability extends to both the residence owner and the electric utility (under suitable contractual obligations).

The perspective of the residence owner is quantified by energy-use statistics computed in a Proposed Physically-Based REMS Simulation. The energy-use statistics are computed using a discrete-event simulation of a typical single-family residence. The perspective of the electric utility is quantified using a production costing algorithm in a proposed aggregate primary energy source utilization (PESU) simulation. The production costing algorithm computes a probabilistic economic dispatch, quantifying the primary energy sources needed to meet the electric load. Further, the production costing algorithm quantifies the generated energy, the generated environmental air pollution, power system reliability (loss of load probability and unserviced energy), and average electricity cost to meet the electric load.

The traditional energy management functions are two forms of direct load control (DLC): water heater (WH) DLC and heating, ventilation, and air conditioning (HVAC) DLC. The DLC energy management function is the direct electric utility control of specific appliances (e.g. WH and HVAC).

The smart grid energy management functions are smart thermostat, smart appliance scheduling, and smart appliance scheduling with a stationary battery. The smart thermostat energy management function adjusts the temperature set point of the HVAC system during demand response (DR). The smart appliance scheduling energy management function delays the use of key residential appliances (smart appliances) during DR. The smart appliance scheduling with a stationary battery energy management function adds a stationary battery to the smart appliance scheduling function. The stationary battery adds an additional level of flexibility to reduce the residential electric load during DR.

The use of REMS has the potential to provide significant benefits for both the residence owner and electric utility. The Proposed Physically-Based REMS Simulation provides a test bed to quantify the performance of the various energy management functions within multiple climate regions. The Proposed Aggregate PESU Simulations quantifies the power system performance (fuel required, environmental air pollution generated, reliability index, and average electricity cost) under varying levels of REMS market penetration.

1.3 Research Motivation and Key Contributions

The objective of this research is to analyze automated residential energy management technology using primary energy source utilization; specifically, a production costing analysis is performed for the ability of residential energy management functions to achieve demand response (DR). The ability of multiple proposed technologies are compared with the addition of plug-in electric vehicle (PEV); photovoltaic (PV); and the combination of PEV and PV.

To achieve this goal, novel probabilistic appliance use models are used in a discrete-event simulation formulation (the Proposed Physically-Based Residential-Energy-Management-System Simulation). The output of this simulation is aggregated to quantify the impact of the residential automation technology on different power system operating areas (the Proposed Aggregate Primary-Energy-Source-Utilization Simulation). These two levels of system simulation provide quantified system performance from both the residence owner and electric utility perspectives on the prospective automated residential energy management functions.

Additional consideration is provided for the impact of PEV charging, PV variable distributed generation, and the ability of small scale (4.8 kWh) battery energy storage to assist in automated DR performance. A comparison is provided of traditional energy management functions (direct load control) and smart grid enabled energy management functions. Each parameter is parametrically adjusted to study the impact of each using simulation.

1.4 Outline

Chapter 2 introduces existing literature related to the current research. Chapter 3 describes the Proposed Physically-Based Residential-Energy-Management-System Simulation. Chapter 4 contains the proposed physically-based residential energy management simulation results. Chapter 5 describes the Proposed Aggregate Primary-Energy-Source-Utilization Simulation. Chapter 6 contains the primary-energy-source-utilization simulation results. Chapter 7 summarizes the conclusions made in this dissertation.

2 LITERATURE REVIEW

This chapter introduces existing research that is related to the impact of residential energy management technology on primary energy source utilization (PESU). The existing research is within five areas: direct load control, residential demand response, residential energy management system simulations, related markets outlook, and PESU. These five research areas provide a background overview of the existing research in this general area of investigation.

2.1 Direct Load Control

This section of the literature review introduces existing research related to direct load control (DLC). Direct load control is a popular methodology for residential energy management. Specifically, DLC consists of the external control of residential electric equipment. This section introduces existing literature related to residential DLC. First is an introduction of literature documenting two theoretical research areas of DLC: optimal scheduling and heuristic scheduling. Second is an introduction of the economics of DLC. Third is an introduction of literature documenting DLC payback models. Fourth (and finally) is an introduction of literature documenting electric utility demonstration projects with DLC.

2.1.1 Optimal Scheduling

A popular theoretical consideration found in existing literature is the optimal scheduling of direct load control (DLC). This topic computes the optimal time to apply DLC. The optimization methodologies used in existing literature are listed in Table 1.

The objectives of the optimization methodologies used in existing literature are listed in Table 2.

Table 1: Direct load control [DLC] optimal scheduling methodologies.

Method	Reference
Dynamic programming	[4], [5], [6], [7], and [8]
Evolutionary algorithm	[9] and [10]
Fuzzy dynamic programming	[11]
Lagrange method	[12] and [13]
Linear programming	[4], [14], [15], [16], and [17]
Multivariable predictive control	[18]
Steepest-descent parameter	[19]

Table 2: Direct load control [DLC] optimal scheduling objectives.

Objective	Reference
Customer comfort	[9], [16], and [19]
Distribution system losses	[13]
General target load curve	[18]
Peak demand	[4], [5], [6], [9], [14], [15], [16], and [19]
Production costs	[5], [6], [7], [8], [9], [11], [12], and [16]

The use of linear and dynamic programming to achieve maximum peak demand and minimum production costs have been the most popular optimization methodologies and optimization objectives.

The application of optimization strategies to schedule DLC for a variety of objectives provide interesting results. The current work simulates DLC energy management functions in a comparison of smart appliance energy management functions. Each methodology has merit. It is the expected that for a large portion of consumers to allow electric utility interaction beyond the electricity meter, the historical delimiter between the electric utility and the residential operation, the electric utility customer must understand why the consumers are giving up control. Further, the consumer should understand why the electric utility control is doing what it is doing. Both of these requirements are more difficult to explain when using optimization methodologies. An alternative to optimized scheduling is heuristic scheduling. Next is an introduction of literature documenting heuristic DLC scheduling.

2.1.2 Heuristic Scheduling

Heuristic scheduled direct load control (DLC) has been documented in [20] and [21]. Note, the use of heuristic control methods is used in the current research, described in later chapters of this dissertation.

In [20], a collection of apartment air conditioners in a large apartment building were aggregated to provide peak load shaving energy management. The example in [20] is an apartment building with 449 apartments with communication network connecting each apartment air conditioner. In this example, this communication network was connected to an automated decision maker called the "local intelligent management server (LIMS)." The LIMS computed decisions based on control heuristics using a set of virtual tokens. The virtual tokens were passed to each air conditioner in the network. The use of each air conditioner was modeled as a Markov birth-and-death queuing model (M/M/c/K/m queuing model). Within this scheme, an air conditioner could only run when it had possession of a token, during the energy management period. Based on the electric utility requested service the LIMS computed the number of tokens required. The first numeric example in [20] provided a 380 kW reduction (the historical apartment peak demand was 1,614 kW). To provide this level of service 300 tokens were used. Further, in the first numeric example the air conditioners events included a 15 minute average service request interval (air conditioner on time) and a 7 minute average service interval (air conditioner off time). Notice, these parameters were a function of the weather and the thermal properties of the apartment building. The resulting waiting time for air conditioner service was 32 seconds. The authors in [20] concluded that "each resident may not even notice the on-going peak load shaving process." Further, additional peak shaving could be possible assuming the apartment tenants approved of increased service interruptions.

The work in [20] is a novel application of operations research theory to a theoretical DLC investigation. The application of queuing network theory provides a set of results assuming the use patterns of actual consumers match the input probabilistic models.

In [21], two possible energy management functions for the electric utility control of residential refrigerators were considered. The energy management functions included DLC and a delayed DLC (DLC at specific time in the future). A recursive thermal model of a refrigerator was used to simulate the residential appliance thermal performance with and without energy management. The authors of [21] showed that thermostatically controlled loads were able to provide regulation (up and down) services. Further, more precise control was provided by the delayed DLC but required a more powerful local controller (needed to compute the compressor operation during the control period).

The use of refrigerators with energy management has received little attention in existing literature, although the refrigerator is an energy intensive appliance. In addition to being a large energy user, the refrigerator is a very common electrical appliance. Given the significant market penetrations the ability to use refrigerators for energy management could be beneficial.

The expanded use of DLC is a complicated evolution of technology and personal preferences. High on the list of concerns of both external actors (the residence owner and the electric utility) in this transition is the economic impact of this technology. Next is an introduction of literature documenting the economic consideration of DLC.

2.1.3 Economics

The economics of direct load control (DLC) has been documented in [22] through [24]. The costs of DLC are relatively small per installation; however, many installations are required for substantial effects to be achieved. Inherently, each DLC installation consists of relatively small equipment (on the order of 1-5 kW); whereas, the traditional alternative, a power plant, is typically large (on the order of 10-1,000 MW). The benefits "of directly controlling customer loads depends on the magnitude of the load reduction, the percentage of energy payback, the cost of control equipment, and the length of time the load can be controlled during periods of high fuel costs or during periods of system generation and [transmission and distribution] capacity shortages" [22]. Given these considerations the costs and benefits, in an economic sense, are highly variable.

The annual savings obtained using the central air conditioner DLC was found to be between $139.04 and $177.84 for a typical summer season [23]. Similarly, the annual savings obtained using the DLC of a water heater was found to be approximately $86.00 [23]. The benefits of DLC accrue to the energy customer, the electric utility, and society as a whole. "For every dollar invested in this program, we estimate that society will benefit by $2.40, while ratepayers will benefit by $1.31" [24]. These results provide a baseline from which simulation results can be compared. A head to head comparison requires a larger sampling of results and proper experimental design.

The first three DLC topics addressed were optimized scheduling, heuristic scheduling, and economics. These topics are important theoretical analyses from different perspectives. A common concept described in DLC literature is a phenomenon called payback. Next is an introduction of literature documenting payback models.

2.1.4 Payback

The concept of payback is the back lash of electric load due to postponing thermostatically controlled appliances. If thermostatic control is interrupted, at the point where the original control is returned, there will be an increased demand for electricity. This increased demand occurs because thermal energy is lost or used during the interruption. This phenomenon appears when using thermostatically controlled appliances for direct load control (DLC). The negative effects of payback are compounded by the synchronization of DLC appliances. Potentially, a large number of appliances require payback electricity at the same time when released from DLC. Thus, the natural diversity of appliances use is reduced by DLC and the coincident peak demand due to payback can be higher than the original demand.

The concept of payback is mentioned in most research related to DLC. The following descriptions of payback were particularly detailed to warrant further comment here.

The ratio of payback energy over the energy saved during DLC service interruption yields a payback efficiency measure. For water heater DLC the payback efficiency was listed as 88%, for air conditioner shedding (completely turned off during the control period) the payback efficiency was listed as 92%, and for air conditioner cycling (15 minutes off for each hour of control) the payback efficiency was listed as 100% in [15]. The payback model from [15] is shown in Table 3.

Table 3: Payback model including control duration and payback results [15].

Control Duration	Energy Payback	Payback Demand	Payback Duration
1-5	1-5	1-5	1
6-8	8	5, 3	2
9-10	10	5, 3, 2	3
11-12	11	5, 3, 2, 1	4
13	12	5, 3, 2, 1, 1	5
14	13	5, 3, 2, 1, 1, 1	6
15-16	14	5, 3, 2, 1, 1, 1, 1	7

The payback model shown in Table 3 was modeled with 100% payback efficiency, thus all energy saved is paid back after the control period ends. The terminology used in Table 3 control duration, energy payback, payback demand, and payback duration will be defined further. The control duration (column 1) is the number of consecutive 15 minute periods in the control period. The energy payback (column 2) is units of energy consumed after the control period. The payback demand (column 3) is the pattern of demand during the payback duration (column 4 - 15 minute periods). Notice, the sum of the payback demand is the energy payback and the number of pattern points in the payback demand is the payback duration. To convert from the integer values in Table 3 to engineering values, we must multiply the energy integer values from Table 3 by 8 MWh and the demand integer values by 32 MW. These multipliers (8 MWh and 32 MW) are based on the number and response of the energy management function in [15]. As a comparison to this block payback model, the payback data in [22] is described next.

The payback data in [22] represents the change in central air conditioning load for four control periods during and after the control period. The control days consist of days with ambient temperature above 95 °F. The control load reduction (negative) and payback (positive) load are shown in Table 4.

Table 4: The control and payback load for control days above 95 °F ambient [22].

Control Period	1-5p [kW]	2-6p [kW]	6-10p [kW]	1-10p [kW]
2p	-1.10			-1.16
3p	-1.22	-1.20		-1.26
4p	-1.31	-1.28		-1.33
5p	-1.21	-1.45		-1.42
6p	-1.15	-1.20		-1.25
7p	0.80	-1.13	-1.05	-1.19
8p	0.46	0.84	-1.15	-1.08
9p	0.59	0.76	-1.20	-0.90
10p	0.34	0.36	-0.97	-0.68
11p			-0.72	-0.45
12p			0.95	1.29
1a			0.26	1.02
2a			0.18	1.13
3a				0.36

The payback data from [22] shown in Table 4 has an average payback efficiency of 33%. This is a very optimistic result. This indicates that for 1 unit of energy saved 0.33 units of energy will be repaid. This is significantly different than the payback model in [15].

Next is an introduction of literature documenting electric utility demonstration projects with DLC.

2.1.5 Demonstration Projects

Electric utility experience with direct load control (DLC) programs from multiple electric utilities have been documented in existing literature. A partial listing of available literature and the electric utility whom sponsored the demonstration project is shown in Table 5.

Table 5: Reviewed direct load control [DLC] demonstration projects.

Electric Utility	Reference
Allegheny Electric Cooperative, Inc.	[26]
American Electric Power	[27] and [28]
Arkansas Power and Light	[28]
Athens Automation and Control Experiment Athens Utility Board/Electric Power Research Institute/ Department of Energy/Oak Ridge National Laboratory	[29] and [30]
Atlantic Electric Company	[31]
Carolina Power and Light Company	[32]
Detroit Edison Company	[27], [28], [33], and [34]
Florida Power and Light Corporation	[35]
Florida Power Corporation	[36], [37], and [38]
Minnkota Power Cooperative	[28]
New England Power Services Company	[39] and [40]
North Carolina Electric Membership Corporation	[41]
Northern States Power Company	[42]
Oglethorpe Power Corporation	[43]
Pacific Gas and Electric Company	[28], [44], and [45]
South Carolina Electric and Gas Company	[28] and [46]
Southern California Edison	[27], [47], and [48]
Taiwan Power Company	[49], [50], [51], [52], and [53]
Wisconsin Electric Power Company	[54] and [55]

The demonstration projects mentioned in Table 5 address the topics previously introduced. Highlights from the demonstration projects related to scheduling, economics, and payback and will be described next.

The demonstration projects mentioned in Table 5 address DLC scheduling in [38], [42], and [44]. In [44], DLC was used for reliability purposes. In [44], nine reliability based events were listed along with the DLC performance achieved during the control periods. The reliability events and DLC results are summarized in Table 6.

Table 6: Reliability based direct load control [DLC] events [44].

Date	Peak Demand [MW]	Time-of-Peak Demand [hr]	Estimated Load Management Contribution	Reason
5/26	12,069	16	145.0	Loss of 500 kV intertie; 730 MW thermal generator out of service
6/6	13,416	15	128.0	Two thermal plants totaling 1,236 MW out of service
7/11	14,252	16	181.0	Extremely high temperatures in the Interior Valleys
7/12	14,708	17	177.5	Continued heat storm through the service territory
7/13	15,156	16	175.7	Continued heat storm through the service territory
8/3	13,577	16	139.8	Two thermal plants totaling 1,080 MW out of service
8/12	14,089	16	156.1	Loss of 500 kV intertie
8/15	14,866	16	142.5	730 MW Thermal generator out of service and high area temperatures
5/16	14,997	16	151.8	730 MW Thermal generator out of service and high area temperatures

The results in Table 6 consist of 70,000 residential customers. As a result of the high number of DLC events in the study period (1983), 2,022 residential customers withdrew from the program. The total load reduction included residential (air conditioning DLC) and commercial DLC.

Fixed duty cycle control scheduling was described in [38] and [42]. In [42], control was applied from 12p (noon) to 6p. The DLC consisted of 30 minutes on and 30 minutes off for one season, and 15 minutes on and 15 minutes off for a second season. It was highlighted in [42] that the 30-minute duty cycle was too harsh for the customers, and some complaints were even received for the 15-minute duty cycle option. A similar fixed scheduling scheme was described in [38]. The DLC was applied from 6a to 10a and again from 6p to 10p in the winter and 12p (noon) to 9p in the summer. In [38], continuous disconnection was applied to the water heaters and pool pumps and the heating, ventilation, and air conditioning system was cycled twice an hour during the control periods.

The difference in level of sophistication between the scheduling functions in the demonstration projects and the optimization and heuristic scheduling literature were drastically different. Also, the reliability-based DLC from [44] was not addressed in any other reviewed literature. Further, the simulation of random outages and extreme weather events, seen in Table 6, would be difficult without power system operating data.

The cost of DLC infrastructure was described in [41] and the potential energy savings of DLC in [23]. The estimated cost of connecting 150,000 consumer appliances (water heaters and air conditioners) was $27 million or equivalently $180 per installed control point [41]. The annual energy cost savings for air conditioner DLC was found to be between $139.04 and $177.84 in annual energy costs for a typical summer season or around $86.00 in annual energy costs for water heater DLC [23]. Both the installation cost and energy savings costs accrue to the electric utility. The claim that DLC is not beneficial to electric utilities was supported in [46] and [56]. No DLC options showed net positive benefits in [46] and a net increase in system costs was found in [56]. However, the analyses in [23], [41], [46], and [56] did not include the fuel cost savings and congestion relief that is achievable with DLC.

A payback model was introduced in [32]. This model defined the amount of energy that would have been used without DLC as E. The payback demand every 15 minutes following the control period is defined in Table 7.

Table 7: The payback demand every 15 minutes following the control period [32].

Time Elapsed After Restoration of Service	Net Restore Demand [kW]	
	$E \leq 3.164$	$E > 3.164$
0:15	$-0.2 \cdot E^2 + 1.4 \cdot E + 0.2$	2.442
0:30	$\max\{0, 0.6 \cdot E - 0.1\}$	1.798
0:45	$\max\{0, 0.5 \cdot E - 0.2\}$	1.295
1:00	$\max\{0, 0.3 \cdot E - 0.2\}$	0.852
1:15	$\max\{0, 0.2 \cdot E - 0.1\}$	0.533
1:30	$\max\{0, 0.2 \cdot E - 0.2\}$	0.489
1:45	$\max\{0, 0.2 \cdot E - 0.2\}$	0.346
2:00	$\max\{0, 0.2 \cdot E - 0.6\}$	0.177

The payback model in Table 7 will be defined further with an example. In addition to the amount of demand immediately following the control period, a residual demand R was defined in [32]. The residual demand was defined as the amount of demand from the controlled appliances that continues to operate during the control period. The residual demand is defined in Equation 1, as a function of the average demand during the control period with no control b.

$$R = 0.0094 + 0.029 \cdot b \tag{1}$$

An example from [32] of using Equitation 1 was where b was 0.509 kW and E was 1.019 kWh, then R was $0.009 + 0.029 \cdot 0.509 = 0.024$ kW. The results of applying the equations from Table 7 are shown in Table 8.

Table 8: The payback demand following the direct load control [DLC] (*b=0.509*, *E=1.019*) [32].

Time Elapsed After Restoration of Service	Net Restore Demand [kW]
0:15	1.442
0:30	0.511
0:45	0.252
1:00	0.166
1:15	0.104
1:30	0.045
1:45	Less than 0.001
2:00	0

Three DLC payback models from existing literature have been introduced. Two were introduced in Section 2.1.4 and one in the current section. The normalized payback demand from each reference is shown in Figure 3.

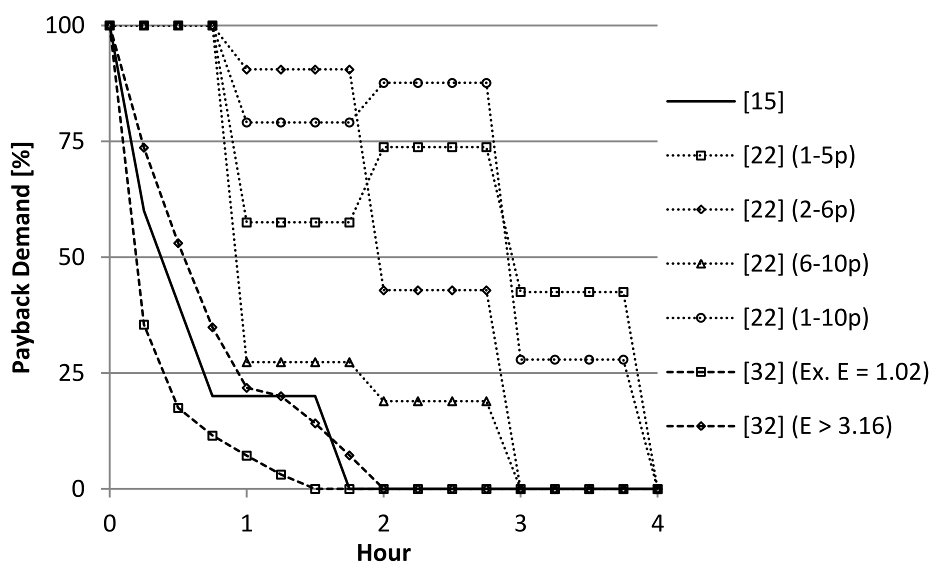

Figure 3: Payback model comparison.

In Figure 3, the x-axis represents the time following the control event and the y-axis represents the payback demand in percent of peak payback demand. The peak demand for each payback model in Figure 3 is 160 MW [15], 0.80 kW [22] (control period 1-5p), 0.84 kW [22] (control period 2-6p), 0.95 kW [22] (control period 6-10p), 1.29 kW [22] (control period 1-10p), 1.40 kW [32] (example E = 1.02), and 2.40 kW [32]

(E > 3.16). The payback model in [15] is the cumulative group DLC response; whereas, in [22] and [32], the payback demand is for individual devices, thus the need to normalize the payback demand in Figure 3. The controlled appliances were water heaters in [15] and [32], and air-conditioners in [22]. Notice, the payback demand is monotonically decreasing in all models but [22] (1-5p) and [22] (1-10p), highlighting an unexpected payback response that is a function of load device and timing.

A geographical variation in payback was described in [57]: "Reported values of energy payback percentages are lower in the northern states (Detroit Edison 25%, American Electric Power 50%) and higher in the southern utilities (Arkansas [Power and Light] and Mississippi [Power and Light] report almost 100%)." Payback is a phenomenon related to thermostatically controlled appliances; thus, it is intuitive that a higher payback could be expected in areas with cooler ambient temperatures. Notice, payback will also be effected by the amount of appliance use.

Finally, in many of the DLC demonstration project descriptions of average appliance performance was cited for air conditioner and water heater DLC power reduction. Typical results for air conditioner DLC was 0.92 kW (40% cycling) [30], 1.00-1.60 kW (50% cycling) [39], 1.73-1.95 kW (weighted average of 67% and 100% cycling-based on consumer preference program participation), and 1.00 kW [58]. Typical results shown for water heater DLC was 0.70-0.92 kW [29], 0.26 kW [39], and 0.60-1.00 kW [58]. These quantities represent average DLC performance per appliance. The air conditioning cycling percentages specify the percentage of time the air conditioners were removed from service. This is a common technique to balance energy management performance and customer satisfaction. The water heater control method across all references was to remove service during the entire control period. The variance in average results can be explained by the different demonstration projects control methods, appliance sizes, ambient temperatures, and appliance use patterns.

Many electricity utilities have experience with DLC. The objective of the current work is to compare traditional energy management functions (including DLC) to smart grid enabled energy management functions. The use of information technology capabilities provides the technical ability to increase communications beyond DLC, but the benefit of additional communication capability is yet thoroughly compared.

Next is a description of literature documenting residential demand response research. This description provides example system performance levels from existing research literature.

2.2 Residential Demand Response

This section of the literature review introduces existing research related to residential demand response (DR). The unique challenges of residential DR include working with a highly fragmented and diversified electricity demand sector [59]. The importance of DR has been emphasized by the Federal Energy Regulatory Commission (FERC). The FERC identified DR as one of three initiatives [60]; smart grid and renewable energy integration were the other two.

The first report that will be introduced was drafted in response to legislation mandating an analysis that "identifies and quantifies the national benefits of demand response and makes a recommendation on achieving levels of such benefits" [61]. To achieve this, the authors of [61] reviewed ten reports that quantified the benefits of DR.

The ten studies reviewed were divided into three groups: *illustrative*, *integrated resource planning*, and *program performance*. The *illustrative* studies simulated competitive market performance with DR. The *integrated resource planning* studies simulated the required level of DR to achieve adequate avoided supply costs in long range resource planning (in a vertically integrated electric utility and competitive market). The *program performance* studies documented results of pilot studies completed in the 2001 to 2004 timeframe.

The gross benefits ($) of DR computed in each of the ten studies reviewed was normalized by peak load (kW), DR program duration (yr), and participation rate (a level of 10% participation rate was used, e.g. 10% of electricity customers participated in DR) in [61]. This normalization facilitated the comparison of the result from the different studies. The normalized results are shown in Figure 4.

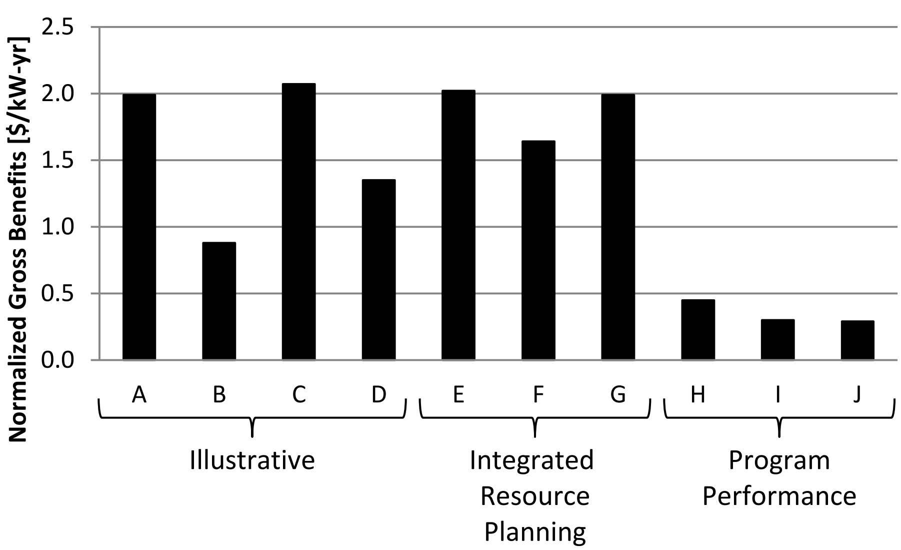

Figure 4: Normalized gross benefits of demand response [DR] [61].

From the normalized gross benefits in Figure 4, it is clear that the *illustrative* and *integrated resource planning* studies results are considerably higher than the *program* *performance* studies. In [61], this was attributed to the difference in analytic methods. Whereas, the *illustrative* and *integrated resource planning* studies extrapolated DR cost and performances into the future, assuming perfect foresight of demand and participation, the *program performance* analyses measured the DR performance of pilot projects. This does not imply that the *program performance* analyses quantified results would be replicable in the future. The number of uncontrollable factors effecting DR benefits are too numerous to make this type of a claim; rather, some combination of these results can be expected in future DR performance analysis.

The studies reviewed in [61] included participation of commercial, industrial, and residential customers. The focus of the current research is residential DR. Residential DR has unique constraints unlike commercial and industrial DR.

Five DR pilot studies were reviewed in [62], two of the five studies included residential participation. A description of the results in the two residential DR pilot studies is provided next to introduce residential DR performance.

Two Puget Sound Energy (PSE) residential DR programs were described in [62]: the personal energy management program and the home comfort control program. The personal energy management program provided residential energy consumers feedback on their energy use. The feedback included electricity bills showing time-of-use data and education on how to shift electricity use away from peak times. Over a three-month test period this program showed three to four percent shift in electricity demand from times of peak electricity use to times of off peak electricity use. The home comfort control program included networked thermostats that could be monitored and controlled via the internet. Remote controllability was available to both the residence owner and PSE.

Control options included increasing the air conditioner temperature set point in each volunteer's residence by two or four degrees Celsius. The option to override the PSE control was available; however, this option incurred a financial penalty if used. The program participation included 105 volunteers. The pilot program consisted of 41 two-hour setback periods. The energy savings showed average energy savings of two kilowatt hours with the four degrees Celsius setback control option (negligible savings were achieved with the two degrees Celsius setback control option). Notice, the override option was only used three times in the test period.

One residential and one commercial/industrial Wabash Valley Power Association DR program was described in [62]. The residential program was called "It Pays to be COOL." This program was an air conditioner and water heater direct load control (DLC) program. Annual payments of $25.00 were provided for residential customers who participated in the program. The estimated DR capacity potential of this program was 30 MW in the summer and 20 MW in the winter.

The final residential DR pilot study that will be introduced was published in [63] and summarized in [64]. This pilot study tested the DR performance using controllable equipment and residential participation within a two way communication system. The pilot study was a collaborative effort among the Pacific Northwest National Laboratory, three utilities (Clallam County Public Utility District, the City of Port Angeles, and Portland General Electric), IBM Watson Research Center, Invensys Controls, and Whirlpool.

The pilot study consisted of controllable equipment and residential participation: five 40 hp water pumps (with total nameplate capacity of 150 kW), two diesel generators (nameplate capacity 175 kW and 600 kW), 30 kW micro turbine, and 112 residential participants (approximately 75 kW). The controllable equipment and participating residences were not fed by a single distribution feeder. The pilot study operated a virtual feeder that included all of the controllable equipment and participating residences.

Two constraint scenarios were tested: 750 kW peak capacity constraint and 500 kW peak capacity constraint (i.e. the capacity of the virtual feeder was limited to the two levels: 750 kW and 500 kW, and controlled to keep the feeder demand below these set points). Each piece of controllable equipment was managed via a price signal that was updated every five minutes. The price signal was provided by an internet connection. The field demonstration was conducted between early 2006 and early 2007.

The field demonstration in [63] and [64] showed improved aggregate virtual feeder peak load reduction. The residential thermostatic load response is exemplified in Figure 5.

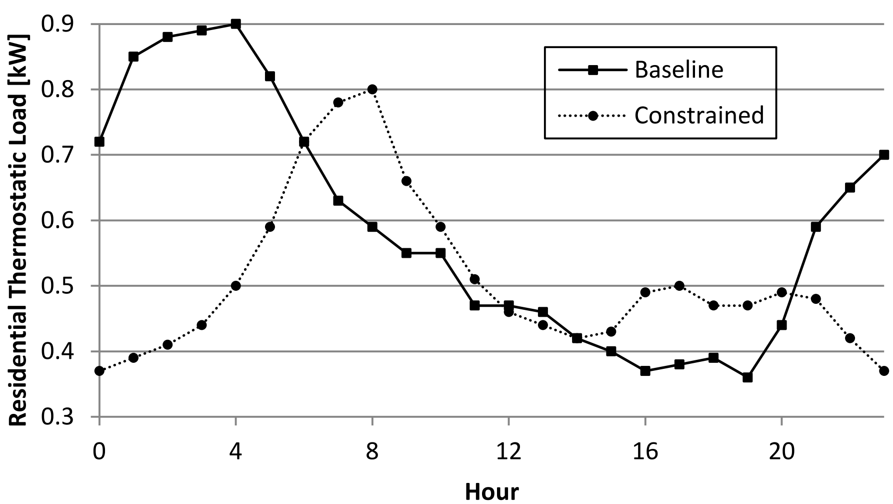

Figure 5: Baseline and constrained residential thermostatic load [63] and [64].

The results in Figure 5 highlight the differences between a daily *baseline* (uncontrolled) load demand and a daily 500 kW capacity *constrained* load demand.

Differences shown in Figure 5 are the reduced peak demand (*baseline* 0.9 kW and *constrained* 0.8 kW), delayed peak demand (*baseline* hour 4 and *constrained* hour 8), and reduced energy use (*baseline* 14.2 kWh and *constrained* 12.2 kWh). The aggregate virtual feeder peak load reduction over the entire field demonstration was estimated to be 5% for the 750 kW constraint scenario and 20% for the 500 kW constraint scenario. Notice, the example day in Figure 5 has an 11% reduction in peak load use.

This section has introduced existing research related to residential DR. Normalized gross benefits in the range of 0.30 to 2.07 $/kW-yr for residential, industrial, and commercial DR was summarized from [61]. Residential DR pilot studies summarized included energy use information feedback, air conditioner DLC, water heater DLC [62], and a two way communication systems [63] and [64].

The variety of residential DR programs underscores the confusion surrounding the potential benefits of residential DR, and highlights a need for a comparative analysis of DR capabilities. The current research provides a thorough analysis of DLC and smart grid residential DR using computer simulations.

Next is a description of literature documenting computer simulation of energy management systems similar to the current research methodology, providing typical results from existing research literature.

2.3 Residential Energy Management System Simulations

This section of the literature review introduces existing research related to residential energy management system (REMS) simulation. A number of REMS simulation frameworks have been described in existing literature. Each simulation framework introduced in this section simulated the use of smart appliances within a residential setting.

2.3.1 Scheduling Methodologies

In [65] through [69], multiple-agent-system theory was used to schedule the smart appliances. In [70], the technical and economic performance of three control schemes was computed for an example residence: traditional direct load control (DLC), enhanced DLC, and coordinated end-use switching. In [71], the cost to run each smart appliance was used to schedule the optimal timing of each smart appliance using an exhaustive search algorithm. In [72], a fuzzy inference system was developed to identify the current grid conditions (peak, off-peak, or pre-peak) and a rule-based control system was used to control the smart appliances. Similarly, in [73] a fuzzy distributed controller was documented. In [74], the smart appliances were scheduled based on a three level control heuristics approach: first, the smart appliances that are on all the time were scheduled (e.g. refrigerator); second, the large energy consuming smart appliances were scheduled; and last, all the other smart appliances were scheduled. Two versions of instantaneous demand limiting control were compared in [75]. Computational intelligence methods particle swarm optimization [76] and genetic algorithms [77] were used to optimize the scheduling of each smart appliance. In [78], a deterministic scheduling problem was solved using a general mixed integer programming method and a stochastic scheduling problem was solved using a scenario tree method. In [79] through [84], a three level control method was described: local prediction (neural network), global planning (iterative distributed dynamic programming), and local scheduling (integer linear programming). A linear programming algorithm using future price prediction was documented in [85]. In [86], a Markov chain model of the smart appliance use was assumed and a Q-learning method was used to learn varying consumer behavior and optimally schedule the smart appliance use to minimize discomfort of the customer and energy cost. In [87], (as in [76]) particle swarm optimization was used to schedule the smart appliance use; however, the smart appliances were generalized as interruptible loads with unique operating characteristics (capacity [kW], rate [$/kW], maximum off time [hr], and minimum on time [hr]). In [88], smart appliances were scheduled to a future time with the lowest forecasted cost for electricity.

2.3.2 Methodology Dichotomy

The methodology used to schedule the operation of the smart appliances in the residential energy management system (REMS) simulation work listed above varied considerably. In general, the scheduling methods can be divided into two classes: causal and non-causal. The causal methodologies use only data that had been created before computing the control actions; whereas, the non-causal simulation methodologies used future data in calculating the control actions. This differentiation provides a set of simulation frameworks that can operate in real-time (causal) and cannot (non-causal). Causal simulations are documented in [72] through [75], [86], and [88]. Non-causal simulation frameworks are documented in the remainder of the papers ([65] through [71], [76] through [85], and [87]).

Theoretically, the causal simulation frameworks will achieve inferior performance compared to the non-causal simulation frameworks due to the limited future knowledge. However, the causal frameworks provide improved performance over uncontrolled operation. Further, the causal frameworks can be implemented beyond a simulation test bed. Causal frameworks can be used as a control system within a residence or as part of a hardware-in-the-loop test bed.

A key limitation of most of the REMS simulation literature is that an electric utility perspective is not considered. An exception to this limitation is in [88]. The aggregate impact of load shifting and demand elasticity was introduced in [88]; however, further research related to the aggregate impact of REMS is required. Limited potential will be achieve via REMS if the objectives of the residence owner alone is considered. Both the residence owner and electric utility are considered in the current research.

Poignant conclusions from [89] highlight common results from much of the REMS simulation literature. Specifically, residential energy management infringes upon electricity use during the control period but only to a certain degree. The severity of this degree will be a personal preference for each electricity user. Payback is an unintended consequence that is inevitable when leveraging thermostatically controlled appliances. The economic performance will depend on the electricity rate structure. As the price differential of on-peak versus off peak increases the REMS performance becomes more attractive.

Next is a description of the projected market outlook in three related areas addressed by Pike Research, providing insight into the future of the nascent REMS industry.

2.4 Related Markets Outlook

The market outlooks of three related technologies were published in the second half of 2010: virtual power plants [90], building energy management systems [91], and smart appliances [92].

Virtual power plants, as defined in [90], are the software enabled coordination of multiple small generation or demand-side (storage inclusive) resources for power system applications. An example of a virtual power plant could be an entire neighborhood of residential energy management system (REMS) enabled residences. The market forecast in [90] was prefaced with adjectives describing virtual power plants including "nebulous technology," and "complicity," and "uncertainty." The current uncertainties surrounding virtual power plants is similar to the uncertainties around the smart grid, the technology vision is more developed than the technical details. However, it was estimated that the total worldwide virtual power plant capacity was 19,428 MW in 2009, and was expected to grow substantially in the near term future [90].

Building energy management systems are the commercial/industrial sibling of REMS. The potential market growth of this technology was correlated to the projected growth of energy efficiency. The potential market growth was attributed to include the emphasis from the government and desire of end users to save electricity and ultimately money [91]. It is assumed that if power system level benefits and economic incentives are achieved in the commercial market, the next market to be addressed will be the residential market.

The actuator for virtual power plants and building/residential energy management systems is the smart appliance. Identified drivers to increase the market share of smart appliances were dynamic pricing; standards; control and privacy; and education [92]. It was documented that nearly half of these drivers had been addressed [92]. The nearly completed drivers were standards and control and privacy; whereas, dynamic pricing and education were less developed drivers. Smart appliances are stuck in a catch-22 situation. The market share is limited by the limited support and the limited support is limited by the low market share.

The current research quantifies the impact of energy management technology in electric utility terms using primary energy source utilization (PESU). Next is a description of literature documenting PESU, providing an introduction to PESU and an electric utility centric analysis of electric load modifications.

2.5 Primary Energy Source Utilization

The study of primary energy source utilization (PESU) is the analysis of the power system primary fuel sources (e.g. coal, natural gas, nuclear, etc.) required to meet electric load over a specific simulation horizon (e.g. one year). Related results include generated energy, generated environmental air pollution (EAP), fuel cost, and amount of fuel used. Primary energy source utilization analyses have been performed investigating the impact of plug-in electric vehicles (PEVs) [93] and [94]; demand response (DR) [95]; and direct load control (DLC) [96] through [98]. The results in each of these documents will be described next to introduce PESU.

The PESU results in [93] included the impact of PEV charging on the system load, EAP (vehicle and power system), and the marginal cost of electricity. The results in [93] showed the percent of energy from each available generator type in the Xcel Energy generation fleet for four vehicle charging cases. The results showed that natural gas was used to meet the majority of the PEV charging load. Also, as the PEV charging load was shifted later in the evening (delayed to 10p) the coal utilization increased. Further, the EAP results in [93] included a small decrease in generated nitrogen oxide and a significant reduction in generated carbon dioxide. A similar analysis was presented in [94].

A PESU analysis of the impact of DR in New England was presented in [95]. The DR energy bid into a day-ahead DR program (DADRP) market, and was dispatched based on the clearing market price (like supply side resources).

The simulated base case and DADRP energy results are shown in Table 9.

Table 9: Base case and day-ahead demand response program [DADRP] energy by plant and fuel type [95].

Plant Type	Fuel Type	Base Case [GWh]	DADRP [GWh]
Combined Cycle	Gas	19,197	19,226
	Gas/Oil	298	303
Combustion Turbine	Gas	75	74
	Gas/Oil	0	1
	Oil	5	5
DR	Various	0	3
Steam	Gas	241	231
	Gas/Oil	343	284
	Oil	4,294	4,264
	Coal	7,706	7,707

The results in Table 9 indicate an increased utilization of the combined cycle type plants and a reduced utilization of the oil and gas fueled steam type plants in the DADRP scenario compared to the base case scenario. Notice, the results in Table 9 are the data from [95] only for the plant and fuel types that the level of generated energy changed from the base case to the DADRP scenario. Further, the energy production in Table 9 is for a summer season only.

A PESU analysis of DLC was documented in [96]. The impact of water heater, air conditioning, and space heating was investigated for multiple durations for different electric utilities. The utilities considered were the Electric Power Research Institute

Synthetic Electric Utility Systems. The production cost savings for the different devices and timing considered are shown in Table 10.

Table 10: Direct load control [DLC] production cost savings [96].

Connected Load	Device	Production Cost Savings [k$ ($/device)]		
		Sys. A-Summer	Sys. D-Summer	Sys. F-Winter
500	Water Heater (6h)	32.0 (0.21)	193.3 (1.24)	59.1 (0.38)
500	Water Heater (12h)	35.8 (0.23)	310.7 (1.99)	
500	Air Conditioning	73.2 (0.66)	781.0 (7.04)	
1,000	Air Conditioning	133.9 (0.66)	781.0 (7.04)	
500	Space Heating			74.2 (4.64)

The results in [96] showed the range of production cost savings from $0.20 to $7.04 per load point per week. Further, the authors of [96] commented that high production cost savings were available in electric utilities with high marginal costs.

A second PESU analysis of DLC was documented in [97]. Four scenarios were considered:

- Scenario 1: No DLC dispatch and unit commitment coordinated.
- Scenario 2: DLC dispatch and unit commitment coordinated (no DLC capacity was used as system spinning capacity).
- Scenario 3: DLC dispatch and unit commitment were coordinated and all DLC capacity was used as system spinning capacity.
- Scenario 4: DLC dispatch and unit commitment were coordinated and 50% of DLC capacity was used as system spinning capacity.

The DLC production cost savings for each scenario are shown in Table 11.

Table 11: Direct load control [DLC] production cost savings [97].

Cost Savings	Scenario 1	Scenario 2	Scenario 3	Scenario 4
$	109,550	111,636	259,411	142,325
%	0.98	1.00	2.33	1.30

The results in Table 11 indicate that the use of DLC capacity as spinning reserve provides considerable cost savings.

A similar PESU analysis of DLC as [96] and [97] is presented in [98]. The authors in [98] point out three possible negative benefits of DLC:

- "The drop in the savings curve caused by the increase in load control from 20 to 30 MW illustrates that a flatter load curve does not necessarily imply a lower production cost and that DLC strategies, if not properly coordinated, can result in negative benefits."
- "As the level of control is increased, the benefits increase up to a certain threshold then level out."
- "When the energy payback of a DLC scheme is less than 100%, the utility loses some revenues due to the decrease in energy sales."

In general, PESU is an analysis used to quantify the power system fuel utilization and subsequent EAP generated to meet electric load. Further, PESU results provide an electric utility centric view of potential changes in electric load. The tradeoff of varying levels of automation from the residence owner and electric utility is a key focus of the current research.

This chapter described existing research in five areas: DLC, residential DR, residential energy management system simulations, related markets outlook, and PESU. These research areas provide background in the general area of the current research. Next is a summary of the conclusions from the reviewed literature.

2.6 Summary

First, theoretical direct load control (DLC) research themes were described. The theoretical DLC research themes described included optimized DLC scheduling, heuristic DLC scheduling, and economics of DLC. Further, payback models from DLC literature were compared. Additionally, literature describing multiple demonstration projects was introduced. Material related to the identified research themes (scheduling, economics, and payback) from the DLC demonstration projects were compared to the similar material from the theoretical DLC literature. It was shown that significant variation in literature results exists.

Second, residential demand response (DR) studies were described. Multiple references included quantified results of residential DR performance. The unique challenges of residential DR were highlighted. The variety of residential DR program results underscores the confusion surrounding the potential benefits of residential DR and highlights a need for a comparative analysis of DR capabilities.

Third, the methodologies and common results from residential energy management system (REMS) simulations were described. Specifically, residential energy management infringes upon electricity use during the control period but only to a certain degree. Payback is an unintended consequence that is inevitable when modifying the use of thermostatically controlled appliances. The economic performance will depend on the electricity rate structure. As the price differential of on-peak versus off peak increases the REMS performance becomes more attractive.

Fourth, market potentials of virtual power plants, building energy management systems, and smart appliances were described. These market potentials indicate impending market growth in the near term future. It is expected that significant market growth is contingent on establishing evidence of a mutual benefit for the residence owner and the electric utility.

Finally, the concept of primary energy source utilization (PESU) was described and literature related to this type of analysis was described. The use of PESU for the investigation of the impacts of plug-in electric vehicles, DR, and DLC was described.

The current research will provide a test bed for energy management functions, quantifying the effects of the load changes using PESU. The variety of REMS underscores existing confusion surrounding the potential benefits of residential energy management. This confusion further highlights a need for a comparative analysis. By testing residential energy management options in a single analysis, an equitable comparison can be made.

This chapter has described existing research that is related to the impact of residential energy management technology on PESU. Next is a description of the REMS simulation formulation.

3 PROPOSED PHYSICALLY-BASED RESIDENTIAL-ENERGY-MANAGEMENT-SYSTEM SIMULATION

This dissertation compares the performance of direct load control (DLC), a traditional form of energy management, with the performance of smart grid enabled energy management functions. The various energy management functions are compared in their ability to provide automated demand response (DR). Specifically, this dissertation documents simulations of five energy management functions, by testing various levels of residential energy management system (REMS) complexity. Through simulation, the potential ability of residential appliances to provide automated DR will be quantified. Providing a quantified indication of what technology (energy management functions) provide the most significant automated DR. Further, the use of photovoltaic and plug-in electric vehicle distributed energy resources are considered in conjunction with the residential energy management functions.

The Proposed Physically-Based REMS Simulation (PPRS) is described in this chapter. The PPRS quantifies the performance of an individual residence using a variety of energy management functions (DLC, smart thermostat, smart appliance scheduling, and smart appliance scheduling with a stationary battery). In general, this simulation quantifies the benefits of the energy management functions to the residence owner.

First is a definition of the PPRS components. Second is a description of the PPRS formulation. Third is a validation of initial PPRS results. Last is a summary of this chapter..

3.1 Simulation Components

A block diagram of the Proposed Physically-Based Residential-Energy-Management-System Simulation (PPRS) components is shown in Figure 6. The PPRS consists of five energy management functions. Not all components are used in each energy management function. Specifically, the direct load control (DLC) energy management function does not include a controller; rather, the DLC controlled appliance responds to an electric utility DLC signal. Further, the smart appliance scheduling (SAS) energy management functions do not include the stationary battery. The stationary battery is only included in the smart appliance scheduling with a stationary battery (SASB) energy management function.

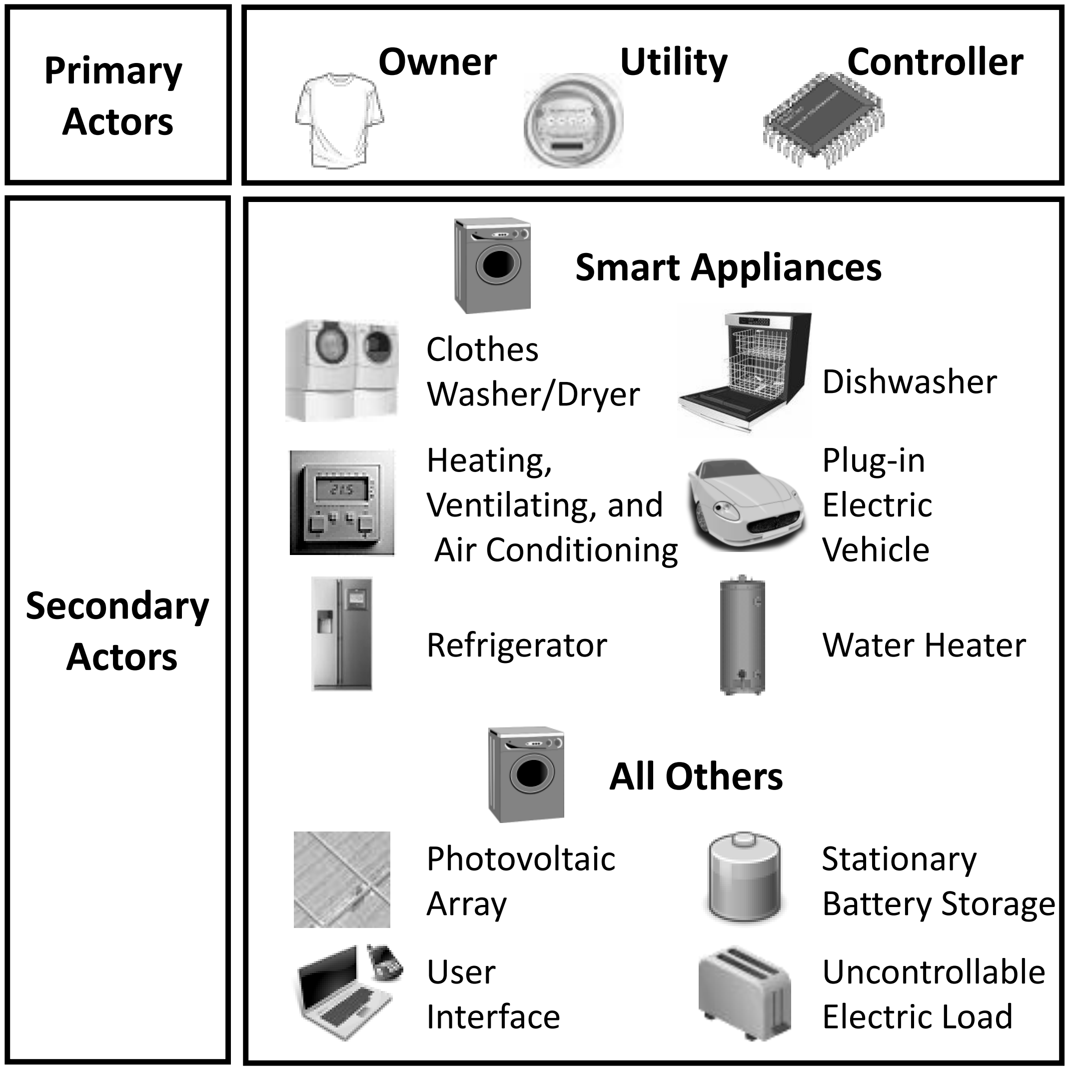

Figure 6: Proposed Physically-Based Residential-Energy-Management-System Simulation [PPRS] components [99].

The primary actors in Figure 6 include the owner, electric utility, and the controller. Secondary actors in Figure 6 include two groups of equipment: smart appliances (clothes washer; clothes dryer; dishwasher; heating, ventilation, and air conditioning [HVAC] system; plug-in electric vehicle; refrigerator; and water heater) and all others (photovoltaic [PV] array, stationary battery system, user interface, and uncontrollable electric load).

The primary actors initiate system events. The owner initiates appliance events by turning on appliances. The electric utility provides operating data such as DLC signal, hourly time-of-use electricity price (not considered), or times of required demand response (DR). The smart thermostat and DLC energy management functions do not include the controller.

The controller is used in the SAS and SASB energy management functions. The controller delays the use of the smart appliances before and during DR. The performance of the smart appliances can be delayed but not interrupted. The HVAC system and refrigerator provide critical thermal services; as such, the amount of time that these appliances are curtailed is limited to specific amounts of time. Specifically, the HVAC service is interrupted for 15 minutes each half hour during the DR period. The refrigerator service is interrupted for a maximum of one hour (60 minutes).

The PV array produces onsite electric energy. The stationary battery storage system provides energy storage capabilities to the system. The user interface (personal computer or handheld electronic device) provides an interface for the owner to monitor the system performance and provide override commands. The uncontrollable electric loads represent residential plug loads that require electricity with no capability to be interrupted.

This section defined the PPRS components. Next is a description of the PPRS formulation.

3.2 Simulation Formulation

The Proposed Physically-Based Residential-Energy-Management-System Simulation (PPRS) was developed in Matlab/Simulink to quantify the electricity use of a typical residence with and without energy management functions. Five energy management functions are simulated for four power system areas in the United States. The PPRS is structured as a discrete event simulation.

The simulation begins by scheduling all the events for the simulation horizon (e.g. one day) then processing each event sequentially. The simulation does not use any knowledge of future events during the simulation execution, leading to a control methodology that could be used in real-time. The simulation events consist of appliances starting, changes in photovoltaic array output, and demand response. Each event can schedule a new events and/or changes the residential electricity load. After each event is processed, the appliance energy and residence energy are analyzed. Next is a description of the probabilistic appliance use models.

3.2.1 Appliance Use Models

Each appliance in the Proposed Physically-Based Residential-Energy-Management-System Simulation is modeled as a constant electric load for a specific duration. The electric load and duration for each appliance is shown in Table 12.

Table 12: Residential appliances electric load and duration values [99].

Appliance	Electric Load [kW]	Duration [hr]
Air Conditioner/Furnace	3.5/0.35	Varies
Clothes Dryer	5.0	0.75
Clothes Washer	0.5	0.50
Dishwasher	1.8	0.75
Plug-in Electric Vehicle (PEV)	1.4	8.00
Refrigerator	0.8	0.25
Water Heater	4.5	0.25

The electric load data is from [99]. The heating, ventilation, and air conditioning (HVAC) load data in Table 12 is decomposed into two appliances based on the ambient temperature: air conditioner (AC) and furnace. The HVAC duration in Table 12 varies based on a thermal simulation of a simplified residence, described further below. The AC electric load data in Table 12 represents a 2.5 ton HVAC system with seasonal energy efficiency ratio of 12. The refrigerator electric load data in Table 12 represents a side-by-side refrigerator. The appliance durations (except the HVAC), in Table 12, were selected based on the average appliance energy use described further in Section 3.3.

Probabilistic models are used for the number of times that each appliance is used and the time of the day that the appliance is used. The number of times that appliance i is used in a daily simulation is a truncated normally distributed random variable with mean μ_i, and standard deviation σ_i; defined in Table 13. Notice, the mean value is function of the appliance annual energy use, the appliance energy use per event, and appliance seasonal use distribution S_i, defined in Figure 7 for each appliance. The subscript i represents each appliance (for clothes dryer i is *CD*, for clothes washer i is *CW*, for dishwasher i is *Dw*, for refrigerator i is *Ref*, and for water heater i is *WH*).

Table 13: Appliance use normally distributed random value parameters.

Appliance	μ_i	σ_i
Clothes Dryer	$1.0082 \cdot S_i$	1
Clothes Washer	$1.0521 \cdot S_i$	1
Dishwasher	$0.1918 \cdot S_i$	1
Refrigerator	$17.7534 \cdot S_i$	2
Water Heater	$11.3072 \cdot S_i$	2

The values in Table 13 were selected based on the annual appliance energy use. The validation of these values is left for the next section of this chapter.

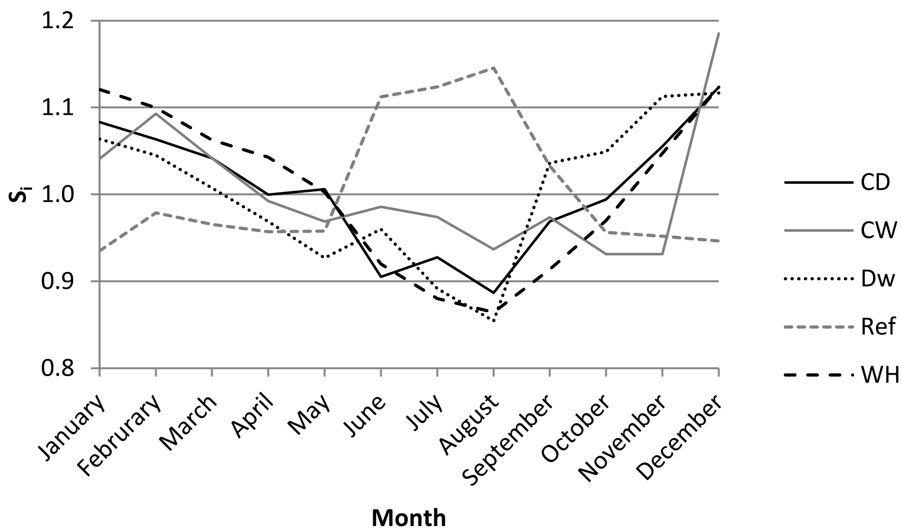

Figure 7: Residential appliance seasonal use multiplier for each appliance.

The distribution parameters μ_i and σ_i result in variability around the expected annual energy use per appliance. The seasonal variability functions in Figure 7 will result in seasonal variability for the use of each appliance.

The times that each appliance is used is based on probability distribution functions (PDFs) for each appliance. The PDF for each appliance is shown in Figure 8.

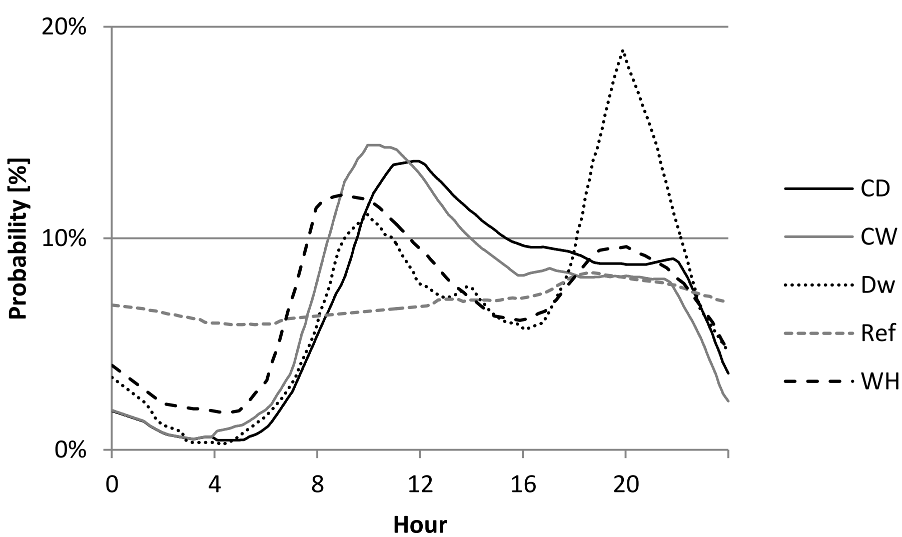

Figure 8: Residential appliance timing probability distribution functions [PDFs] for each appliance.

The annual energy use, the data used to compute the seasonal variability functions (Figure 7), and data used to compute the timing PDFs (Figure 8) are based on data in [100]. Using an inverse-transform method [101], random appliance starting times are generated based on the timing PDF for each appliance. The use of probabilistic models results in realistic appliance use that varies similar to the data in [100].

The residential appliances run a random number of times and each appliance use begins at a random time. To illustrate the random appliance use, three daily use simulations; clothes dryer, clothes washer, and dishwasher; are shown in Figure 9.

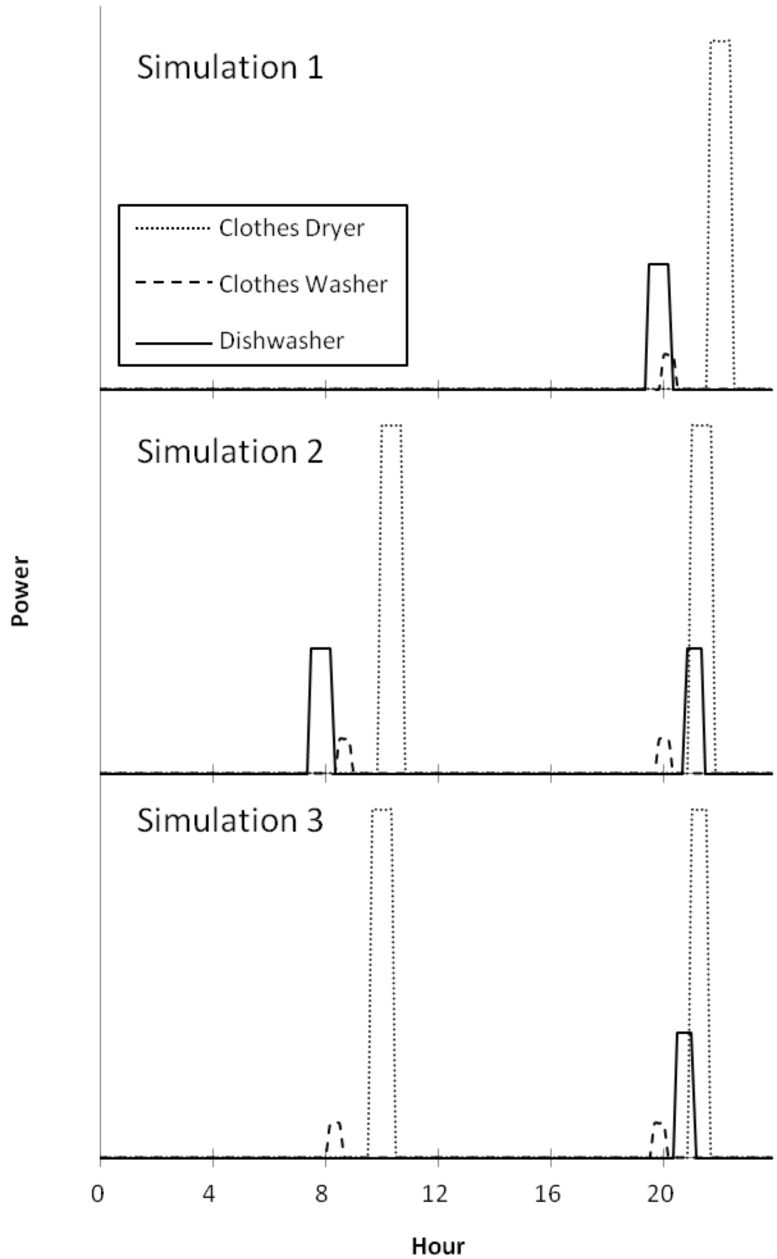

Figure 9: Example appliance use for three simulations.

In Figure 9, Simulation 1 is an example with one clothes dryer, clothes washer, and dishwasher event each in the evening. Similarly, Simulation 2 is an example with two events for each appliance, one grouping of appliance uses in the morning and another grouping in the evening. Finally, Simulation 3 is an example with a single dishwasher event in the evening and two sets of clothes dryer and clothes washer events. This variation models random consumer behavior.

The PEV is recharged every day. The time that the PEV starts to recharge is based on a probabilistic model. The PEV recharging time PDF is shown in Figure 10.

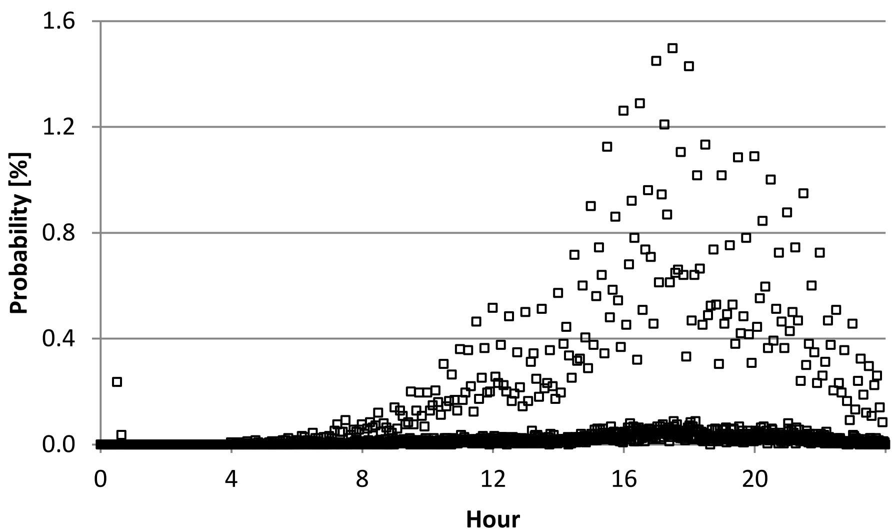

Figure 10: Plug-in electric vehicle [PEV] timing probability density function [PDF].

The data used to compute the PDF in Figure 10 is from [102]. This distribution represents the times survey respondents recorded they returned home from a trip driving a car and the car was not used again for eight or more hours.

The duration of the HVAC system depends on a thermal simulation of a residence heating and cooling system. The thermal simulation models the temperature change within the residence based on the ambient temperature and the indoor temperature set point. Next is a description of the ambient temperature data and assumed indoor temperature set point data.

3.2.2 Temperature and Irradiance Data

Four power system areas of the United States are analyzed: Versailles Kentucky (ECAK), Mercury Nevada (SNV), Stillwater Oklahoma (SPPS), and Necedah Wisconsin (WUMS). These four power system areas were selected to consist of different power system operation areas and different climate zones. Different climate zones were selected to study the impact of ambient temperature on the automated demand response ability of various energy management functions.

The daily average temperature for each power system area is shown in Figure 11.

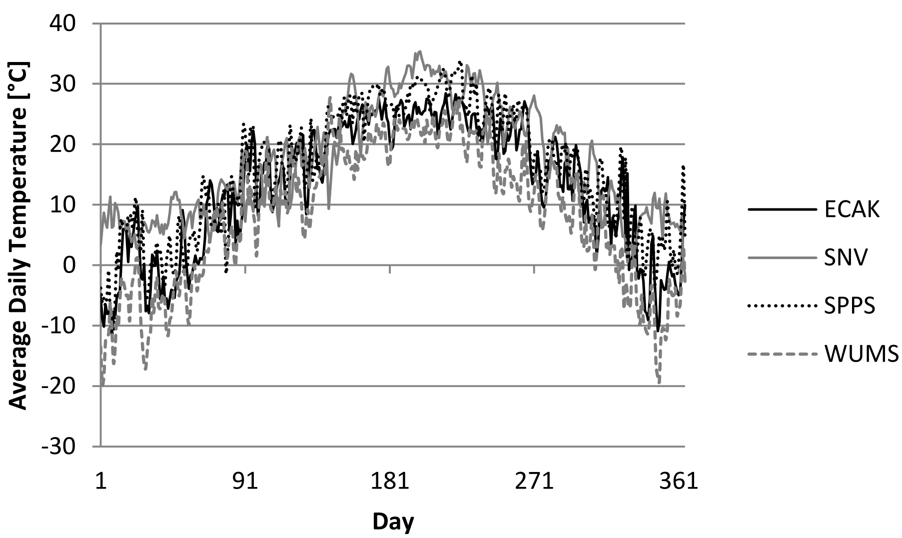

Figure 11: Daily average temperature for each power system area.

The annual daily average temperature patterns confirm the intuition that SNV observed the highest summer peak temperature at 35.4 °C, followed by SPPS at 33.9 °C, ECAK at 28.4 °C, and WUMS at 27.7 °C. Also, the coldest winter temperature was observed in WUMS at -19.8 °C, followed by ECAK at -11.4 °C, SPPS at -11.3 °C, and SNV at -1.5 °C. Overall, the average annual temperature ranks the power system areas WUMS at 8.3 °C, ECAK at 12.9 °C, SPPS at 15.6 °C, and SNV at 17.1 °C.

The daily cumulative irradiance for each power system area is shown in Figure 12.

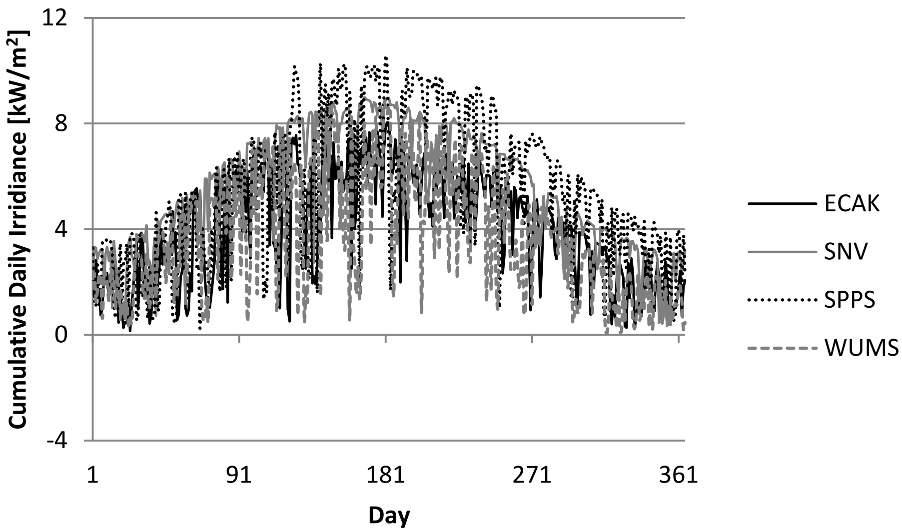

Figure 12: Daily cumulative irradiance for each power system area.

The cumulative daily irradiance in Figure 12 is the sum of the hourly irradiance for each power system area. This summation results in a value [kW/m^2] that is proportional to the daily energy available from the photovoltaic array. Similar to Figure 11, the annual average cumulative daily irradiance ranks the power system areas: WUMS at 3.78 kW/m^2, ECAK at 4.05 kW/m^2, SPPS at 5.51 kW/m^2, and SNV at 5.51 kW/m^2.

The average temperature data shown in Figure 11 and cumulative irradiance data shown in Figure 12 summarizes 8760 hourly outdoor temperature and PV energy production data points in the PPRS: ECAK [103], SNV [104], SPPS [105], and WUMS [106].

For the Proposed Physically-Based Residential-Energy-Management-System Simulation (PPRS), the results from two days are described in Chapter 4. The two days represent extreme temperature seasons: winter and summer. These days were selected as good candidates for the use of energy management functions. The daily temperature data for both seasons and for each power system area is shown in Figure 13 and Figure 14.

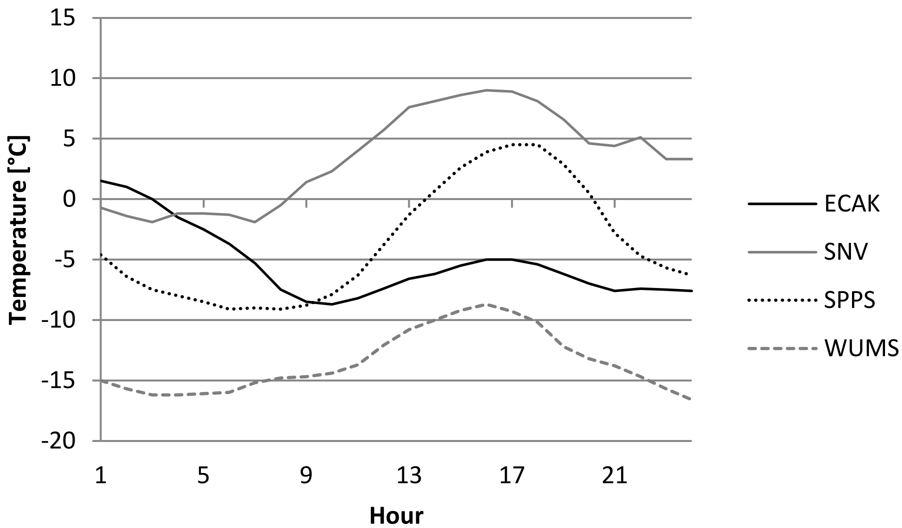

Figure 13: The winter hourly temperature for each power system area.

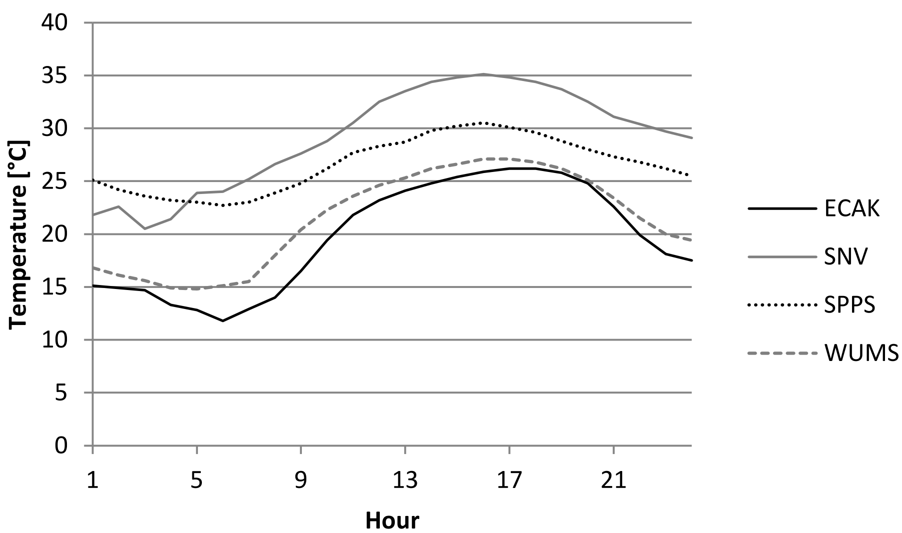

Figure 14: The summer hourly temperature for each power system area.

The daily irradiance data for both seasons and for each power system area is shown in Figure 15 and Figure 16.

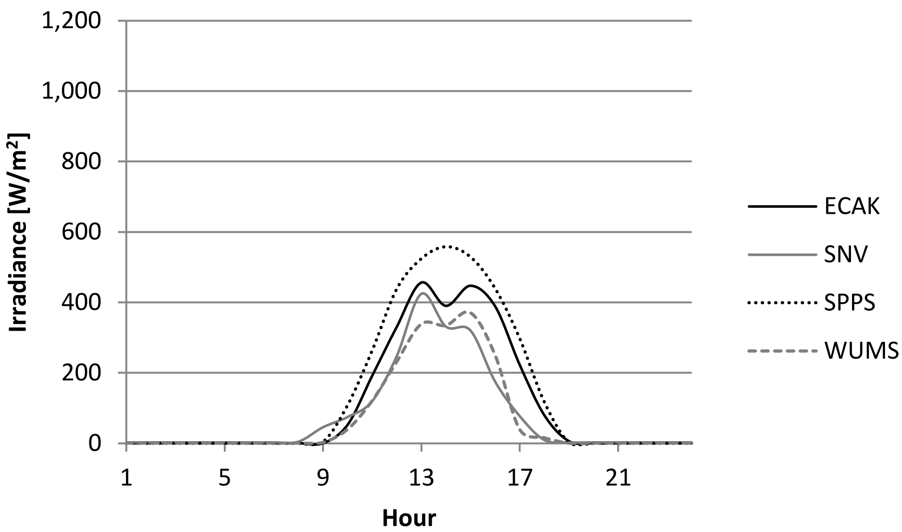

Figure 15: The winter hourly irradiance for each power system area.

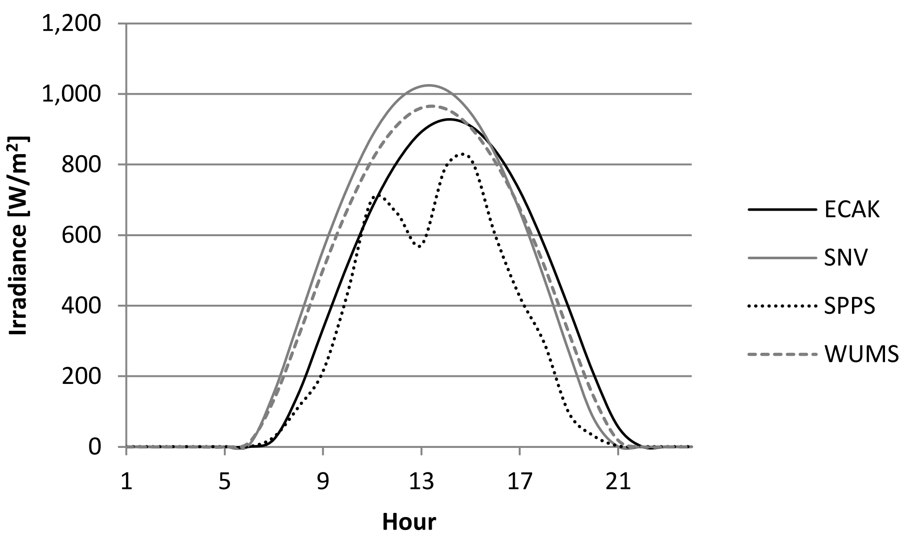

Figure 16: The summer hourly irradiance for each power system area.

The appliance use models, outdoor temperature data, and irradiance data specifies the details of all the PPRS components of Figure 6, except the uncontrolled electric load. Next is a description of the uncontrolled electric load.

3.2.3 Uncontrolled Electric Load

The uncontrollable electric load (UEL) represents residential plug load that require electricity with no capability to be interrupted. The deterministic daily UEL profile is shown in Figure 17.

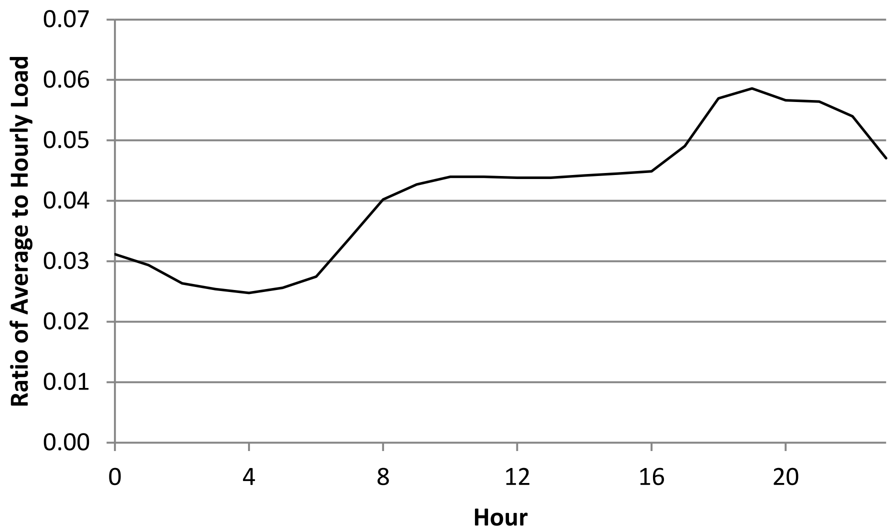

Figure 17: Daily uncontrolled electric load [UEL] profile.

The profile in Figure 17 is the ratio of the annual UEL energy use (4,914 kWh) to the hourly UEL demand. The actual hourly UEL is the product of the hourly UEL demand and the UEL seasonal use distribution S_{UEL}. The UEL seasonal use distribution is shown in Figure 18.

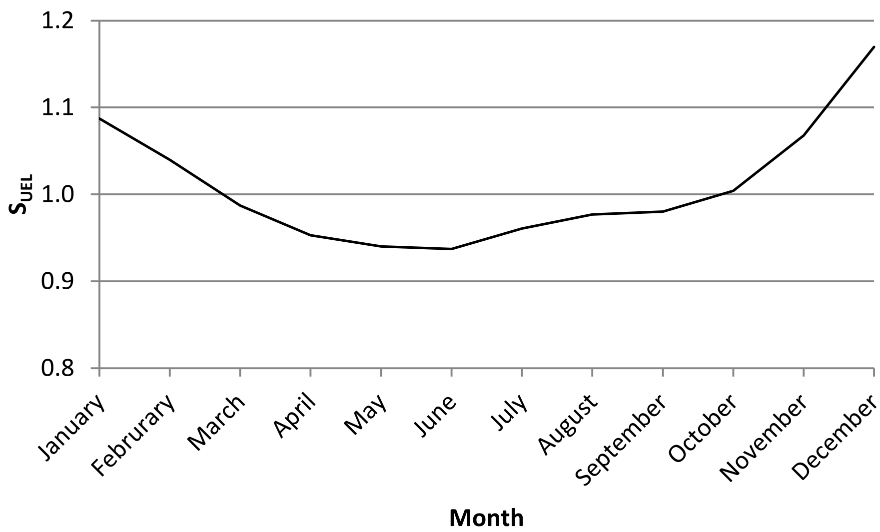

Figure 18: Uncontrolled electric load seasonal use multiplier.

The annual UEL energy use, the data used to compute the daily UEL profile (Figure 17) and the UEL seasonal use multiplier (Figure 18) are based on data in [100].

The data described up to this point outlines the methodology to generate the simulated appliance use. This is used in the base case simulation to quantify the residential electric load. The use patterns are modified in each of the energy management functions simulations to model the application of automation technology within a residence. Next is a description of the logic used to modify each appliance use pattern.

3.2.4 Control Heuristics

Five energy management functions are included in the Proposed Physically-Based Residential-Energy-Management-System Simulation (PPRS): water heater (WH) direct load control (DLC); heating, ventilation, and air conditioning (HVAC) DLC; smart thermostat (ST); smart appliance scheduling (SAS); and smart appliance scheduling with a stationary battery (SASB). In the two forms of DLC the controlled appliance (WH and HVAC) is controlled for an electric utility specified time period (demand response [DR] period) with limited service during this time period to the controlled appliance only. The ST energy management function increases (for times that air conditioning is needed) or decreases (for times that heating is needed) the indoor temperature set point during the DR period. The SAS energy management function delays the use of the smart appliances (clothes dryer, clothes washer, dishwasher, HVAC, refrigerator, and WH) prior to and during the DR period. The SASB energy management function adds a stationary battery dispatching function to the SAS energy management function.

All energy management functions (WH DLC, HVAC DLC, ST, SAS, and SASB) start from a base case sequence of appliance use and the use of the smart appliances is modified. In the HVAC DLC energy management function the HVAC utilization is rescheduled during the DR period. The HVAC is rescheduled so that within every half-hour during the DR period the HVAC is not allowed to run for n_{off} minutes (e.g. 15 minutes). Within each half-hour increment in the DR period the specific n_{off} minutes are selected randomly to minimize the impact of synchronized payback. This type of grouping scheme is common within DLC demonstration literature [30], [39], and [58]. The WH DLC removes service to the WH for the entire DR period (with all WH energy use rescheduled after the DR period, i.e. 100% payback efficiency).

In the ST energy management function, the indoor temperature set point is relaxed during the DR period. During the summer and warmer days in the transitional months (average temperature greater than or equal to 20 °C) the indoor temperature set point is increased from 20 °C to 26 °C. During the winter and cooler days in the transitional months (average daily temperature less than 20 °C) the indoor temperature set point is decreased from 20 °C to 14 °C.

The SAS allows the smart appliances to be delayed if the appliance is scheduled to start just before or during the DR period. One caveat of this rule is for the refrigerator. The refrigerator is delayed for a maximum of one hour (60 minutes), because the internal temperature of the refrigerator must remain cold during the DR period. It is assumed that the internal temperature of the refrigerator will not rise to unsafe levels in a single hour [107]. All the other smart appliances are delayed if they are started such that they will run into the DR period. All of the delayed appliances are rescheduled in a priority-based sequential sequence (e.g. clothes washer, clothes dryer, dishwasher, and plug-in electric vehicle). A sequential sequence is needed so that a new daily peak is not created when all delayed appliances are restarted (i.e. synchronized payback) after the DR period.

In the SASB energy management function, a battery dispatching function is added to the appliance rescheduling in the SAS energy management function. The stationary battery is only dispatched during DR. The battery output is limited to 120 V and 15 A (1.8 kW). The battery capacity is 4.8 kWh. The battery is scheduled to recharge at 4a.

This chapter defined the PPRS components and described the PPRS formulation . Next is a description of the initial PPRS results. Validation compares initial PPRS appliance energy results and residential appliance energy use data from three references.

3.3 Validation

Typical appliance energy use data from [108], [109], and [110] was used in the development of the probabilistic appliance use models. Initial simulated appliance energy use is compared with the data from these references as validation of the appliance use models. The average annual appliance energy use data for each reference is shown in Table 14, along with the average and standard deviation of the appliance reference data.

Table 14: Annual appliance reference energy use average and standard deviation.

Appliance	[108]	[109]	[110]	Average	Standard Deviation
Clothes Dryer [kWh]	1,020.0	1,079.0	919.8	1,006.3	80.5
Clothes Washer [kWh]	144.0	120.0	96.4	120.1	23.8
Dishwasher [kWh]	516.0	512.0	105.1	377.7	236.1
HVAC [kWh]	23,100.0	2,796.0	9,198.0	11,698.0	10,380.3
Refrigerator [kWh]	2,292.0	1,462.0	4,642.8	2,798.9	1,649.9
Water Heater [kWh]	6,156.0	2,552.0	1,296.5	3,334.8	2,522.6

The clothes dryer, clothes washer, dishwasher, refrigerator, and water heater reference data averages in Table 14 were used to compute the mean number of appliance events in each simulation for the clothes dryer, clothes washer, dishwasher, refrigerator, and water heater. The heating, ventilation, and air conditioning (HVAC) appliance use is scheduled based on a thermal simulation of a residence. The data in Table 14 is a reference point of from which the simulated appliance energy use can be compared.

The initial annual Proposed Physically-Based Residential-Energy-Management-System Simulation (PPRS) appliance energy use results are shown in Table 15.

Table 15: Initial annual Proposed Physically-Based Residential-Energy-Management-System Simulation [PPRS] appliance energy use.

Appliance	ECAK	SNV	SPPS	WUMS
Clothes Dryer [kWh]	1,030.3	1,014.2	1,018.5	1,010.9
Clothes Washer [kWh]	120.4	120.5	122.2	122.5
Dishwasher [kWh]	388.9	388.3	389.3	386.4
HVAC [kWh]	1,938.5	4,056.0	4,024.9	1,386.3
Refrigerator [kWh]	2,814.8	2,814.5	2,812.4	2,814.6
Water Heater [kWh]	3,355.4	3,335.4	3,351.0	3,357.3

Initial annual PPRS appliance energy use in Table 15 is the weighted average of the average appliance energy use in the first day of each month of the year. The monthly average appliance energy use is weighted by the number of days in the month. Each simulated day was repeated 750 times.

All the initial annual PPRS appliance energy use is within plus or minus 2.5% from the equivalent average appliance reference data in Table 14, except the simulated HVAC annual energy use. The simulated HVAC annual energy use is clustered around the minimum HVAC reference data point. Notice, the average percent difference is 2% compared to the minimum HVAC reference data point.

The validation of the simulated appliance use model has shown that the annual appliance use (clothes dryer, clothes washer, dishwasher, refrigerator, and water heater) is similar to the average of the reference data. The HVAC appliance use has significant regional variability that approximates the minimum HVAC reference data point.

This chapter has defined the PPRS components and described the PPRS formulation and validation. Next is a summary of this chapter.

3.4 Summary

This dissertation compares the performance of direct load control (DLC), a traditional form of energy management, with the performance of smart grid enabled energy management functions. The various energy management functions are compared in their ability to provide automated demand response (DR). Specifically, this dissertation documents simulations of five energy management functions, by testing various levels of residential energy management system (REMS) complexity. Providing a quantified indication of what technology (energy management functions) provide the most significant automated DR.

The Proposed Physically-Based REMS Simulation (PPRS) quantifies the performance of an individual residence using a variety of control options (DLC, smart thermostat, smart appliance scheduling, and smart appliance scheduling with a stationary battery). The PPRS was developed in Matlab/Simulink to quantify the electricity use of a typical residence. The PPRS is structured as a discrete event simulation. Five energy management functions are simulated for four power system areas of the United States.

Four power system areas of the United States are analyzed: Versailles Kentucky, Mercury Nevada, Stillwater Oklahoma, and Necedah Wisconsin. These four power system areas were selected to consist of different power system operation areas and different climate zones. Finally, it was shown that average PPRS appliance energy use results were similar to the residential appliance energy use data from three references.

This chapter described the PPRS. Next is a description of the PPRS results.

4 PROPOSED PHYSICALLY-BASED RESIDENTIAL-ENERGY-MANAGEMENT-SYSTEM SIMULATION RESULTS

This dissertation compares the performance of direct load control (DLC), a traditional form of energy management, with the performance of smart grid enabled energy management functions. The various energy management functions are compared in their ability to provide automated demand response (DR). Specifically, this dissertation documents simulations of five energy management functions, by testing various levels of residential energy management system (REMS) complexity. Further, the use of photovoltaic (PV) and plug-in electric vehicle (PEV) distributed energy resources are considered in conjunction with the residential energy management functions.

The Proposed Physically-Based REMS Simulations (PPRS) quantifies the performance of an individual residence using a variety of energy management functions (water heater [WH] DLC; heating, ventilation, and air conditioning [HVAC] DLC; smart thermostat [ST]; smart appliance scheduling [SAS]; and smart appliance scheduling with a stationary battery [SASB]). Four power system areas of the United States are analyzed: Versailles Kentucky, Mercury Nevada, Stillwater Oklahoma, and Necedah Wisconsin. These four power system areas were selected to consist of different power system operation areas and different climate zones. Different climate zones were selected to study the impact of ambient temperature on the automated DR ability of various energy management functions.

The following statistics will be computed for each PPRS energy management function: daily energy use, peak power, and DR energy. Notice, DR energy is the PPRS daily energy use during the DR period. For the results in this chapter, the DR period is from 4p to 7p. This assumption is relaxed in Chapters 5 and 6. Comparison of these statistics for each energy management function illustrates the benefits of the residential energy management functions to the residence owner.

Five energy management functions are included in the PPRS: WH DLC, HVAC DLC, ST, SAS, and SASB. All energy management functions start from a base case sequence of appliance use and the use of key appliances is modified for each energy management function. The probabilistic appliance use models require repeated simulation iterations to compute distributions of the quantified results.

First is a justification of the number of independent replications . The number of independent replications is selected using a sequential analytical procedure and a graphical. Both methods were outlined in [111].

Second is a presentation of the base case (BC) results. The BC consists of four distributed energy resource scenarios: A, B, C, and D. Each BC distributed energy resource scenario includes no energy management function. The BC Scenario A simulates the residence with each appliance (clothes dryer, clothes washer, dishwasher, HVAC, WH, and uncontrolled electric load). The BC Scenario B simulates all the appliances in Scenario A and adds a PEV. The BC Scenario C simulates all the appliances in Scenario A and adds a PV array. The BC Scenario D simulates all the appliances in Scenario A and adds both the PEV and the PV.

Third is a presentation of the WH DLC energy management function results. Fourth is a presentation of the HVAC DLC energy management functions. Fifth is a presentation of the ST energy management function results. Both forms of DLC and the

ST energy management functions include the four distributed energy resource scenarios. Where no DER is included in Scenario A, the additional load due to PEV is added in Scenario B, the PV generation is added in Scenario C, and the combination of PEV and PV is added in Scenario D.

Sixth is a presentation of, the SAS energy management function results. Unlike the results from the first three simulated energy management functions, the last two simulated energy management function investigate not only the impact of the energy management functions and distributed energy resources but also the impact of the use of individual smart appliances. There are seven smart appliances in the PPRS formulation. The SAS energy management function is tested with all combinations of the seven smart appliances with (smart) and without communication capabilities, resulting in 128 combinations. The 128 combinations range from no smart appliances to all seven smart appliances.

Seventh is a presentation of, the SASB energy management function results. Similar to the SAS energy management function, the SASB energy management function is tested with all combinations of the seven smart appliances.

Eight (and finally) is a summary of the PPRS results.

The WH DLC, HVAC DLC, and ST results in this chapter are summarized using box and whisker plots. The results illustrated in the box and whisker plot are defined in Figure 19.

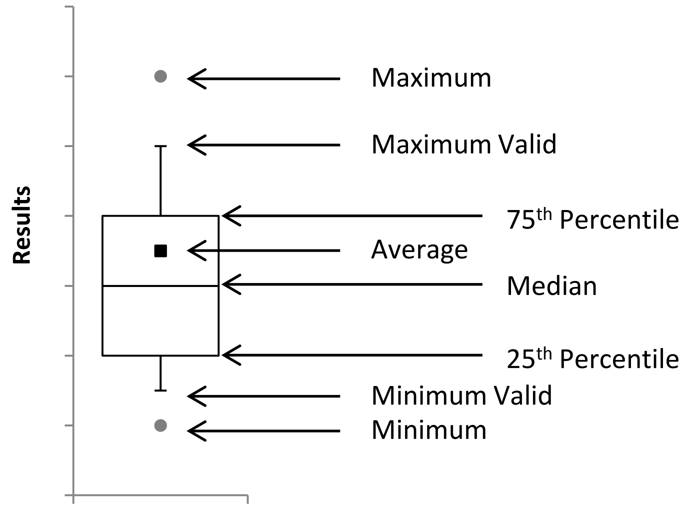

Figure 19: Box and whisker results definition [112].

Multiple box and whisker plots are used to describe the simulated distribution results for the WH DLC, HVAC DLC, and ST energy management functions based on the results defined in Figure 19. Simulation results include a finite number of values generated randomly from an underlying unknown distribution. The box and whisker plots provide graphic description of the sample population distributions. The descriptive statistics defined in Figure 19 include maximum φ_{max}, maximum valid ϑ_{max}, 75th percentile ρ_{75}, average, median, 25th percentile ρ_{25}, minimum valid ϑ_{min}, and minimum φ_{min}. The minimum and maximum are the minimum and maximum values observed in the set of repeated iterations. The average, median, 75th percentile, and 25th percentile are the computed based on the repeated iteration sample population for each energy management function. The minimum and maximum valid values are defined in Equation 2 and Equation 3.

$$\vartheta_{min} = max\{\varphi_{min}, \rho_{25} - 1.5 \cdot (\rho_{75} - \rho_{25})\} \quad (2)$$
$$\vartheta_{max} = min\{\varphi_{max}, \rho_{75} + 1.5 \cdot (\rho_{75} - \rho_{25})\} \quad (3)$$

The minimum (maximum) valid value defined in Equation 2 (Equation 3) can be interpreted as the maximum (minimum) value within 1.5 times the inter-quartile range below (above) the 25th percentile (75th percentile).

4.1 Repeated Iteration Justification

Probabilistic appliance use models were defined in Chapter 3. Their repeated use in the Proposed Physically-Based Residential-Energy-Management-System Simulation (PPRS) results in unknown distributions for the key results: daily energy use, peak power, and demand response energy. The number of independent replications is selected using a sequential analytical procedure and a graphical consideration.

The number of independent replications is picked based on a sequential procedure defined in [111]. Which is an adaptation of the below algorithm, that was initially intended to remove the initial transient phase of a simulation.

0. Make n_0 replications of the simulation and set $n = n_0$.

1. Compute $\bar{X}(n)$ and $\delta(n, \varsigma)$ from $X_1, X_2, \dots X_n$.

2. If $\delta(n, \varsigma)/\bar{X}(n) \leq \upsilon'$, use $\bar{X}(n)$ as the point estimate for the true (but unknown population mean) and stop. Otherwise, replace n by $n + 1$, make an additional replication of the simulation, and go to step 1.

Notice, $\delta(n, \varsigma) = t_{n-1,1-\varsigma/2} \cdot \sqrt{S_n^2/n}$, the initial number of replications used is 10 ($n_0 = 10$), the confidence level is 99% ($\varsigma = 0.99$), the relative error 1% ($\upsilon = 0.01, \upsilon' = \upsilon/(1 + \upsilon)$), and the resulting n is 507.

As a second method to select the number of independent replications is picked based on a graphical procedure defined in [111]. The residence daily energy use sample average (Ave - left hand side y-axis) and sample variance (Var - right hand side y-axis) in three independent experiments for 10 to 1000 iterations is shown in Figure 20.

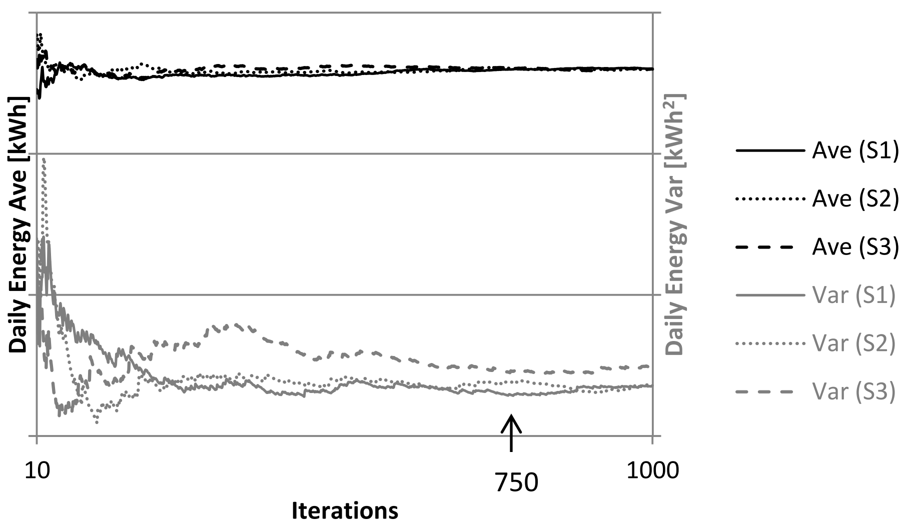

Figure 20: Simulated residence demand sample average [Ave] and variance [Var].

Notice, the iterations include varying amounts of appliance use representing common appliance use patterns. The magnitude of the sample average and sample variance is not of concern. Rather, the fact that the sample average and sample variance are not changing significantly as more iterations are performed suggests that the sample population is characterized by the collected data. The sample average and sample variance in Figure 20 settles to a final value after 750 independent replications in all three experiments. This is the number of independent replications used in the remainder of this dissertation. The three seed values were arbitrarily selected S1 was 1, S2 was 1,234, and S3 was 123,456,789.

Next is a presentation of the PPRS base case results.

4.2 Base Case

The Proposed Physically-Based Residential-Energy-Management-System Simulation (PPRS) base case (BC) consists of a residence with no added controls. This simulation represents a typical residence from which the other energy management function simulations can be compared. The PPRS BC consists of four separate distributed energy resource scenarios. The PPRS BC Scenario A simulates the residence with each appliance (clothes dryer; clothes washer; dishwasher; heating, ventilation, and air conditioning; water heater [WH]; and uncontrolled electric load). The PPRS BC Scenario B simulates all the appliances in Scenario A and adds the plug-in electric vehicle (PEV). This distributed energy resource scenario represents a near term future of a household that charges a PEV daily in the evening after the vehicle arrives home. The PPRS BC Scenario C simulates all the appliances in Scenario A and adds the photovoltaic (PV) array. The PPRS BC Scenario D simulates all the appliances in Scenario A and adds both the PEV and the PV.

Statistics of the PPRS BC Scenario A, Scenario B, Scenario C, and Scenario D daily energy are shown in Figure 21, Figure 22, Figure 23, and Figure 24, respectively. The PPRS BC daily energy is shown for each power system area and for the two extreme weather seasons: winter (Win) and summer (Sum). These days were selected to highlight the performance of the PPRS BC in the coldest (Win) and hottest (Sum) ambient temperatures. The extreme temperatures and days used for each power system area (Versailles Kentucky [ECAK], Mercury Nevada [SNV], Stillwater Oklahoma [SPPS], and Necedah Wisconsin [WUMS]) and season are shown in Table 16.

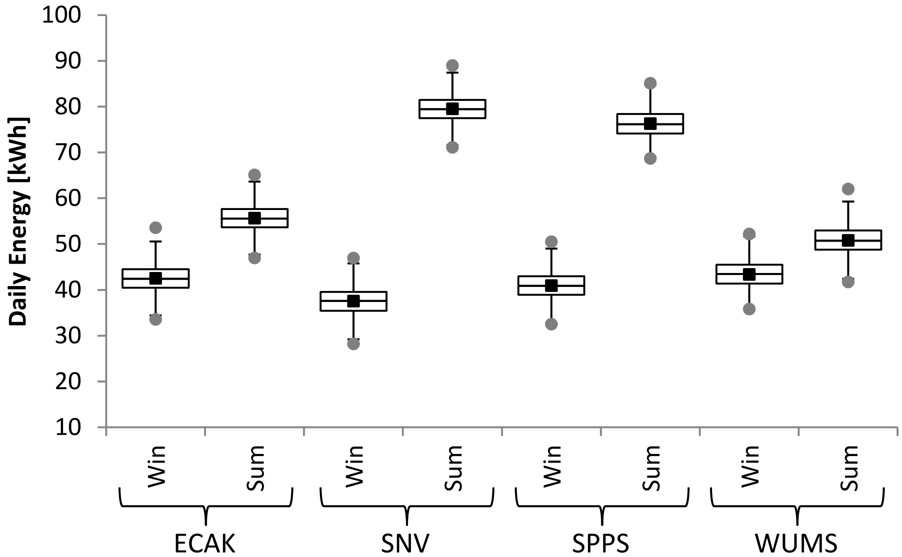

Figure 21: The Proposed Physically-Based Residential-Energy-Management-System Simulation [PPRS] base case [BC] Scenario A daily energy.

The PPRS BC Scenario A daily energy in Figure 21 represents the daily energy use on the coldest and warmest days for each power system area. These days are strong candidates for the application of an energy management function. Further, the seasonal variation for each location is apparent from Figure 21. Most notably, SNV and SPPS have significantly increased summer daily energy use than winter daily energy use; whereas, ECAK and WUMS have only slightly higher summer daily energy use than winter daily energy use. The PPRS BC models a typical residence with no energy management. The PPRS BC is a baseline from which the other energy management function simulations can be compared.

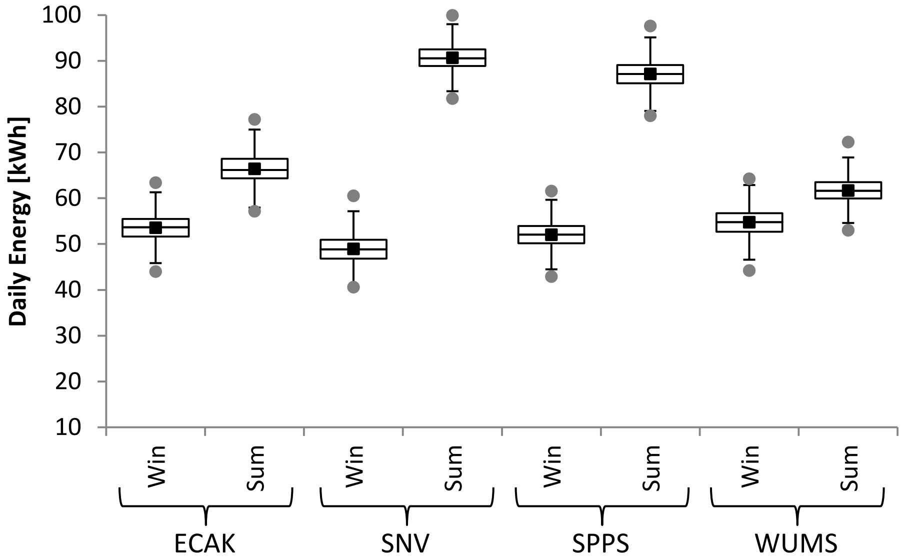

Figure 22: The Proposed Physically-Based Residential-Energy-Management-System Simulation [PPRS] base case [BC] Scenario B daily energy.

The PPRS BC Scenario B daily energy in Figure 22 represents a residence where a PEV is recharged on a daily basis. Notice, the increase in average (across all power system areas) winter PPRS BC Scenario B daily energy use is 27.4% (11.2 kWh) and increase in average summer PPRS BC Scenario B daily energy use is 17.3% (10.9 kWh) compared to the average winter and summer PPRS BC Scenario A daily energy, respectively.

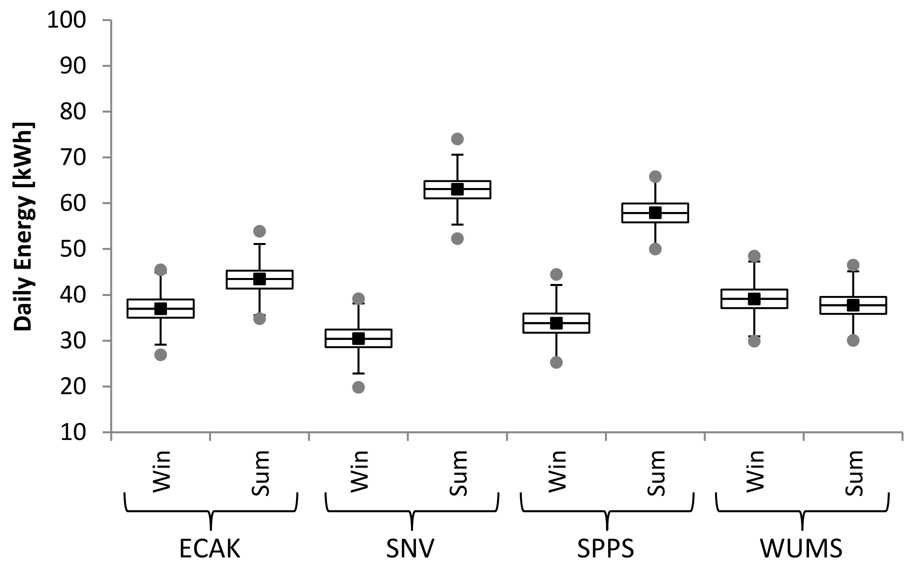

Figure 23: The Proposed Physically-Based Residential-Energy-Management-System Simulation [PPRS] base case [BC] Scenario C daily energy.

The PPRS BC Scenario C daily energy in Figure 23 represents a residence with a 20 m^2 PV array with 10% efficiency. Notice, the decrease in average winter PPRS BC Scenario C daily energy is 14.8% (6.0 kWh) and decrease in summer PPRS BC Scenario C daily energy use is 23.1% (15.0 kWh) compared to the average winter and summer PPRS BC Scenario A daily energy, respectively.

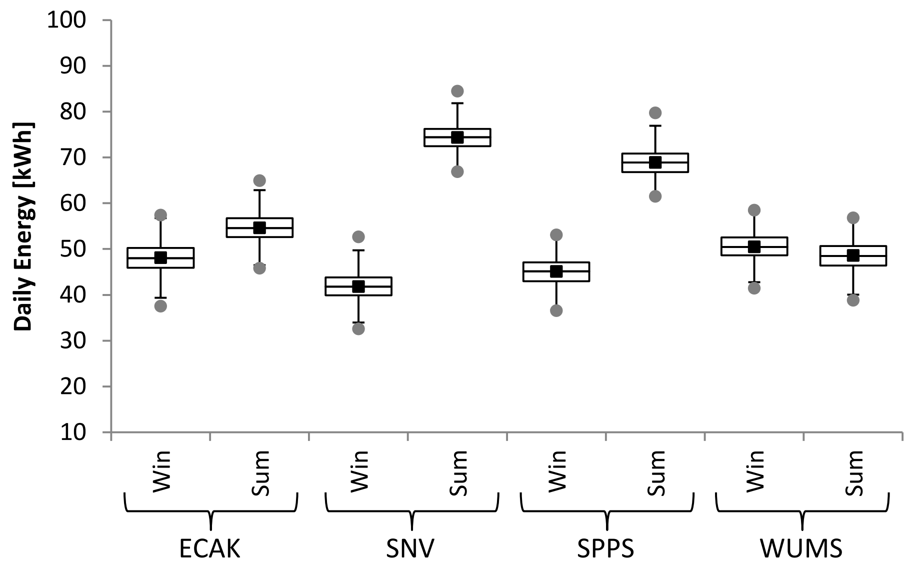

Figure 24: The Proposed Physically-Based Residential-Energy-Management-System Simulation [PPRS] base case [BC] Scenario D daily energy.

The PPRS BC Scenario D daily energy in Figure 24 represents a residence with PEV and PV array. Notice, the increase in average winter PPRS BC Scenario D daily energy is 12.8% (5.3 kWh) and the decrease in average summer PPRS BC Scenario D daily energy use is 5.6% (decrease 3.9 kWh) compared to the average winter and summer PPRS BC Scenario A daily energy, respectively.

Table 16: The seasonal temperature and simulated days for each power system area.

Season	ECAK [°C (Day)]	SNV [°C (Day)]	SPPS [°C (Day)]	WUMS [°C (Day)]
Summer	34.8 (215)	41.2 (198)	40.3 (224)	32.6 (223)
Winter	-16.0 (348)	-5.5 (330)	-16.4 (8)	-26.8 (348)

The temperatures and simulated days in Table 16 are average daily temperature on the simulated day for each location and season used in the Chapter 4. The summer temperature is the maximum daily average temperature for each power system area. Similarly, the winter temperature is the minimum daily average temperature for each power system area. Each day corresponds to the annual day which the extreme average temperature was experienced.

Statistics of the PPRS BC Scenario A, Scenario B, Scenario C, and Scenario D peak power are shown in Figure 25, Figure 26, Figure 27, and Figure 28, respectively. The PPRS BC peak power is shown for each power system area and for the two unique seasons with extreme temperatures where energy management utilization would be expected: winter and summer. The extreme temperatures and days used for each power system area and season are shown in Table 16.

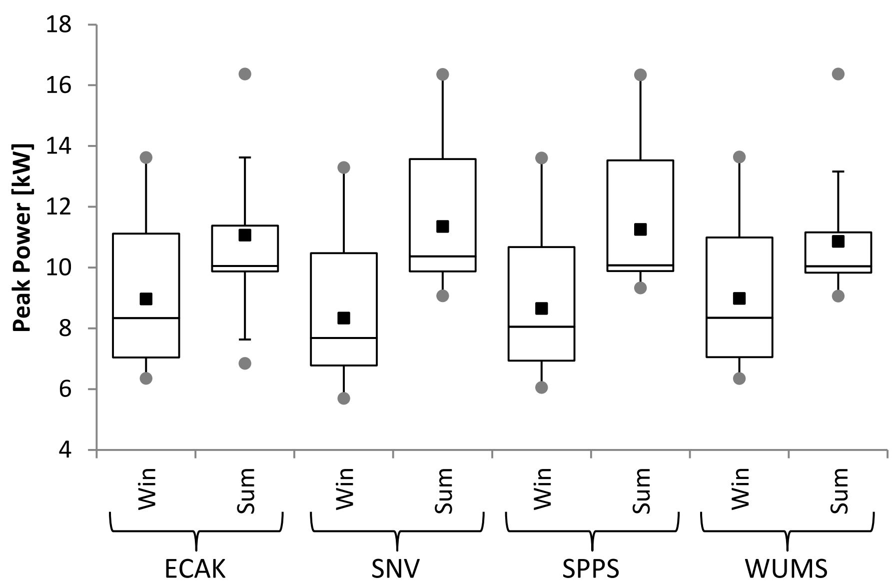

Figure 25: The Proposed Physically-Based Residential-Energy-Management-System Simulation [PPRS] base case [BC] Scenario A peak power.

The PPRS BC Scenario A peak power in Figure 25 indicates that the highest peak demand occurs in the summer for all the power system areas, as expected.

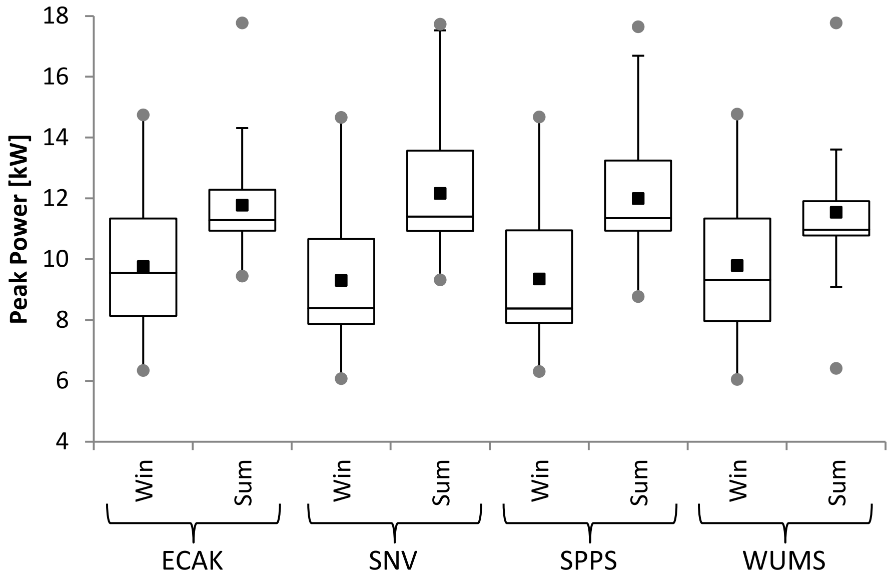

Figure 26: The Proposed Physically-Based Residential-Energy-Management-System Simulation [PPRS] base case [BC] Scenario B peak power.

The PPRS BC Scenario B peak power in Figure 26 indicate an increase in average winter PPRS BC Scenario B peak power of 9.4% (0.8 kW) and an increase in average summer PPRS BC Scenario B peak power of 6.6% (0.7 kW) compared to the average winter and summer PPRS BC Scenario B peak power, respectively.

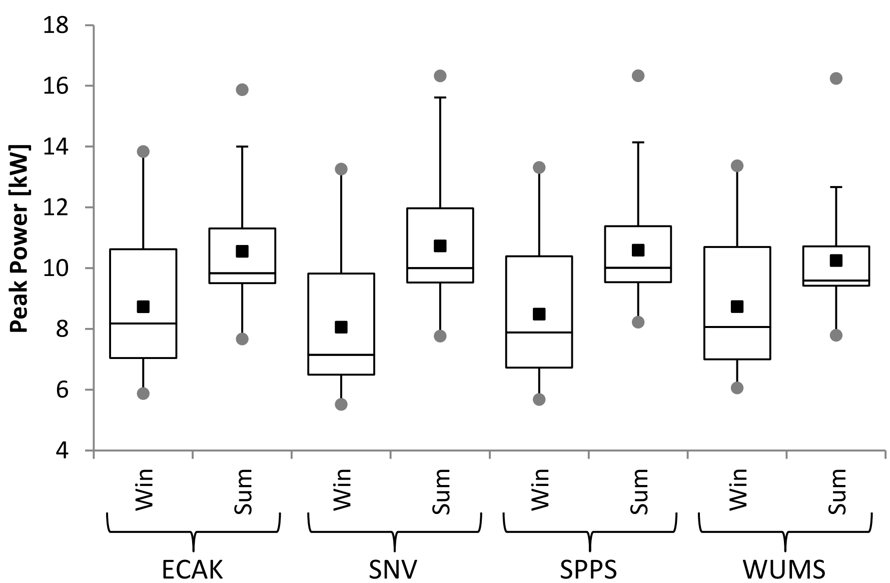

Figure 27: The Proposed Physically-Based Residential-Energy-Management-System Simulation [PPRS] base case [BC] Scenario C peak power.

The PPRS BC Scenario C peak power in Figure 27 indicate a decrease in average winter PPRS BC Scenario C peak power of 2.6% (0.2 kW) and a decrease in average summer PPRS BC Scenario C peak power of 5.4% (0.6 kW) compared to the average winter and summer PPRS BC Scenario A peak power, respectively.

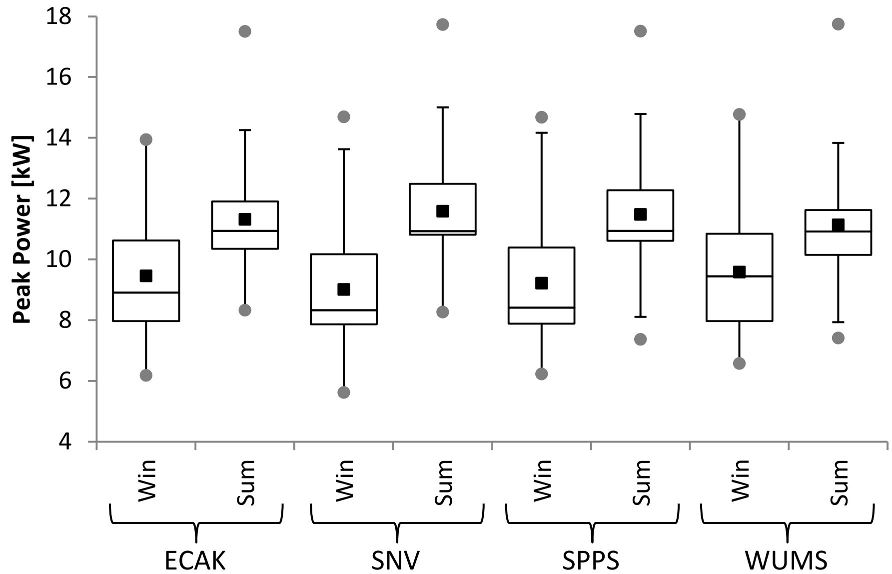

Figure 28: The Proposed Physically-Based Residential-Energy-Management-System Simulation [PPRS] base case [BC] Scenario D peak power.

The PPRS BC Scenario D peak power in Figure 28 indicate an increase in average winter PPRS BC Scenario D peak power of 6.7% (0.6 kW) and an increase in average summer PPRS BC Scenario D peak power increase of 2.2% (0.2 kW) compared to the average winter and summer PPRS BC Scenario A peak power, respectively.

Statistics of the PPRS BC Scenario A, Scenario B, Scenario C, and Scenario D demand response (DR) energy are shown in Figure 29, Figure 30, Figure 31, and Figure 32, respectively. The PPRS WH DLC peak power is shown for each power system area and for the two unique seasons with extreme temperatures where energy management utilization would be expected: winter and summer. The extreme temperatures and days used for each power system area and season are shown in Table 16.

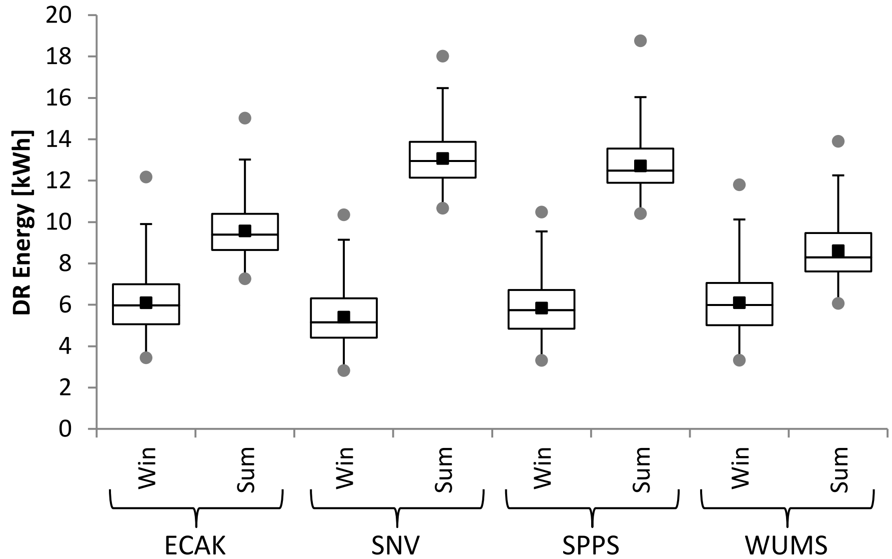

Figure 29: The Proposed Physically-Based Residential-Energy-Management-System Simulation [PPRS] base case [BC] Scenario A demand response [DR] energy.

The PPRS BC Scenario A DR energy in Figure 29 indicate that the average winter PPRS BC Scenario A DR energy represents 14.3% (5.9 kWh) and the average summer PPRS BC Scenario A DR energy represents 16.8% (11.0 kWh) of the average winter and summer PPRS BC Scenario A daily energy (4p to 7p is 12.5% of the day), respectively.

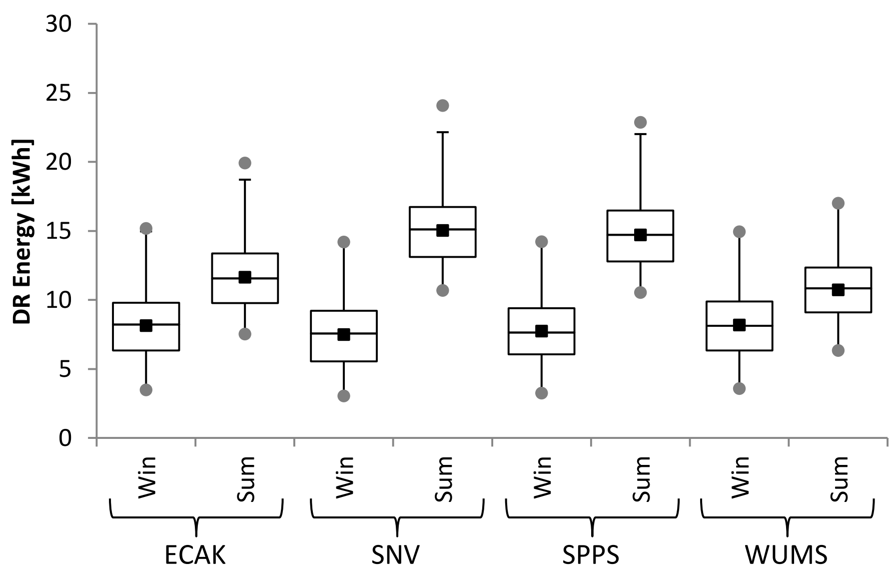

Figure 30: The Proposed Physically-Based Residential-Energy-Management-System Simulation [PPRS] base case [BC] Scenario B demand response [DR] energy.

The PPRS BC Scenario B DR energy in Figure 30 indicate that the average winter PPRS BC Scenario B DR energy represents 15.1% (7.9 kWh) and the average summer PPRS BC Scenario B DR energy represents 17.0% (13.0 kWh) of the average winter and summer PPRS BC Scenario B daily energy, respectively. Further, the PPRS BC Scenario B DR energy in Figure 30 indicate an increase in average winter BC Scenario B DR energy of 34.8% (2.0 kWh) and an increase in average summer BC Scenario B DR energy of 19.3% (2.0 kWh) compared to the average winter and summer PPRS BC Scenario A DR energy, respectively.

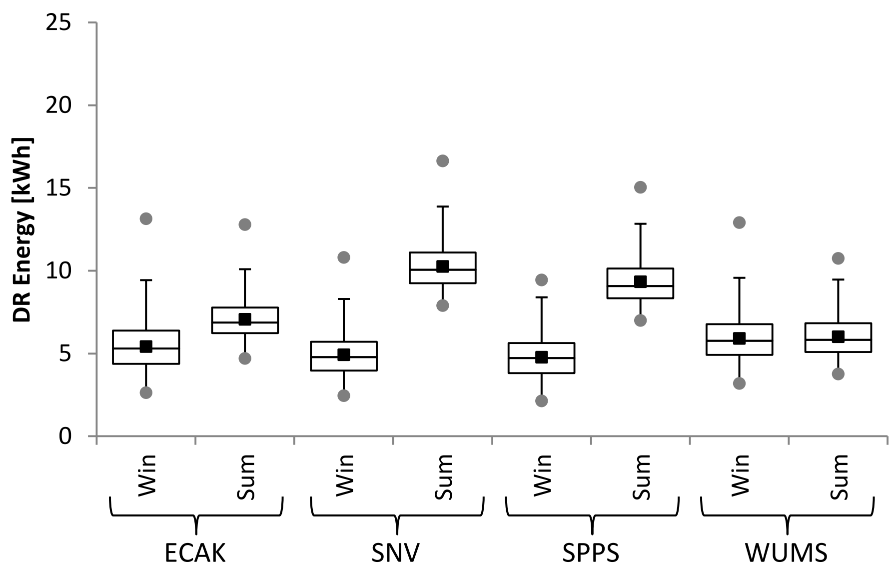

Figure 31: The Proposed Physically-Based Residential-Energy-Management-System Simulation [PPRS] base case [BC] Scenario C demand response [DR] energy.

The PPRS BC Scenario C DR energy in Figure 31 indicate that the PPRS BC Scenario C average winter PPRS BC Scenario C DR energy represents 15.1% (5.3 kWh) and the average summer PPRS BC Scenario C DR energy represents 16.2% (8.2 kWh) of the average winter and summer PPRS BC Scenario C daily energy, respectively. Further, the PPRS BC Scenario C DR energy in Figure 31 indicate a decrease in average winter PPRS BC Scenario C DR energy of 10.4% (0.6 kWh) and a decrease in average summer

PPRS BC Scenario C DR energy of 26.1% (2.8 kWh) compared to the average winter and summer PPRS BC Scenario A DR energy, respectively.

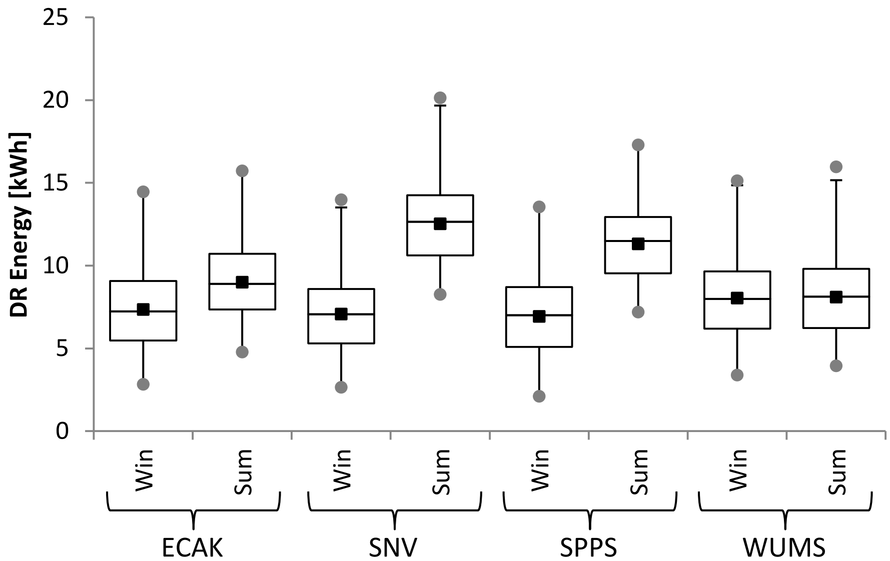

Figure 32: The Proposed Physically-Based Residential-Energy-Management-System Simulation [PPRS] base case [BC] Scenario D demand response [DR] energy.

The PPRS BC Scenario D DR energy in Figure 32 indicate that the average winter PPRS BC Scenario D DR energy represents 15.8% (7.3 kWh) and the average summer PPRS BC Scenario D DR energy represents 16.6% (10.2 kWh) of the average winter and summer PPRS BC Scenario D daily energy (4p to 7p is 12.5% of the day), respectively. Further, the PPRS BC Scenario D DR energy in Figure 32 indicate an increase in average winter PPRS BC Scenario D DR energy of 25.4% (1.5 kWh) and a decrease in average summer PPRS BC Scenario D DR energy of 6.8% (0.8 kWh) compared to the average winter and summer PPRS BC Scenario D DR energy, respectively.

Next is a presentation of the PPRS WH direct load control results.

4.3 Water Heater Direct Load Control

The Proposed Physically-Based Residential-Energy-Management-System Simulation (PPRS) direct load control (DLC) is provided in two forms: water heater (WH) and heating, ventilation, and air conditioning (HVAC). In both of these forms, the controlled appliance (WH and HVAC) is controlled for an electric utility specified time period (demand response [DR] period from 4p to 7p) with limited service during this time to the specific directly controlled appliance only. The WH DLC removes service to the WH for the entire DR period (with all WH energy use rescheduled after the DR period, i.e. 100% payback efficiency).

Statistics of the PPRS WH DLC Scenario A, Scenario B, Scenario C, and Scenario D daily energy are shown in Figure 33, Figure 34, Figure 35, and Figure 36, respectively. The PPRS WH DLC daily energy is shown for each power system area (Versailles Kentucky [ECAK], Mercury Nevada [SNV], Stillwater Oklahoma [SPPS], and Necedah Wisconsin [WUMS]) and for the two unique seasons with extreme temperatures where energy management utilization would be expected: winter (Win) and summer (Sum). The extreme temperatures and days used for each power system area and season are shown in Table 16.

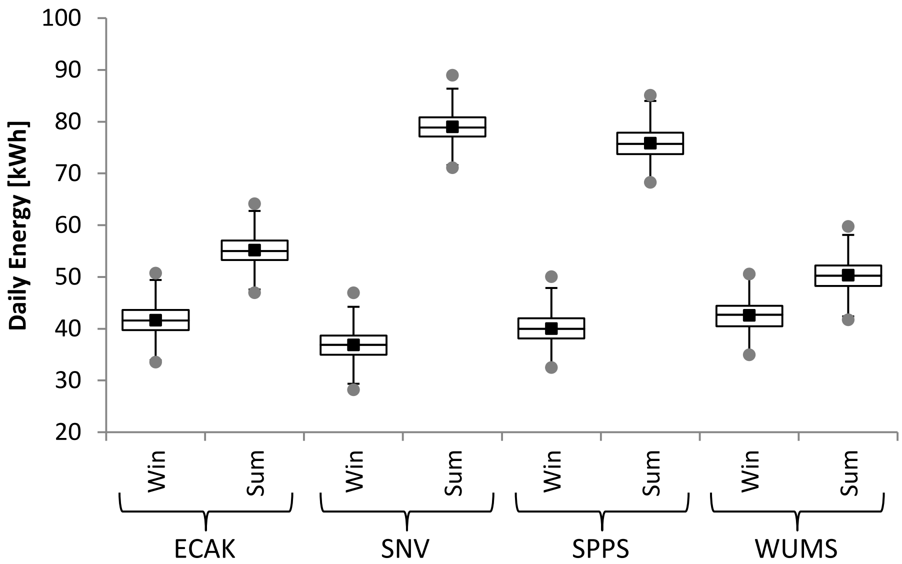

Figure 33: The Proposed Physically-Based Residential-Energy-Management-System Simulation [PPRS] water heater [WH] direct load control [DLC] Scenario A daily energy.

The PPRS WH DLC Scenario A daily energy use in Figure 33 represents the daily energy use on the coldest and warmest day for each power system area, where the use of the WH is eliminated from 4p to 7p. These days are strong candidates for the application of an energy management function. Notice, the decrease in average winter PPRS WH DLC Scenario A daily energy is 1.9% (0.8 kWh) and the decrease in average summer PPRS WH DLC Scenario A daily energy is 0.7% (0.5 kWh) compared to the average winter and summer PPRS base case (BC) Scenario A daily energy, respectively.

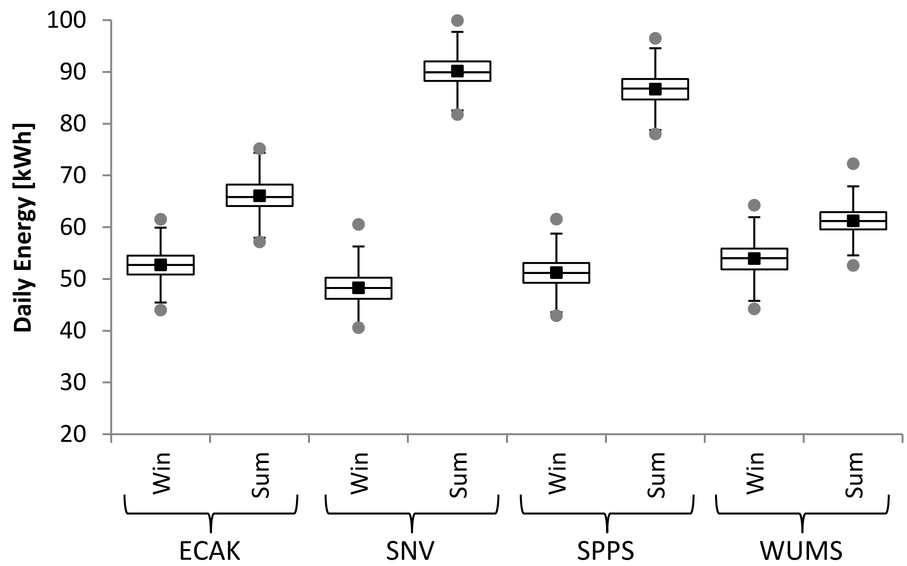

Figure 34: The Proposed Physically-Based Residential-Energy-Management-System Simulation [PPRS] water heater [WH] direct load control [DLC] Scenario B daily energy.

The PPRS WH DLC Scenario B daily energy in Figure 34 represents a residence with WH DLC and where a plug-in electric vehicle (PEV) is recharged on a daily basis. Notice, the decrease in average winter PPRS WH DLC Scenario B daily energy is 1.5% (0.8 kWh) and the decrease in average summer PPRS WH DLC Scenario B daily energy is 0.6% (0.4 kWh) compared to the average winter and summer PPRS BC Scenario B daily energy, respectively.

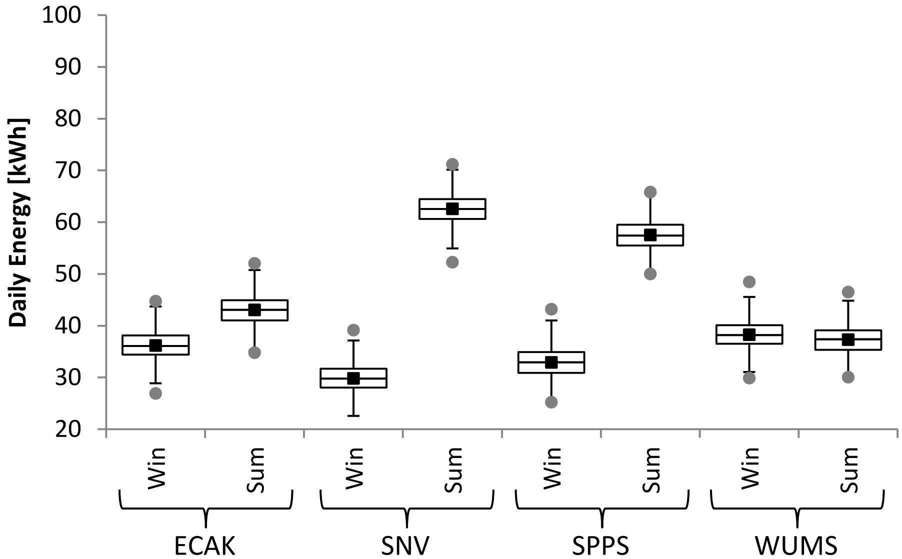

Figure 35: The Proposed Physically-Based Residential-Energy-Management-System Simulation [PPRS] water heater [WH] direct load control [DLC] Scenario C daily energy.

The PPRS WH DLC Scenario C daily energy in Figure 35 represents a residence with WH DLC and a photovoltaic (PV) array. Notice, the decrease in average winter PPRS WH DLC Scenario C daily energy is 2.2% (0.8 kWh) and the decrease in average summer PPRS WH DLC Scenario C daily energy is 0.9% (0.4 kWh) compared to the average winter and summer PPRS BC Scenario C daily energy, respectively.

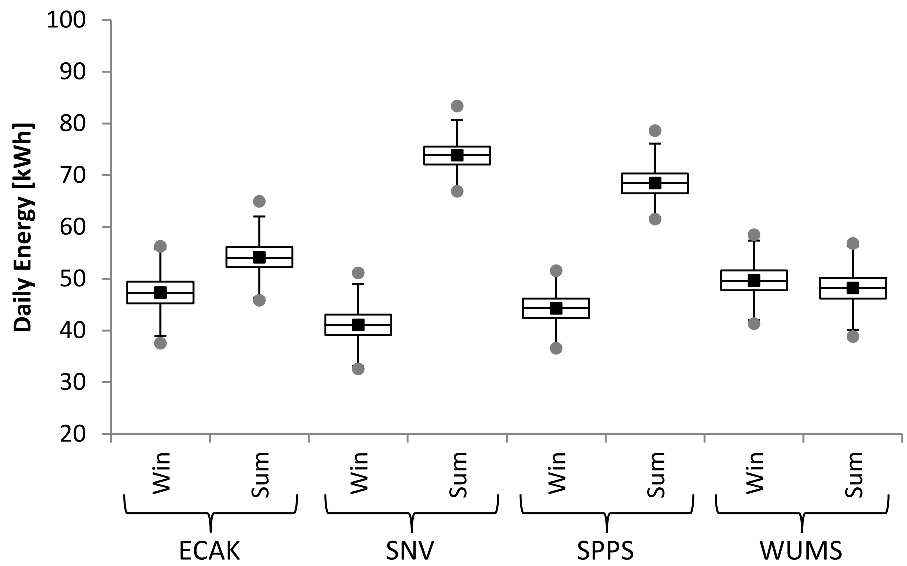

Figure 36: The Proposed Physically-Based Residential-Energy-Management-System Simulation [PPRS] water heater [WH] direct load control [DLC] Scenario D daily energy.

The PPRS WH DLC Scenario D daily energy in Figure 36 represents a residence with WH DLC, PEV, and PV array. Notice, the decrease in average winter PPRS WH DLC Scenario D daily energy is 1.7% (0.8 kWh) and the decrease in average summer PPRS WH DLC Scenario D daily energy is 0.8% (0.5 kWh) compared to the average winter and summer PPRS BC Scenario D daily energy, respectively.

Statistics of the PPRS WH DLC Scenario A, Scenario B, Scenario C, and Scenario D peak power are shown in Figure 37, Figure 38, Figure 39, and Figure 40, respectively. The PPRS WH DLC peak power is shown for each power system area and for the two unique seasons with extreme temperatures where energy management utilization would be expected: winter and summer. The extreme temperatures and days used for each power system area and season are shown in Table 16.

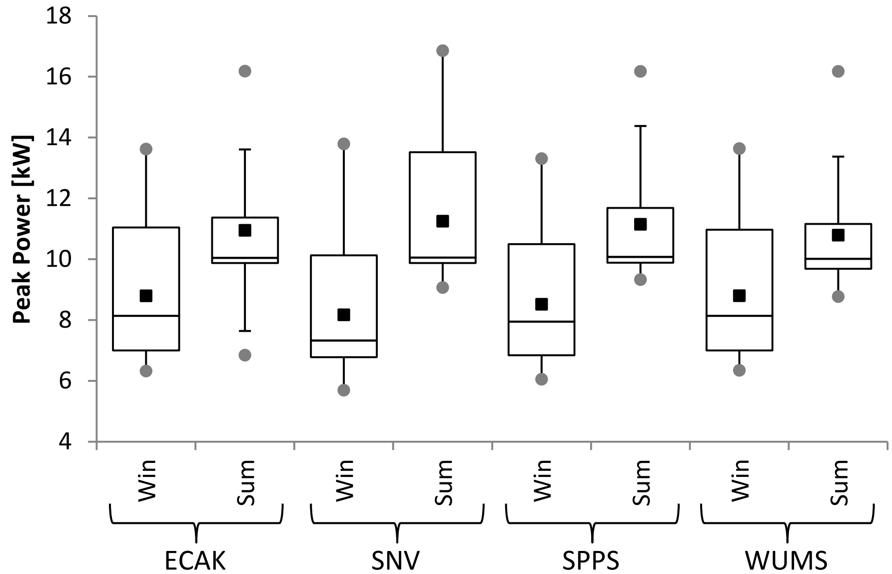

Figure 37: The Proposed Physically-Based Residential-Energy-Management-System Simulation [PPRS] water heater [WH] direct load control [DLC] Scenario A peak power.

The PPRS WH DLC Scenario A peak power in Figure 37 indicate a decrease in average winter PPRS WH DLC Scenario A peak power of 1.9% (0.2 kW) and a decrease in average summer PPRS WH DLC Scenario A peak power of 0.9% (0.1 kW) compared to the average winter and summer PPRS BC Scenario A peak power, respectively.

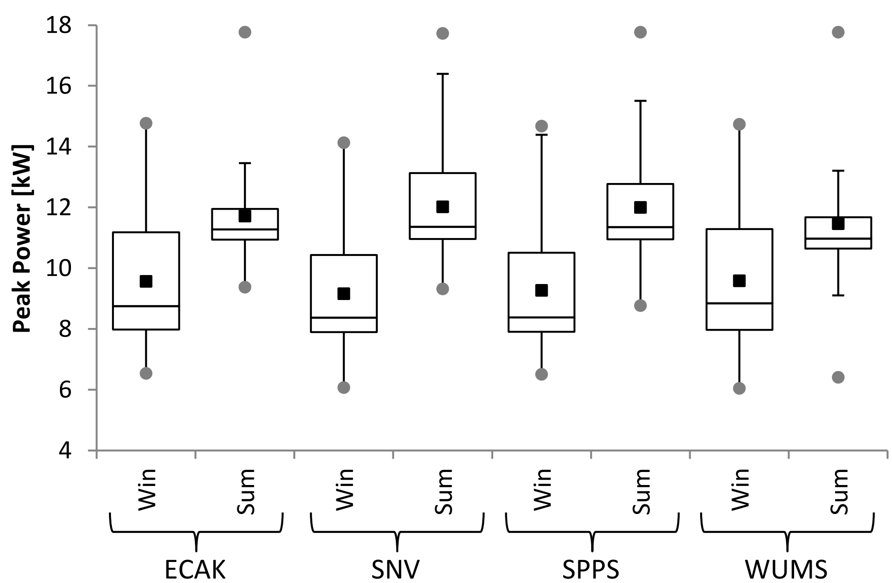

Figure 38: The Proposed Physically-Based Residential-Energy-Management-System Simulation [PPRS] water heater [WH] direct load control [DLC] Scenario B peak power.

The PPRS WH DLC Scenario B peak power in Figure 38 indicate a decrease in average winter PPRS WH DLC Scenario B peak power of 1.6% (0.2 kW) and a decrease in average summer PPRS WH DLC Scenario B peak power of 0.6% (0.1 kW) compared to the average winter and summer PPRS BC Scenario B peak power, respectively.

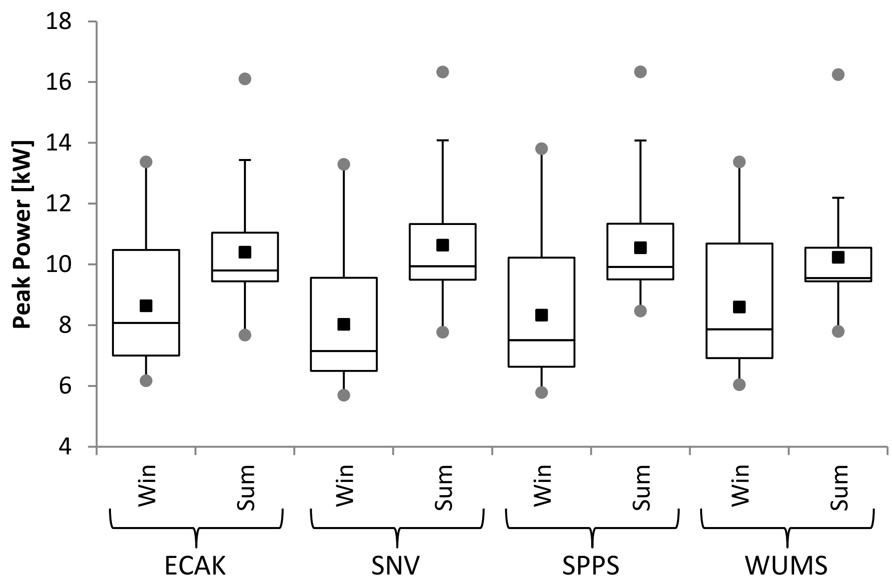

Figure 39: The Proposed Physically-Based Residential-Energy-Management-System Simulation [PPRS] water heater [WH] direct load control [DLC] Scenario C peak power.

The PPRS WH DLC Scenario C peak power in Figure 39 indicate a decrease in average winter PPRS WH DLC Scenario C peak power decrease of 1.3% (0.1 kW) and a decrease in average summer PPRS WH DLC Scenario C peak power of 0.8% (0.1 kW) compared to the average winter and summer PPRS BC Scenario C peak power, respectively.

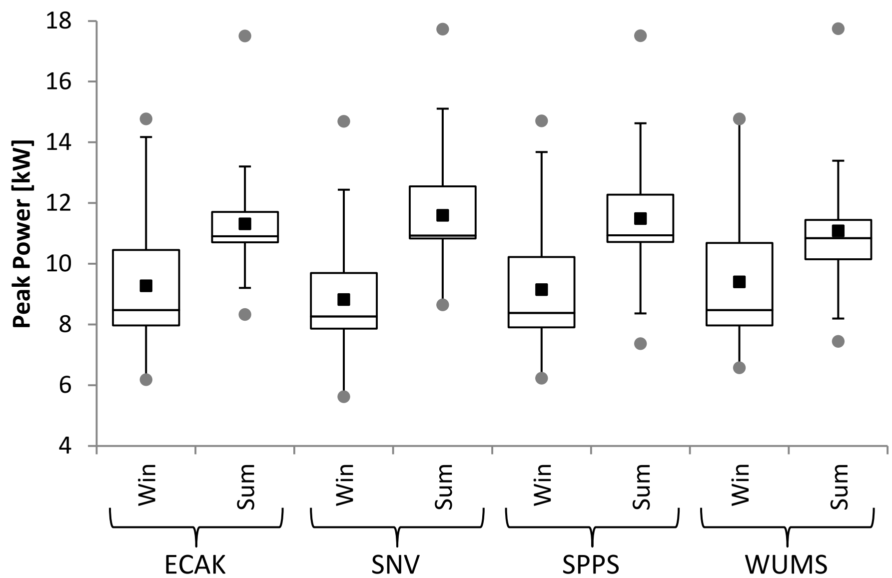

Figure 40: The Proposed Physically-Based Residential-Energy-Management-System Simulation [PPRS] water heater [WH] direct load control [DLC] Scenario D peak power.

The PPRS WH DLC Scenario D peak power in Figure 40 indicate a decrease in average winter PPRS WH DLC Scenario D peak power of 1.7% (0.2 kW) and a decrease in average summer PPRS WH DLC Scenario D peak power of 0.1% (less than 0.1 kW) compared to the average winter and summer PPRS BC Scenario D peak power, respectively.

Statistics of the PPRS WH DLC Scenario A, Scenario B, Scenario C, and Scenario D DR energy are shown in Figure 41, Figure 42, Figure 43, and Figure 44, respectively. The PPRS WH DLC DR energy is shown for each power system area and for the two unique seasons with extreme temperatures where energy management utilization would be expected: winter and summer. The extreme temperatures and days used for each power system area and season are shown in Table 16.

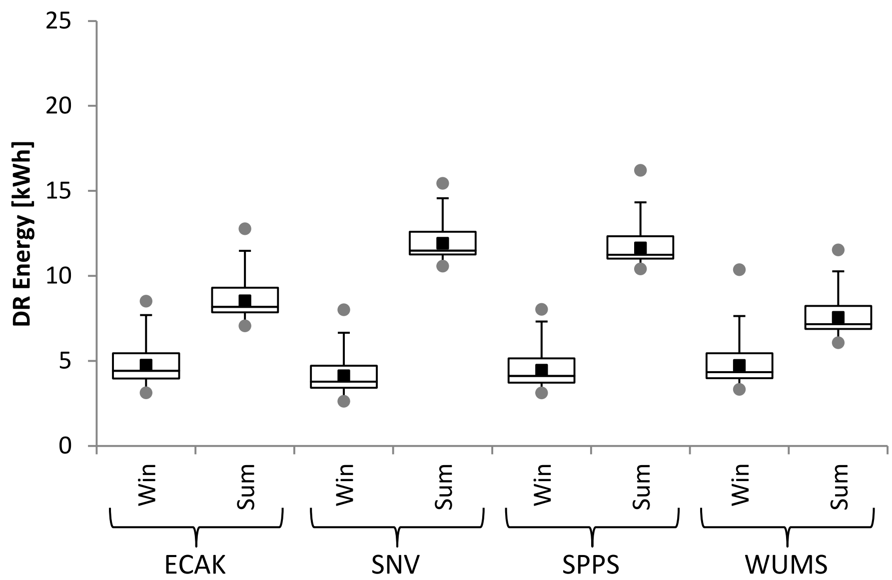

Figure 41: The Proposed Physically-Based Residential-Energy-Management-System Simulation [PPRS] water heater [WH] direct load control [DLC] Scenario A demand response [DR] energy.

The PPRS WH DLC Scenario A DR energy in Figure 41 indicate that the average winter PPRS WH DLC Scenario A DR energy represents 11.2% (4.5 kWh) and the average summer PPRS WH DLC Scenario A DR energy represents 15.2% (9.9 kWh) of the average winter and summer PPRS WH DLC Scenario A daily energy, respectively. Further, the PPRS WH DLC Scenario A DR energy in Figure 41 indicate a decrease in average winter PPRS WH DLC Scenario A DR energy of 23.0% (1.3 kWh) and a decrease in average summer PPRS WH DLC Scenario A DR energy of 10.1% (1.1 kWh) compared to the average winter and summer PPRS BC Scenario A DR energy, respectively.

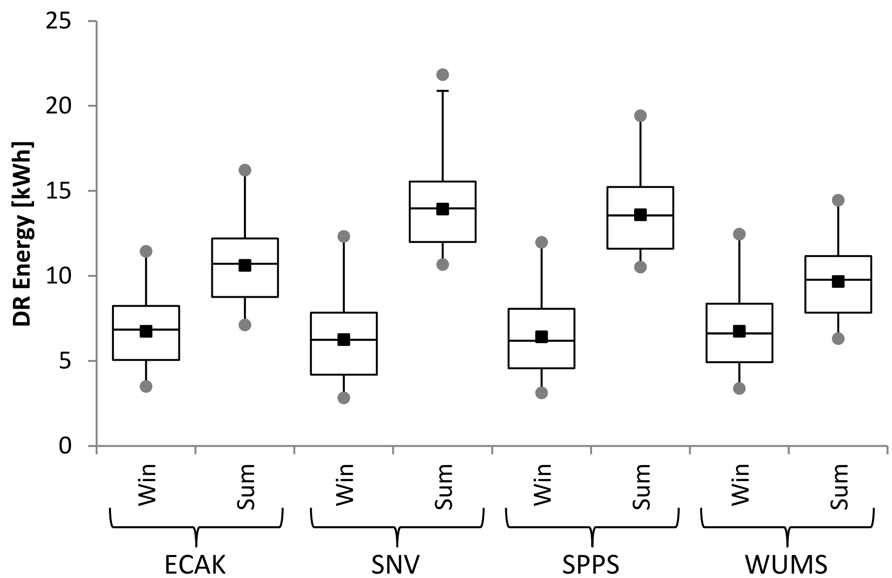

Figure 42: The Proposed Physically-Based Residential-Energy-Management-System Simulation [PPRS] water heater [WH] direct load control [DLC] Scenario B demand response [DR] energy.

The PPRS WH DLC Scenario B DR energy in Figure 42 indicate that the average winter PPRS WH DLC Scenario B DR energy represents 12.7% (6.5 kWh) and the average summer PPRS WH DLC Scenario B DR energy represents 15.7% (12.0 kWh) of the average winter and summer PPRS Scenario B daily energy, respectively. Further, the PPRS WH DLC Scenario B DR energy in Figure 42 indicate a decrease in average winter PPRS WH DLC Scenario B DR energy of 17.2% (1.4 kWh) and a decrease in average summer PPRS WH DLC Scenario B DR energy of 8.5% (1.1 kWh) compared to the average winter and summer PPRS BC Scenario B DR energy, respectively.

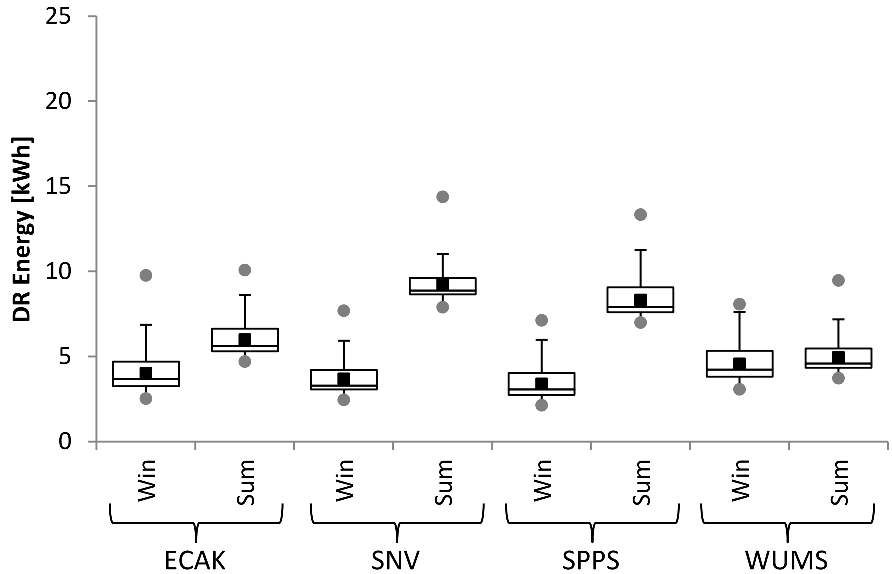

Figure 43: The Proposed Physically-Based Residential-Energy-Management-System Simulation [PPRS] water heater [WH] direct load control [DLC] Scenario C demand response [DR] energy.

The PPRS WH DLC Scenario C DR energy in Figure 43 indicate that the PPRS WH DLC Scenario C average winter DR energy represents 11.4% (3.9 kWh) and the average summer DR energy represents 14.2% (7.1 kWh) of the average winter and summer PPRS WH DLC Scenario C daily energy (4p to 7p is 12.5% of the day), respectively. Further, the PPRS WH DLC Scenario C DR energy in Figure 43 indicate an average winter decrease of 25.7% (1.3 kWh) and an average summer decrease of 13.5% (1.0 kWh) compared to the average winter and summer PPRS BC Scenario C DR energy, respectively.

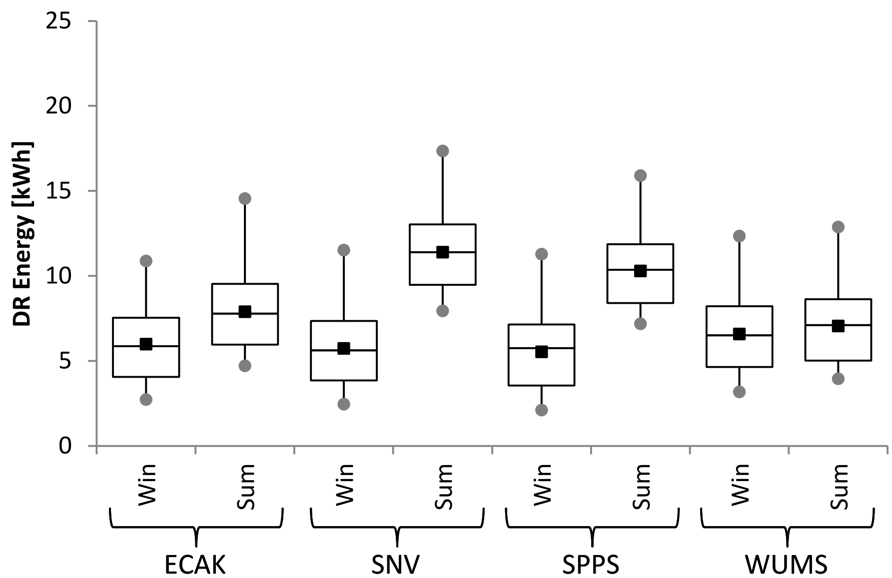

Figure 44: The Proposed Physically-Based Residential-Energy-Management-System Simulation [PPRS] water heater [WH] direct load control [DLC] Scenario D demand response [DR] energy.

The PPRS WH DLC Scenario D DR energy in Figure 44 indicate that the average winter PPRS WH DLC Scenario D DR energy represents 13.1% (6.0 kWh) and the average summer PPRS WH DLC Scenario D DR energy represents 15.0% (9.2 kWh) of the average winter and summer PPRS WH DLC Scenario D daily energy, respectively. Further, the PPRS WH DLC Scenario D DR energy in Figure 44 indicate a decrease in average winter DR energy of 19.0% (1.4 kWh) and a decrease in average summer DR energy of 10.8% (1.1 kWh) compared to the average winter and summer PPRS BC Scenario D DR energy, respectively.

Next is a presentation of the PPRS HVAC DLC results

4.4 Heating, ventilation, and Air Conditioning Direct Load Control

The Proposed Physically-Based Residential-Energy-Management-System Simulation (PPRS) direct load control (DLC) is provided in two forms: water heater (WH) and heating, ventilation, and air conditioning (HVAC). In both of these forms, the controlled appliance (WH or HVAC) is controlled for an electric utility specified time period (demand response [DR] period from 4p to 7p) with limited service during this time to the specific directly controlled appliance only. In the HVAC DLC energy management function the HVAC utilization is rescheduled during the DR period. The HVAC is rescheduled so that within every half hour during the DR period the HVAC is not allowed to run for n_{off} minutes (e.g. 15 minutes). Within the half hour of the specific n_{off} minutes are selected randomly to minimize the impact of payback. This type of grouping scheme is common with DLC [30], [39], and [58].

Statistics of the PPRS HVAC DLC Scenario A, Scenario B, Scenario C, and Scenario D daily energy are shown in Figure 45, Figure 46, Figure 47, and Figure 48, respectively. The PPRS HVAC DLC daily energy is shown for each power system area (Versailles Kentucky [ECAK], Mercury Nevada [SNV], Stillwater Oklahoma [SPPS], and Necedah Wisconsin [WUMS]) and for the two unique seasons with extreme temperatures where energy management utilization would be expected: winter (Win) and summer (Sum). The extreme temperatures and days used for each power system area and season are shown in Table 16.

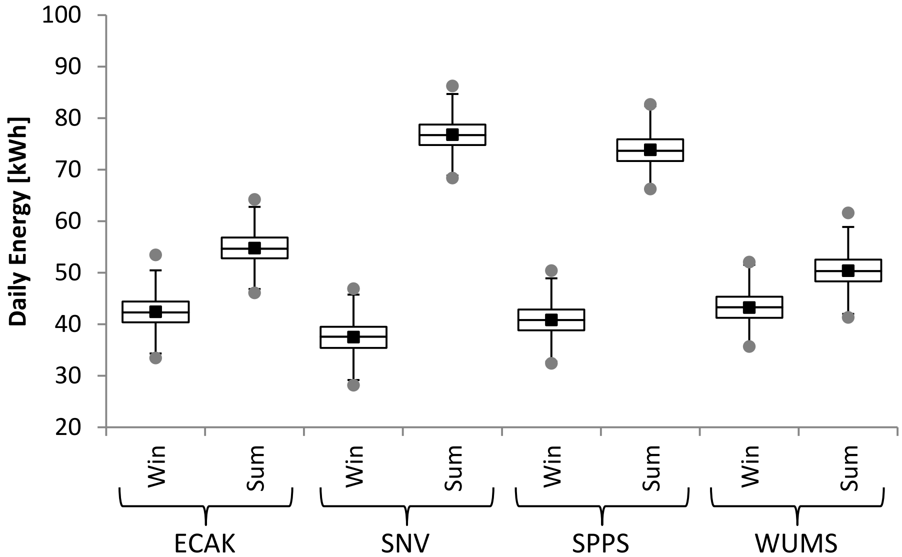

Figure 45: The Proposed Physically-Based Residential-Energy-Management-System Simulation [PPRS] heating, ventilation, and air conditioning [HVAC] direct load control [DLC] Scenario A daily energy.

The PPRS HVAC DLC Scenario A daily energy use in Figure 45 represents the daily energy use on the coldest and warmest day for each power system area, where the use of the HVAC is cycled for 15 minute increments from 4p to 7p. These days are strong candidates for the application of an energy management function. Notice, the decrease in average winter PPRS HVAC DLC Scenario A daily energy is 0.2% (0.1 kWh) and the decrease in average summer PPRS HVAC DLC Scenario A daily energy is 2.3% (1.6 kWh) compared to the average winter and summer PPRS base case (BC) Scenario A daily energy, respectively. This indicates that the HVAC thermal simulation model used includes less than 100% payback efficiency. This result is similar to the results in [22].

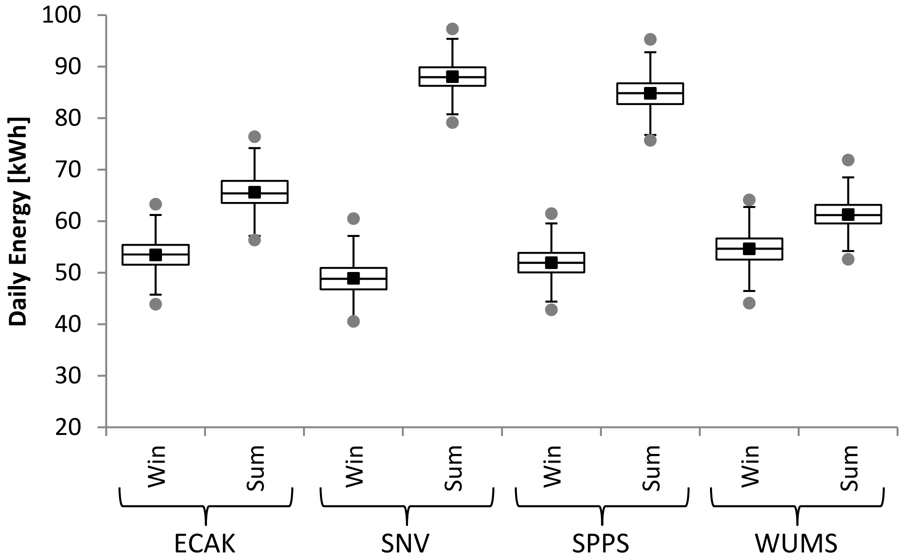

Figure 46: The Proposed Physically-Based Residential-Energy-Management-System Simulation [PPRS] heating, ventilation, and air conditioning [HVAC] direct load control [DLC] Scenario B daily energy.

The PPRS HVAC DLC Scenario B daily energy in Figure 46 represents a residence with HVAC DLC and where a plug-in electric vehicle (PEV) is recharged on a daily basis. Notice, the decrease in average winter PPRS HVAC DLC Scenario B daily energy is 0.2% (0.1 kWh) and the decrease in average summer PPRS HVAC DLC Scenario B daily energy is 1.9% (1.5 kWh) compared to the average winter and summer PPRS BC Scenario B daily energy, respectively.

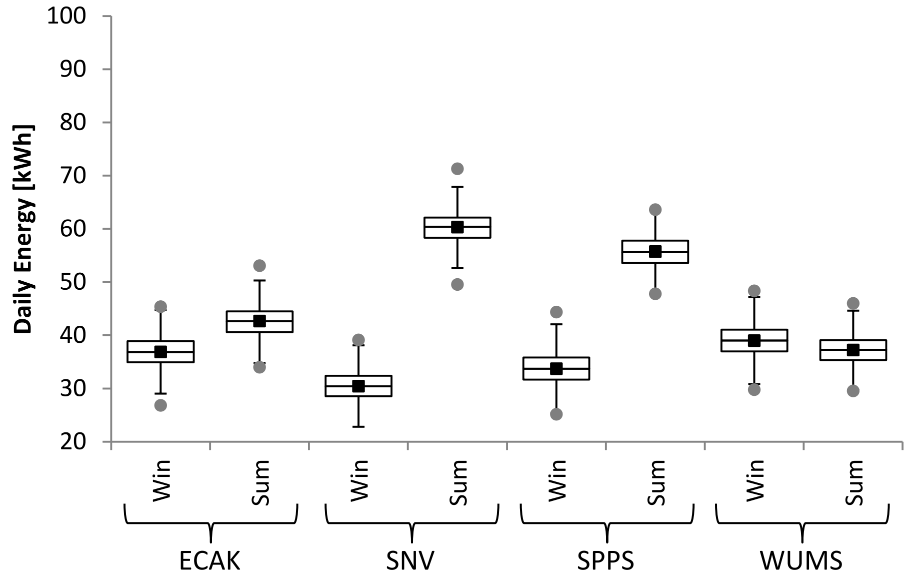

Figure 47: The Proposed Physically-Based Residential-Energy-Management-System Simulation [PPRS] heating, ventilation, and air conditioning [HVAC] direct load control [DLC] Scenario C daily energy.

The PPRS HVAC DLC Scenario C daily energy in Figure 47 represents a residence with HVAC DLC and a photovoltaic (PV) array. Notice, the decrease in average winter PPRS HVAC DLC Scenario C daily energy is 0.3% (0.1 kWh) and the decrease in average summer PPRS HVAC DLC Scenario C daily energy is 2.9% (1.6 kWh) compared to the average winter and summer PPRS BC Scenario C daily energy, respectively.

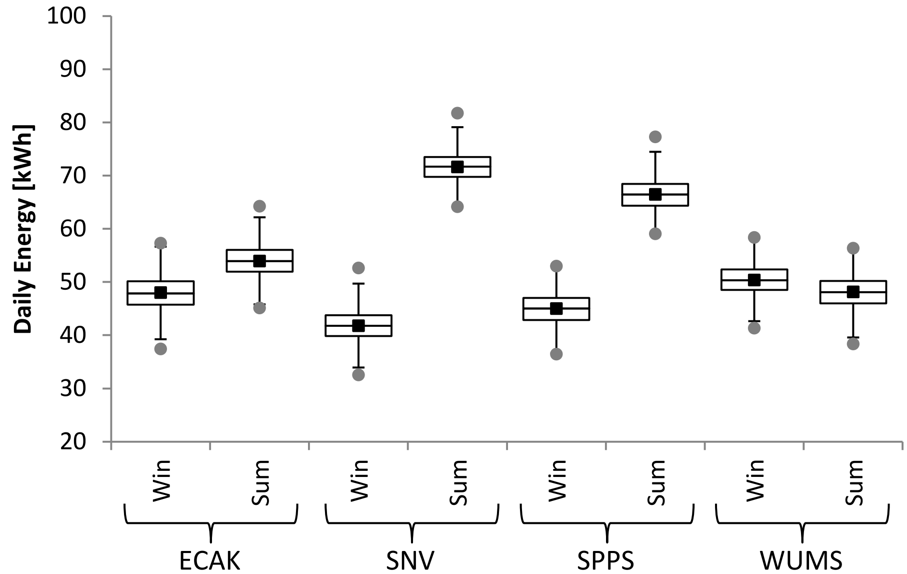

Figure 48: The Proposed Physically-Based Residential-Energy-Management-System Simulation [PPRS] heating, ventilation, and air conditioning [HVAC] direct load control [DLC] Scenario D daily energy.

The PPRS HVAC DLC Scenario D daily energy in Figure 48 represents a residence with HVAC DLC, PEV, and PV array. Notice, the decrease in average winter PPRS HVAC DLC Scenario D daily energy is 0.2% (0.1 kWh) and the decrease in average summer PPRS HVAC DLC Scenario D daily energy is 2.4% (1.6 kWh) compared to the average winter and summer PPRS BC Scenario D daily energy, daily energy.

Statistics of the PPRS HVAC DLC Scenario A, Scenario B, Scenario C, and Scenario D peak power are shown in Figure 49, Figure 50, Figure 51, and Figure 52, respectively. The PPRS HVAC DLC peak power is shown for each power system area and for the two unique seasons with extreme temperatures where energy management utilization would be expected: winter and summer. The extreme temperatures and days used for each power system area and season are shown in Table 16.

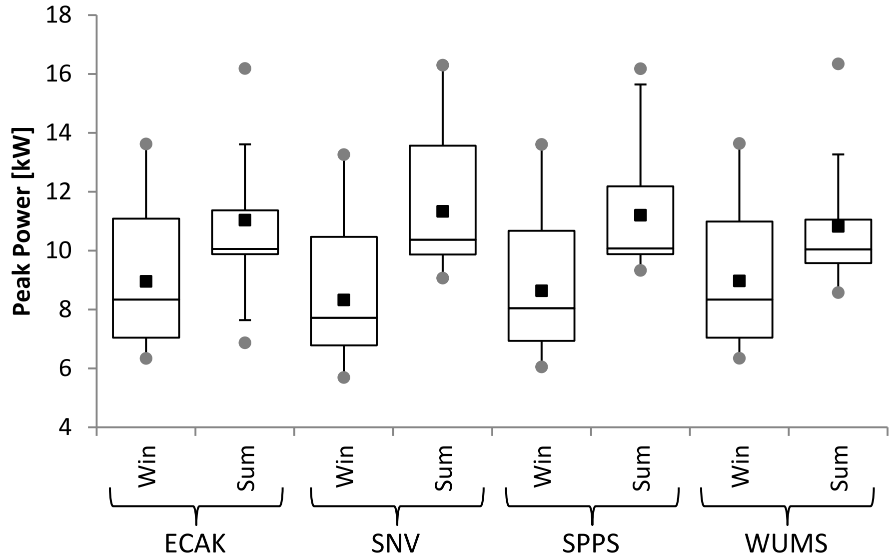

Figure 49: The Proposed Physically-Based Residential-Energy-Management-System Simulation [PPRS] heating, ventilation, and air conditioning [HVAC] direct load control [DLC] Scenario A peak power.

The PPRS HVAC DLC Scenario A peak power in Figure 49 indicate a decrease in average winter PPRS HVAC DLC Scenario A peak power of 0.1% (less than 0.1 kW) and a decrease in average summer PPRS HVAC DLC Scenario A peak power of 0.3% (less than 0.1 kW) compared to the average winter and summer PPRS BC Scenario A peak power, respectively.

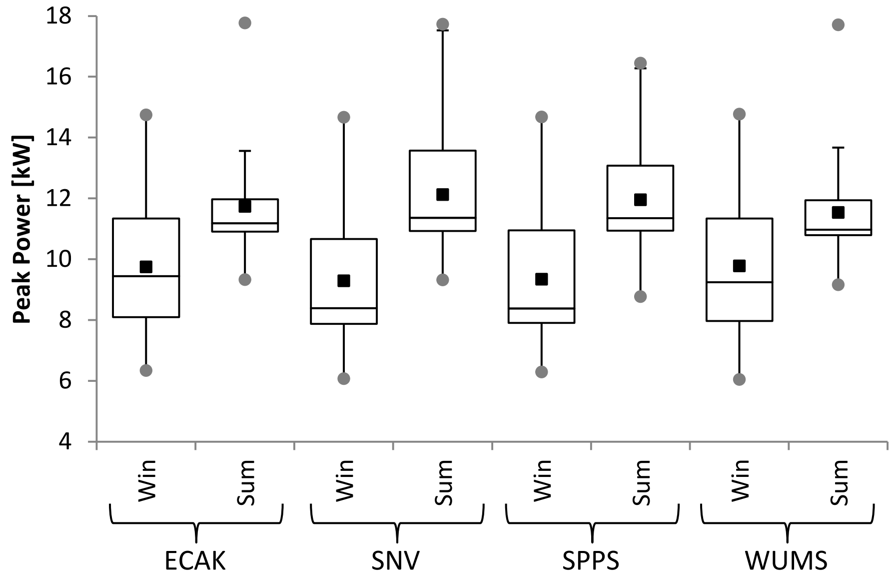

Figure 50: The Proposed Physically-Based Residential-Energy-Management-System Simulation [PPRS] heating, ventilation, and air conditioning [HVAC] direct load control [DLC] Scenario B peak power.

The PPRS HVAC DLC Scenario B peak power in Figure 50 indicate a decrease in average winter PPRS HVAC DLC Scenario B peak power of 0.1% (less than 0.1 kW) and a decrease in average summer PPRS HVAC DLC Scenario B peak power decrease of 0.3% (less than 0.1 kW) compared to the average winter and summer PPRS BC Scenario B peak power, respectively.

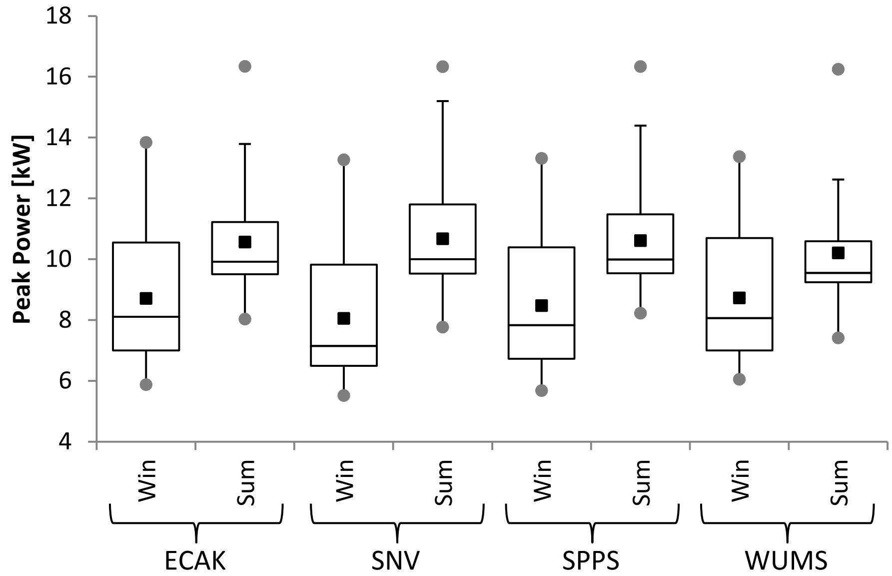

Figure 51: The Proposed Physically-Based Residential-Energy-Management-System Simulation [PPRS] heating, ventilation, and air conditioning [HVAC] direct load control [DLC] Scenario C peak power.

The PPRS HVAC DLC Scenario C peak power in Figure 51 indicate a decrease in average winter PPRS HVAC DLC Scenario C peak power of 0.2% (less than 0.1 kW) and a decrease in average summer PPRS HVAC DLC Scenario C peak power of 0.2% (less than 0.1 kW) compared to the average winter and summer PPRS BC Scenario C peak power, respectively.

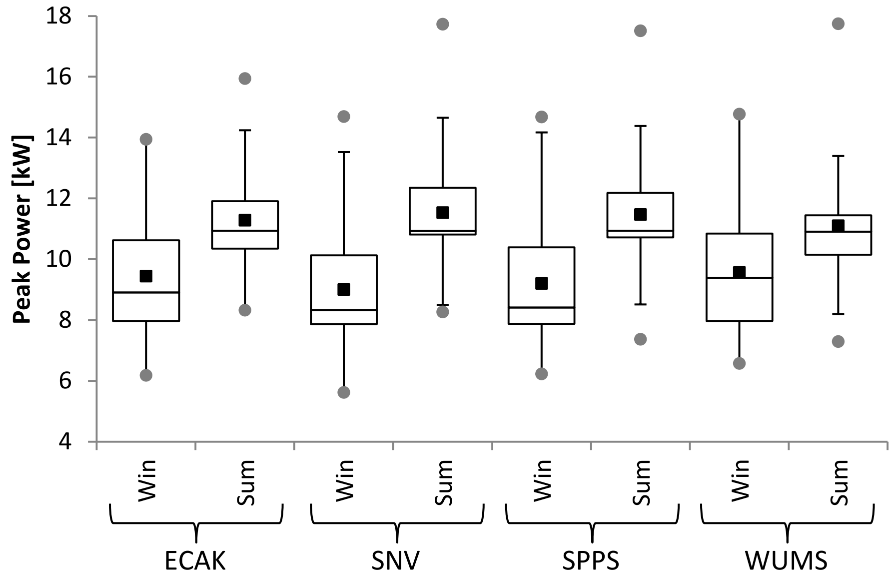

Figure 52: The Proposed Physically-Based Residential-Energy-Management-System Simulation [PPRS] heating, ventilation, and air conditioning [HVAC] direct load control [DLC] Scenario D peak power.

The PPRS HVAC DLC Scenario D peak power in Figure 52 indicate a decrease in average winter PPRS HVAC DLC Scenario D peak power of 0.1% (less than 0.1 kW) and a decrease in average summer PPRS HVAC DLC Scenario D peak power of 0.3% (less than 0.1 kW) compared to the average winter and summer PPRS BC Scenario D peak power, respectively.

Statistics of the PPRS HVAC DLC Scenario A, Scenario B, Scenario C, and Scenario D DR energy are shown in Figure 53, Figure 54, Figure 55, and Figure 56, respectively. The PPRS HVAC DLC DR energy is shown for each power system area and for the two unique seasons with extreme temperatures where energy management utilization would be expected: winter and summer. The extreme temperatures and days used for each power system area and season are shown in Table 16.

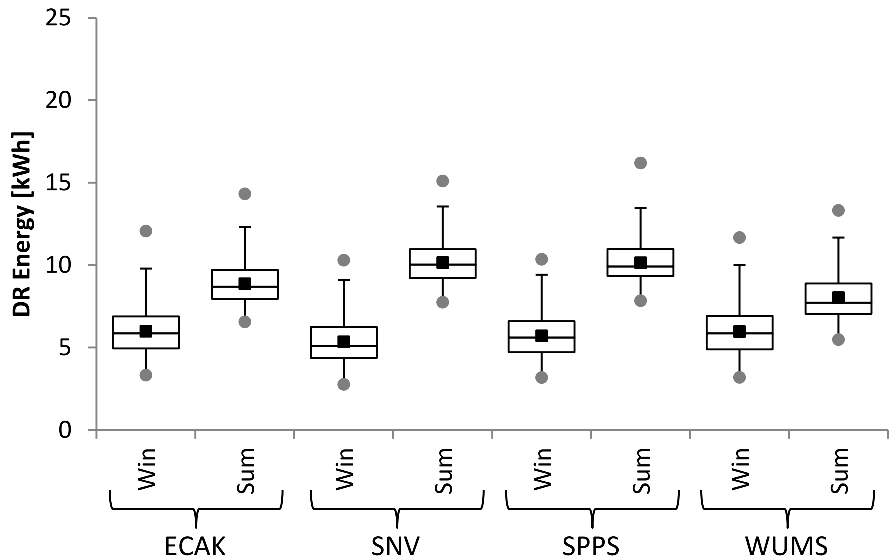

Figure 53: The Proposed Physically-Based Residential-Energy-Management-System Simulation [PPRS] heating, ventilation, and air conditioning [HVAC] direct load control [DLC] Scenario A demand response [DR] energy.

The PPRS HVAC DLC Scenario A DR energy in Figure 53 indicate that the average winter PPRS HVAC DLC Scenario A DR energy represents 14.0% (5.8 kWh) and the average summer PPRS HVAC DLC Scenario A DR energy represents 14.5% (9.3 kWh) of the average winter and summer PPRS HVAC DLC Scenario A daily energy, respectively. Further, the PPRS HVAC DLC Scenario A DR energy in Figure 53 indicate a decrease in average winter PPRS HVAC DLC Scenario A DR energy of 1.8% (0.1 kWh) and a decrease in average summer PPRS HVAC DLC Scenario A DR energy of 14.1% (1.7 kWh) compared to the winter and summer PPRS BC Scenario A DR energy, respectively.

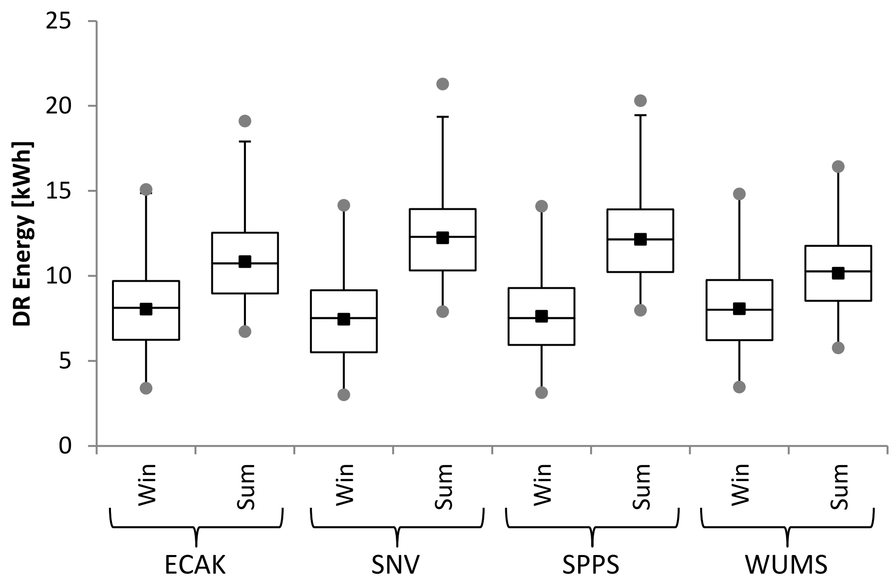

Figure 54: The Proposed Physically-Based Residential-Energy-Management-System Simulation [PPRS] heating, ventilation, and air conditioning [HVAC] direct load control [DLC] Scenario B demand response [DR] energy.

The PPRS HVAC DLC Scenario B DR energy in Figure 54 indicate that the average winter PPRS HVAC DLC Scenario B DR energy represents 14.9% (7.8 kWh) and the average summer PPRS HVAC DLC Scenario B DR energy represents 15.1% (11.3 kWh) of the average winter and summer PPRS HVAC DLC Scenario B daily energy, respectively. Further, the PPRS HVAC DLC Scenario B DR energy in Figure 54 indicate a decrease in average winter PPRS HVAC DLC Scenario B DR energy of 1.3% (0.1 kWh) and a decrease in average summer PPRS HVAC DLC Scenario B DR energy of 12.1% (1.7 kWh) compared to the average winter and summer PPRS BC Scenario B DR energy, respectively.

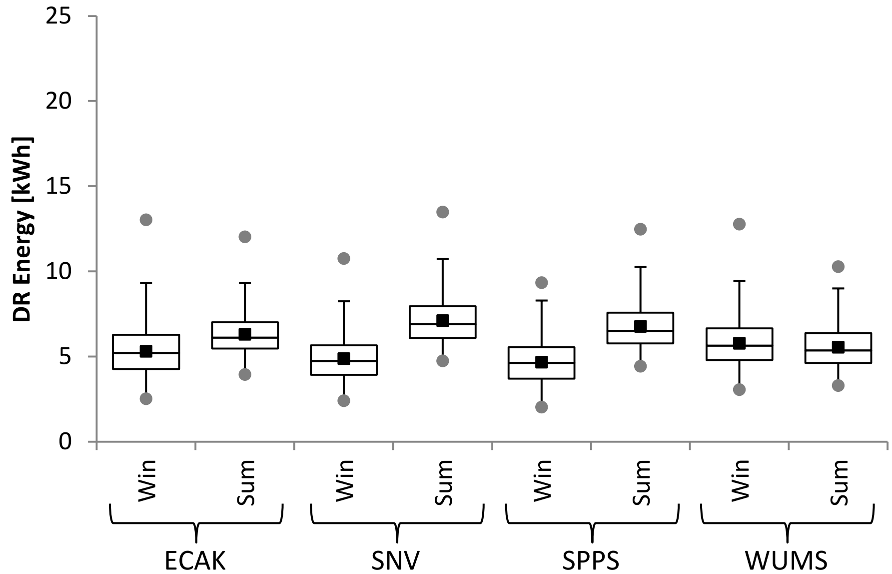

Figure 55: The Proposed Physically-Based Residential-Energy-Management-System Simulation [PPRS] heating, ventilation, and air conditioning [HVAC] direct load control [DLC] Scenario C demand response [DR] energy.

The PPRS HVAC DLC Scenario C DR energy in Figure 55 indicate that the average winter PPRS HVAC DLC Scenario C DR energy represents 14.7% (5.2 kWh) and the average summer PPRS HVAC DLC Scenario C DR energy represents 13.1% (6.4 kWh) of the average winter and summer PPRS HVAC DLC Scenario C daily energy, respectively. Further, the PPRS HVAC DLC Scenario C DR energy in Figure 55 indicate a decrease in average winter PPRS HVAC DLC Scenario C DR energy of 1.9% (0.1 kWh) and a decrease in average summer PPRS HVAC DLC Scenario C DR energy of 19.2% (1.7 kWh) compared to the average winter and summer PPRS BC Scenario C DR energy, respectively.

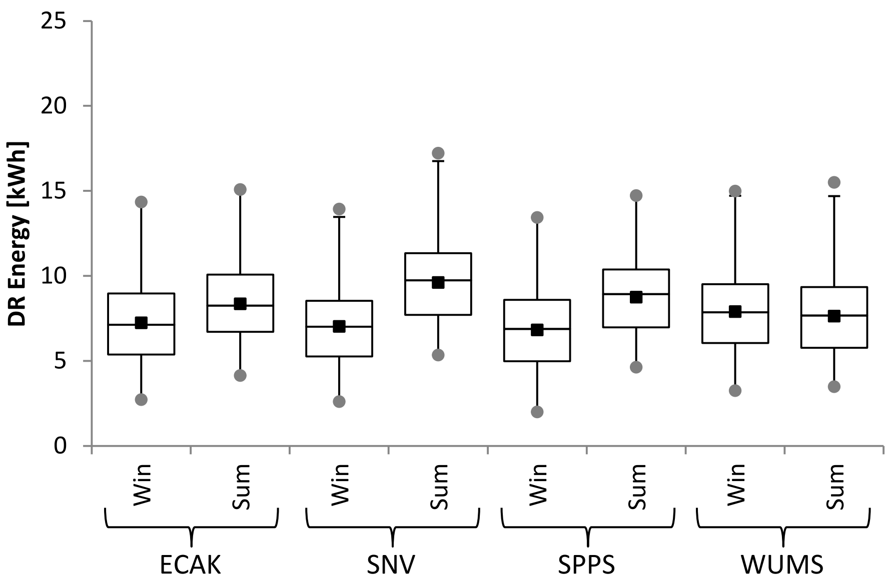

Figure 56: The Proposed Physically-Based Residential-Energy-Management-System Simulation [PPRS] heating, ventilation, and air conditioning [HVAC] direct load control [DLC] Scenario D demand response [DR] energy.

The PPRS HVAC DLC Scenario D DR energy in Figure 56 indicate that the average winter PPRS HVAC DLC Scenario D DR energy represents 15.7% (7.2 kWh) and the average summer PPRS HVAC DLC Scenario D DR energy represents 14.3% (8.6 kWh) of the average winter and summer PPRS HVAC DLC Scenario D daily energy, respectively. Further, the PPRS HVAC DLC Scenario D DR energy in Figure 56 indicate a decrease in average winter PPRS HVAC DLC Scenario D DR energy of 1.4% (0.1 kWh) and a decrease in average summer PPRS HVAC DLC Scenario D DR energy of 14.7% (1.6 kWh) compared to the average winter and summer PPRS BC Scenario D DR energy, respectively.

Next is a presentation of the PPRS smart thermostat results.

4.5 Smart Thermostat

The Proposed Physically-Based Residential-Energy-Management-System Simulation (PPRS) smart thermostat (ST) consists of a residence (with the same sequence of appliance use as the base case [BC]) with a ST. The PPRS ST energy management function increases (for times that air conditioning is needed) or decreases (for times that heating is needed) the indoor temperature set point during the demand response (DR) period. During the summer and warmer days in the transitional months (with average temperature greater than or equal to 20 °C) the indoor temperature set point is increased from 20 °C to 26 °C. During the winter and cooler days in the transitional months (with average daily temperature less than 20 °C) the indoor temperature set point is decreased from 20 °C to 14 °C.

Statistics of the PPRS ST Scenario A, Scenario B, Scenario C, and Scenario D daily energy are shown in Figure 57, Figure 58, Figure 59, and Figure 60, respectively. The PPRS ST daily energy is shown for each power system area (Versailles Kentucky [ECAK], Mercury Nevada [SNV], Stillwater Oklahoma [SPPS], and Necedah Wisconsin [WUMS]) and for the two unique seasons with extreme temperatures where energy management utilization would be expected: winter (Win) and summer (Sum). The extreme temperatures and days used for each power system area and season are shown in Table 16.

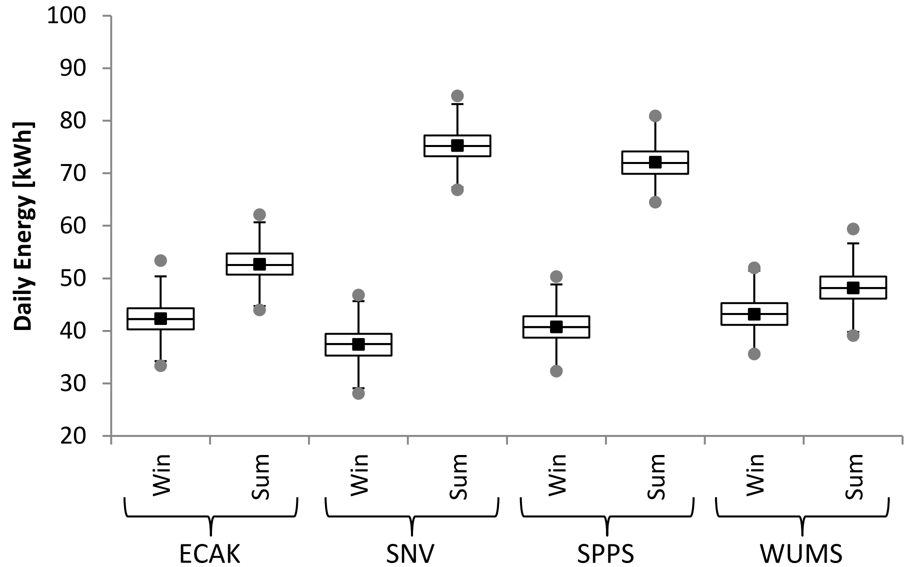

Figure 57: The Proposed Physically-Based Residential-Energy-Management-System Simulation [PPRS] smart thermostat [ST] Scenario A daily energy.

The PPRS ST Scenario A daily energy use in Figure 57 represents the daily energy use on the coldest and warmest day for each power system area, where the indoor temperature set point is adjusted based on the ambient temperature from 4p to 7p. These days are strong candidates for the application of an energy management function. Notice, the decrease in average winter PPRS ST Scenario A daily energy is 0.4% (0.2 kWh) and the decrease in average summer PPRS ST Scenario A daily energy is 5.3% (3.5 kWh) compared to the average winter and summer PPRS BC Scenario A daily energy, respectively.

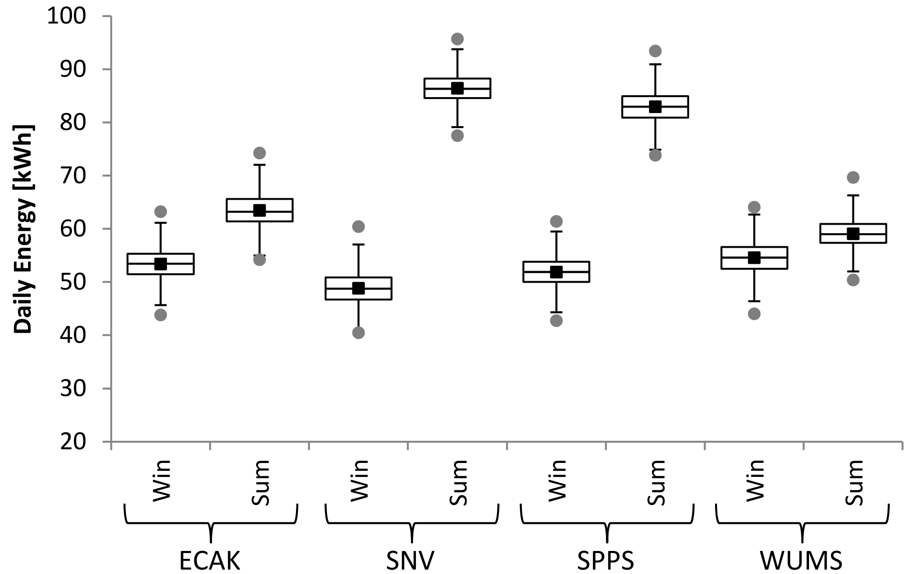

Figure 58: The Proposed Physically-Based Residential-Energy-Management-System Simulation [PPRS] smart thermostat [ST] Scenario B daily energy.

The PPRS ST Scenario B daily energy in Figure 58 represents a residence with ST and where a plug-in electric (PEV) is recharged on a daily basis. Notice, the decrease in average winter PPRS ST Scenario B daily energy is 0.3% (0.2kWh) and decrease in the average summer PPRS ST Scenario B daily energy use is 4.6% (3.5 kWh) compared to the average winter and summer PPRS BC Scenario B daily energy use, respectively.

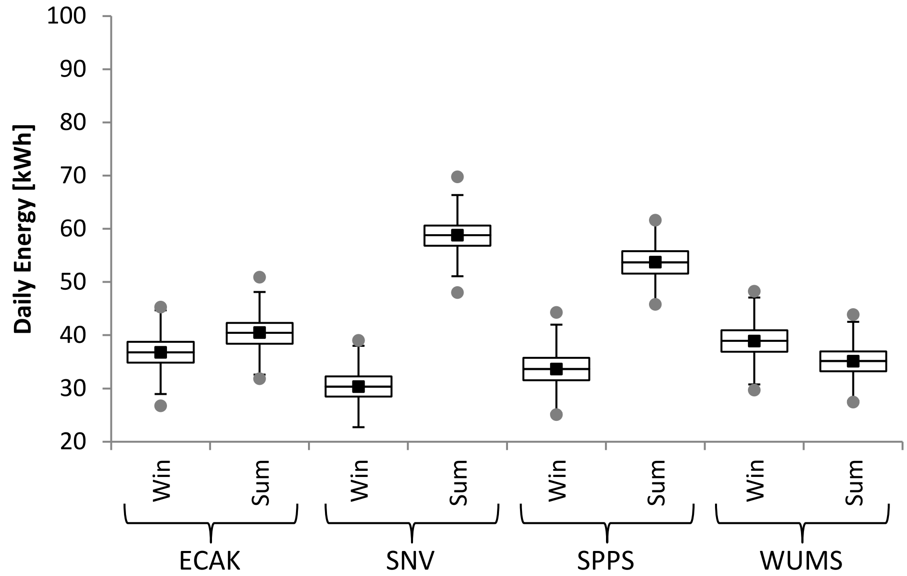

Figure 59: The Proposed Physically-Based Residential-Energy-Management-System Simulation [PPRS] smart thermostat [ST] Scenario C daily energy.

The PPRS ST Scenario C daily energy in Figure 59 represents a residence with ST and a photovoltaic (PV) array. Notice, the decrease in average winter PPRS ST Scenario C daily energy is 0.5% (0.2 kWh) and the decrease in average summer PPRS ST Scenario C daily energy is 6.9% (3.5 kWh) compared to the average winter and summer PPRS BC Scenario C daily energy, respectively.

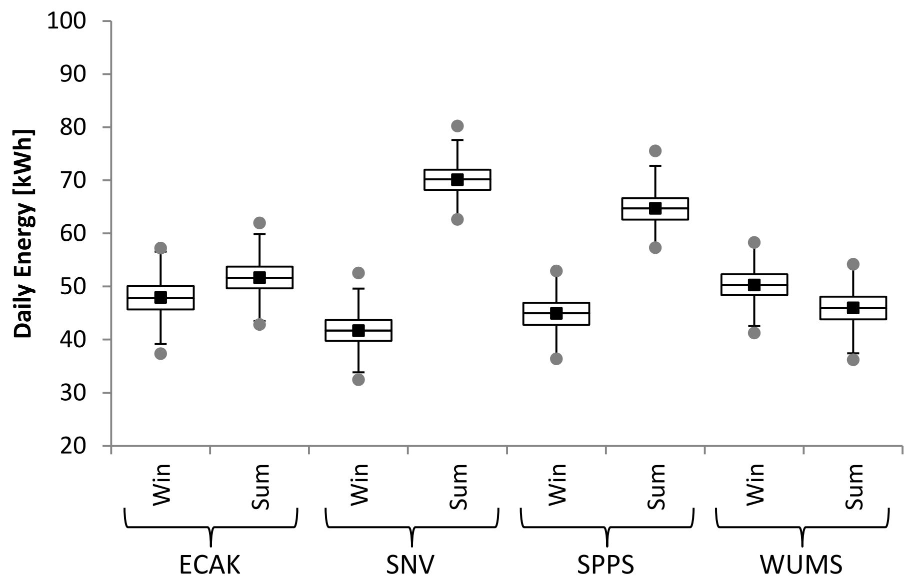

Figure 60: The Proposed Physically-Based Residential-Energy-Management-System Simulation [PPRS] smart thermostat [ST] Scenario D daily energy.

The PPRS ST Scenario D daily energy in Figure 60 represents a residence with ST, PEV, and PV array. Notice, the decrease in average winter PPRS ST Scenario D daily energy is 0.4% (0.2 kWh) and the decrease in average summer PPRS ST Scenario D daily energy is 5.7% (3.5 kWh) compared to the average winter and summer PPRS BC Scenario D daily energy, respectively.

Statistics of the PPRS ST Scenario A, Scenario B, Scenario C, and Scenario D peak power are shown in Figure 61, Figure 62, Figure 63, and Figure 64, respectively. The PPRS ST peak power is shown for each power system area and for the two unique seasons with extreme temperatures where energy management utilization would be expected: winter and summer. The extreme temperatures and days used for each power system area and season are shown in Table 16.

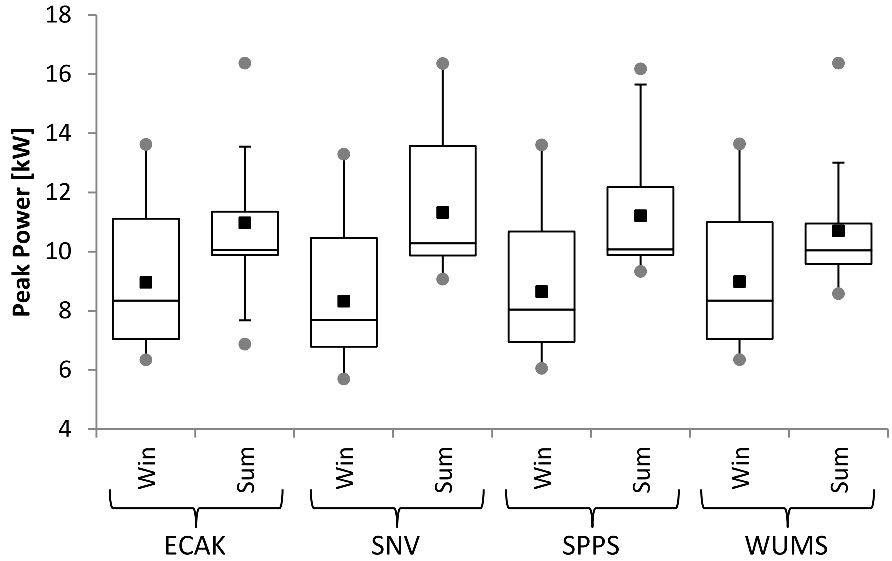

Figure 61: The Proposed Physically-Based Residential-Energy-Management-System Simulation [PPRS] smart thermostat [ST] Scenario A peak power.

The PPRS ST Scenario A peak power in Figure 61 indicate a decrease in average winter PPRS ST Scenario A peak power of 0.1% (less than 0.1 kW) and a decrease in average summer PPRS ST Scenario A peak power of 0.7% (0.1 kW) compared to the average winter and summer PPRS BC Scenario A peak power, respectively.

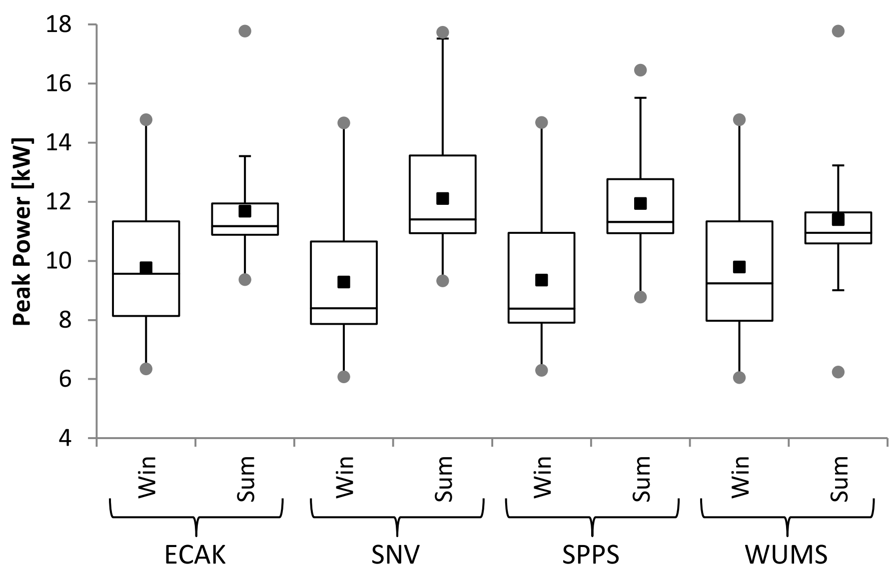

Figure 62: The Proposed Physically-Based Residential-Energy-Management-System Simulation [PPRS] smart thermostat [ST] Scenario B peak power.

The PPRS ST Scenario B peak power in Figure 62 indicate a decrease in average winter PPRS ST Scenario B peak power of 0.1% (less than 0.1 kW) and a decrease in average summer PPRS ST Scenario B peak power of 0.8% (0.1 kW) compared to the average winter and summer PPRS BC Scenario B peak power, respectively.

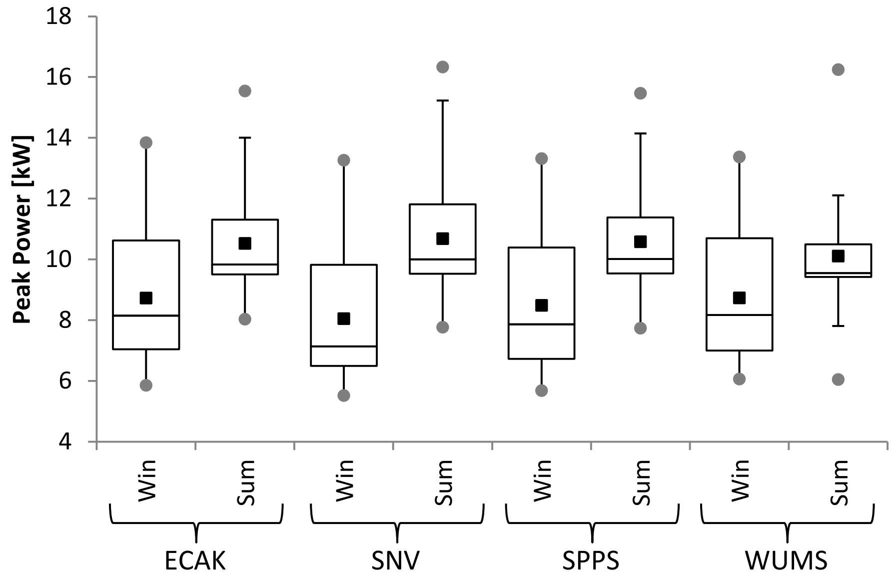

Figure 63: The Proposed Physically-Based Residential-Energy-Management-System Simulation [PPRS] smart thermostat [ST] Scenario C peak power.

The PPRS ST Scenario C peak power in Figure 63 indicate a decrease in average winter PPRS ST Scenario C peak power of 0.1% (less than 0.1 kW) and a decrease in average summer PPRS ST Scenario C peak power of 0.6% (0.1 kW) compared to the average winter and summer PPRS BC Scenario C peak power, respectively.

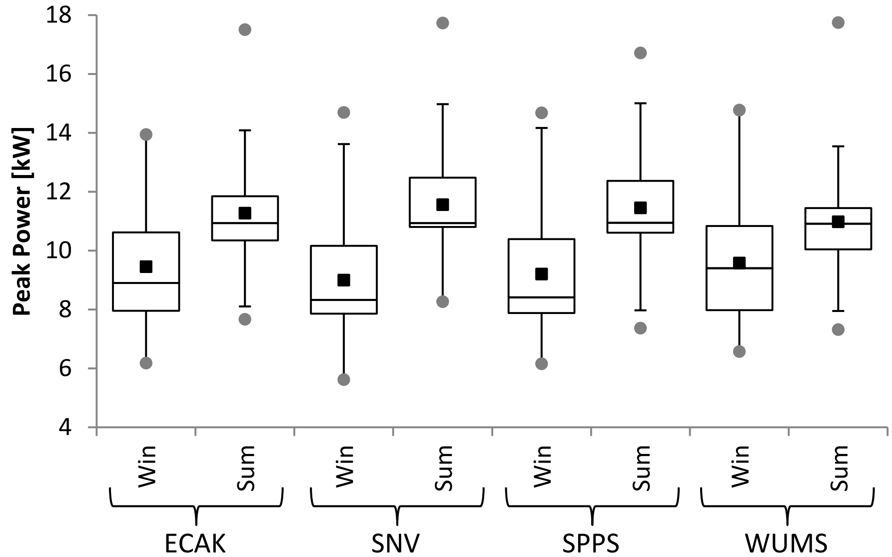

Figure 64: The Proposed Physically-Based Residential-Energy-Management-System Simulation [PPRS] smart thermostat [ST] Scenario D peak power.

The PPRS ST Scenario D peak power in Figure 64 indicate a decrease in average winter PPRS ST Scenario D peak power of 0.1% (less than 0.1 kW) and a decrease in average summer PPRS ST Scenario D peak power of 0.6% (0.1 kW) compared to the average winter and summer PPRS BC Scenario D peak power, respectively.

Statistics of the PPRS ST Scenario A, Scenario B, Scenario C, and Scenario D DR energy are shown in Figure 65, Figure 66, Figure 67, and Figure 68, respectively. The PPRS ST DR energy is shown for each power system area and for the two unique seasons with extreme temperatures where energy management utilization would be expected: winter and summer. The extreme temperatures and days used for each power system area and season are shown in Table 16.

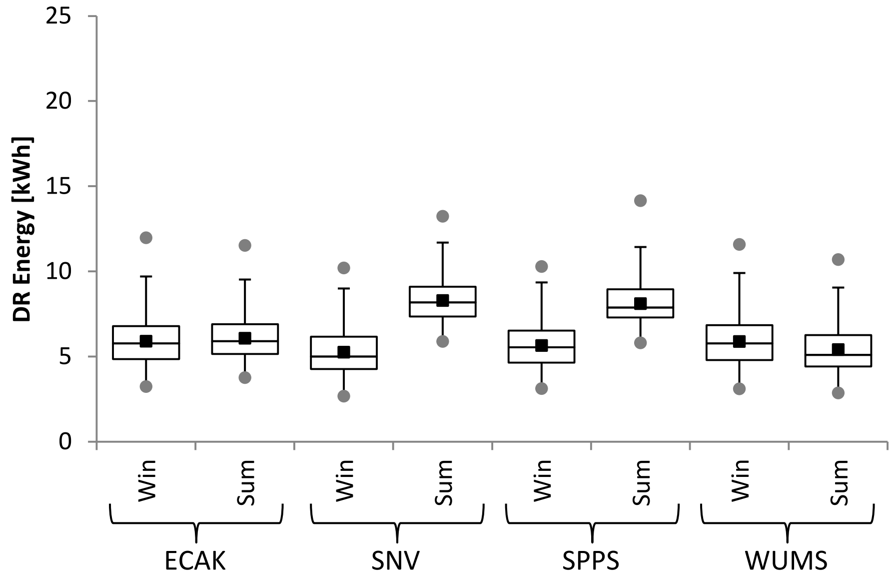

Figure 65: The Proposed Physically-Based Residential-Energy-Management-System Simulation [PPRS] smart thermostat [ST] Scenario A demand response [DR] energy.

The PPRS ST Scenario A DR energy in Figure 65 indicate that the average winter PPRS ST Scenario A DR energy represents 13.9% (5.7 kWh) and the average summer PPRS ST Scenario A DR energy represents 11.2% (7.0 kWh) of the winter and summer PPRS ST Scenario A daily energy, respectively. Further, the PPRS ST Scenario A DR energy in Figure 65 indicate a decrease in average winter PPRS ST Scenario A DR energy of 3.3% (0.2 kWh) and a decrease in average summer PPRS ST Scenario A DR energy of 36.7% (4.0 kWh) compared to the average winter and summer PPRS BC Scenario A DR energy, respectively.

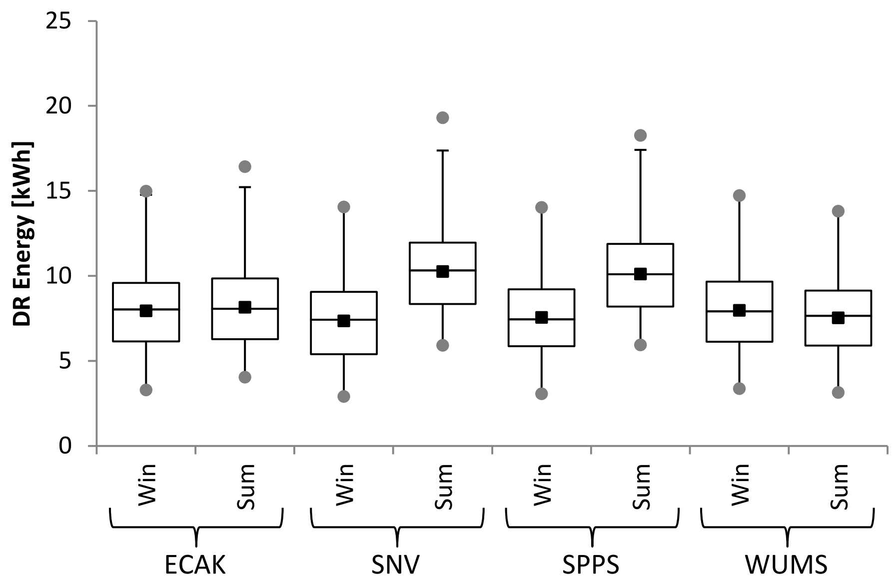

Figure 66: The Proposed Physically-Based Residential-Energy-Management-System Simulation [PPRS] smart thermostat [ST] Scenario B demand response [DR] energy.

The PPRS ST Scenario B DR energy in Figure 66 indicate that the average winter PPRS ST Scenario B DR energy represents 14.8% (7.7 kWh) and average summer PPRS ST Scenario B DR energy represents 12.4% (9.0 kWh) of the average winter and summer PPRS ST Scenario B daily energy, respectively. Further, the PPRS ST Scenario B DR energy in Figure 66 indicate a decrease in average winter PPRS ST Scenario B DR energy of 2.4% (0.2 kWh) and a decrease in average summer PPRS ST Scenario B DR energy of 30.8% (4.0 kWh) compared to the average winter and summer PPRS BC Scenario B DR energy, respectively.

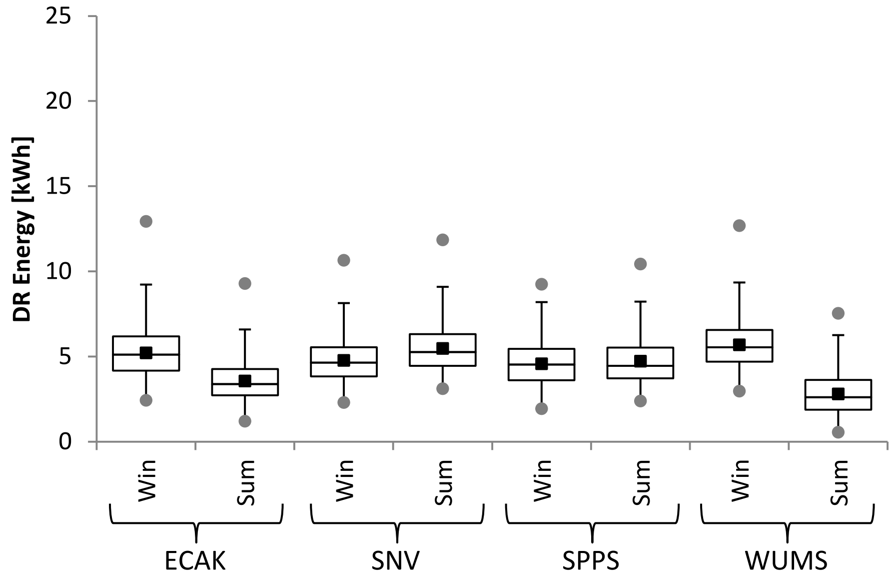

Figure 67: The Proposed Physically-Based Residential-Energy-Management-System Simulation [PPRS] smart thermostat [ST] Scenario C demand response [DR] energy.

The PPRS ST Scenario C DR energy in Figure 67 indicate that the average winter PPRS ST Scenario C DR energy represents 14.5% (5.1 kWh) and the average summer PPRS ST Scenario C DR energy represents 8.8% (4.1 kWh) of the average winter and summer PPRS ST Scenario C daily energy, respectively. Further, the PPRS ST Scenario C DR energy in Figure 67 indicate a decrease in average winter PPRS ST Scenario C DR energy of 3.7% (0.2 kWh) and a decrease in average summer PPRS ST Scenario C DR energy of 49.7% (4.0 kWh) compared to the average winter and summer PPRS BC Scenario C DR energy, respectively.

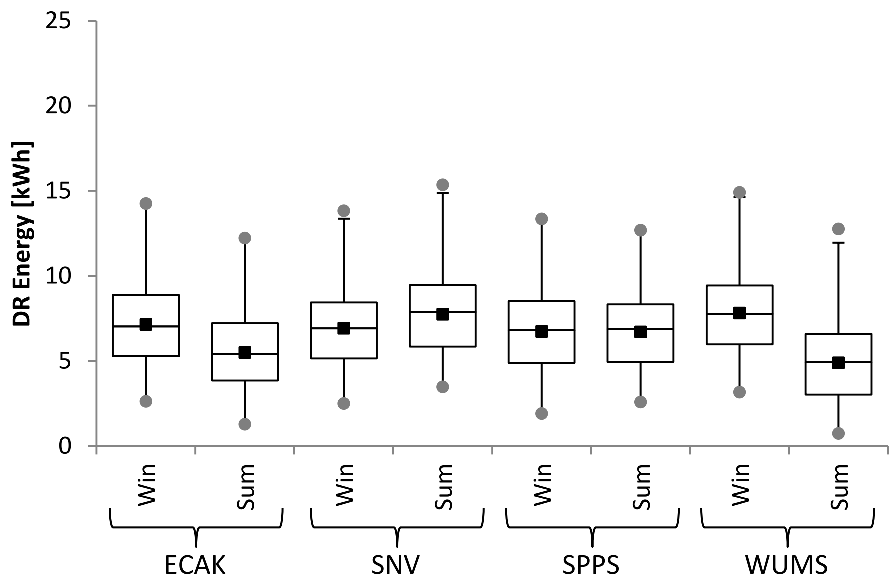

Figure 68: The Proposed Physically-Based Residential-Energy-Management-System Simulation [PPRS] smart thermostat [ST] Scenario D demand response [DR] energy.

The PPRS ST Scenario D DR energy in Figure 68 indicate that the average winter PPRS ST Scenario D DR energy represents 15.5% (7.2 kWh) and the average summer PPRS ST Scenario D DR energy represents 10.7% (6.2 kWh) of the average winter and summer PPRS ST Scenario D daily energy, respectively. Further, the PPRS ST Scenario D DR energy in Figure 68 indicate a decrease in average winter ST Scenario D DR energy of 2.6% (0.2 kWh) and a decrease in average summer S ST Scenario D DR energy of 39.4% (4.0 kWh) compared to the average winter and summer PPRS BC Scenario D DR energy, respectively.

Next is a presentation of the PPRS SAS results.

4.6 Smart Appliance Scheduling

In the Proposed Physically-Based Residential-Energy-Management-System Simulation (PPRS) smart appliance scheduling (SAS) energy management function the use of the smart appliances (clothes washer [CW]; clothes dryer [CD]; dishwasher [Dw];

heating, ventilation, and air conditioning [HVAC]; plug-in electric vehicle [PEV], and refrigerator [Ref]) can be delayed if the smart appliance is scheduled to start before (such that the smart appliance will continue to operate during the demand response [DR] period) or during the DR period.

Two caveats to this heuristic control rule is the HVAC and Ref. The HVAC operation is the same as the ST in the SAS energy management function. The Ref is delayed for a maximum of one hour because the refrigerator internal temperature must stay below 40 °F [113]. It is assumed that the internal temperature of the Ref will not drop to unsafe levels in a single hour [107]. All the other smart appliances are delayed if they are started such that they will run into the DR period.

All of the delayed appliances are rescheduled in a priority-based sequential sequence (e.g. CW, CD, Dw, and PEV). This sequence is needed so that a new daily peak is not created when all the delayed appliances are restarted.

Unlike the results from the first three PPRS energy management functions, the last two PPRS energy management function simulations investigate the use of individual smart appliances. There are seven smart appliances in the PPRS formulation. The SAS energy management function is tested with all combinations of the seven smart appliances with (smart) and without communication capabilities, resulting in 128 combinations, from no smart appliances to all seven smart appliances. Again, each PPRS SAS result is shown for each power system area (Versailles Kentucky [ECAK], Mercury Nevada [SNV], Stillwater Oklahoma [SPPS], and Necedah Wisconsin [WUMS]).

The average winter and summer PPRS SAS Scenario A daily energy for each smart appliance permutation simulation is shown in Figure 69 and Figure 70, respectively.

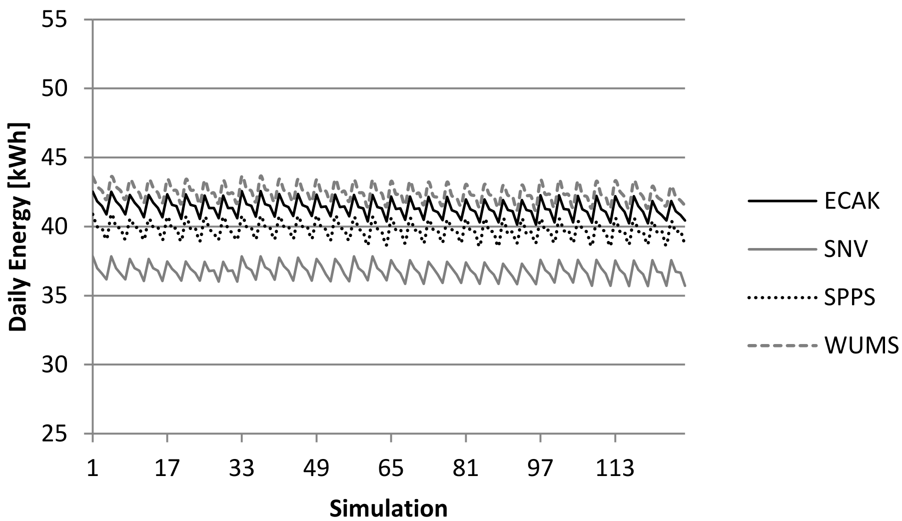

Figure 69: The average winter Proposed Physically-Based Residential-Energy-Management-System Simulation [PPRS] smart appliance scheduling [SAS] Scenario A daily energy.

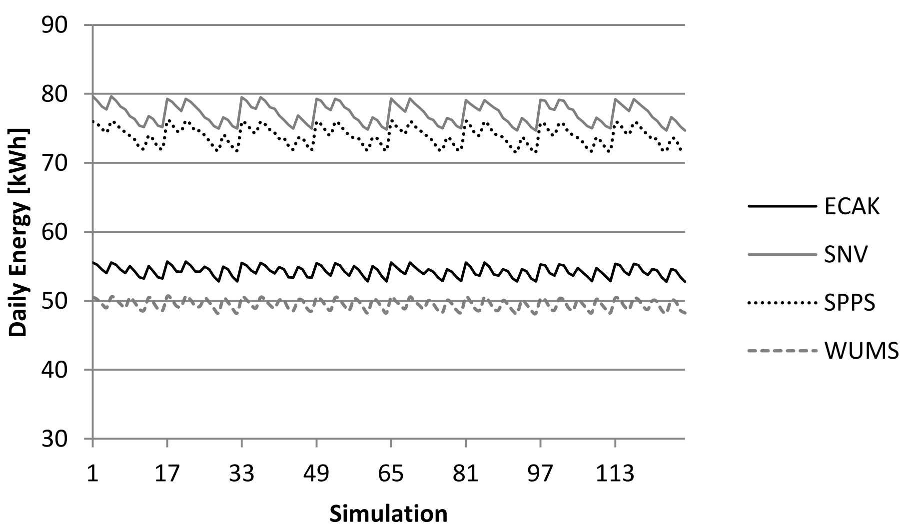

Figure 70: The average summer Proposed Physically-Based Residential-Energy-Management-System Simulation [PPRS] smart appliance scheduling [SAS] Scenario A daily energy.

The average winter and summer PPRS SAS Scenario A daily energy shown in Figure 69 and Figure 70, respectively, indicate that the WH, Ref, and PEV intelligence has the most significant impact on the daily energy use. Specifically, the WH, Ref, and PEV intelligence result in small amounts of unserviced energy. Theoretically, the average winter and summer PPRS SAS daily energy should be the same for all permutations of smart appliances.

The effect of the various smart appliances in the average seasonal PPRS SAS Scenario A daily energy is between 0.1% (less than 0.1 kWh) increase and 5.6% (2.3 kWh) decrease in the winter and between 0.1% (0.1 kWh) increase and 5.4% (3.6 kWh) decrease in the summer, compared to the respective average seasonal PPRS SAS Scenario A Simulation 1 (no smart appliances) daily energy. Notice, the average winter (summer) PPRS Scenario A Simulation 1 daily energy is 41.2 kWh (65.4 kWh).

The average winter and summer PPRS SAS Scenario B daily energy for each smart appliance permutation simulation is shown in Figure 71 and Figure 72, respectively.

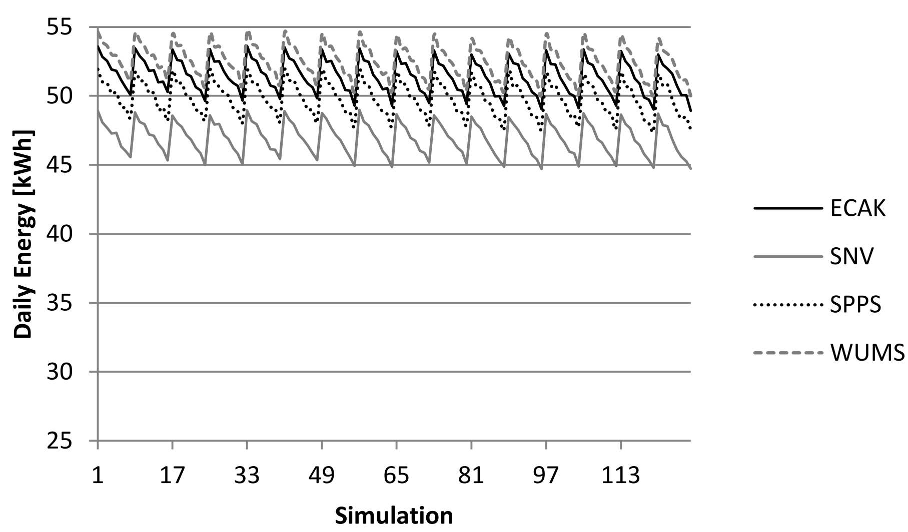

Figure 71: The average winter Proposed Physically-Based Residential-Energy-Management-System Simulation [PPRS] smart appliance scheduling [SAS] Scenario B daily energy.

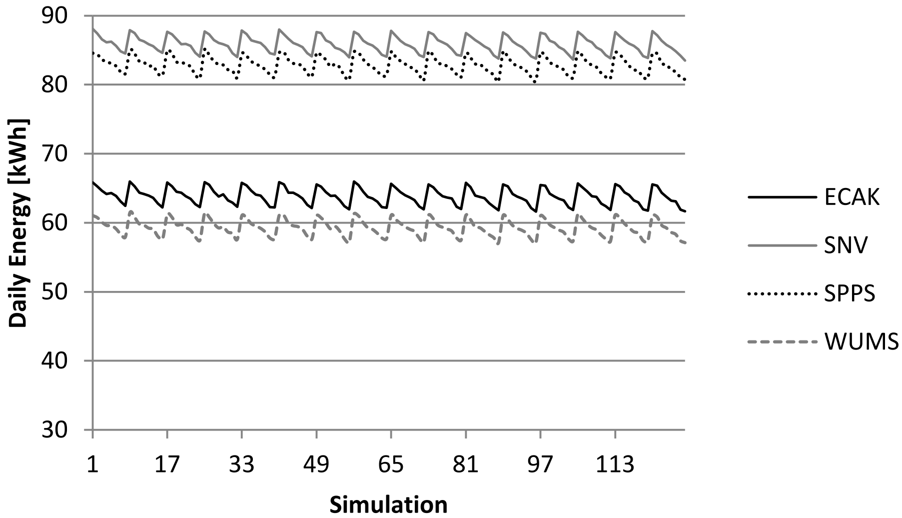

Figure 72: The average summer Proposed Physically-Based Residential-Energy-Management-System Simulation [PPRS] smart appliance scheduling [SAS] Scenario B daily energy.

The average winter and summer PPRS SAS Scenario B daily energy shown in Figure 71 and Figure 72, respectively, depict the same pattern as the PPRS SAS Scenario A winter and summer average daily energy.

The effect of the various smart appliances in the average seasonal PPRS SAS Scenario B daily energy is between 0.1% (less than 0.1 kWh) increase and 8.6% (4.5 kWh) decrease in the winter and between 0.4% (0.3 kWh) increase and 5.7% (4.2 kWh) decrease in the summer, compared to the average respective seasonal PPRS SAS Scenario B Simulation 1 (no smart appliances) daily energy. Notice, the average winter (summer) PPRS Scenario B Simulation 1 daily energy is 52.3 kWh (74.9 kWh).

The average winter and summer PPRS SAS Scenario C daily energy for each smart appliance permutation simulation is shown in Figure 73 and Figure 74, respectively.

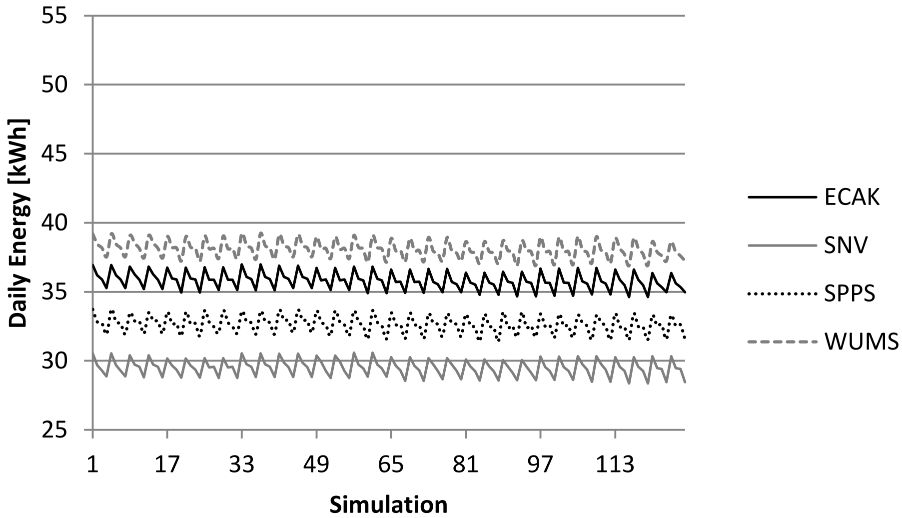

Figure 73: The average winter Proposed Physically-Based Residential-Energy-Management-System Simulation [PPRS] smart appliance scheduling [SAS] Scenario C daily energy.

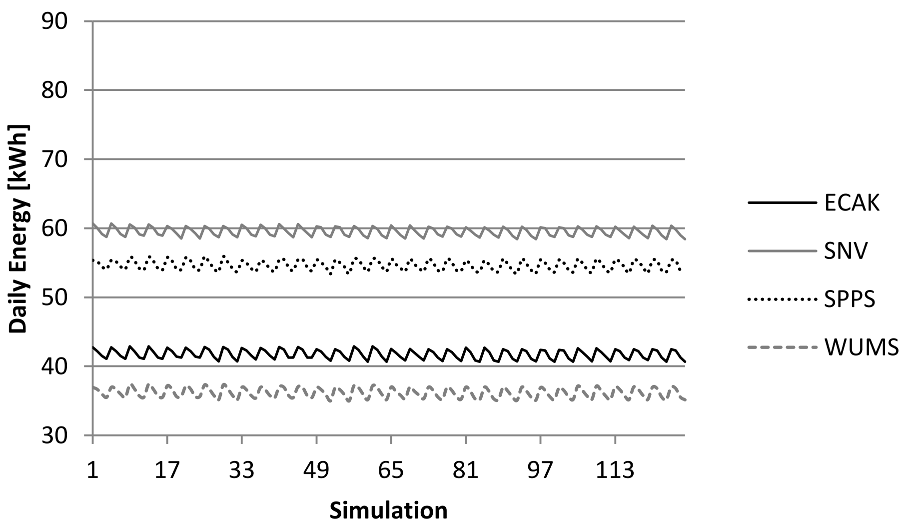

Figure 74: The average summer Proposed Physically-Based Residential-Energy-Management-System Simulation [PPRS] smart appliance scheduling [SAS] Scenario C daily energy.

The average winter and summer PPRS SAS Scenario C daily energy shown in Figure 73 and Figure 74, respectively, depict the same pattern as the average winter and summer PPRS SAS Scenario A daily energy.

The effect of the various smart appliances in the average seasonal PPRS SAS Scenario C daily energy is between 0.1% (less than 0.1 kWh) increase and 6.5% (2.3

kWh) decrease in the winter and between 0.6% (0.3 kWh) increase and 4.4% (2.1 kWh) decrease in the summer, compared to the respective average seasonal PPRS SAS Scenario C Simulation 1 (no smart appliances) daily energy. Notice, the average winter (summer) PPRS Scenario C Simulation 1 daily energy is 35.1 kWh (48.9 kWh).

The average winter and summer PPRS SAS Scenario D daily energy for each smart appliance permutation simulation is shown in Figure 75 and Figure 76, respectively.

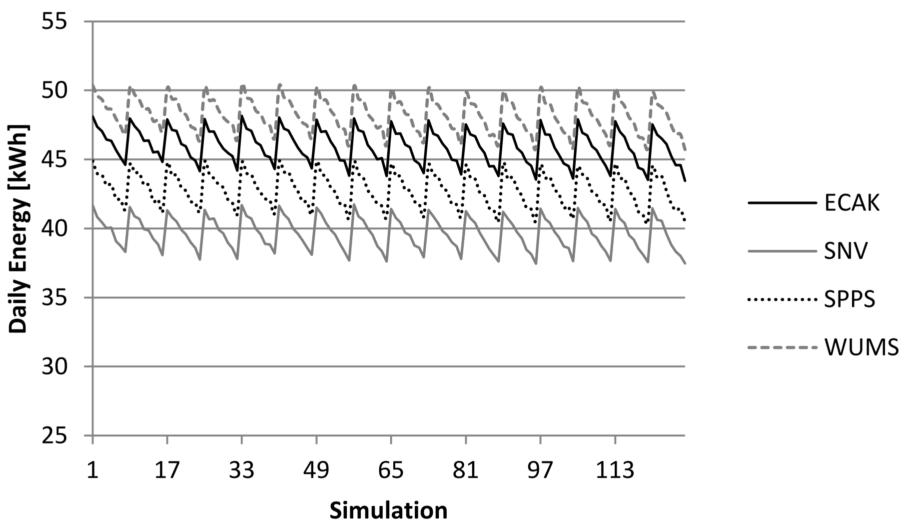

Figure 75: The average winter Proposed Physically-Based Residential-Energy-Management-System Simulation [PPRS] smart appliance scheduling [SAS] Scenario D daily energy.

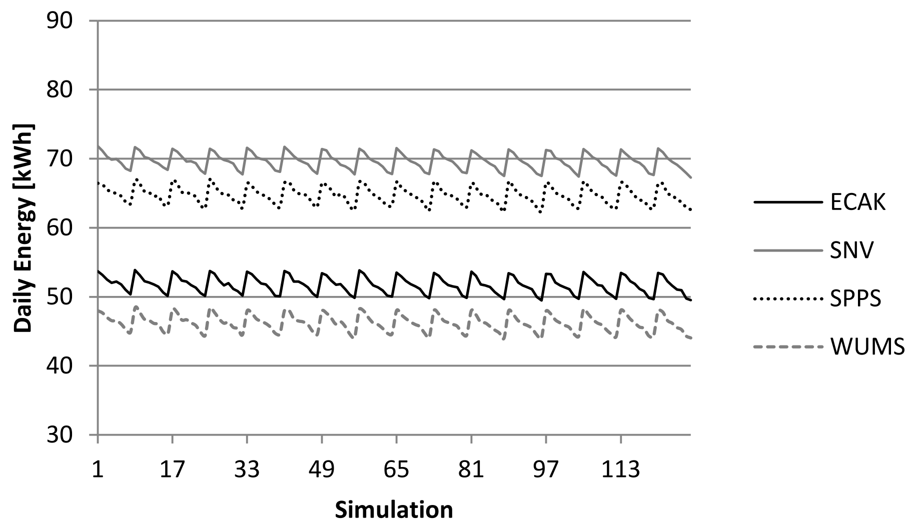

Figure 76: The average summer Proposed Physically-Based Residential-Energy-Management-System Simulation [PPRS] smart appliance scheduling [SAS] Scenario D daily energy.

The average winter and summer PPRS SAS Scenario D winter and summer average daily energy shown in Figure 75 and Figure 76, respectively, depict the same pattern as the average winter and summer PPRS SAS Scenario A daily energy.

The effect of the various smart appliances in the average seasonal PPRS SAS Scenario D daily energy is between 0.1% (less than 0.1 kWh) increase and 9.8% (4.5 kWh) decrease in the winter and between 0.5% (0.3 kWh) increase and 7.1% (4.2 kWh) decrease in the summer, compared to the respective average seasonal PPRS SAS Scenario D Simulation 1 (no smart appliances) daily energy. Notice, the average winter (summer) PPRS SAS Scenario D Simulation 1 daily energy is 46.3 kWh (60.0 kWh) in the summer.

The average winter and summer PPRS SAS Scenario A peak power for each smart appliance permutation simulation is shown in Figure 77 and Figure 78, respectively.

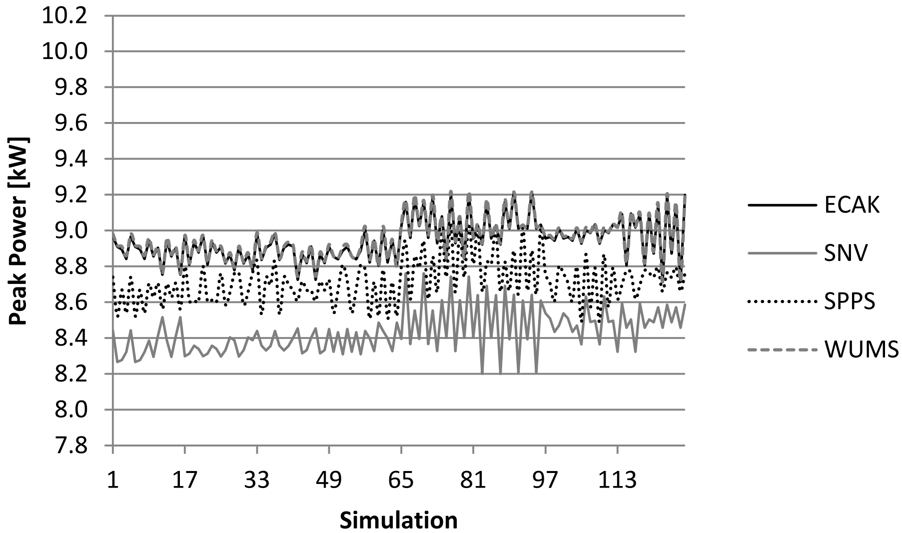

Figure 77: The average winter Proposed Physically-Based Residential-Energy-Management-System Simulation [PPRS] smart appliance scheduling [SAS] Scenario A peak power.

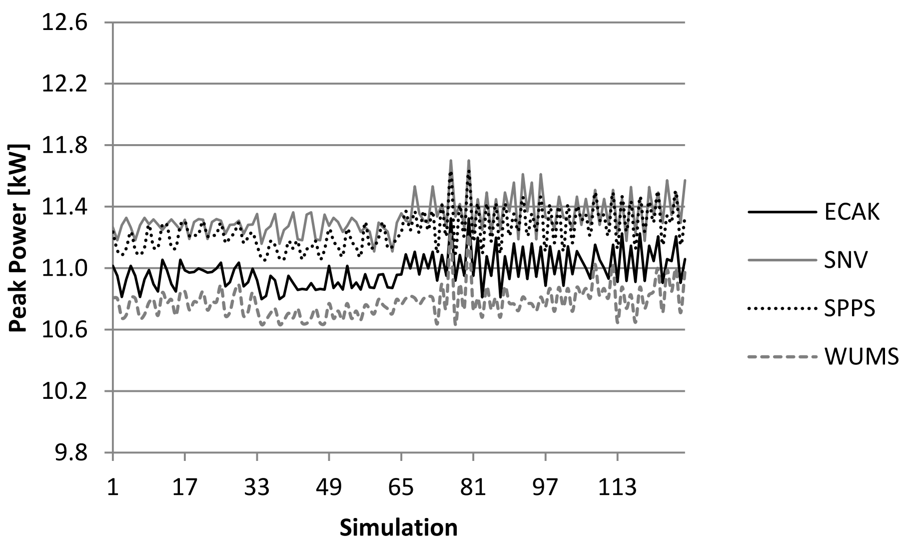

Figure 78: The average summer Proposed Physically-Based Residential-Energy-Management-System Simulation [PPRS] smart appliance scheduling [SAS] Scenario A peak power.

The average winter and summer PPRS SAS Scenario A peak power shown in Figure 77 and Figure 78, respectively, indicate that the smart clothes dryer has a noticeable effect on the average peak power. Each simulation above Simulation 65 includes a smart clothes dryer. Each simulation above Simulation 65 results in a higher average winter and summer PPRS SAS Scenario A peak power than the simulations below Simulation 64. Notice, the power demand of the clothes dryer (5.0 kW) is the highest of the simulated appliances.

The effect of the various smart appliances in the average seasonal PPRS SAS Scenario A peak power is between 3.2% (0.3 kW) increase and 2.9% (0.3 kW) decrease in the winter and between 3.5% (0.4 kW) increase and 1.6% (0.2 kW) decrease in the summer, compared to the respective average seasonal PPRS SAS Scenario A Simulation 1 (no smart appliances) peak power. Notice, the average winter (summer) PPRS Scenario A Simulation 1 peak power is 8.8 kW (11.1 kW).

The average winter and summer PPRS SAS Scenario B peak power for each smart appliance permutation simulation is shown in Figure 79 and Figure 80, respectively.

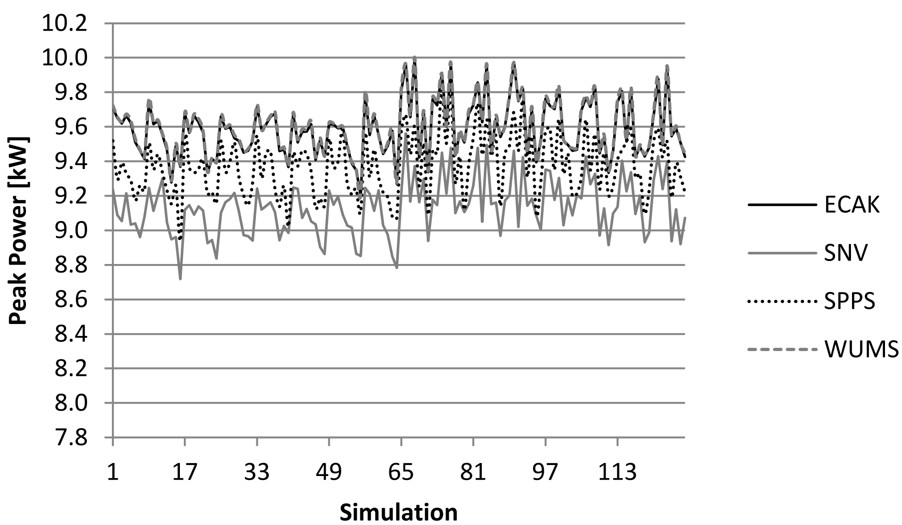

Figure 79: The average winter Proposed Physically-Based Residential-Energy-Management-System Simulation [PPRS] smart appliance scheduling [SAS] Scenario B peak power.

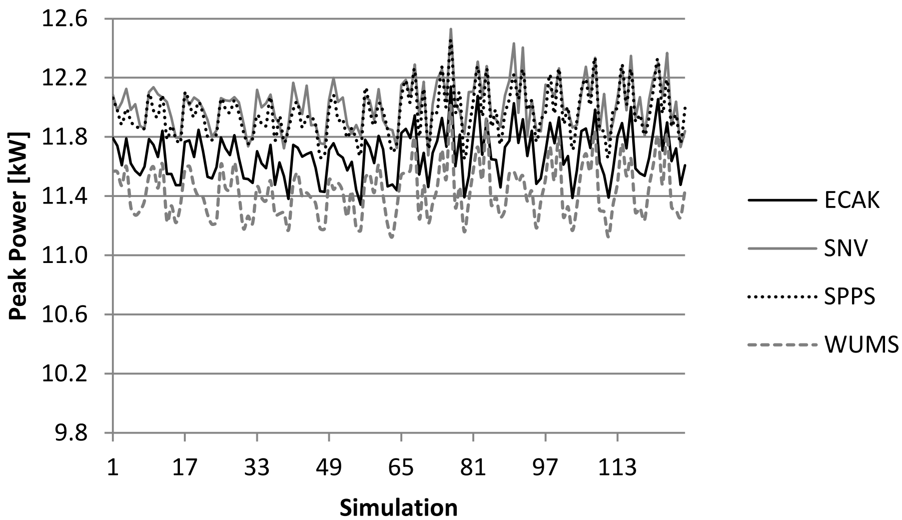

Figure 80: The average summer Proposed Physically-Based Residential-Energy-Management-System Simulation [PPRS] smart appliance scheduling [SAS] Scenario B peak power.

The average winter and summer PPRS SAS Scenario B winter and summer average peak power shown in Figure 79 and Figure 80, respectively, indicate the same pattern as the average winter and summer PPRS SAS Scenario A peak power.

The effect of the various smart appliances in the average seasonal PPRS SAS Scenario B peak power is between 3.1% (0.3 kW) increase and 5.6% (0.5 kW) decrease in the winter and between 3.4% (0.4 kW) increase and 3.6% (0.4 kW) decrease in the summer, compared to the respective average seasonal PPRS SAS Scenario B Simulation 1 (no smart appliances) peak power. Notice, the average winter (summer) PPRS Scenario B Simulation 1 peak power is 9.5 kW (11.9 kW).

The average winter and summer PPRS SAS Scenario C peak power for each smart appliance permutation simulation is shown in Figure 81 and Figure 82, respectively.

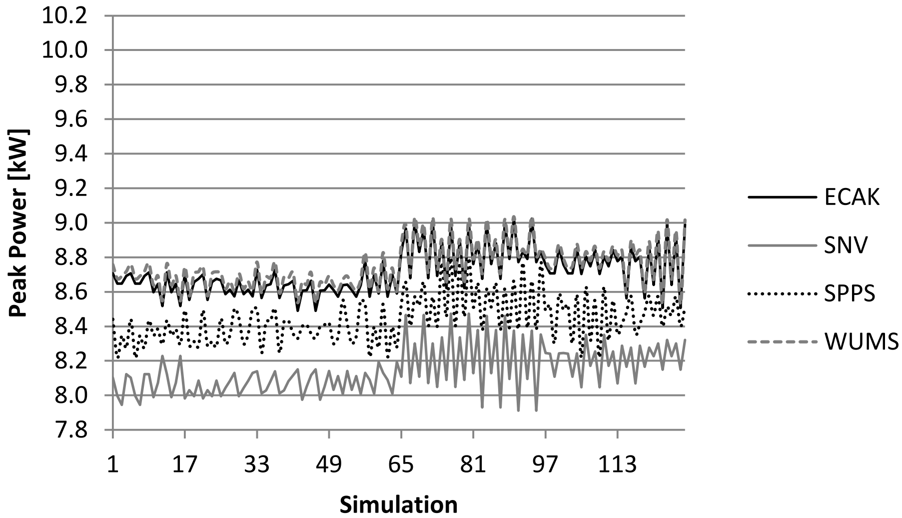

Figure 81: The average winter Proposed Physically-Based Residential-Energy-Management-System Simulation [PPRS] smart appliance scheduling [SAS] Scenario C peak power.

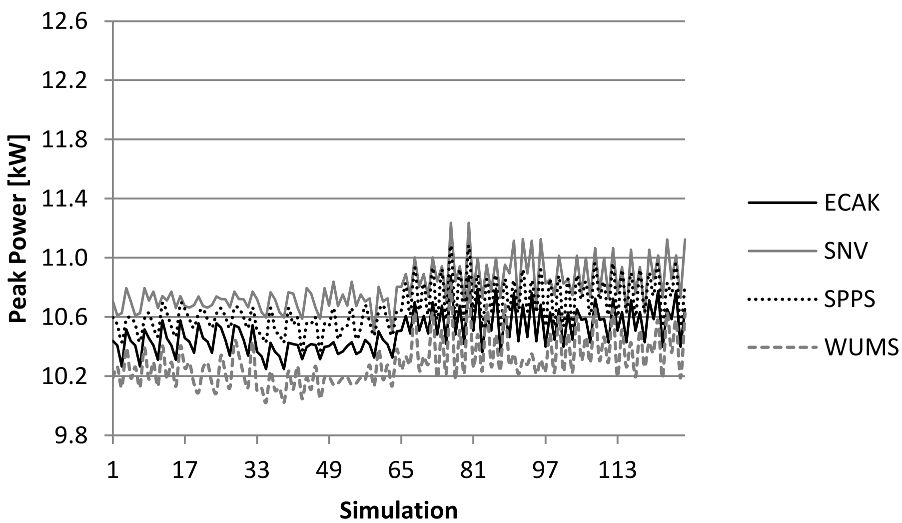

Figure 82: The average summer Proposed Physically-Based Residential-Energy-Management-System Simulation [PPRS] smart appliance scheduling [SAS] Scenario C peak power.

The average winter and summer PPRS SAS Scenario C peak power shown in Figure 81 and Figure 82, respectively, indicate the same pattern as the average winter and summer PPRS SAS Scenario A peak power.

The effect of the various smart appliances in the average seasonal PPRS SAS Scenario C peak power is between 3.9% (0.3 kW) increase and 2.5% (0.2 kW) decrease in the winter and between 5.0% (0.5 kW) increase and 1.9% (0.2 kW) decrease in the summer, compared to the respective average seasonal PPRS SAS Scenario C Simulation 1 (no smart appliances) peak power. Notice, the average winter (summer) PPRS Scenario C Simulation 1 peak power is 8.5 kW (10.5 kW).

The average winter and summer PPRS SAS Scenario D peak power for each smart appliance permutation simulation is shown in Figure 83 and Figure 84, respectively.

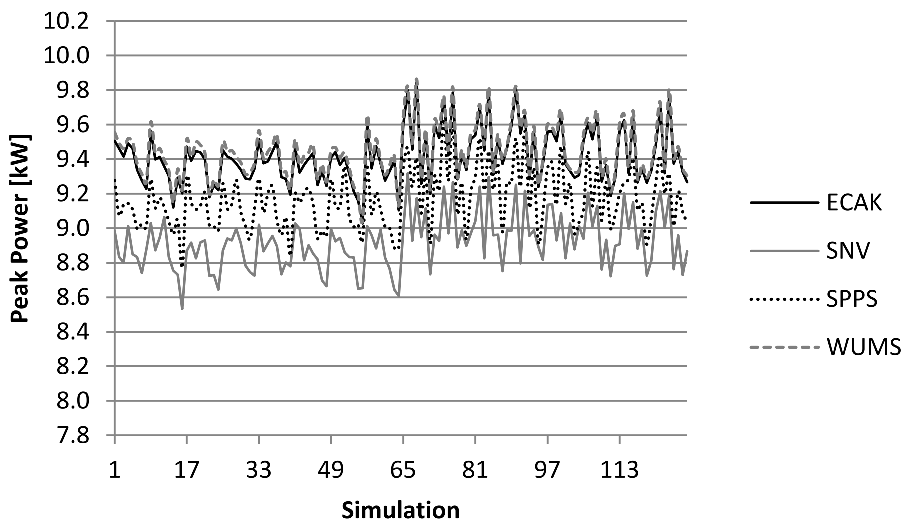

Figure 83: The average winter Proposed Physically-Based Residential-Energy-Management-System Simulation [PPRS] smart appliance scheduling [SAS] Scenario D peak power.

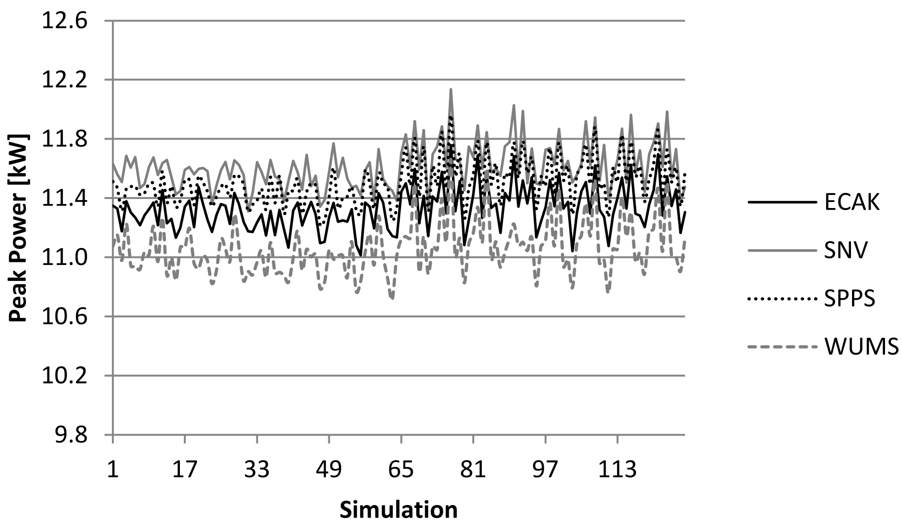

Figure 84: The average summer Proposed Physically-Based Residential-Energy-Management-System Simulation [PPRS] smart appliance scheduling [SAS] Scenario D peak power.

The average winter and summer PPRS SAS Scenario D peak power shown in Figure 83 and Figure 84, respectively, indicate the same pattern as the average winter and summer PPRS SAS Scenario A peak power.

The effect of the various smart appliances in the average seasonal PPRS SAS Scenario D peak power is between 3.6% (0.3 kW) increase and 5.2% (0.5 kW) decrease in the winter and between 4.3% (0.5 kW) increase and 2.9% (0.3 kW) decrease in the summer, compared to the respective average seasonal PPRS SAS Scenario D Simulation 1 (no smart appliances) peak power. Notice, the average winter (summer) PPRS SAS Scenario D Simulation 1 peak power is 9.3 kW (11.4 kW).

The average winter and summer PPRS SAS Scenario A DR energy for each smart appliance permutation simulation is shown in Figure 85 and Figure 86, respectively.

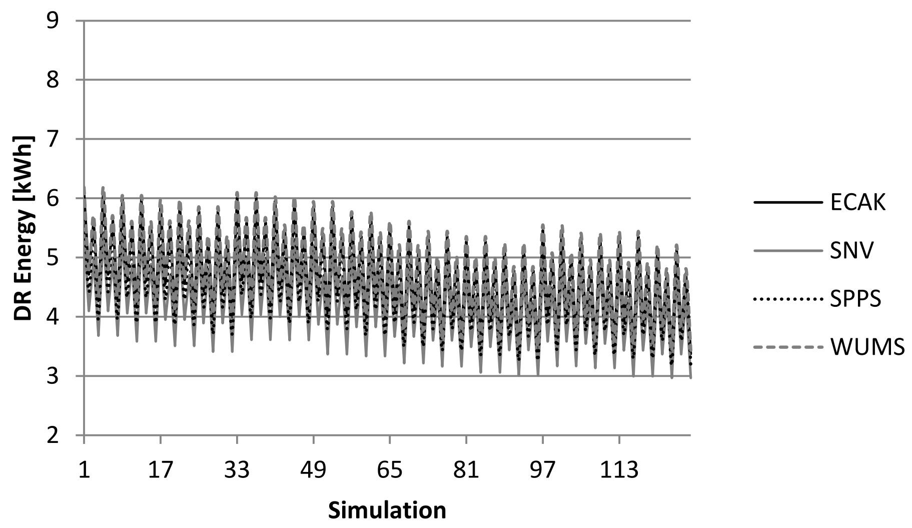

Figure 85: The average winter Proposed Physically-Based Residential-Energy-Management-System Simulation [PPRS] smart appliance scheduling [SAS] Scenario A DR energy.

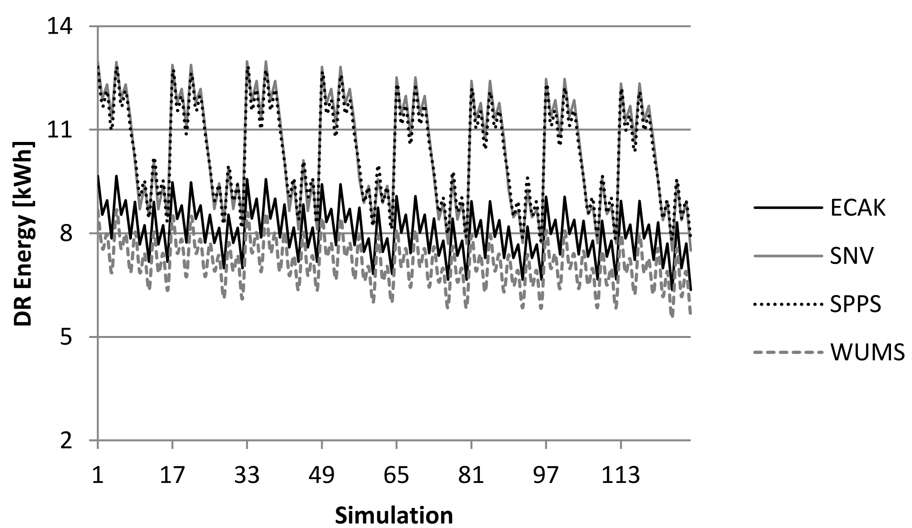

Figure 86: The average summer Proposed Physically-Based Residential-Energy-Management-System Simulation [PPRS] smart appliance scheduling [SAS] Scenario A DR energy.

The average winter and summer PPRS SAS Scenario A DR energy shown in Figure 85 and Figure 86, respectively, indicate that the number of smart appliances is inversely proportional to the average winter and summer PPRS SAS Scenario A DR energy. Different combinations of smart appliances achieved the minimum DR energy for the different distributed energy resource scenarios, power system areas, and seasons.

For the average winter and summer PPRS SAS Scenario A the minimum DR energy was observed in Simulation 124 (CD, CW, Dw, HVAC, Ref, and WH).

The effect of the various smart appliances in the average seasonal PPRS SAS Scenario A DR energy is between less than 0.1% (less than 0.1 kWh) increase and 45.0% (2.7 kWh) decrease in the winter and between less than 0.1% (less than 0.1 kWh) increase and 37.8% (4.2 kWh) decrease in the summer, compared to the respective average seasonal PPRS SAS Scenario A Simulation 1 (no smart appliances) DR energy. Notice, the average winter (summer) PPRS Scenario A Simulation 1 DR energy is 5.9 kWh (11.0 kWh).

The average winter and summer PPRS SAS Scenario B DR energy for each smart appliance permutation simulation is shown in Figure 87 and Figure 88, respectively.

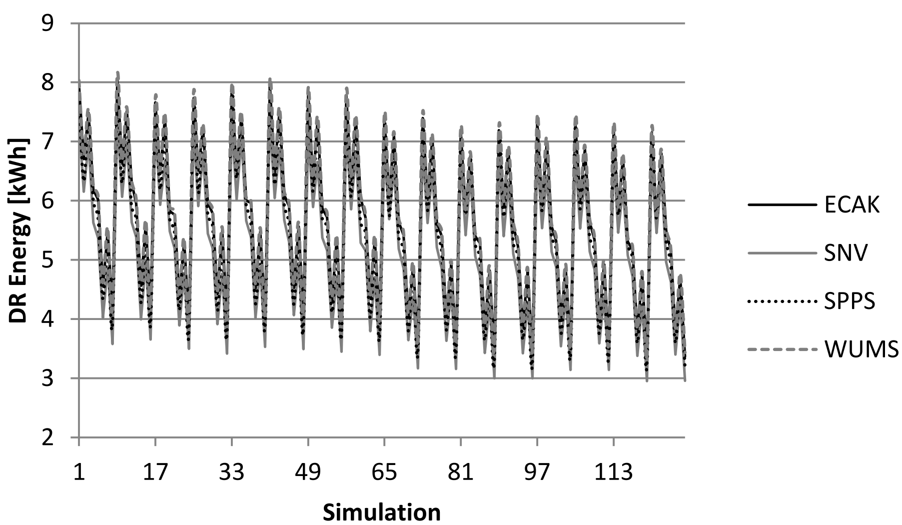

Figure 87: The average winter Proposed Physically-Based Residential-Energy-Management-System Simulation [PPRS] smart appliance scheduling [SAS] Scenario B demand response [DR] energy.

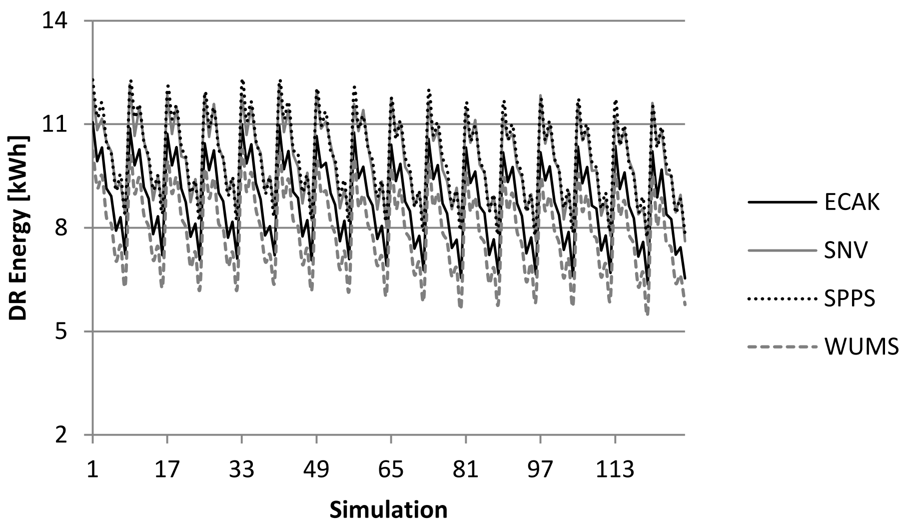

Figure 88: The average summer Proposed Physically-Based Residential-Energy-Management-System Simulation [PPRS] smart appliance scheduling [SAS] Scenario B demand response [DR] energy.

The average winter and summer PPRS SAS Scenario B DR energy shown in Figure 87 and Figure 88, respectively, depict the same pattern as the average winter and summer PPRS SAS Scenario A DR energy. Different combinations of smart appliances achieved the minimum DR energy for the different distributed energy resource scenarios, power system areas, and seasons. For the average winter and summer PPRS SAS Scenario B the minimum DR energy was observed in Simulation 120 (CD, CW, Dw, PEV, Ref, and WH); except for the SPPS power system area PPRS SAS Scenario B winter, the minimum DR energy was observed in Simulation 128 (all smart appliances).

The effect of the various smart appliances in the average seasonal PPRS SAS Scenario B DR energy is between 0.7% (0.1 kWh) increase and 58.6% (4.6 kWh) decrease in the winter and between 0.5% (0.1 kWh) increase and 40.5% (4.6 kWh) decrease in the summer, compared to the respective average seasonal PPRS SAS Scenario B Simulation 1 (no smart appliances) DR energy. Notice, the average winter (summer) PPRS Scenario B Simulation 1 DR energy is 7.8 kWh (11.4 kWh).

The average winter and summer PPRS SAS Scenario C DR energy for each smart appliance permutation simulation is shown in Figure 89 and Figure 90, respectively.

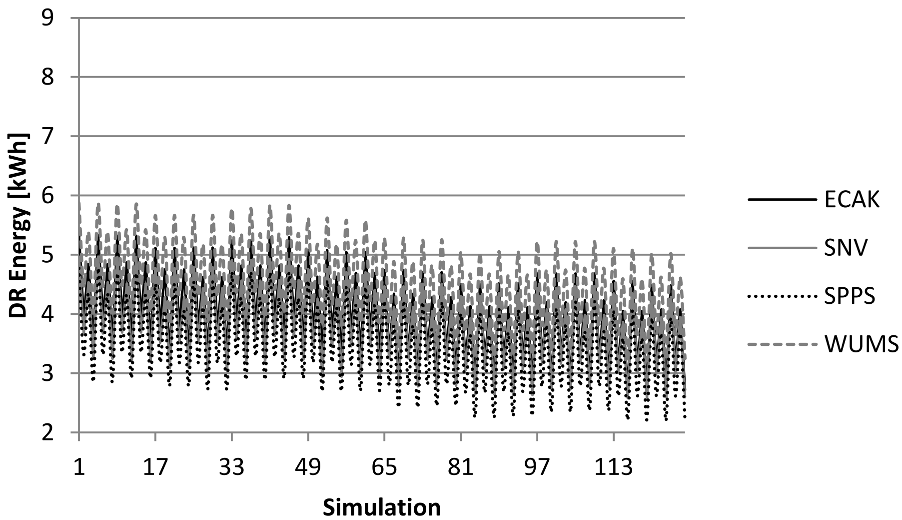

Figure 89: The average winter Proposed Physically-Based Residential-Energy-Management-System Simulation [PPRS] smart appliance scheduling [SAS] Scenario C demand response [DR] energy.

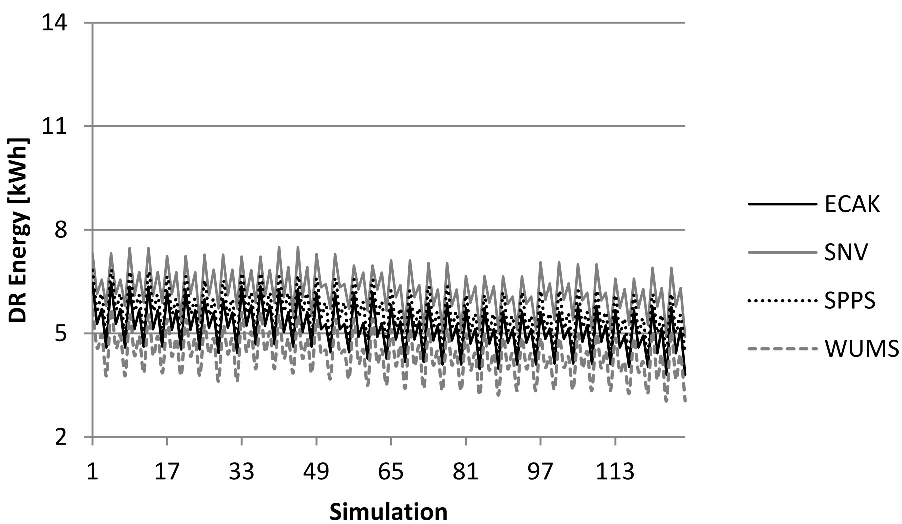

Figure 90: The average summer Proposed Physically-Based Residential-Energy-Management-System Simulation [PPRS] smart appliance scheduling [SAS] Scenario C demand response [DR] energy.

The average winter and summer PPRS SAS Scenario C winter and summer average DR energy shown in Figure 87 and Figure 88, respectively, depict the same pattern as the average winter and summer PPRS SAS Scenario A DR energy. Different combinations of smart appliances achieved the minimum DR energy for the different distributed energy resource scenarios, power system areas, and seasons. For the average winter and summer PPRS SAS Scenario C the minimum DR energy was observed in Simulation 116 (CD, CW, Dw, Ref, and WH) for ECAK, SNV, and WUMS winter and SPPS summer and Simulation 124 (CD, CW, Dw, Ref, HVAC, and WH) for SPPS winter and ECAK, SNV, and WUMS summer.

The effect of the various smart appliances in the average seasonal PPRS SAS Scenario C DR energy is between less than 0.1% (less than 0.1 kWh) increase and 49.4% (2.6 kWh) decrease in the winter and between 0.6% (less than 0.1 kWh) increase and 31.9% (2.5 kWh) decrease in the summer, compared to the respective average seasonal PPRS SAS Scenario C Simulation 1 (no smart appliances) DR energy. Notice, the average winter (summer) PPRS Scenario C Simulation 1 DR energy is 5.2 kWh (6.6 kWh).

The average winter and summer PPRS SAS Scenario D average DR energy for each smart appliance permutation simulation is shown in Figure 91 and Figure 92, respectively.

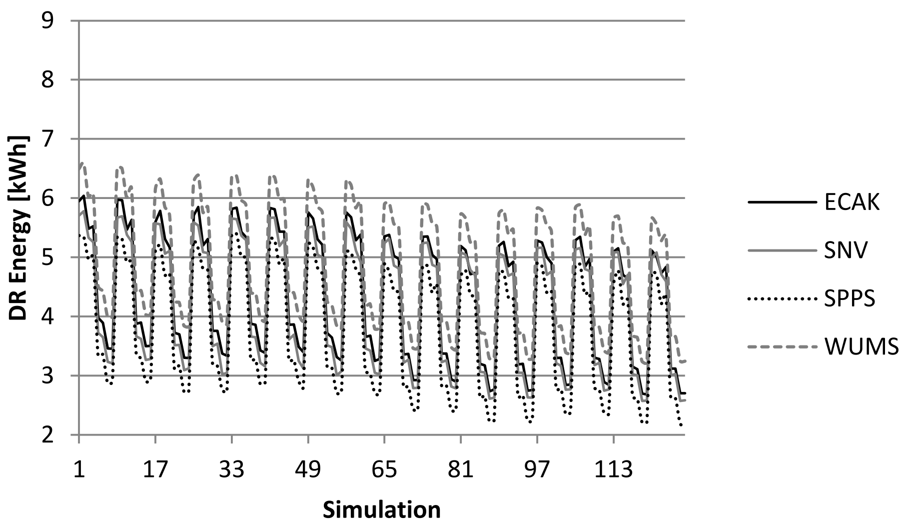

Figure 91: The average winter Proposed Physically-Based Residential-Energy-Management-System Simulation [PPRS] smart appliance scheduling [SAS] Scenario D demand response [DR] energy.

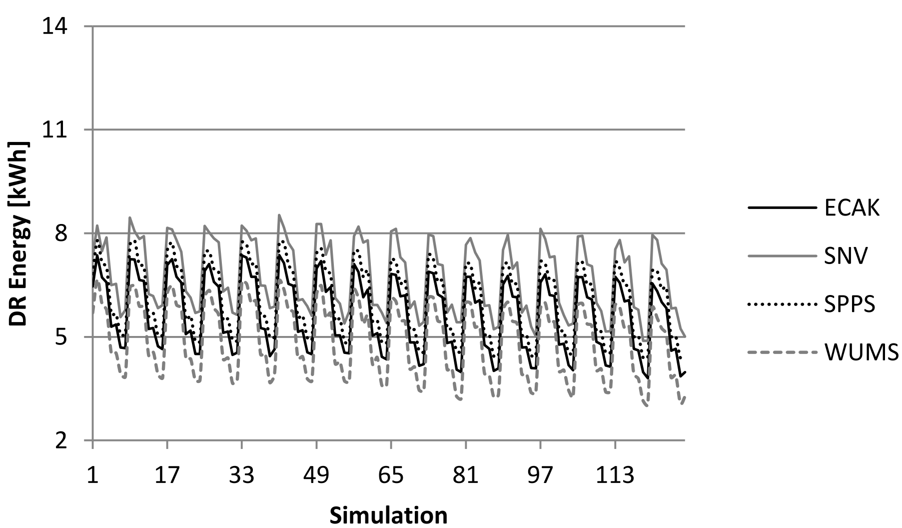

Figure 92: The average summer Proposed Physically-Based Residential-Energy-Management-System Simulation [PPRS] smart appliance scheduling [SAS] Scenario D demand response [DR] energy.

The average winter and summer PPRS SAS Scenario D DR energy shown in Figure 91 and Figure 92, respectively, depict the same pattern as the average winter and summer PPRS SAS Scenario A DR energy. Different combinations of smart appliances achieved the minimum DR energy for the different distributed energy resource scenarios, power system areas, and seasons. For the average winter and summer PPRS SAS

Scenario D the minimum DR energy was observed in Simulation 116 (CD, CW, Dw, Ref, and WH) for ECAK, SNV, and WUMS winter and SPPS summer and Simulation 124 (CD, CW, Dw, HVAC, Ref, and WH) for SPPS winter and ECAK, SNV, and WUMS summer. Notice, the same PPRS SAS minimum DR energy for the PPRS SAS Scenario D was observed as in Scenario B.

The effect of the various smart appliances in the average seasonal PPRS SAS Scenario D DR energy is between 0.8% (0.1 kWh) increase and 63.2% (4.6 kWh) decrease in the winter and between 0.6% (0.1. kWh) increase and 53.5% (4.6 kWh) decrease in the summer, compared to the respective average seasonal PPRS SAS Scenario D Simulation 1 (no smart appliances) DR energy. Notice, the average winter PPRS SAS Scenario D Simulation 1 DR energy is 7.2 kWh (8.6 kWh).

Next is a presentation of the PPRS smart appliance scheduling with a stationary battery results.

4.7 Smart Appliance Scheduling with a Stationary Battery

In the Proposed Physically-Based Residential-Energy-Management-System Simulation (PPRS) smart appliance scheduling with a stationary battery (SASB) energy management function the use of the smart appliances (clothes washer [CW]; clothes dryer [CD]; dishwasher [Dw]; heating, ventilation, and air conditioning [HVAC]; plug-in electric vehicle [PEV], and refrigerator [Ref]) can be delayed if the smart appliance is scheduled to start before (such that the smart appliance will continue to operate during the demand response [DR] period) or during the DR period. Further, a battery dispatching function is added to the appliance rescheduling in the PPRS smart appliance scheduling (SAS) energy management function. The stationary battery is dispatched during the DR period. The battery output is limited to 120 V and 15 A (1.8 kW). The battery capacity is 4.8 kWh. The battery is scheduled to charge at 4a. Again, each PPRS SASB result is shown for each power system area (Versailles Kentucky [ECAK], Mercury Nevada [SNV], Stillwater Oklahoma [SPPS], and Necedah Wisconsin [WUMS]).

The average winter and summer PPRS SASB Scenario A daily energy for each smart appliance permutation simulation is shown in Figure 93 and Figure 94, respectively.

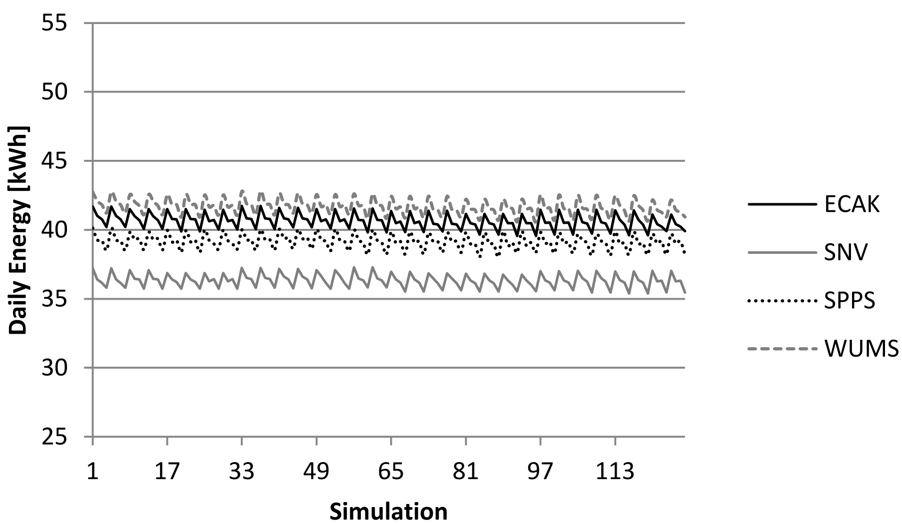

Figure 93: The average winter Proposed Physically-Based Residential-Energy-Management-System Simulation [PPRS] smart appliance scheduling with a stationary battery [SASB] Scenario A daily energy.

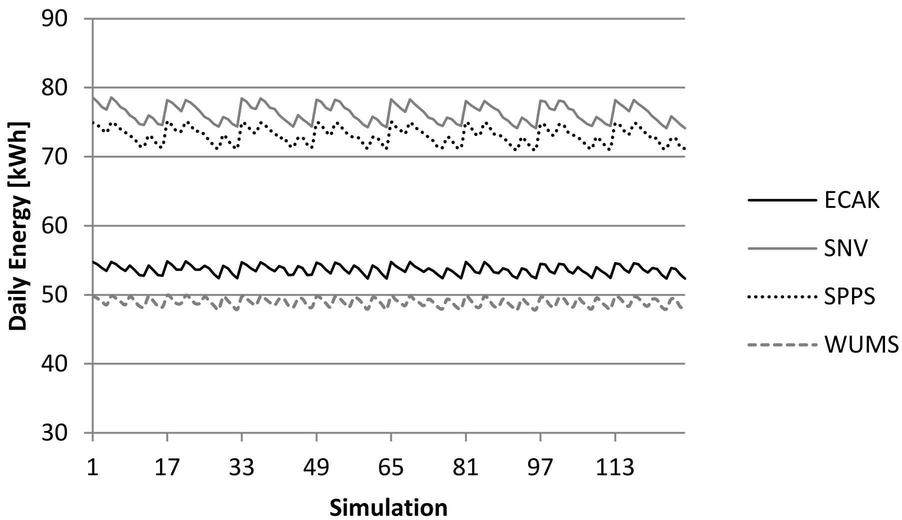

Figure 94: The average summer Proposed Physically-Based Residential-Energy-Management-System Simulation [PPRS] smart appliance scheduling with a stationary battery [SASB] Scenario A daily energy.

The average winter and summer PPRS SASB Scenario A daily energy shown in Figure 93 and Figure 94, respectively, depict the same pattern as the average winter and summer PPRS SAS Scenario A daily energy. The pattern with the winter and summer average daily energy is that the WH, Ref, and PEV intelligence has the most significant impact on the daily energy use due to unserviced energy.

The effect of the various smart appliances in the average seasonal PPRS SASB Scenario A daily energy is between 0.1% (less than 0.1 kWh) increase and 5.0% (2.0 kWh) decrease in the winter and between 0.1% (0.1 kWh) increase and 4.8% (3.2 kWh) decrease in the summer, compared to the respective average seasonal PPRS SASB Scenario A Simulation 1 (no smart appliances) daily energy. Notice, the average winter (summer) PPRS SASB Scenario A Simulation 1 daily energy use is 40.4 kWh (64.5 kWh).

The average winter and summer PPRS SASB Scenario B daily energy for each smart appliance permutation simulation is shown in Figure 95 and Figure 96, respectively.

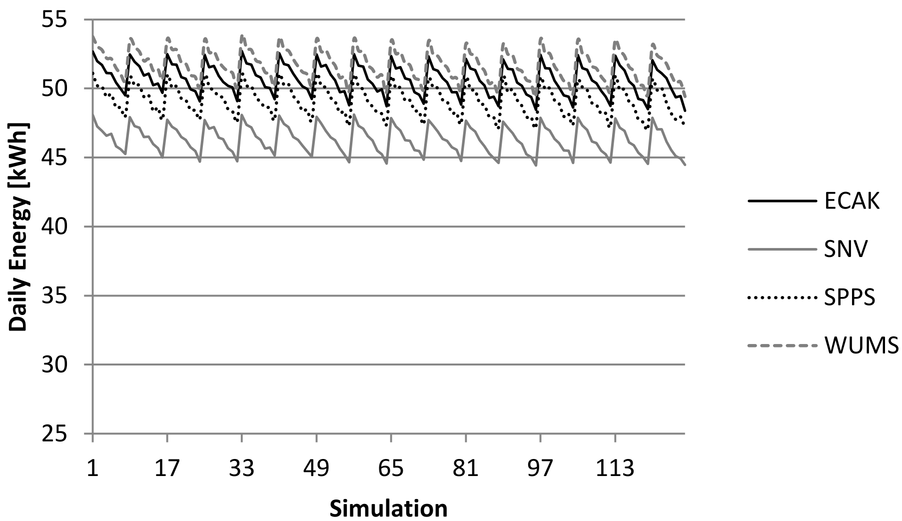

Figure 95: The average winter Proposed Physically-Based Residential-Energy-Management-System Simulation [PPRS] smart appliance scheduling with a stationary battery [SASB] Scenario B daily energy.

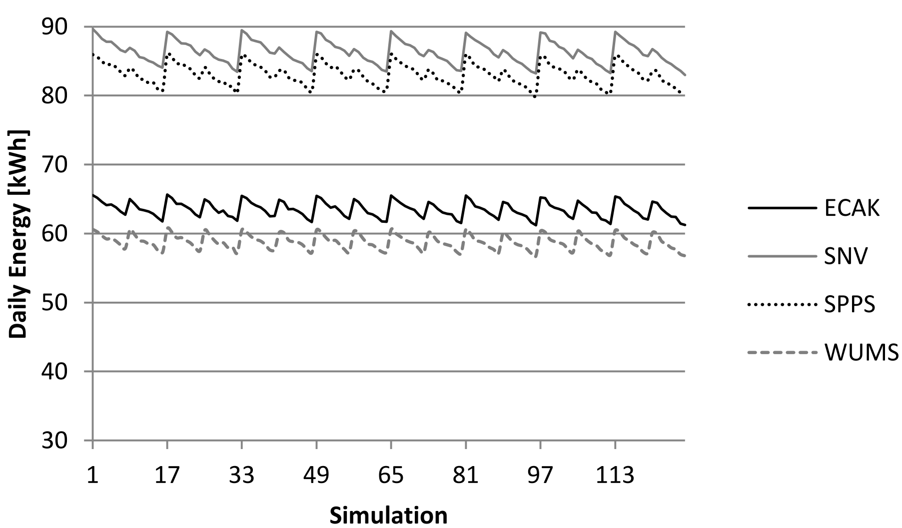

Figure 96: The average summer Proposed Physically-Based Residential-Energy-Management-System Simulation [PPRS] smart appliance scheduling with a stationary battery [SASB] Scenario B daily energy.

The average winter and summer PPRS SASB Scenario B daily energy shown in Figure 95 and Figure 96, respectively, depict the same pattern as the average winter and summer PPRS SAS Scenario A daily energy.

The effect of the various smart appliances in the average seasonal PPRS SASB Scenario B daily energy is between 0.1% (less than 0.1 kWh) increase and 7.9% (4.1 kWh) decrease in the winter and between 0.1% (0.1 kWh) increase and 6.9% (5.2 kWh) decrease in the summer, compared to the respective average seasonal PPRS SASB Scenario B Simulation 1 (no smart appliances) daily energy. Notice, the average winter (summer) PPRS SASB Scenario B Simulation 1 daily energy use is 51.4 kWh in (75.4 kWh).

The average winter and summer PPRS SASB Scenario C daily energy for each smart appliance permutation simulation is shown in Figure 97 and Figure 98, respectively.

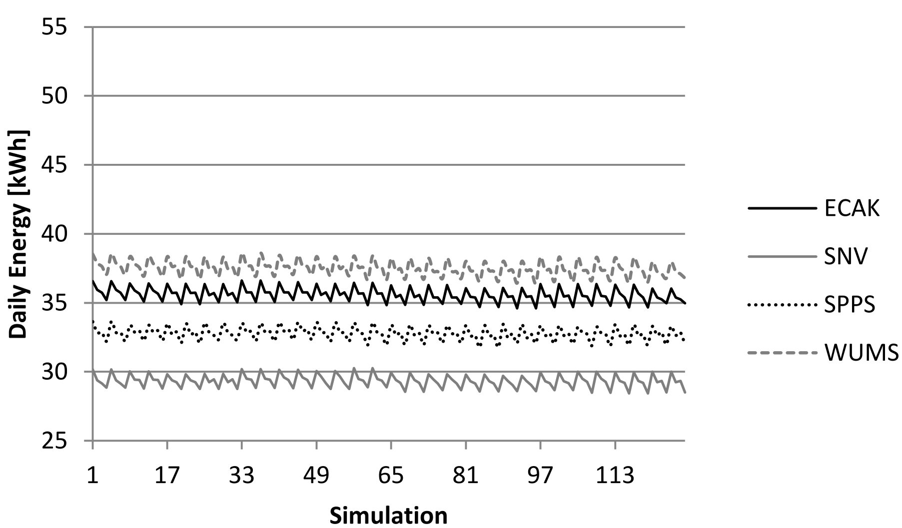

Figure 97: The average winter Proposed Physically-Based Residential-Energy-Management-System Simulation [PPRS] smart appliance scheduling with a stationary battery [SASB] Scenario C daily energy.

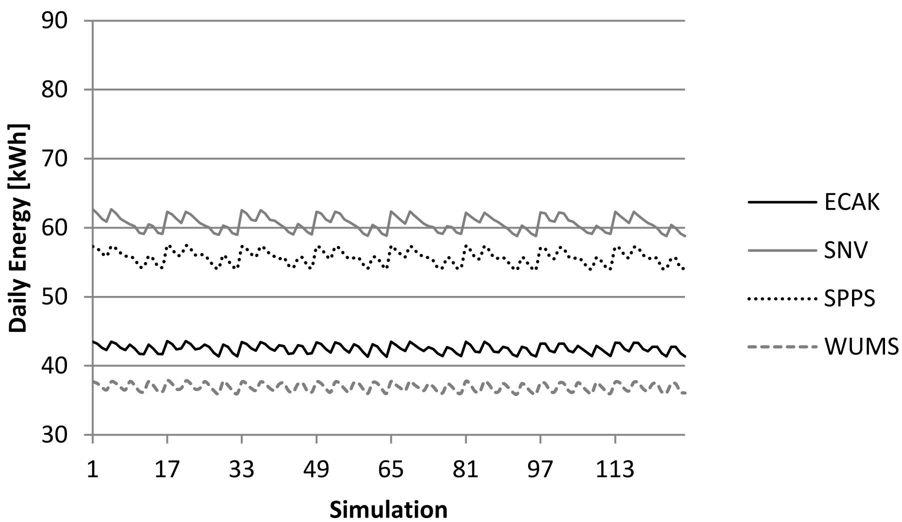

Figure 98: The average summer Proposed Physically-Based Residential-Energy-Management-System Simulation [PPRS] smart appliance scheduling with a stationary battery [SASB] Scenario C daily energy.

The average winter and summer PPRS SASB Scenario C daily energy shown in Figure 97 and Figure 98, respectively, depict the same pattern as the average winter and summer PPRS SAS Scenario A daily energy.

The effect of the various smart appliances in the average seasonal PPRS SASB Scenario C daily energy is between 0.2% (0.1 kWh) increase and 5.5% (1.9 kWh) decrease in the winter and between 0.2% (0.1 kWh) increase and 5.4% (2.8 kWh) decrease in the summer, compared to the respective average seasonal PPRS SASB Scenario A Simulation 1 (no smart appliances) daily energy. Notice, the average winter (summer) PPRS SASB Scenario C Simulation 1 daily energy use is 34.7 kWh (50.3 kWh).

The average winter and summer PPRS SASB Scenario D daily energy for each smart appliance permutation simulation is shown in Figure 99 and Figure 100, respectively.

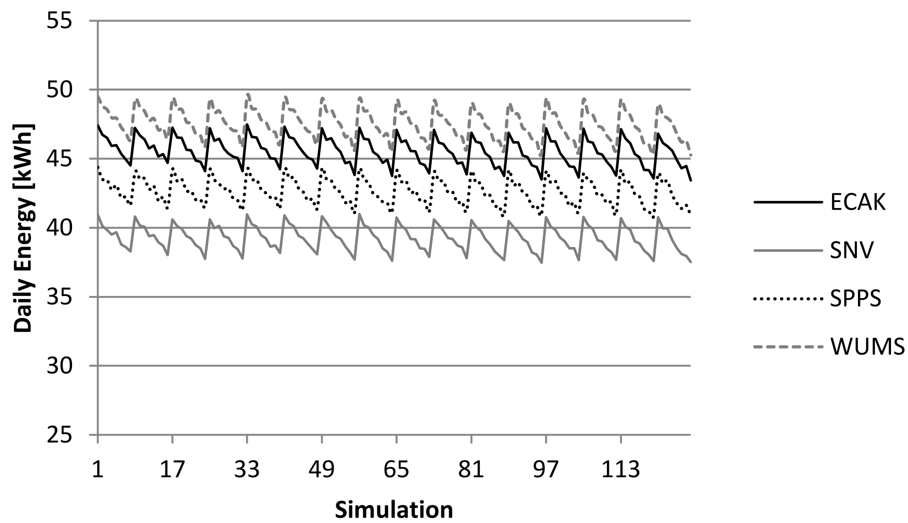

Figure 99: The average winter Proposed Physically-Based Residential-Energy-Management-System Simulation [PPRS] smart appliance scheduling with a stationary battery [SASB] Scenario D daily energy.

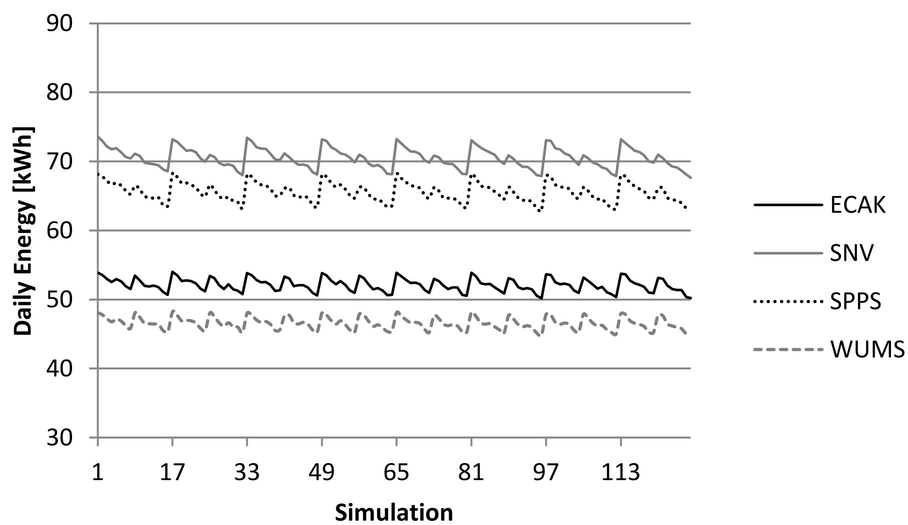

Figure 100: The average summer Proposed Physically-Based Residential-Energy-Management-System Simulation [PPRS] smart appliance scheduling with a stationary battery [SASB] Scenario D daily energy.

The average winter and summer PPRS SASB Scenario D daily energy shown in Figure 99 and Figure 100, respectively, depict the same pattern as the average winter and summer PPRS SAS Scenario A daily energy.

The effect of the various smart appliances in the average seasonal PPRS SASB Scenario D daily energy is between 0.1% (less than 0.1 kWh) increase and 8.4% (3.8 kWh) decrease in the winter and between 0.2% (0.1 kWh) increase and 7.4% (4.6 kWh) decrease in the summer, compared to the respective average seasonal PPRS SASB Scenario D Simulation 1 (no smart appliances) daily energy. Notice, the average winter (summer) PPRS SASB Scenario D Simulation 1 daily energy use is 41.2 kWh (65.4 kWh).

The average winter and summer PPRS SASB Scenario A peak power for each smart appliance permutation simulation is shown in Figure 101 and Figure 102, respectively.

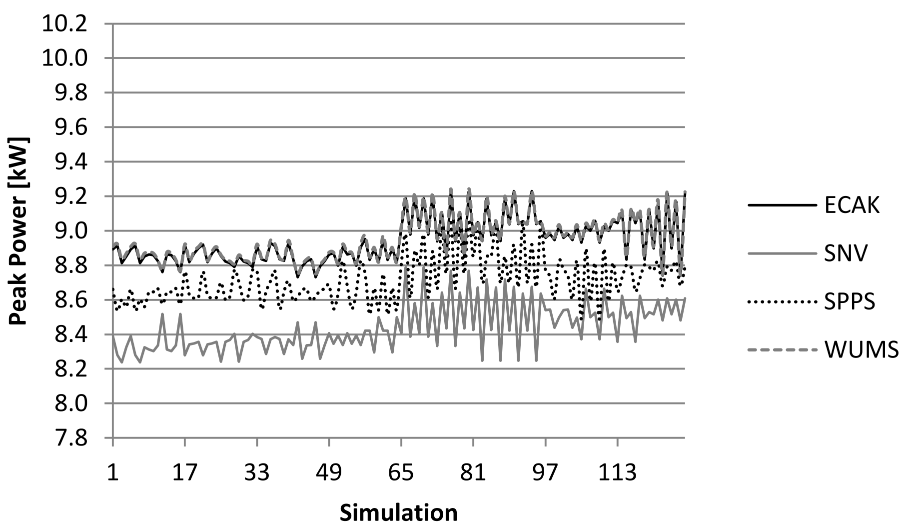

Figure 101: The average winter Proposed Physically-Based Residential-Energy-Management-System Simulation [PPRS] smart appliance scheduling with a stationary battery [SASB] Scenario A peak power.

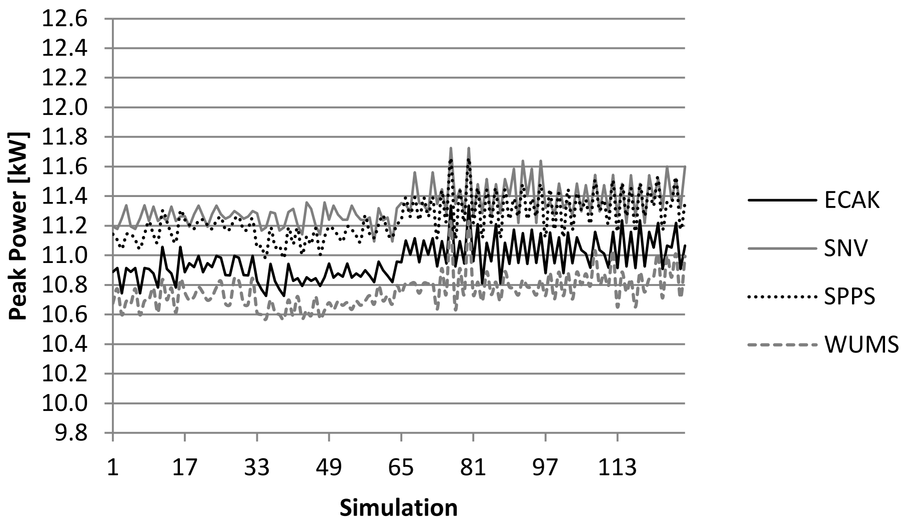

Figure 102: The average summer Proposed Physically-Based Residential-Energy-Management-System Simulation [PPRS] smart appliance scheduling with a stationary battery [SASB] Scenario A peak power.

The average winter and summer PPRS SASB Scenario A peak power shown in Figure 101 and Figure 102, respectively, indicate the same pattern as the average winter and summer PPRS SAS Scenario A power. The pattern is that the smart clothes dryer has a noticeable effect on the peak power.

The effect of the various smart appliances in the average seasonal PPRS SASB Scenario A peak power is between 4.2% (0.4 kW) increase and 1.9% (0.2 kW) decrease in the winter and between 4.7% (0.1 kW) increase and 1.2% (0.1 kW) decrease in the summer, compared to the respective average seasonal PPRS SASB Scenario A Simulation 1 (no smart appliances) peak power. Notice, the average winter (summer) PPRS SASB Scenario A Simulation 1 peak power is 8.7 kW (11.0 kW).

The average winter and summer PPRS SASB Scenario B peak power for each smart appliance permutation simulation is shown in Figure 103 and Figure 104, respectively.

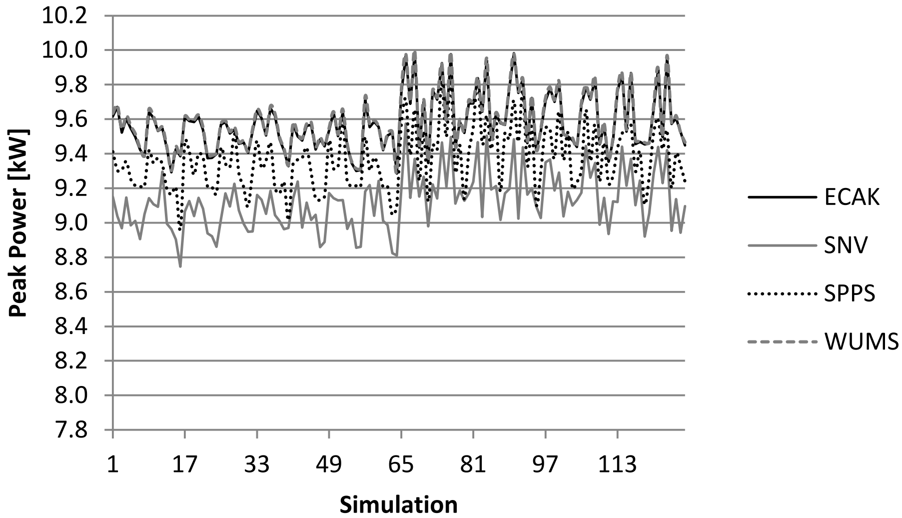

Figure 103: The average winter Proposed Physically-Based Residential-Energy-Management-System Simulation [PPRS] smart appliance scheduling with a stationary battery [SASB] Scenario B peak power.

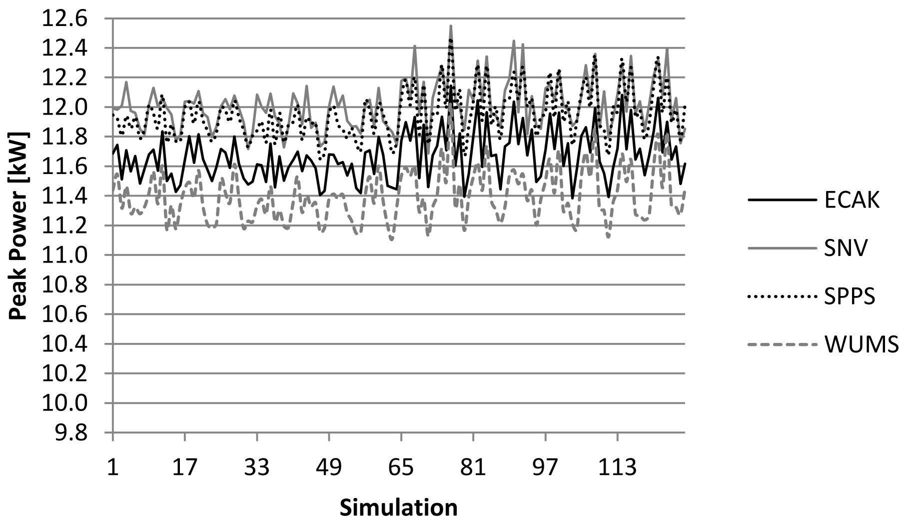

Figure 104: The average summer Proposed Physically-Based Residential-Energy-Management-System Simulation [PPRS] smart appliance scheduling with a stationary battery [SASB] Scenario B peak power.

The average winter and summer PPRS SASB Scenario B peak power shown in Figure 103 and Figure 104, respectively, indicate the same pattern as the average winter and summer PPRS SAS Scenario A peak power.

The effect of the various smart appliances in the average seasonal PPRS SASB Scenario B peak power is between 4.2% (0.4 kW) increase and 4.0% (0.4 kW) decrease in the winter and between 4.5% (0.5 kW) increase and 2.6% (0.3 kW) decrease in the summer, compared to the respective average seasonal PPRS SASB Scenario B Simulation 1 (no smart appliances) peak power. Notice, the average winter (summer) PPRS SASB Scenario B Simulation 1 peak power is 9.5 kW (11.8 kW).

The average winter and summer PPRS SASB Scenario C peak power for each smart appliance permutation simulation is shown in Figure 105 and Figure 106, respectively.

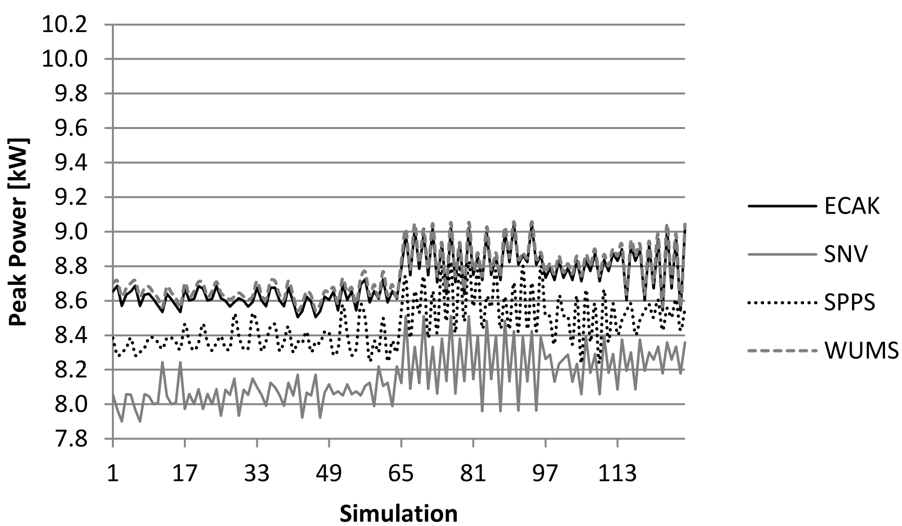

Figure 105: The average winter Proposed Physically-Based Residential-Energy-Management-System Simulation [PPRS] smart appliance scheduling with a stationary battery [SASB] Scenario C peak power.

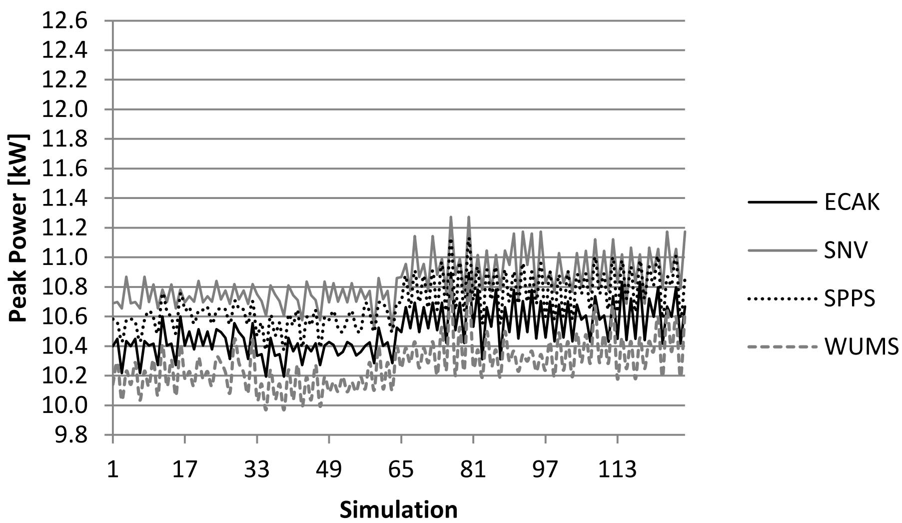

Figure 106: The average summer Proposed Physically-Based Residential-Energy-Management-System Simulation [PPRS] smart appliance scheduling with a stationary battery [SASB] Scenario C peak power.

The average winter and summer PPRS SASB Scenario C peak power shown in Figure 105 and Figure 106, respectively, indicate the same pattern as the average winter and summer PPRS SAS Scenario A peak power.

The effect of the various smart appliances in the average seasonal PPRS SASB Scenario C peak power is between 4.9% (0.4 kW) increase and 1.8% (0.2 kW) decrease in the winter and between 5.6% (0.6 kW) increase and 1.8% (0.2 kW) decrease in the summer, compared to the respective average seasonal PPRS SASB Scenario C Simulation 1 (no smart appliances) peak power. Notice, the average winter (summer) PPRS SASB Scenario C Simulation 1 peak power is 8.4 kW (10.5 kW).

The average winter and summer PPRS SASB Scenario D peak power for each smart appliance permutation simulation is shown in Figure 107 and Figure 108, respectively.

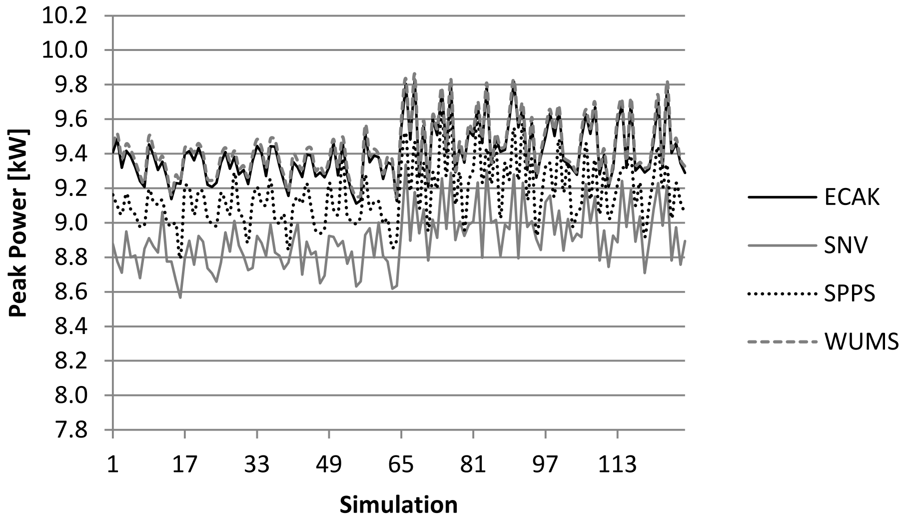

Figure 107: The average winter Proposed Physically-Based Residential-Energy-Management-System Simulation [PPRS] smart appliance scheduling with a stationary battery [SASB] Scenario D peak power.

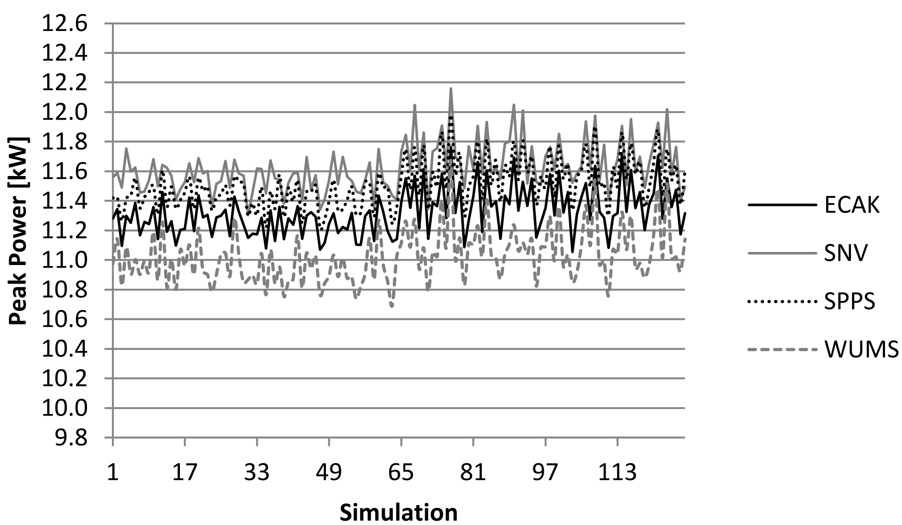

Figure 108: The average summer Proposed Physically-Based Residential-Energy-Management-System Simulation [PPRS] smart appliance scheduling with a stationary battery [SASB] Scenario D peak power.

The average winter and summer PPRS SASB Scenario D peak power shown in Figure 107 and Figure 108, respectively, indicate the same pattern as the average winter and summer PPRS SAS Scenario A peak power.

The effect of the various smart appliances in the average seasonal PPRS SASB Scenario D peak power is between 4.8% (0.4 kW) increase and 3.5% (0.3 kW) decrease in the winter and between 5.2% (0.6 kW) increase and 2.1% (0.2 kW) decrease in the summer, compared to the respective average seasonal PPRS SASB Scenario D Simulation 1 (no smart appliances) peak power. Notice, the average winter (summer) PPRS SASB Scenario D Simulation 1 peak power is 8.8 kW (11.1 kW).

The average winter and summer PPRS SASB Scenario A DR energy for each smart appliance permutation simulation is shown in Figure 109 and Figure 110, respectively.

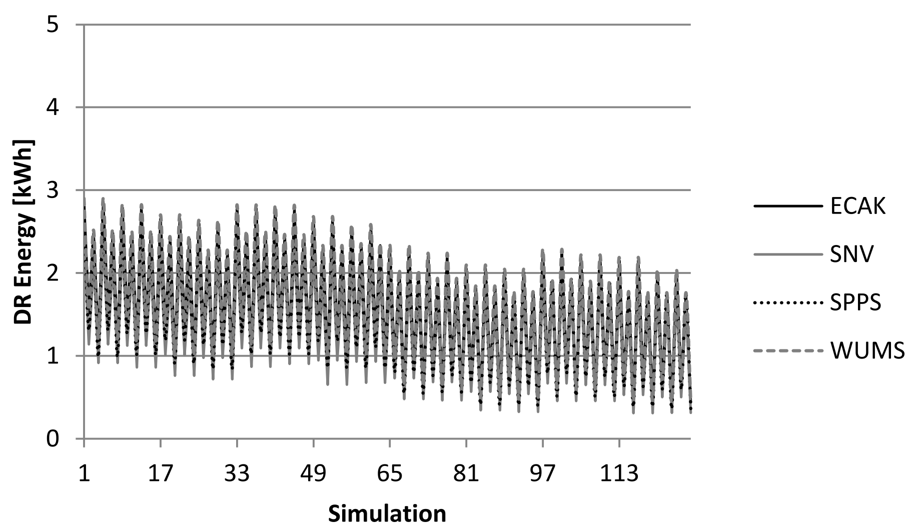

Figure 109: The average winter Proposed Physically-Based Residential-Energy-Management-System Simulation [PPRS] smart appliance scheduling with a stationary battery [SASB] Scenario A demand response [DR] energy.

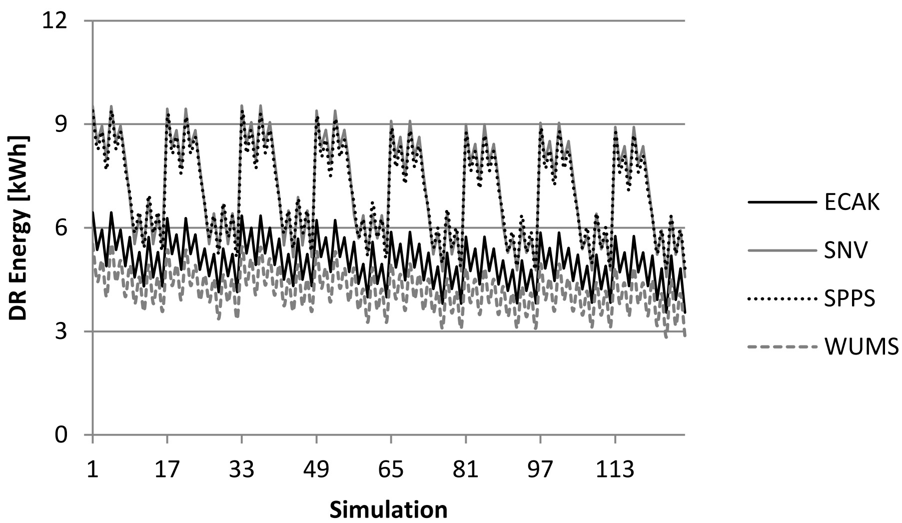

Figure 110: The average summer Proposed Physically-Based Residential-Energy-Management-System Simulation [PPRS] smart appliance scheduling with a stationary battery [SASB] Scenario A demand response [DR] energy.

The average winter and summer PPRS SASB Scenario A DR energy shown in Figure 109 and Figure 110, respectively, depict the same pattern as the average winter and summer PPRS SAS Scenario A DR energy. The pattern with the average winter and summer PPRS SAS Scenario A DR energy is that the number of smart appliances is inversely proportional to the average DR energy. Different combinations of smart appliances achieved the minimum DR energy for the different distributed energy resource scenarios, power system areas, and seasons. For the average winter and summer PPRS SASB Scenario A the minimum DR energy was observed in Simulation 124 (CD; CW; Dw; heating, ventilation, and air conditioning; Ref; and WH); except for the SNV power system area PPRS SASB Scenario A winter, the minimum DR energy was observed in Simulation 116 (CD, CW, Dw, Ref, and WH).

The effect of the various smart appliances in the average seasonal PPRS SASB Scenario A DR energy is between less than 0.1% (less than 0.1 kWh) increase and 85.7% (2.3 kWh) decrease in the winter and between less than 0.1% (less than 0.1 kWh) increase and 48.6% (3.8 kWh) decrease in the summer, compared to the respective average seasonal PPRS SASB Scenario A Simulation 1 (no smart appliances) DR energy. Notice, the average winter (summer) PPRS SASB Scenario A Simulation 1 DR energy is 2.7 kWh (7.7 kWh).

The average winter and summer PPRS SASB Scenario B DR energy for each smart appliance permutation simulation is shown in Figure 111 and Figure 112, for the DR energy, respectively.

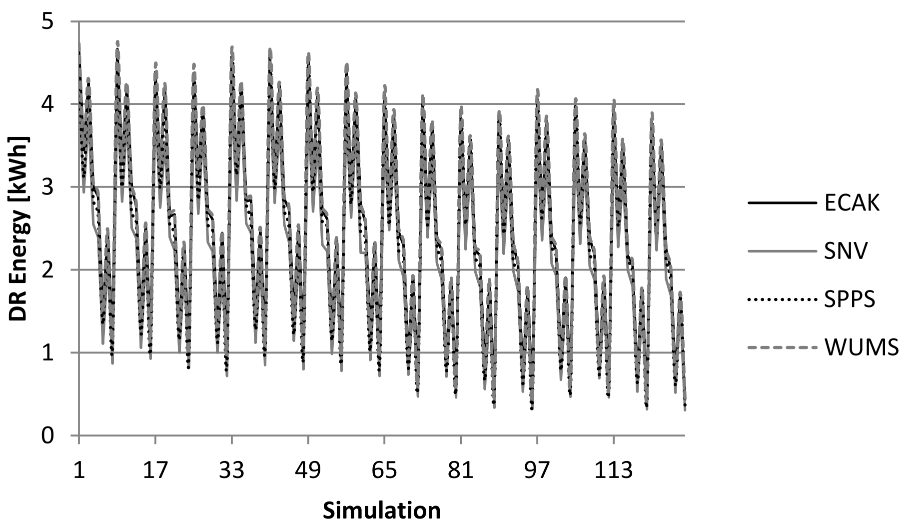

Figure 111: The average winter Proposed Physically-Based Residential-Energy-Management-System Simulation [PPRS] smart appliance scheduling with a stationary battery [SASB] Scenario B demand response [DR] energy.

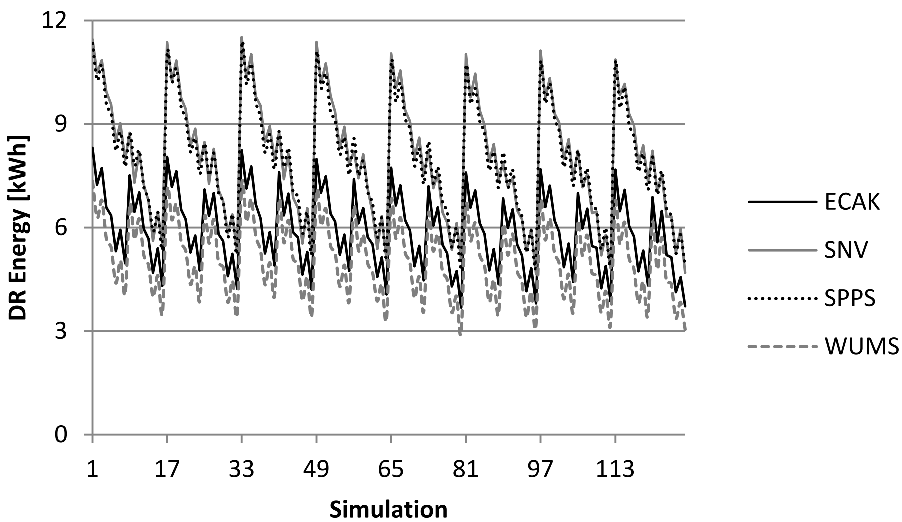

Figure 112: The average summer Proposed Physically-Based Residential-Energy-Management-System Simulation [PPRS] smart appliance scheduling with a stationary battery [SASB] Scenario B demand response [DR] energy.

The average winter and summer PPRS SASB Scenario B DR energy shown in Figure 111 and Figure 112, respectively, depict the same pattern as the average winter and summer PPRS SAS Scenario A DR energy. Different combinations of smart appliances achieved the minimum DR energy for the different distributed energy resource scenarios, power system areas, and seasons. For the average winter and summer PPRS SASB Scenario B the minimum DR energy was observed in Simulation 128 (all smart appliances); ECAK and WUMS summer the minimum DR energy was observed in Simulation 80 (CD, HVAC, PEV, Ref, and WH); and SNV summer minimum DR energy was observed in Simulation 96 (CD, Dw, HVAC, PEV, Ref, and WH).

The effect of the various smart appliances in the average seasonal PPRS SASB Scenario B DR energy is between 0.2% (less than 0.1 kWh) increase and 91.5% (4.1 kWh) decrease in the winter and between 0.1% (less than 0.1 kWh) increase and 58.0% (5.6 kWh) decrease in the summer, compared to the respective average seasonal PPRS

SASB Scenario B Simulation 1 (no smart appliances) DR energy. Notice, the average winter (summer) PPRS SASB Scenario B Simulation 1 DR energy is 4.5 kWh (9.6 kWh).

The average winter and summer PPRS SASB Scenario C DR energy for each smart appliance permutation simulation is shown in Figure 113 and Figure 114, respectively.

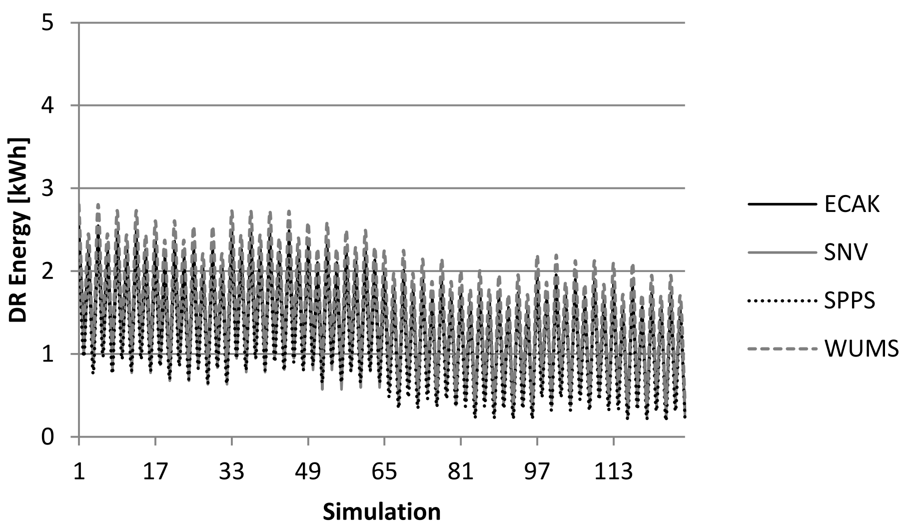

Figure 113: The average winter Proposed Physically-Based Residential-Energy-Management-System Simulation [PPRS] smart appliance scheduling with a stationary battery [SASB] Scenario C demand response [DR] energy.

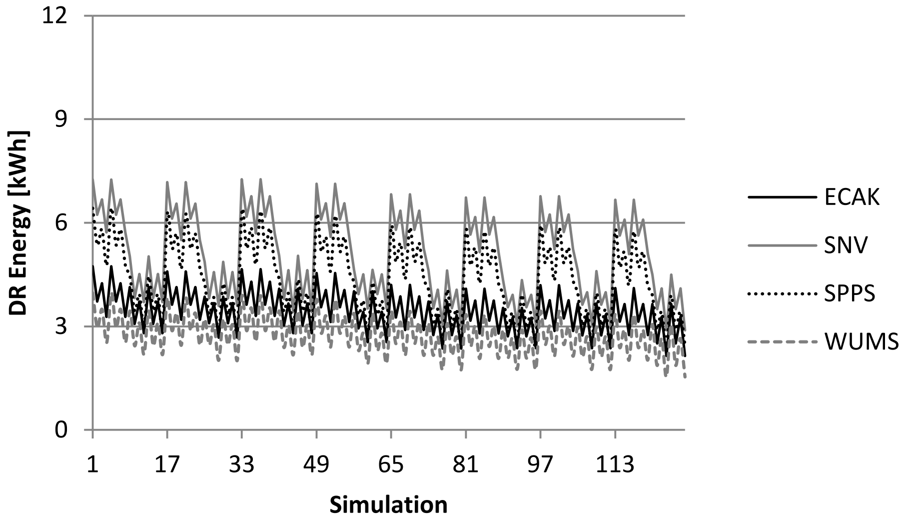

Figure 114: The average summer Proposed Physically-Based Residential-Energy-Management-System Simulation [PPRS] smart appliance scheduling with a stationary battery [SASB] Scenario C demand response [DR] energy.

The average winter and summer PPRS SASB Scenario D DR energy shown in Figure 113 and Figure 114, respectively, depict the same pattern as the average winter and summer PPRS SAS Scenario A DR energy. Different combinations of smart appliances achieved the minimum DR energy for the different distributed energy resource scenarios, power system areas, and seasons. For the average winter and summer PPRS SASB Scenario A the minimum DR energy was observed in Simulation 124 (CD, CW, Dw, HVAC, Ref, and WH); except for the SNV power system area PPRS SASB Scenario A winter, the minimum DR energy was observed in Simulation 116 (CD, CW, Dw, Ref, and WH). Notice, the same PPRS SASB minimum DR energy for Scenario C was observed as in the PPRS SASB Scenario A.

The effect of the various smart appliances in the average seasonal PPRS SASB Scenario C DR energy is between less than 0.1% (less than 0.1 kWh) increase and 88.7% (2.2 kWh) decrease in the winter and between less than 0.1% (less than 0.1 kWh) increase and 59.7% (3.3 kWh) decrease in the summer, compared to the respective average seasonal PPRS SASB Scenario C Simulation 1 (no smart appliances) DR energy. Notice, the average winter (summer) PPRS SASB Scenario C Simulation 1 DR energy is 2.5 kWh (5.6 kWh).

The average winter and summer PPRS SASB Scenario D DR energy for each smart appliance permutation simulation is shown in Figure 115 and Figure 116, respectively.

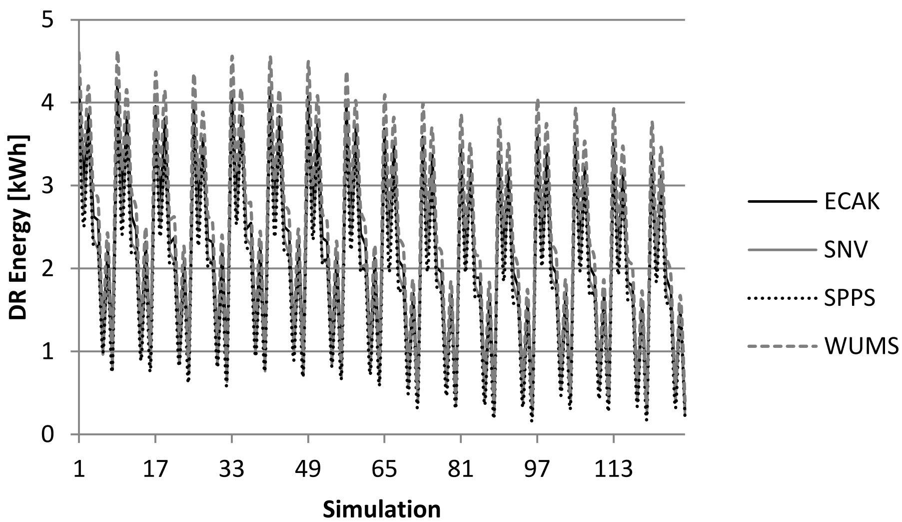

Figure 115: The average winter Proposed Physically-Based Residential-Energy-Management-System Simulation [PPRS] smart appliance scheduling with a stationary battery [SASB] Scenario D demand response [DR] energy.

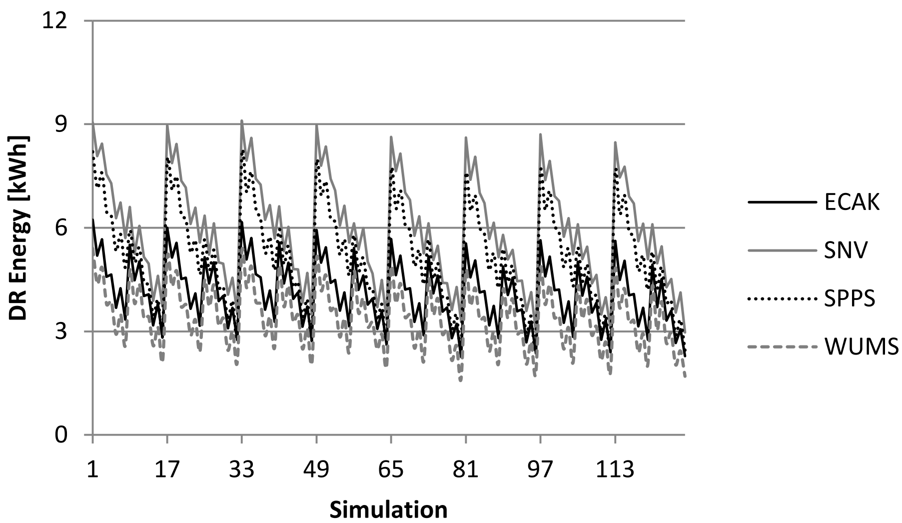

Figure 116: The average summer Proposed Physically-Based Residential-Energy-Management-System Simulation [PPRS] smart appliance scheduling with a stationary battery [SASB] Scenario D demand response [DR] energy.

The average winter and summer PPRS SASB Scenario D DR energy shown in Figure 115 and Figure 116, respectively, depict the same pattern as the average winter and summer PPRS SAS Scenario A DR energy. Different combinations of smart appliances achieved the minimum DR energy for the different distributed energy resource scenarios, power system areas, and seasons. For the average winter and summer PPRS SASB Scenario D the minimum DR energy was observed in Simulation 128 (all smart appliances); ECAK and WUMS summer the minimum DR energy was observed in Simulation 80 (CD, HVAC, PEV, Ref, and WH); and SNV summer minimum DR energy was observed in Simulation 96 (CD, Dw, HVAC, PEV, Ref, and WH). Notice, the same PPRS SASB minimum DR energy for Scenario D was observed as in the PPRS SASB Scenario B.

The effect of the various smart appliances in the average seasonal PPRS SASB Scenario D DR energy is between 0.2% (less than 0.1 kWh) increase and 93.4% (3.9 kWh) decrease in the winter and between 0.2% (less than 0.1 kWh) increase and 67.7%

(4.9 kWh) decrease in the summer, compared to the respective average seasonal PPRS SASB Scenario D Simulation 1 (no smart appliances) DR energy. Notice, the average winter (summer) PPRS SASB Scenario D Simulation 1 DR energy is 4.1 kWh (7.2 kWh).

This chapter has described the PPRS results. First, the number of independent replications was justified. Second, the PPRS BC results were presented. Third, the PPRS WH direct load control (DLC) results were presented. Fourth, the PPRS HVAC DLC results were presented. Fifth, the PPRS smart thermostat results were presented. Sixth, the PPRS SAS results were presented. Seventh, the PPRS SASB results were presented. Next is a summary of the key findings from the PPRS results.

4.8 Summary

This dissertation documents simulations of five energy management functions, testing various levels of residential energy management system (REMS) complexity. Both traditional energy management (direct load control [DLC]) and smart grid enabled energy management functions are compared. The energy use of a typical single-family residence is compared under a variety of energy management functions. Further, the use of photovoltaic (PV) and plug-in electric vehicle (PEV) distributed energy resources are considered in conjunction with the residential energy management functions.

The Proposed Physically-Based REMS Simulations (PPRS) quantifies the performance of an individual residence using a variety of energy management functions (water heater [WH] DLC; heating, ventilation, and air conditioning [HVAC] DLC; smart thermostat [ST]; smart appliance scheduling [SAS]; and smart appliance scheduling with a stationary battery [SASB]). Four power system areas of the United States are analyzed: Versailles Kentucky (ECAK), Mercury Nevada (SNV), Stillwater Oklahoma (SPPS), and

Necedah Wisconsin (WUMS). These four power system areas were selected to consist of different power system operation areas and different climate zones. Different climate zones were selected to study the impact of ambient temperature on the automated demand response (DR) ability of various energy management functions.

The following statistics were computed for each PPRS energy management function: daily energy use, peak power, and DR energy. Notice, DR energy is the daily energy use during the DR period. For the results in this chapter, the DR period was from 4p to 7p.

The PPRS base case (BC) models a typical residence with no energy management. The PPRS BC results are a baseline from which the other energy management functions results can be compared. The PPRS DLC is provided in two forms: WH and HVAC. In both of these forms, the controlled appliance (WH or HVAC) is controlled for an electric utility specified time period with limited service during this time to the specific controlled appliance only. The PPRS ST energy management function increases (for times that air conditioning is needed) or lowers (for times that heating is needed) the indoor temperature set point during the DR period. The PPRS SAS energy management function allows the smart appliances (clothes washer, clothes dryer, dishwasher, PEV, and refrigerator) to be delayed if the smart appliance is scheduled to start before (such that the smart appliance will continue to operate during the DR period) or during the DR period. The PPRS SASB adds a stationary battery dispatching function to the SAS energy management function.

In this section the results for each power system area have been averaged to summarize the PPRS results. The average winter and summer PPRS daily energy, peak power, and DR energy is the average of the respective average daily energy, peak power, and DR energy for each power system area: ECAK, SNV, SPPS, and WUMS. In the figures in this section the average PPRS SAS and SASB daily energy, peak power, and DR energy have both bars and error bars. The bars indicate the average winter and summer PPRS Simulation 128 (all smart appliances) daily energy, peak power, and DR energy averaged over each power system area, respectively. The error bars indicate the range of average PPRS SAS and SASB daily energy, peak power, and DR energy for all the permutations of the smart appliances. The SAS and SASB energy management functions were tested with all combinations of the seven smart appliances with (smart) and without communication capabilities, resulting in 128 combinations, from no smart appliances to all seven smart appliances.

A summary of the average winter and summer PPRS daily energy for all energy management functions is shown in Figure 117 and Figure 118, respectively.

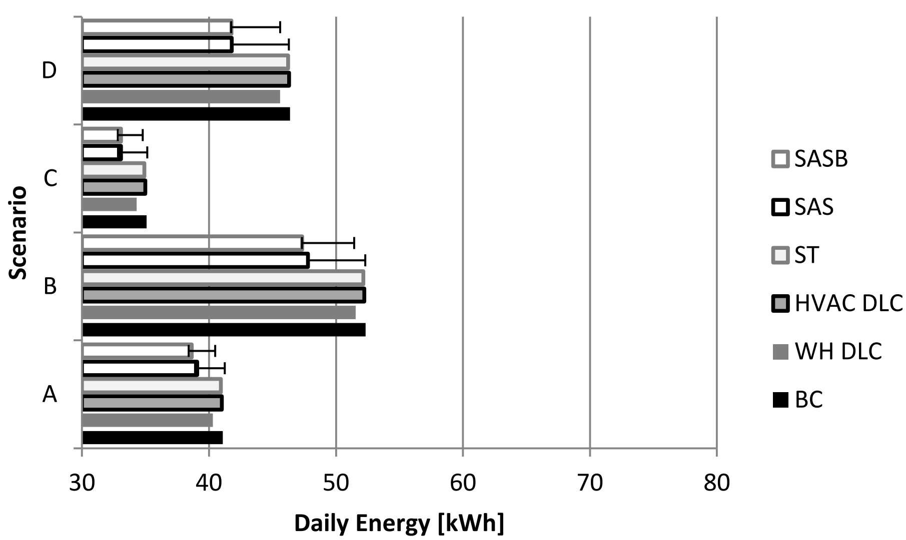

Figure 117: The average winter Proposed Physically-Based Residential-Energy-Management-System Simulation [PPRS] daily energy summary.

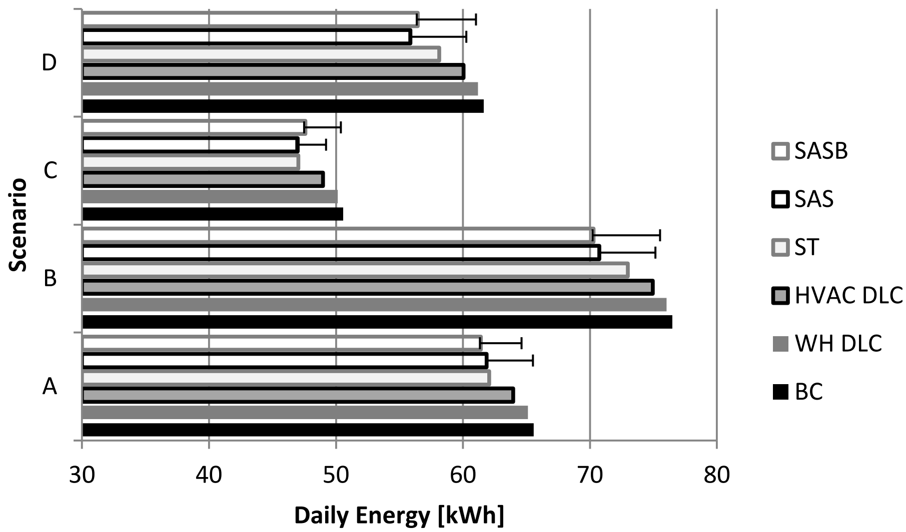

Figure 118: The average summer Proposed Physically-Based Residential-Energy-Management-System Simulation [PPRS] daily energy summary.

The impact of the energy management functions on the PPRS daily energy is highlighted in Figure 117 and Figure 118. The average winter PPRS SASB daily energy provides the most significant savings of 7.8% (3.5 kWh) across all the power system areas compared to the average winter PPRS BC daily energy. The average summer PPRS SAS daily energy results provide the most significant savings of 7.4% (4.7 kWh) across all the power system areas compared to the average summer PPRS BC daily energy. These results are representative of the payback efficiency of each energy management function; thus, the higher the energy savings, the lower the payback efficiency.

The impact of the PEV; PV; and combination of PEV and PV on the PPRS daily energy is also highlighted in Figure 117 and Figure 118. In the average winter and summer PPRS daily energy for all energy management functions, the PEV causes an increase of 25.8% (10.4 kWh) and 16.2% (10.3 kWh) compared to the average winter and summer PPRS Scenario A daily energy, respectively. In the average winter and summer

PPRS daily energy for all energy management functions, the PV causes a decrease of 14.8% (5.9 kWh) and 23.3% (14.8 kWh) compared to the average winter and summer PPRS Scenario A daily energy. In the average winter and summer PPRS daily energy for all energy management functions, the combination of PEV and PV causes 11.2% (4.5 kWh) increase and 7.0% (4.4 kWh) decrease compared to the average winter and summer PPRS Scenario A daily energy. The combination of PEV and PV is the net summation of the PPRS Scenario B and Scenario C results (where PV provides a negative contribution). Thus, there is no synergistic combined effect of the PEV and PV on the PPRS daily energy.

The PPRS SAS and SASB error bars in Figure 117 and Figure 118 indicate that the use of smart appliances result in reduction in daily energy. Specifically, the average winter and summer PPRS SAS and SASB Simulation 128 is within less that 1% of the minimum seasonal PPRS SAS and SASB daily energy for all permutations of smart appliances.

A summary of the average winter and summer PPRS peak power for all energy management functions is shown in Figure 119 and Figure 120, respectively.

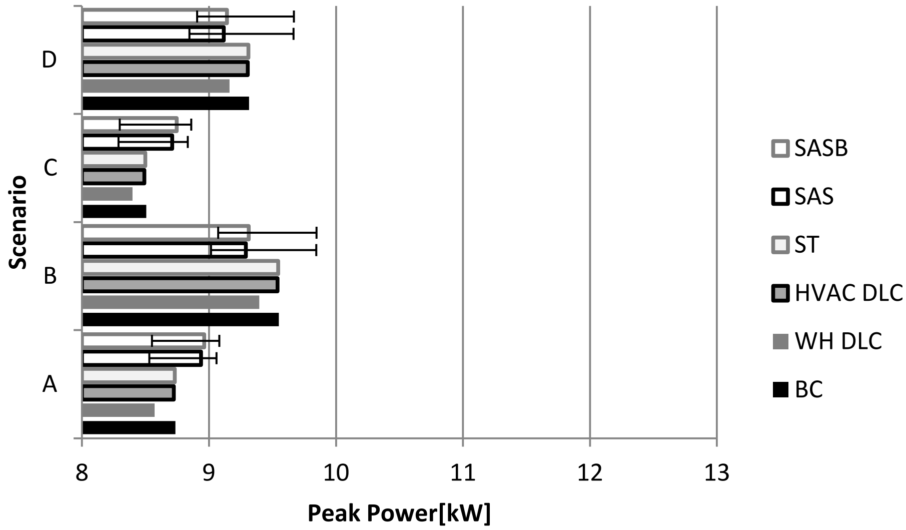

Figure 119: The average winter Proposed Physically-Based Residential-Energy-Management-System Simulation [PPRS] peak power summary.

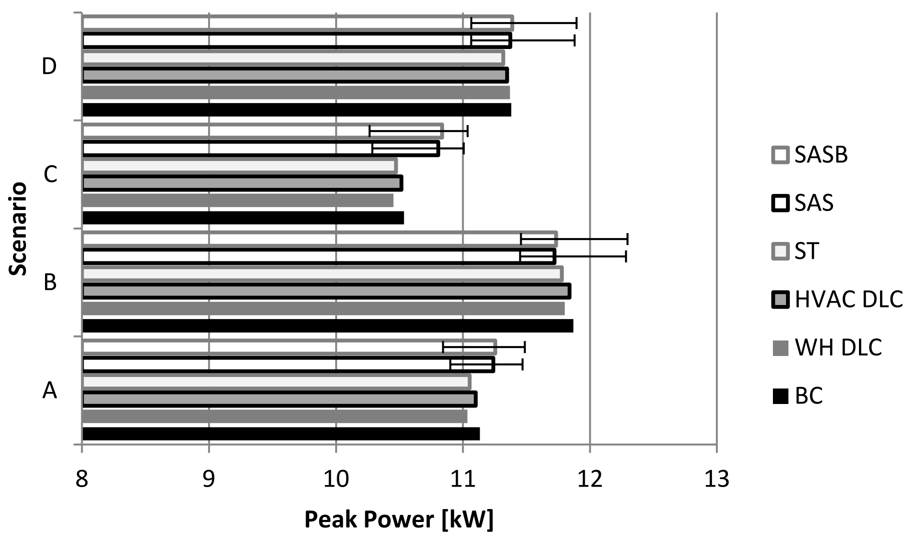

Figure 120: The average summer Proposed Physically-Based Residential-Energy-Management-System Simulation [PPRS] peak power summary.

The impact of the energy management functions on the PPRS peak power is highlighted in Figure 119 and Figure 120. The average winter PPRS WH DLC peak power provides the most significant savings of 1.6% (0.1 kW) across all the power system areas compared to the average winter PPRS BC peak power. The average summer PPRS SASB peak power provides the most significant savings of 0.7% (0.1 kW) across all the power system areas compared to the average summer PPRS BC peak power.

The impact of the PEV; PV; and combination of PEV and PV on the PPRS peak power is also highlighted in Figure 119 and Figure 120. In the average winter and summer PPRS peak power for all energy management functions, the PEV causes an increase of 7.6% (0.7 kW) and 5.9% (0.7 kW) compared to the average winter and summer PPRS Scenario A peak power, respectively. In the average winter and summer PPRS peak power for all energy management functions, the PV causes a decrease of 2.5% (0.2 kW) and 4.8% (0.5 kW) compared to the average winter and summer PPRS Scenario A peak power, respectively. In the average winter and summer PPRS peak power for all energy management functions, the combination of PEV and PV causes an increase of 5.1% (0.4 kW) and 2.0% (0.2 kW) compared to the average winter and summer PPRS Scenario A peak power, respectively. The combination of PEV and PV is the net summation of the PPRS Scenario B and Scenario C peak power (PV provides a negative contribution). Thus, there is no synergistic combined effect of the PEV and PV on the PPRS peak power.

The PPRS SAS and SASB error bars in Figure 119 and Figure 120 indicate that the use of smart appliances result in both an increase and a decrease in PPRS peak power depending on the timing of the smart appliance use. The distributions of PPRS peak power are slightly skewed towards an increase in peak power. This is due to the reduction in natural diversity of the appliance use, which is common in energy management research [15], [22], and [32].

A summary of the average winter and summer PPRS DR energy for all energy management functions is shown in Figure 121 and Figure 122, respectively.

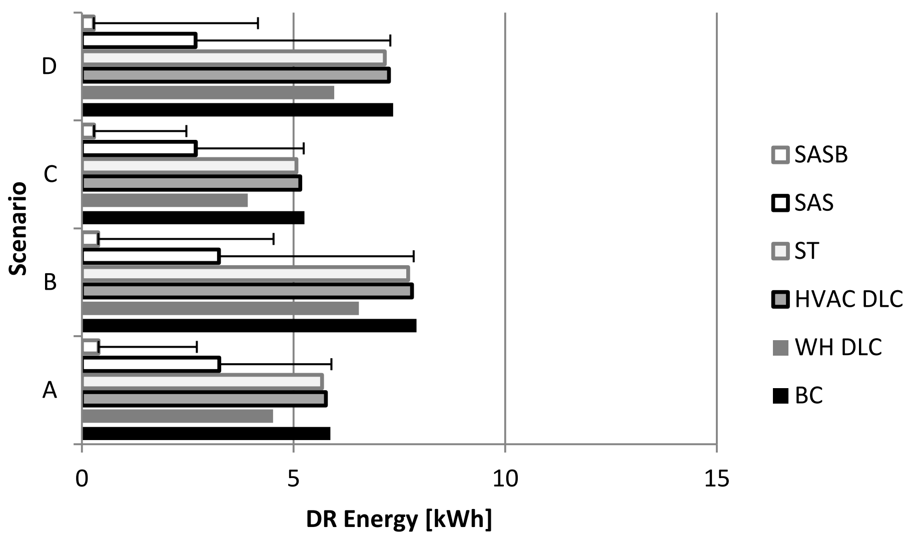

Figure 121: The average winter Proposed Physically-Based Residential-Energy-Management-System Simulation [PPRS] demand response [DR] energy summary.

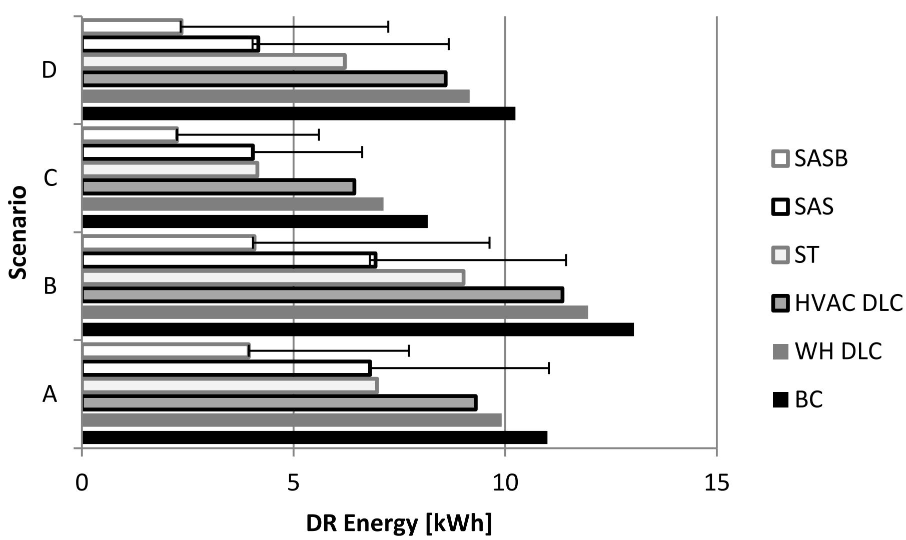

Figure 122: The average summer Proposed Physically-Based Residential-Energy-Management-System Simulation [PPRS] demand response [DR] energy summary.

The impact of the energy management functions on the PPRS DR energy is highlighted in Figure 121 and Figure 122. The average winter PPRS SASB DR energy provides the most significant savings of 94.8% (6.3 kWh) across all the power system areas compared to the average winter PPRS BC DR energy. The average summer PPRS SASB DR energy for all power system areas provides the most significant savings of 70.6% (7.5 kWh) across all the power system areas compared to the average summer PPRS BC DR energy.

The impact of the PEV; PV; and combination of PEV and PV on the PPRS DR energy is also highlighted in Figure 121 and Figure 122. In the average winter and summer PPRS DR energy for all energy management functions, the PEV causes an increase of 24.8% (1.4 kWh) and 16.0% (1.4 kWh) compared to the average winter and summer PPRS Scenario A DR energy, respectively. In the average winter and summer PPRS DR energy for all energy management functions, the PV causes a decrease of 14.9% (0.5 kWh) and 34.9% (2.6 kWh) compared to the average winter and summer PPRS Scenario A DR energy, respectively. In the average winter and summer PPRS Scenario DR energy for all energy management functions, the combination of PEV and PV causes an increase of 10.5% (0.9 kWh) and decrease of 18.7% (1.2 kWh) compared to the average winter and summer PPRS Scenario A DR energy, respectively. The combination of PEV and PV is the net summation of the PPRS Scenario B and Scenario C DR energy (PV provides a negative contribution). Thus, there is no synergistic combined effect of the PEV and PV on the PPRS DR energy.

The PPRS SAS and SASB error bars in Figure 121 and Figure 122 indicate that the use of smart appliances result in drastic reduction in DR energy. Specifically, different combinations of smart appliances achieved the minimum DR energy for the different distributed energy resource scenarios, power system areas, and seasons.

This chapter described the PPRS results. Next is a description of the second major topic of this dissertation, the Proposed Aggregate Primary-Energy-Source-Utilization Simulation.

5 PROPOSED AGGREGATE PRIMARY-ENERGY-SOURCE-UTILIZATION SIMULATION

This dissertation compares the performance of direct load control, a traditional form of energy management, with the performance of smart grid enabled energy management functions. The various energy management functions are compared in their ability to provide automated demand response (DR). Specifically, this dissertation documents simulations of five energy management functions, by testing various levels of residential energy management system complexity. Providing a quantified indication of what technology (energy management functions) provide the most significant automated DR. Further, the use of photovoltaic and plug-in electric vehicle distributed energy resources are considered in conjunction with the residential energy management functions.

To quantify the impact of residential energy management technology on primary energy source utilization (PESU) a probabilistic economic dispatch algorithm is used. Specifically, the Probabilistic Production Costing (PPC) algorithm is used [114]. This economic dispatch algorithm computes the PESU based on an algorithm where the availability of each generator and the electric load are considered random variables.

The PPC algorithm results summarized for each simulated energy management function include the generated energy, the generated environmental air pollution, power system reliability indices (loss of load probability and unserviced energy), and average electricity cost. Further, the PPC algorithm results within the Proposed Aggregate PESU Simulation provide an electric utility centric point of view of residential energy management technology.

First is a description of the PPC algorithm. Second is a summary of the power system input data. Third is a description of the residential energy management aggregation algorithm. Forth is a description of a validation of initial PPC algorithm results. Last is a summary of the PAPS .

5.1 Probabilistic Production Costing Algorithm

The importance of electric energy to modern economic productivity is undeniable. The primary energy sources (petroleum, natural gas, coal, renewable, and nuclear) and the amount of energy used in each end use sector (transportation; industrial; residential and commercial; and electric power) is shown in Figure 123.

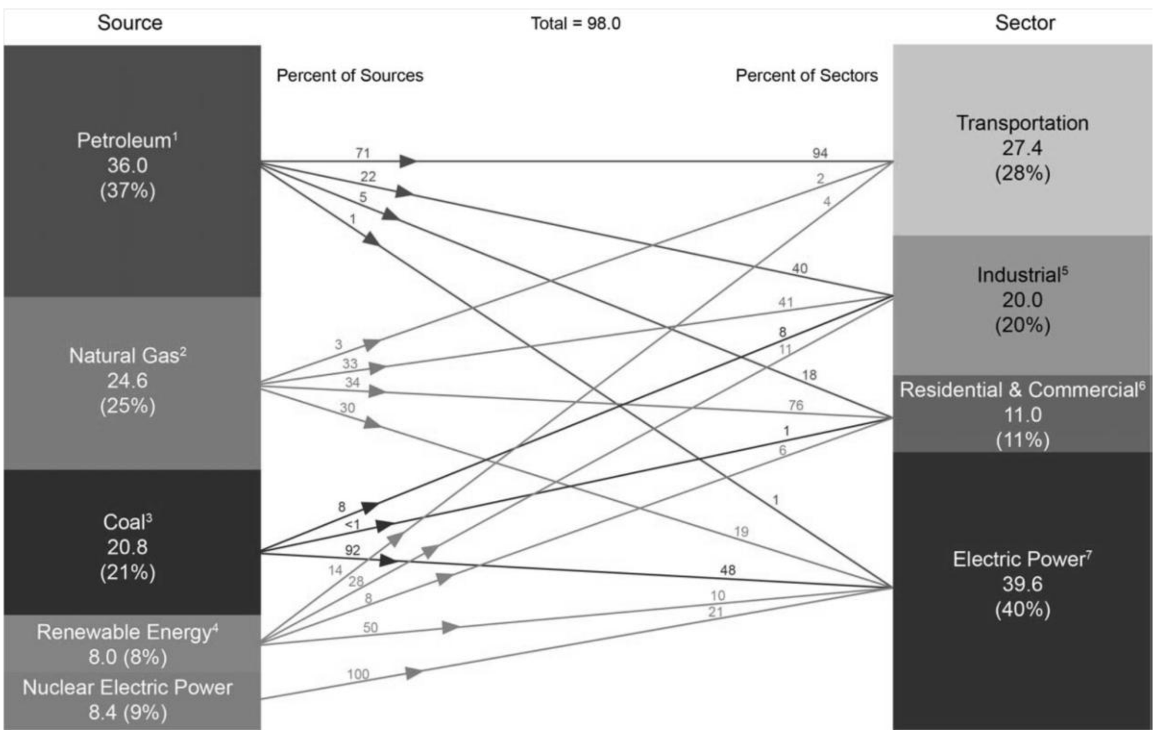

Figure 123: Primary energy source consumption by source and sector in 2010 [115].

The numeric values in Figure 123 are in quadrillion Btu and percentage of source and sector. Further, in Figure 123 notice the electric power sector is the most diversified sector (with five sources providing the total 39.6 quadrillion Btu) and the transportation sector is the least diversified sector (with three sources providing the 27.4 quadrillion Btu).

The economic activity associated with the development, ongoing operation, and future planning of the electric power sector is complex. One tool used to forecast the future economic cost of electric power is production costing. In general, production costing is any methodology by which the operating costs of an economic activity can be projected to a proposed future time frame accounting for the reliability of the various components of the activity. Electric power production costing is a useful tool for policy formulation or the development of planning decisions.

The Probabilistic Production Costing (PPC) algorithm and an application of the PPC algorithm within a graduate level course were summarized in [114]. In the PPC algorithm, the availability of each generator and the electric load are considered random variables. The remainder of this section includes a definition of the generator availability and electric load models and then a description of the probabilistic simulation procedure.

5.1.1 Generator Availability Model

The basic generator availability model is a two state continuous-time Markov chain model, shown in Figure 124.

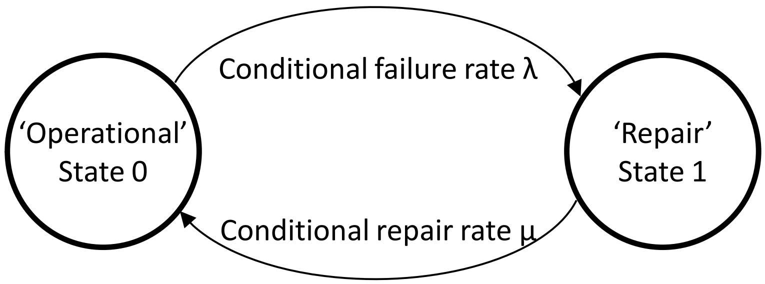

Figure 124: Generator availability two state continuous-time Markov chain model.

The generator availability model shown in Figure 124 consists of two states 'Operational' (State 0) and 'Repair' (State 1) with constant conditional failure rate λ and constant conditional repair rate μ. The constant failure rate and repair rate assumptions represents useful simplifying assumptions because the production costing algorithm is developed to quantify the production cost results for a system in steady state not including infant mortality nor end of life effects on generator availability.

Based on the generator availability model in Figure 124, the limiting probability is the probability of being in state j as time approaches infinity. Notice, the limiting probability is independent of the initial state [116] and is defined in Equation 4.

$$P_j \stackrel{\text{def}}{=} \lim_{t\to\infty} P_{ij}(t) \tag{4}$$

In Equation 4 $P_{ij}(t)$ is the probability of transitioning from state i to state j at time t. The derivation of P_j uses the set of equations in Equation 5, where v_j is the transition rate in state j and q_{kj} is the instantaneous transition rate from state k to state j.

$$\begin{gathered} v_j \cdot P_j = \sum_{k\neq j} q_{kj} \cdot P_k \\ \sum_j P_j = 1 \end{gathered} \tag{5}$$

The relationship between v_i, P_{ij}, and q_{ij} is defined in Equation 6.

$$v_i = \sum_j v_i \cdot P_{ij} = \sum_j q_{ij} \tag{6}$$

The specific set of equations introduced in Equation 5 for the two state continuous-time Markov chain in Figure 124 are shown in Equation 7.

$$\begin{gathered} \lambda \cdot P_0 = \mu \cdot P_1 \\ \mu \cdot P_1 = \lambda \cdot P_0 \\ P_0 + P_1 = 1 \end{gathered} \tag{7}$$

The solution of the set of equations in Equation 7 is shown in Equation 8 and Equation 9.

$$P_0 = \frac{\mu}{\lambda + \mu} \stackrel{\text{def}}{=} p \tag{8}$$

$$P_1 = \frac{\lambda}{\lambda + \mu} \stackrel{\text{def}}{=} q \tag{9}$$

The result in Equation 8 can be interpreted as the percentage of time that the generator is available p. Similarly, the result in Equation 9 can be interpreted as the percentage of time that the generator is unavailable, the forced outage rate q. This two state continuous-time Markov chain model is also known as the up and down state model.

In general, this is the model used to describe the generator availability in the Probabilistic Production Costing (PPC) algorithm. Each generator has an unique availability, thus the availability $p(g)$ and forced outage rates $q(g)$ are a function of generator g. Specifically, the PPC algorithm uses a refinement of this model to include de-rated states of each generator. The up and down state model includes two output levels, the full generator capacity, and zero output (in repair). In reality, generator dispatch is a continuous real-time process. To account for the ability of each generator output between zero output, the minimum output, and the maximum output, a multi-block representation of each generator is used. The output of each generator is a discrete value based on a minimum block size (e.g. 5 MW) and each generator is loaded sequentially. As the block size decreases the model approaches a continuous loading process. The availability of block j is the random variable A_j. In general, the availability of each block does not have to be the same, but constant forced outage rates are used for simplicity.

5.1.2 Electric Load Model

The intuitive fashion to consider electric load is the load as a function of time, a chronological load demand curve. To consider the load as a random variable, the chronological load curve is converted into a load duration curve. This curve describes the amount of time the load is equal to or greater than a specific load l. From the load duration curve, a normalized inverted load duration curve (NILDC) is computed by inverting the load duration curve and normalizing the new y-axis by the simulation length T. Using the relative frequency interpretation of probability, the resulting normalized time describes the probability that the load is greater than or equal to load l. The NILDC $L(l)$ is defined in Equation 10 and depicted in Figure 125, where L is a random variable representing the load.

$$L(l) = Pr\{L > l\} = \frac{t}{T} \tag{10}$$

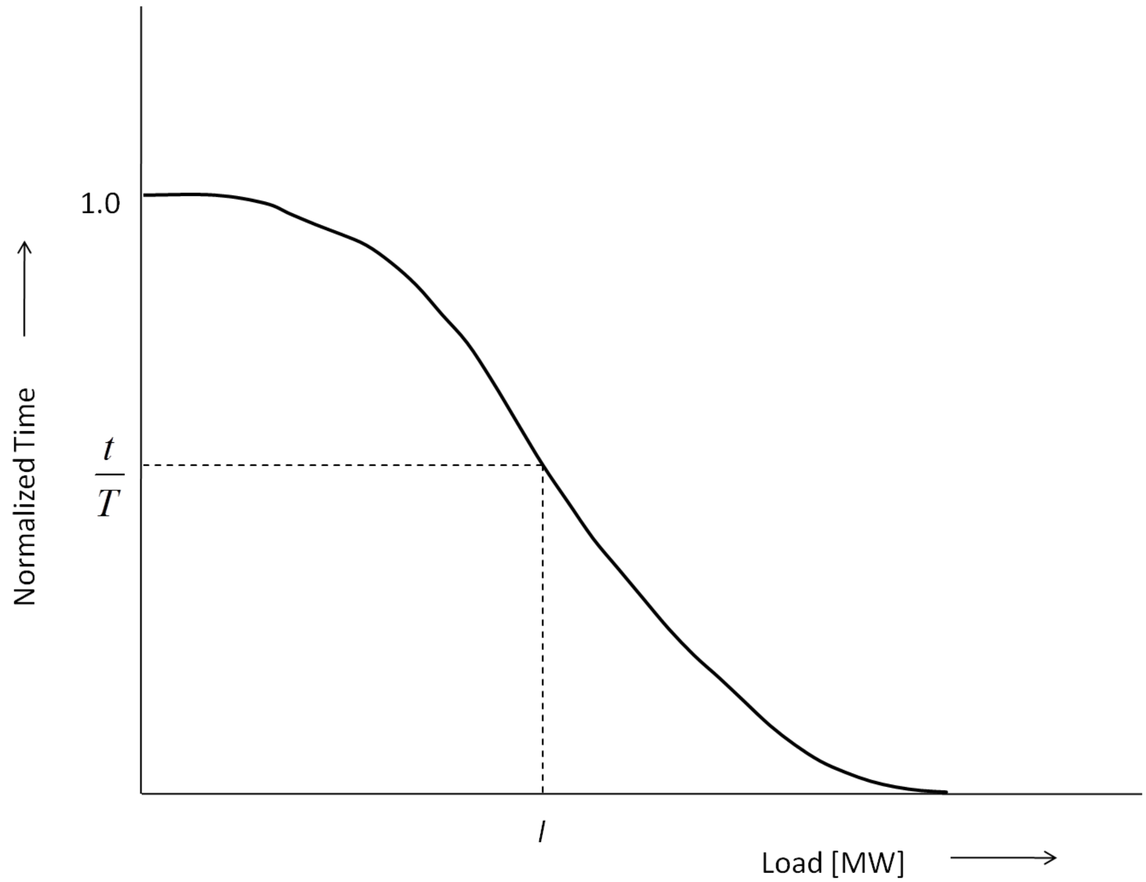

Figure 125: Normalized inverted load duration curve.

The function $L(l)$ defined in Equation 10 and shown, in general, in Figure 125 is the NILDC. This is the function used to model the system load as a random variable.

5.1.3 Probabilistic Simulation Procedure

The Probabilistic Production Costing (PPC) algorithm [114] computes the primary energy source utilization based on an algorithm where the availability of each generator and the electric load are considered random variables. Specifically, the generated energy, the generated environmental air pollution (EAP), reliability indices (loss of load probability and unserviced energy), and average electricity cost will be summarized for each simulated energy management function. The expected power system results provide an electric utility centric point of view of residential energy management technology.

In general, the PPC algorithm is sequential procedure. A load order of the generators is assumed. The output of each generator is discretized into blocks of an arbitrary size. Then each generator is loaded sequentially. For block i the following calculations are performed.

From the previous step the function $L_{i-1}(x)$ is known. The residual load $R_{i-1}(x)$ is defined in Equation 11, where A_j is the availability of generator block j.

$$R_{i-1}(x) = L_{i-1}(x) - \sum_{j=1}^{i-1} A_j \tag{11}$$

Compute the expected generator g operation time $E_{ot}(g)$ [hr] defined in Equation 12, where T is the simulation length in hours, $p(i)$ is the percent of time that generator block i is available defined in Equation 8 ($p(i) = 1 - q(i)$, where $q(i)$ is the forced outage rate for generator block i). Notice, generator block i is a portion of the output from generator g.

$$E_{ot}(g) = T \cdot p(i) \cdot L_{i-1}(0) \tag{12}$$

Compute the expected generated energy $E_{ge}(g)$ [MWh] for generator g defined in Equation 13, where $C(i)$ is the current generator (generator block i corresponds to generator g) output in MW.

$$E_{ge}(g) = T \cdot p(i) \cdot \int_{x=0}^{C(i)} L_{i-1}(x)\, dx \tag{13}$$

Compute the expected cost $E_c(g)$ [$] for generator g defined in Equation 14, where $\alpha(g)$ is the constant heat rate coefficient for generator g, $\beta(g)$ is the linear heat rate coefficient for generator g, and $\gamma(g)$ is the quadratic heat rate coefficient for generator g. Again, generator block i corresponds to generator g.

$$E_c(g) = T \cdot p(i) \cdot \left(\alpha(g) \cdot L_{i-1}(0) + \int_{x=0}^{C(i)} (\beta(g) + 2 \cdot \gamma(g) \cdot x) \cdot L_{i-1}(x) dx \right) \quad (14)$$

Compute the expected EAP $E_e(g)$ [kg] for generator g defined in Equation 15, where $a_e(g)$ is the constant emission rate coefficient for EAP e and generator g, and $b_e(g)$ is the linear emission rate coefficient for EAP e and generator g. Again, generator block i corresponds to generator g.

$$E_e(g) = T \cdot p(i) \cdot \left(a_e(g) \cdot L_{i-1}(0) + b_e(g) \cdot E_{ge}(g) \right) \quad (15)$$

The next function $L_i(x)$ is computed using Equation 16. Again, generator block i corresponds to generator g.

$$L_i(x) = p(i) \cdot L_{i-1}\left(x + \gamma(g)\right) + q(i) \cdot L_{i-1}(x) \quad (16)$$

If there are more generator blocks in the system, the algorithm goes back to the expected generated energy step Equation 12. Otherwise, compute the loss of load probability p_{lol} using Equation 17 and the expected unserviced energy E_u [MWh] using Equation 18, where n is the number of generating blocks in the system.

$$p_{lol} = L_n(0) \quad (17)$$

$$E_u = T \cdot \int_{x=0}^{\infty} L_n(x) dx \quad (18)$$

A block diagram of the PPC algorithm is shown in Figure 126.

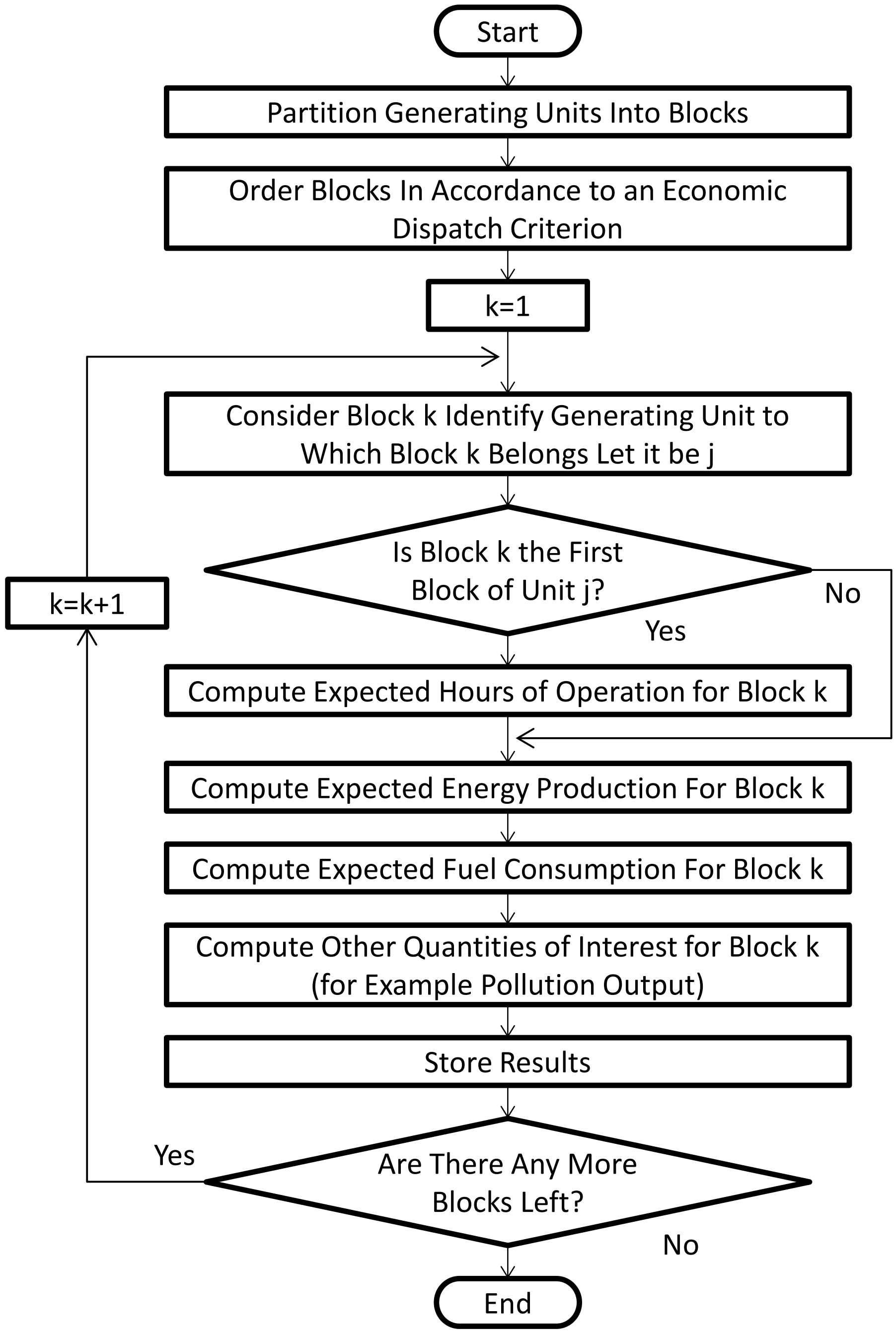

Figure 126: Probabilistic Production Costing [PPC] algorithm block diagram.

The procedure outlined in Figure 126 is the same as the process outlined in Equation 11 through Equation 18.

In general, the PPC algorithm provides the following functionality. Given a forecasted electric load and list of available generators, the expected value of each of the following quantities is computed for each available generating generator:

- generated energy,
- generated EAP,
- loss of load probability,
- unserviced energy, and
- average energy cost.

First was a description of the random variable models for the generator availability and electric load. Second was a description of the simulation procedure. Next is a description of the data used in the PPC algorithm. Specifically, four power system areas are analyzed. Data describing these power system areas has been derived from data in [117].

5.2 Power System Data

The U.S. Environmental Protection Agency (EPA) developed the Integrated Planning Model (IPM) [117]. The IPM is an economic dispatch model used for multiple EPA power system studies. Based on the data in the IPM input and output files, the input for the Probabilistic Production Costing (PPC) algorithm was derived. The PPC input data is summarized in this section. The IPM input data and derivation of the PPC algorithm input is described in Appendix A and tabulated in Appendix B.

Four power system areas of the United States are analyzed: Versailles Kentucky, Mercury Nevada, Stillwater Oklahoma, and Necedah Wisconsin. These four power system areas were selected to consist of different power system operation areas and different climate zones. Different climate zones were selected to study the impact of ambient temperature on the energy management functions ability to provide automated DR.

The remainder of this section describes the PPC algorithm input data for each power system area. The PPC input data consists of fuel data, generator data, and load data.

5.2.1 Fuel Data

Each of the power system operating regions use a variety of primary energy sources. The fuel data consists of fuel type and fuel costs. The fuel types consist of the terminology defined in [117] and the fuel cost is the economic fuel cost. The fuel cost of fuel f is computed as the average fuel cost for each of the Integrated Planning Model (IPM) generators that use fuel f.

In general, hydro, solar, and wind (i.e. renewable) generation is modeled as negative load. Specifically, the hydro energy is 35% realized in the first half of the year, 10% in the third quarter, and 20% in the last quarter. This utilization distribution was defined in [118]. The solar and wind generation is used based on hourly solar insulation and wind speed data, respectively, for each power system area.

Critical IPM data for each IPM generator was the capacity, generated energy, fuel energy, and fuel cost. If any of the critical data was missing or zero the particular IPM generator was ignored. Similarly, if the capacity of an IPM generator was less than 7.5 MW the IPM generator was ignored.

The fuel type and fuel cost is shown in Table 17, Table 18, Table 19, and Table 20 for Versailles Kentucky (ECAK), Mercury Nevada (SNV), Stillwater Oklahoma (SPPS), and Necedah Wisconsin (WUMS) power system areas, respectively.

Table 17: Versailles Kentucky [ECAK] fuel type and fuel cost.

Fuel Type	Fuel Cost [10^{-6}·$/kcal]
Scrubbed-Wet Coal SCR	5.60
Scrubbed-Wet Coal SNCR	5.62
Scrubbed-Wet Coal	5.42
Scrubbed-Dry Coal SCR	5.87
Scrubbed-Dry Coal SNCR	6.31
Unscrubbed Coal	6.67
FB-Unscrubbed Coal SNCR	6.31
Hydro	Negative Load
Combustion Turbine	0.26
Landfill Gas	Ignored
Cgn Biomass	Ignored
Ret. Exist Wet Scrub & SCR	4.99

In Table 17 the 'landfill gas' and 'cgn biomass' fuels consisted of missing data and small generation, respectively. The generated energy ignored in the ECAK power system area was less than 0.1% (23 GWh). The renewable generation in the ECAK power system area consisted of 0.5% (303 GWh) hydro generation.

Table 18: Mercury Nevada [SNV] fuel type and fuel cost.

Fuel Type	Fuel Cost [10^{-6}·$/kcal]
Scrubbed-Wet Coal	2.81
Scrubbed-Dry Coal	4.47
Unscrubbed Coal	2.81
Hydro	Negative Load
Comb. Cycle	0.22
Combustion Turbine	0.25
Wind	Negative Load
Solar	Negative Load
Cgn CC	0.22

In Table 18, no fuel types were ignored due to missing data or small generator capacity. The renewable generations in the SNV power system area consisted of 5.7% (2,065 GWh) hydro, 3.5% (1,262 GWh) wind, and 0.7% (255 GWh) solar generation.

Table 19: Stillwater Oklahoma [SPPS] fuel type and fuel cost.

Fuel Type	Fuel Cost [10^{-6}·$/kcal]
New Landfill Gas	Ignored
Scrubbed-Wet Coal	3.89
Scrubbed-Dry Coal	4.51
Unscrubbed Coal	5.47
FB-Unscrubbed Coal	4.74
FB-Unscrubbed Coal SNCR	4.98
Oil/Gas Steam	0.22
Hydro	Negative Load
Comb. Cycle	0.22
Combustion Turbine	0.25
Wind	Negative Load
Solar	Negative Load
Non Fossil Other	Ignored
Fossil Other	Ignored
Pump Storage	Ignored
Cgn CT	0.22
Cgn CC	0.29
Cgn Biomass	Ignored
Ret. Exist Wet Scrub & SCR	3.85

In Table 19, 'non fossil other', 'fossil other', and 'pumped storage' were ignored due to missing data; whereas, 'cgn biomass' was ignored due to small generator capacity. The ignored generation energy in the SPPS power system area was less than 0.1% (563 GWh). The renewable generations consisted of less than 0.1% (4,290 GWh) hydro, less than 0.1% (2,730 GWh) wind, and less than 0.1% (14 GWh) solar generation.

Table 20: Necedah Wisconsin [WUMS] fuel type and fuel cost.

Fuel Type	Fuel Cost [10^{-6}·$/kcal]
Scrubbed-Wet Coal SCR	6.60
Scrubbed-Dry Coal SCR	6.50
Scrubbed-Dry Coal	5.79
Unscrubbed Coal	6.93
FB-Unscrubbed Coal	4.98
Nuclear	2.08
Hydro	Negative Load
Comb. Cycle	0.24
Combustion Turbine	0.25
Landfill Gas	Ignored
Wind	Negative Load
Cgn CC	0.24
Cgn Biomass	Ignored
Cgn Non Fossil Other	Ignored
Rep. Coal-CC	Ignored
Ret. SCR	7.37
Ret. SNCR	7.42

In Table 20, 'landfill gas' and 'cgn non fossil other', were ignored due missing data; whereas, 'cgn biomass' and 'rep. coal-cc' were ignored due to small generator capacity. The ignored generation energy in the WUMS power system area was 0.6% (369 GWh). The renewable generations consisted of 2.2% (1,621 GWh) hydro and 1.1% (814 GWh) wind generation.

A comparison of the fuel cost for each fuel type and each power system area is shown in Figure 127.

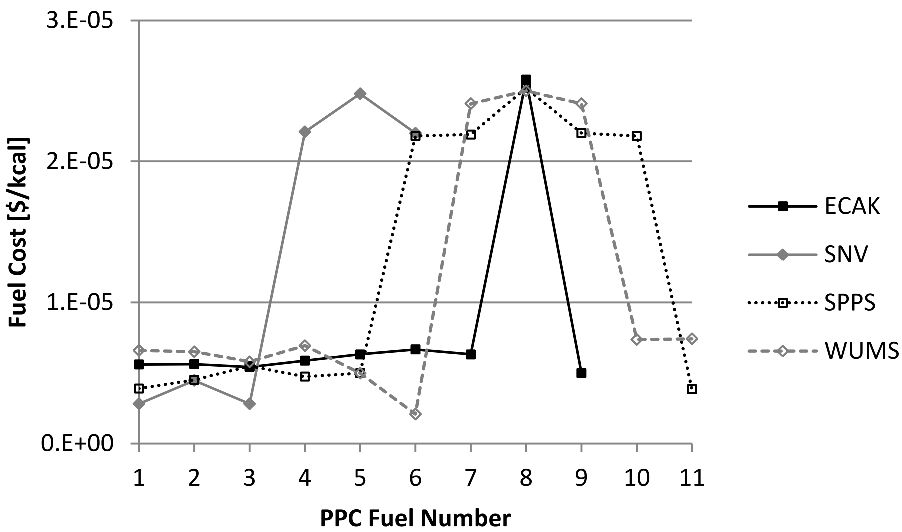

Figure 127: Fuel cost comparisons.

In Figure 127, it is clear that the cost of most of the fuels (73% of all the power system fuels) are approximately $5.0 \cdot 10^{-6}$ $/kcal. The remaining fuels (27% of all the power system fuels) are approximately $2.5 \cdot 10^{-5}$ $/kcal.

5.2.2 Generator Data

Each of the power system areas uses a set of generators; Versailles Kentucky (ECAK) consists of 36 generators, Mercury Nevada (SNV) consists of 21 generators, Stillwater Oklahoma (SPPS) consists of 65 generators, and Necedah Wisconsin (WUMS) consists of 77 generators. The generator data is defined per generator (generator g). The data for each generator consists of minimum capacity [MW], maximum capacity [MW], forced outage rate (FOR), constant heat rate coefficient $\alpha(g)$ [kcal/hr], linear heat rate coefficient $\beta(g)$ [kcal/MWh], quadratic heat rate coefficient $\gamma(g)$ [kcal/(MW)^{2}h], constant emission rate coefficient $a_e(g)$ [kg/h], and linear emission rate coefficient $b_e(g)$ [kg/MWh] where e is a generic place holder for the specific environmental air pollution (EAP): carbon dioxide (CO_2), mercury (MER), nitrogen oxide (NO_x), and sulfur dioxide (SO_2).

The generator data is first summarized by two pie charts for each power system area. The pie charts show the generating capacity and generated energy (based on the IPM results) by fuel type. The generating capacity and generated energy by fuel type is shown in Figure 128, Figure 129, Figure 130, and Figure 131 for the ECAK, SNV, SPPS, and WUMS power system area, respectively.

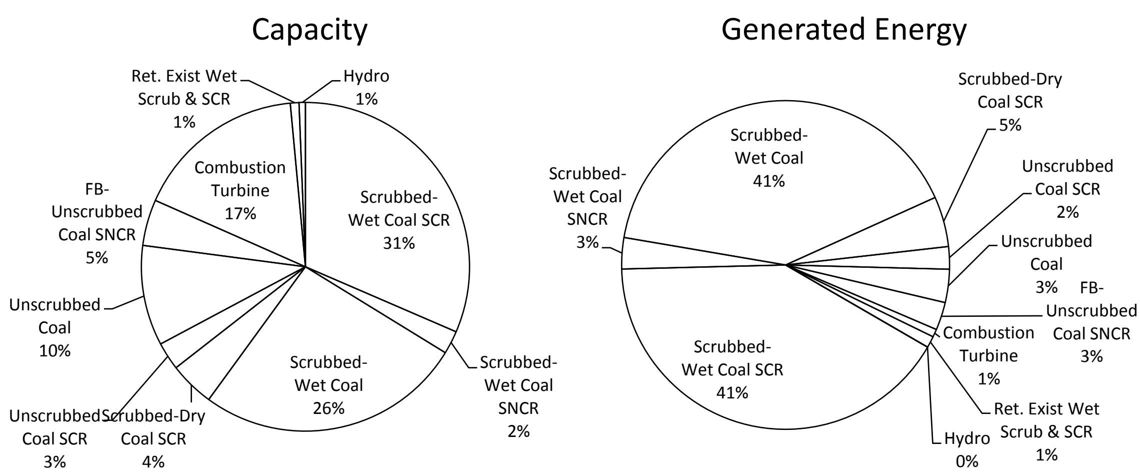

Figure 128: Versailles Kentucky [ECAK] generation capacity and generated energy by fuel type.

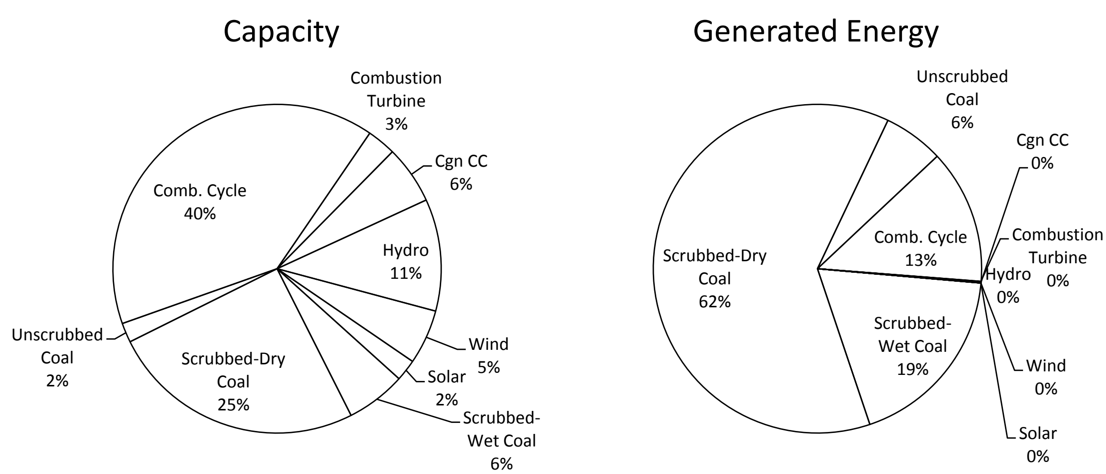

Figure 129: Mercury Nevada [SNV] generation capacity and generated energy by fuel type.

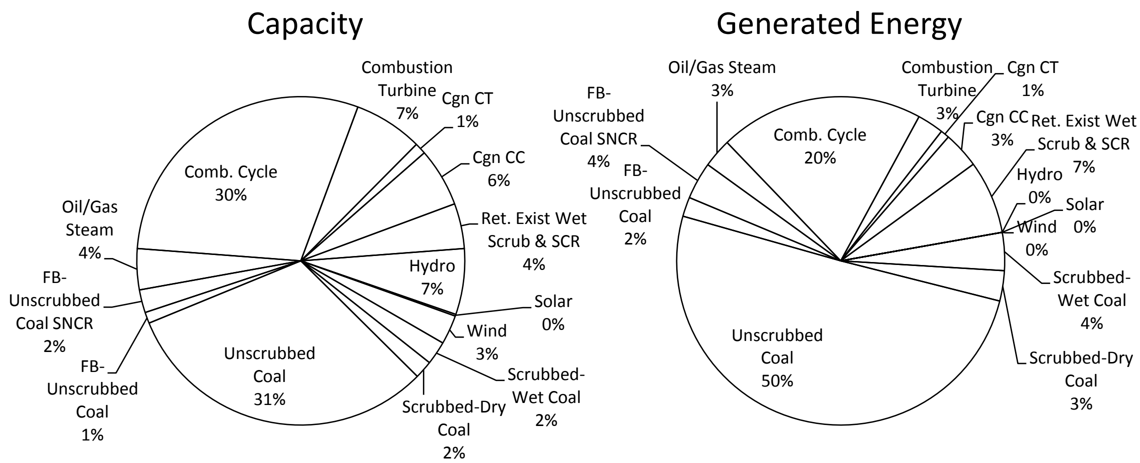

Figure 130: Stillwater Oklahoma [SPPS] generation capacity and generated energy by fuel type.

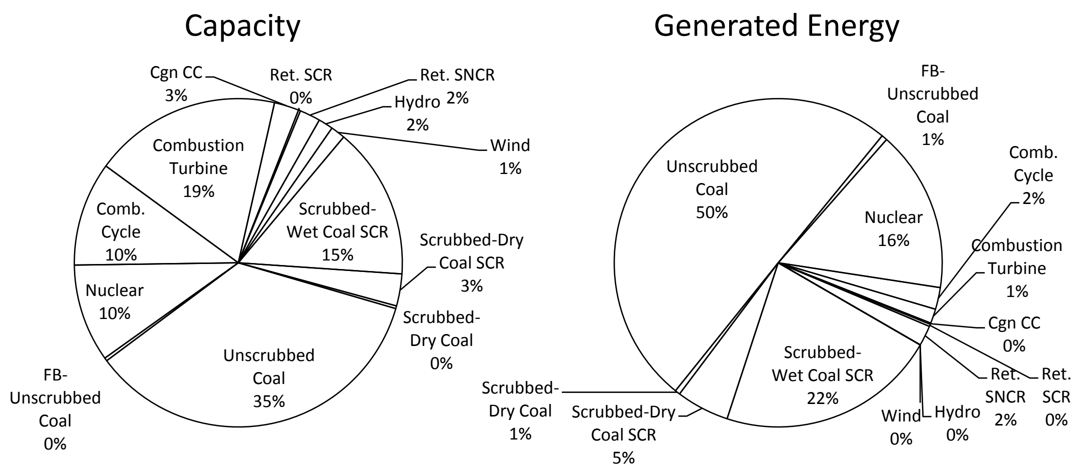

Figure 131: Necedah Wisconsin [WUMS] generation capacity and generated energy by fuel type.

It is shown in Figure 128, Figure 129, Figure 130, and Figure 131 that the generation capacity varies for all the power system areas and the majority of generated energy for all the power system areas is coal.

The maximum capacity for each generator and each power system area is shown in Figure 132.

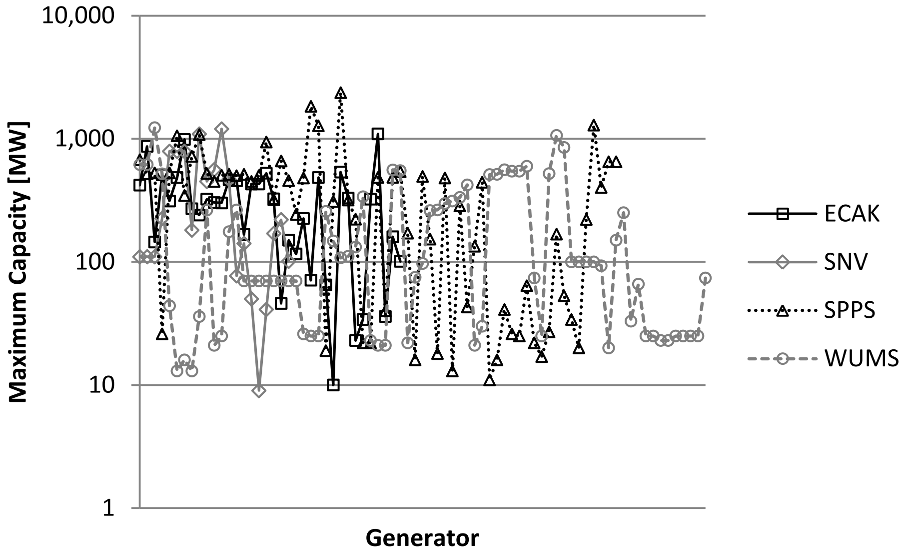

Figure 132: Generator maximum generating capacity.

Notice, the y-axis in Figure 132 is plotted with a logarithmic scale. Each generator data description in [117] includes a maximum capacity. Based on the ratio of maximum to minimum generator capacity (0.35) in [118] the minimum capacity can be computed from the maximum capacity.

A scatter plot of the generator FOR versus generator capacity is shown in Figure 133.

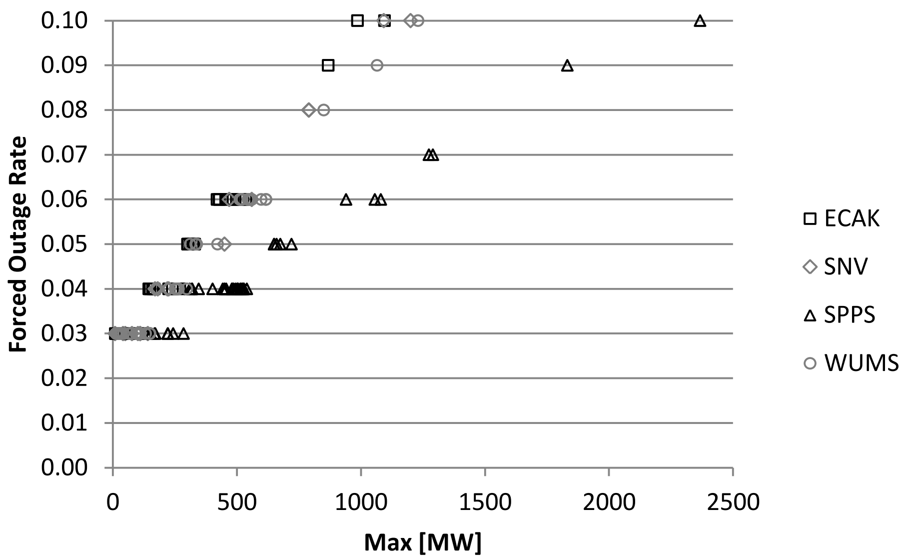

Figure 133: Generator forced outage [FOR] rate versus capacity.

The scatter plot in Figure 133 summarizes the generator FOR data. Further, this scatter plot highlights the linear relationship used to derive the FOR data for each generator. A linear relationship was computed based on the generator FOR data and generator maximum capacity from [118].

Three scatter plots of the generator g constant $\alpha(g)$, linear $\beta(g)$, and quadratic $\gamma(g)$ heat rate coefficients versus generator capacity are shown in Figure 134, Figure 135, and Figure 136, respectively.

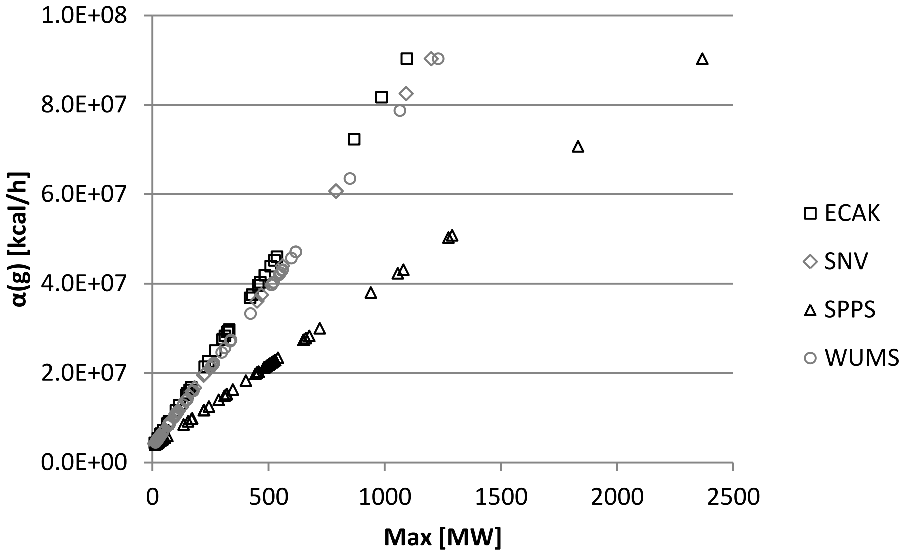

Figure 134: Generator constant heat rate coefficient versus generator capacity.

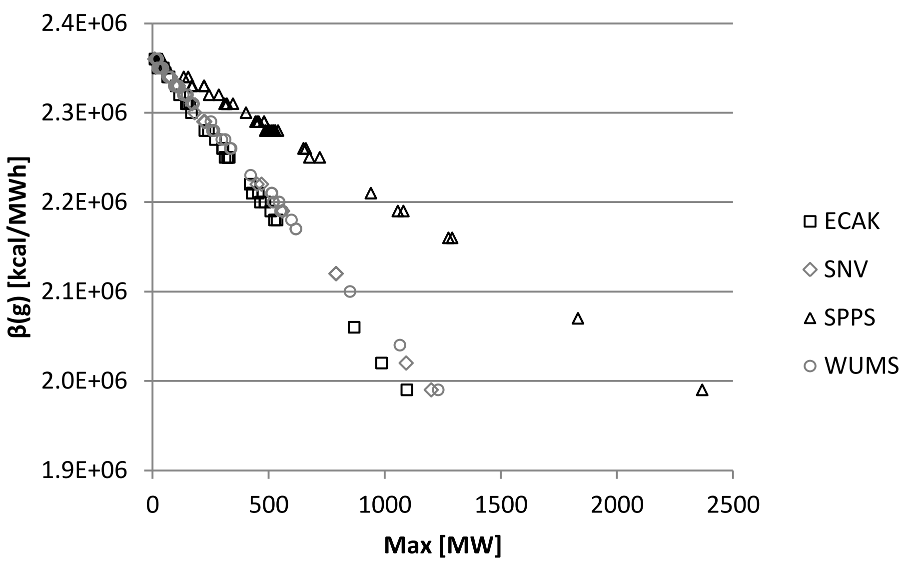

Figure 135: Generator linear heat rate coefficient versus generator capacity.

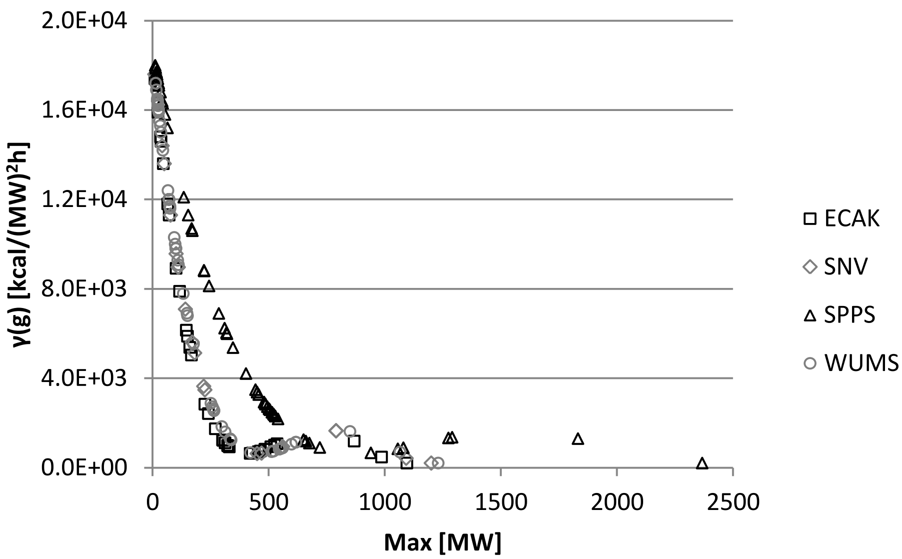

Figure 136: Generator quadratic heat rate coefficient versus generator capacity.

The scatter plots in Figure 134, Figure 135, and Figure 136 summarize the generator heat rate coefficients. Further, these scatter plots highlight the linear relationship used for the constant and linear heat rate coefficient and the fourth order polynomial approximation used to derive the generator heat rate coefficients. The functional approximations were based on the heat rate coefficients in [118]. A fourth order polynomial was used so that negative values for the quadratic heat rate coefficient are avoided.

The remainder of the generator data consists of two emission rate coefficients (a_e and b_e where the subscript is used to denote EAP e) for each pollutant: CO_2, MER, NO_x, and SO_2. As a summary of the generator emission rate data, the ECAK power system area CO_2 emission rate coefficients are shown in Figure 137.

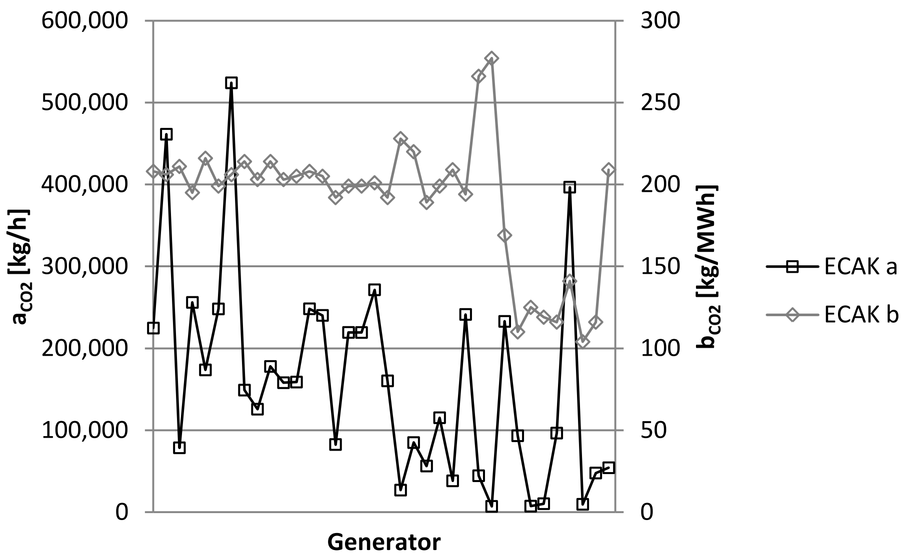

Figure 137: The Versailles Kentucky [ECAK] power system area carbon dioxide [CO_2] emission rate coefficients.

A linear least square method was used to calculate the emission rate coefficients a_e and b_e for each generator. The emission rate coefficients were computed assuming the EAP rate will increase 20% from minimum output to maximum generator output. The linear least square method used an average EAP rate for each EAP. The average EAP rate was computed dividing the generated EAP by the generated energy.

The generator data introduced in this section is described further in Appendix A and Appendix B. Appendix A describes the derivation used to compute the Probabilistic Production Costing (PPC) generator data. Appendix B tabulates the PPC input data introduced in this section.

5.2.3 Load Data

The load data in [117] is hourly chronological load data. The hourly chronological load data is shown in Figure 138 for Versailles Kentucky (ECAK) and

Mercury Nevada (SNV) and Figure 139 for Stillwater Oklahoma (SPPS) and Necedah Wisconsin (WUMS).

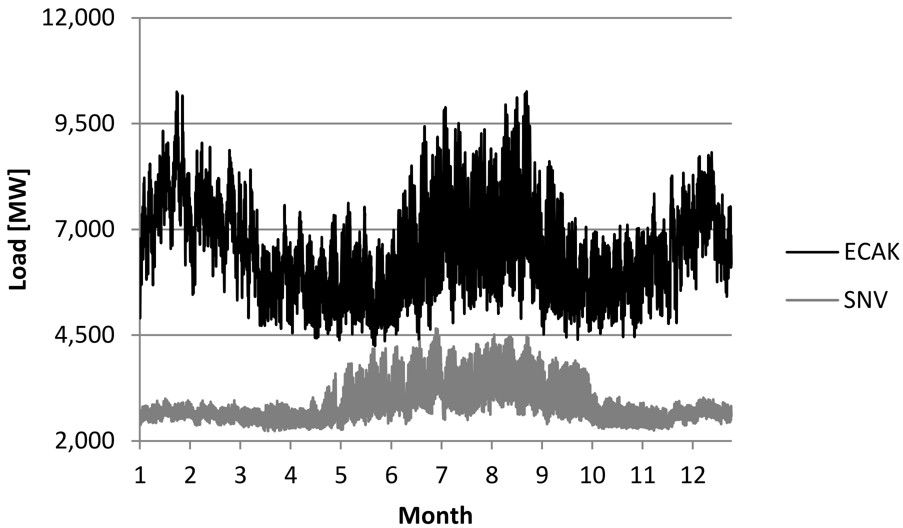

Figure 138: Versailles Kentucky [ECAK] and Mercury Nevada [SNV] hourly chronological load data.

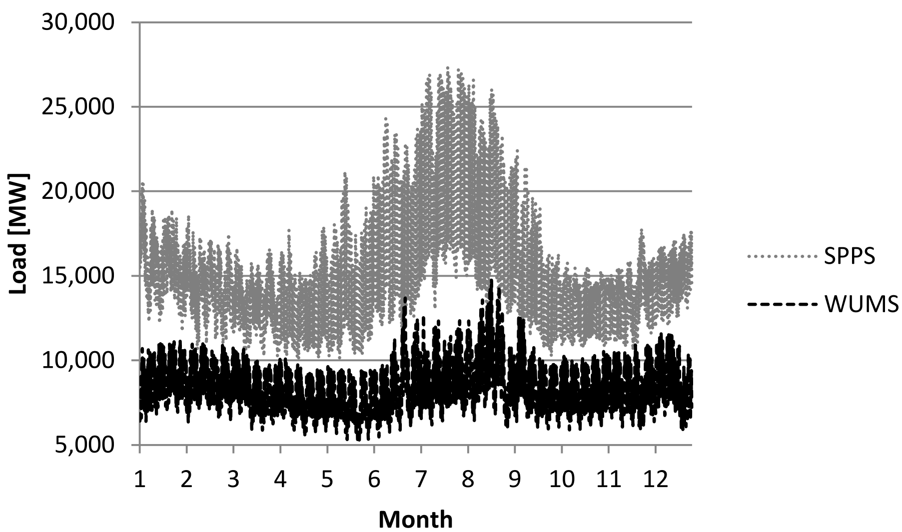

Figure 139: Stillwater Oklahoma [SPPS] and Necedah Wisconsin [WUMS] hourly chronological load data.

Statistics of the hourly chronological load data shown in Figure 138 and Figure 139 are summarized in Table 21.

Table 21: Hourly chronological load data statistics.

	ECAK	SNV	SPPS	WUMS
Minimum [MW]	4,242	2,231	10,090	5,120
Median [MW]	6,507	2,715	14,700	8,727
Maximum [MW]	10,260	4,658	27,360	14,770
Average [MW]	6,635	2,898	15,510	8,694
Standard Deviation [MW]	1,127	496	3,302	1,485
Annual Energy [GWh]	58,120	25,390	135,900	76,160
Annual Load Factor [%]	64.68	62.22	56.70	58.84

The chronological load data shown in Figure 138 and Figure 139 and summarized in Table 21 describes the original Integrated Planning Model load data before the load is adjusted for the renewable energy generation. The annual load factor in Table 21 is the average load divided by the peak load. The annual load factor describes the severity of the peak load. A flat load would have an annual load factor of 1. The smaller the annual load factor the larger the peak load. A large peak load is undesirable from a power system perspective because investment in underutilized generation equipment would be required.

The PPC algorithm uses a probabilistic description of the chronological load. The normalized inverted load duration curve (NILDC) is computed from the hourly chronological load data. A NILDC is a probabilistic description of the load data. To convert from the hourly chronological load data to the NILDC, the range of load levels is divided into 30 increments. The NILDC for each power system area is shown in Figure 140.

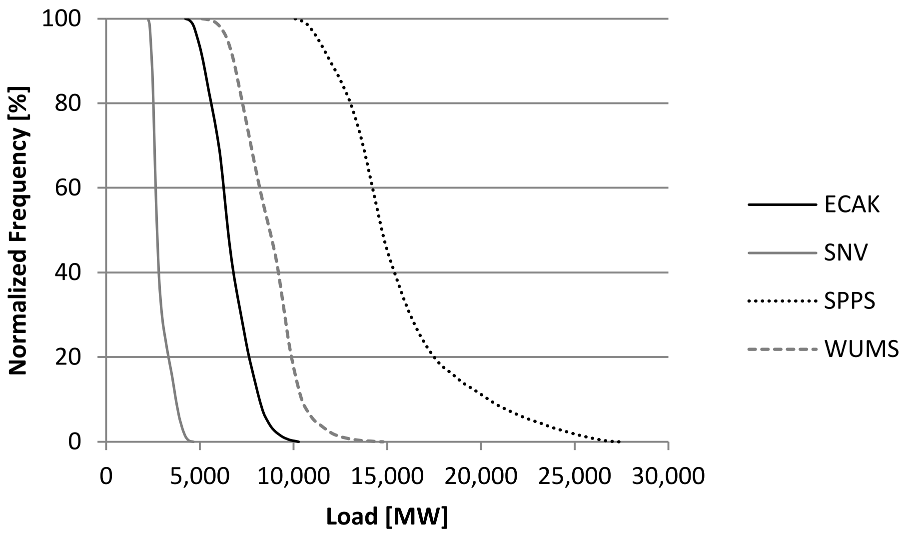

Figure 140: Normalized inverted load duration curve [NILDC] for each power system area.

The resulting NILDC, shown in Figure 140, has horizontal axis units of power and vertical axis units of normalized frequency (probability). The vertical axis indicates the probability that the load is greater than or equal to the horizontal axis power level.

First was a description of the production costing algorithm used. Second was a description of the input data used in the production costing algorithm. Next is a description of the algorithm used to aggregate the residential-energy management results.

5.3 Residential-Energy-Management Aggregation Algorithm

Results from the Proposed Physically-Based Residential-Energy-Management-System Simulation (PPRS) are used in the Proposed Aggregate Primary-Energy-Source-Utilization Simulation (PAPS) to quantify the effect of the change in electric load due to the analyzed energy management functions. The key steps include aggregating a fraction of residences that are assumed to be equipped with residential energy management automation equipment and computing the Probabilistic Production Costing (PPC) algorithm on the modified load.

This section will outline the procedure used to aggregate the PPRS results within the PAPS. A block diagram of the steps used is shown in Figure 141.

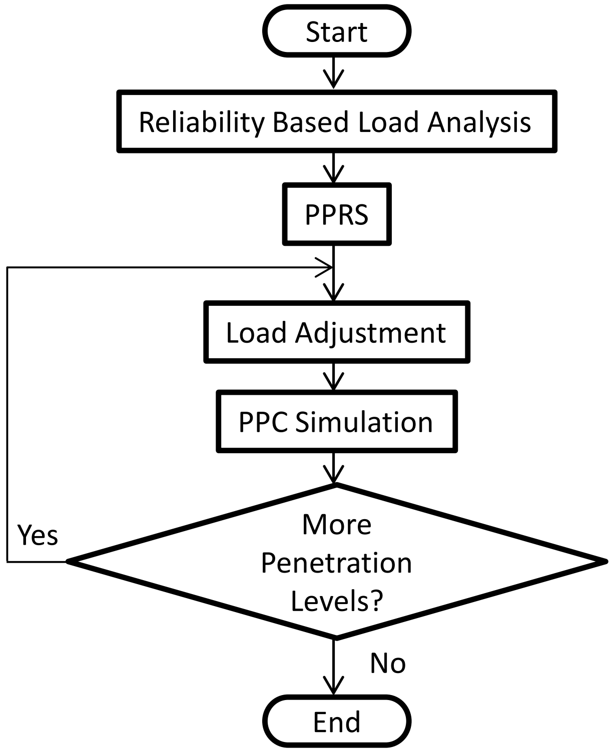

Figure 141: The Proposed Aggregate Primary-Energy-Source-Utilization Simulation [PAPS] block diagram.

The first step in Figure 141 is the *Reliability Based Load Analysis*. In this step the days and times that energy management is needed is computed. The days that energy management is needed is based on reliability considerations. Specifically, the top 50 peak daily load levels are identified as days and times when the reliability of the power system is most stressed.

The second step in Figure 141 is the *PPRS*. The days identified in the first step are simulated with the demand response (DR) period defined as the hour before the peak load hour. The DR period consists of four consecutive hours. The *PPRS* output includes a one minute chronological load curve for each of the 750 repeated iterations. The average hourly chronological load curve is computed for each energy management function. The average hourly chronological load curve is summed for each of the 750 independent replications resulting in a cumulative average hourly chronological load curve. The average chronological load curve is scaled by the factor $\Lambda(d, a, s)$, defined in Equation 19, to match the energy in the residential fraction of the 'original' chronological load curve.

$$\Lambda(d, a, s) = \frac{E_o(d) \cdot R(a) \cdot P(s)}{E_{sim}(d)} \tag{19}$$

In Equation 19, $E_o(d)$ is the energy in the 'original' day d, $R(a)$ is the percentage of residential load defined in Table 22 for power system area a, $P(s)$ is the percentage of residential energy management system (REMS) penetration in simulation s (10%, 20%, and 40%), and $E_{sim}(d)$ is the energy in the simulated load day d.

Table 22: The fraction of each power system area load that is residential [119].

	ECAK	SNV	SPPS	WUMS
Percent Residential Load	31.14	34.39	40.95	32.43

The third step in Figure 141 is the *Load Adjustment*. In this step the 'original' load data from [117] is adjusted for the plug-in electric vehicle (PEV) load (in Scenarios B and D) and the photovoltaic (PV) generation (in Scenarios C and D) and the energy management function load dynamics. The 'original' load is adjusted every non-DR day for the PEV load and PV generation from the REMS enabled residences. The 'original' load is adjusted every DR day based on the scaled cumulative average hourly time series load computed in the *PPRS* step.

The fourth step in Figure 141 is the *PPC Simulation*. First, the adjusted chronological load curve from the *Load Adjustment* step is converted to a NILDC. Then the PPC algorithm is used. Key results from the PPC algorithm are collected: generated energy, generated environmental air pollution, loss of load probability, unserviced energy, and average electricity cost. The last two steps are repeated with the various levels of REMS market penetration: 10%, 20%, and 40%.

Results from the PPRS are used in the PAPS to quantify effect of the change in electric load due to the analyzed energy management functions. This section outlined the procedure used to aggregate the PPRS results within the PAPS. Next is a validation of the initial PPC algorithm results. Specifically, a comparison is provided of initial PPC algorithm results to the original Integrated Planning Model data as validation of the PPC algorithm.

5.4 Validation

Validation of initial Probabilistic Production Costing (PPC) algorithm results is provided. This includes comparing initial PPC algorithm results with the original Integrated Planning Model (IPM) data. Comparison is made with percent difference calculations. Here, percent difference is defined as the original data $x_o(i)$ minus the simulation data $x_s(i)$ divided by the total original data X_o (Equation 20) or the original data (Equation 21) depending on the result. Both versions of percent difference are defined for result i.

$$P_X(i) = \frac{x_o(i) - x_s(i)}{X_o} \cdot 100 \tag{20}$$

$$p_x(i) = \frac{x_o(i) - x_s(i)}{x_o(i)} \cdot 100 \tag{21}$$

The PPC algorithm results consist of three parts: fuel results, generator results, and summary results. The PPC fuel results consist of fuel energy consumed for each fuel type, electric energy generated for each fuel type, and environmental air pollution (EAP) generated: carbon dioxide (CO_2), mercury (MER), nitrogen oxide (NO_x), and sulfur dioxide (SO_2) for each fuel type. The PPC generator results consist of generated energy for each generator, fuel cost for each generator, average electricity cost for each generator, fuel used for each generator, and EAP generated (CO_2, MER, NO_x, and SO_2) for each generator. The PPC summary results statistics include generated energy, generated EAP, fuel cost, loss of load probability (LOLP), unserviced energy (UE), and average electricity cost. The LOLP is the probability that the system generation is incapable of meeting the electric load. The UE is the amount of electric load not fulfilled by the system generation in the simulation.

Next is a comparison of the initial PPC algorithm fuel results with the original IPM data.

5.4.1 Probabilistic Production Costing Fuel Results

Results for each fuel type include fuel energy used, electric energy generated, and environmental air pollution (EAP) generated (carbon dioxide [CO_2], mercury [MER], nitrogen oxide [NO_x], and sulfur dioxide [SO_2]). The Versailles Kentucky (ECAK), Mercury Nevada (SNV), Stillwater Oklahoma (SPPS), and Necedah Wisconsin (WUMS) power system areas consist of 9, 6, 11, and 11 fuels, respectively. Each Probabilistic Production Costing (PPC) fuel result is compared to the original Integrated Planning Model (IPM) data using the percent difference defined in Equation 20.

Percent difference fuel energy consumed by fuel type for each power system area is shown in Table 23, generated energy in Table 24, generated CO_2 in Table 25, generated MER in Table 26, generated NO_x in Table 27, and generated SO_2 in Table 28.

Table 23: Percent difference fuel energy consumed by fuel type.

Fuel	ECAK	SNV	SPPS	WUMS
1	19.47	1.45	1.36	9.04
2	1.39	3.95	0.62	0.87
3	6.61	1.07	14.44	0.05
4	2.97	33.52	0.20	14.22
5	2.10	0.05	0.52	-0.08
6	9.86	3.64	-0.83	5.58
7	3.72		3.48	0.39
8	-0.03		-1.89	-0.32
9	0.46		-0.72	0.34
10			2.09	0.09
11			-1.77	0.39

Table 24: Percent difference generated energy by fuel type.

Fuel	ECAK [%]	SNV [%]	SPPS [%]	WUMS [%]
1	4.70	-1.22	0.00	1.50
2	0.20	-10.76	-0.12	-0.22
3	-6.67	-0.34	0.24	-0.13
4	1.18	38.25	-0.11	-4.67
5	1.47	0.04	-0.02	-0.06
6	8.64	4.36	-1.93	0.22
7	3.64		1.32	-0.57
8	-0.34		-2.42	-1.13
9	0.15		-0.87	0.43
10			1.97	0.08
11			-3.85	-0.31

Table 25: Percent difference generated carbon dioxide [CO_2] by fuel type.

Fuel	ECAK [%]	SNV [%]	SPPS [%]	WUMS [%]
1	18.55	6.25	2.20	12.93
2	1.16	9.74	1.61	2.33
3	8.74	2.32	29.73	0.18
4	2.36	19.65	1.04	17.44
5	1.89	0.03	1.87	0.24
6	9.46	2.48	-0.99	0.00
7	3.35		2.24	-0.53
8	-0.26		-1.45	-1.26
9	0.45		-0.48	0.21
10			1.01	0.18
11			-0.50	0.60

Table 26: Percent difference generated mercury [MER] by fuel type.

Fuel	ECAK [%]	SNV [%]	SPPS [%]	WUMS [%]
1	6.95	5.24	4.03	10.70
2	1.53	19.39	1.50	2.60
3	11.09	4.95	33.19	0.13
4	3.60	0.00	1.49	22.37
5	3.77	0.00	0.46	0.68
6	17.27	0.00	0.00	0.00
7	4.85		0.00	0.00
8	0.00		0.00	0.00
9	0.17		0.00	0.00
10			0.00	0.21
11			-0.93	1.04

Table 27: Percent difference generated nitrogen oxide [NO_x] by fuel type.

Fuel	ECAK [%]	SNV [%]	SPPS [%]	WUMS [%]
1	6.59	7.87	1.63	4.30
2	1.16	13.99	2.54	0.78
3	15.94	1.56	33.19	0.15
4	0.78	3.38	0.73	21.05
5	0.62	0.03	0.46	0.21
6	20.71	1.15	-2.48	0.00
7	1.10		0.94	-0.11
8	-0.03		-4.51	-1.06
9	0.15		-0.34	0.03
10			0.71	0.06
11			-0.13	1.58

Table 28: Percent difference generated sulfur dioxide [SO_2] by fuel type.

Fuel	ECAK [%]	SNV [%]	SPPS [%]	WUMS [%]
1	16.22	2.72	2.84	1.64
2	0.62	12.72	0.68	0.44
3	6.13	17.64	38.71	0.03
4	1.18	0.00	0.14	18.76
5	4.51	0.00	1.10	0.23
6	24.82	0.00	0.00	0.00
7	0.40		0.00	0.00
8	0.00		0.00	0.00
9	0.30		0.00	0.00
10			0.00	0.22
11			-0.52	-0.12

The PPC fuel results have close approximation with the original IPM data. Specifically, the average percent difference for each result is a maximum 7.28% and a minimum -0.53% different than the original IPM data. A number of the EAP results are zero because the corresponding fuel has no production of the specific EAP. The zero EAP results cause a bias in the average results, providing a smaller average than the average of non-zero results. However, the conclusion holds that the PPC fuel results are similar to the original IPM data.

Next is a comparison of initial PPC generation results with the original IPM data.

5.4.2 *Probabilistic Production Costing Generation Results*

Results for each generator include generated energy, fuel cost, average electricity cost, fuel used, and generated environmental air pollution (carbon dioxide [CO_2], mercury [MER], nitrogen oxide [NO_x], and sulfur dioxide [SO_2]). The Versailles Kentucky (ECAK), Mercury Nevada (SNV), Stillwater Oklahoma (SPPS), and Necedah Wisconsin (WUMS) power system areas consist of 36, 21, 65, and 77 generators, respectively. To summarize the generator validation, the percent difference for each set of Probabilistic Production Costing (PPC) generation results is summarized with the minimum, maximum, and average percent difference descriptive statistics.

Percent difference summary statistics for the generated energy are shown in Table 29, fuel cost are shown in Table 30, average electricity cost are shown in Table 31, fuel used are shown in Table 32, generated CO_2 are shown in Table 33, generated MER are shown in Table 34, generated NO_x are shown in Table 35, and generated SO_2 are shown in Table 36.

Table 29: Percent difference statistics for the generator generated energy.

	ECAK [%]	SNV [%]	SPPS [%]	WUMS [%]
Minimum	-3.62	-9.93	-2.58	-0.89
Maximum	3.56	19.02	3.80	1.77
Average	0.36	1.45	-0.26	-0.06

Table 30: Percent difference statistics for the generator fuel cost.

	ECAK [%]	SNV [%]	SPPS [%]	WUMS [%]
Minimum	-1.77	-2.52	-2.90	-1.25
Maximum	5.62	31.30	9.02	5.37
Average	1.30	3.46	-0.09	0.37

Table 31: Percent difference statistics for the average electricity cost.

	ECAK [%]	SNV [%]	SPPS [%]	WUMS [%]
Minimum	6.76	-45.23	-37.19	-24.95
Maximum	57.85	57.06	47.49	69.53
Average	34.43	25.14	16.23	32.83

The percent difference for all of the PPC generator results in this section are computed using Equation 20, except the average electricity cost results in Table 31. The percent difference in Table 31 was computed using Equation 21.

The positive averages in Table 31 indicate that the PPC results are less than the original Integrated Planning Model (IPM) data. This can be explained because of the fact that no operation and maintenance costs are included in the current PPC simulations.

Table 32: Percent difference statistics for the fuel used.

	ECAK [%]	SNV [%]	SPPS [%]	WUMS [%]
Minimum	-1.89	-6.53	-1.63	-0.40
Maximum	5.83	16.44	3.73	5.22
Average	1.29	2.08	0.16	0.40

Table 33: Percent difference statistics for the generated carbon dioxide [CO_2].

	ECAK [%]	SNV [%]	SPPS [%]	WUMS [%]
Minimum	-1.34	-6.33	-1.15	-1.13
Maximum	5.52	11.58	3.91	6.81
Average	1.28	1.94	0.48	0.42

Table 34: Percent difference statistics for the generated mercury [MER].

	ECAK [%]	SNV [%]	SPPS [%]	WUMS [%]
Minimum	-1.72	-6.22	-1.99	-0.13
Maximum	6.52	18.39	5.45	3.91
Average	1.37	1.44	0.62	0.50

Table 35: Percent difference statistics for the generated nitrogen oxide [NO_x].

	ECAK [%]	SNV [%]	SPPS [%]	WUMS [%]
Minimum	-2.36	-9.04	-3.30	-1.10
Maximum	5.06	16.62	5.68	2.50
Average	1.31	1.36	0.40	0.35

Table 36: Percent difference statistics for the generated sulfur dioxide [SO_2].

	ECAK [%]	SNV [%]	SPPS [%]	WUMS [%]
Minimum	-0.89	-4.14	-0.87	-2.06
Maximum	7.76	17.88	6.33	3.32
Average	1.51	1.61	0.67	0.28

The PPC generator results statistics have close approximation with the original IPM data, other than the average electricity cost results. This suggests that on average the PPC generator results for each power system area approximate the original IPM data. Specifically, the PPC generator results for a specific generator may differ from the original IPM data, but the difference on average is less than 3.46% for all results except the average electricity cost results. The simulated average cost results are less than the original IPM data because no operation and maintenance costs were included.

Next is a comparison of initial PPC summary results with the original IPM data.

5.4.3 Probabilistic Production Costing Summary

The Probabilistic Production Costing (PPC) summary result statistics include loss of load probability, generated energy, unserviced energy, fuel cost, and average energy cost. Notice, no original Integrated Planning Model (IPM) data was available for the loss of load probability and unserviced energy, thus no percent difference calculation is possible for these results. The summary result statistics are included for Versailles Kentucky (ECAK), Mercury Nevada (SNV), Stillwater Oklahoma (SPPS), and Necedah

Wisconsin (WUMS) power system areas. The available PPC summary results percent differences are shown in Table 37.

Table 37: The Probabilistic Production Costing [PPC] summary results percent differences.

	ECAK [%]	SNV [%]	SPPS [%]	WUMS [%]
Generated Energy	12.99	30.35	-16.91	-4.83
Fuel Cost	46.90	72.56	-5.55	28.64
Average Energy Cost	38.97	60.60	9.72	31.93

The PPC summary results in Table 37 have moderately accurate results with the original IPM data. The generated energy is slightly higher for ECAK and SNV and slightly lower for SPPS and WUMS. The fuel cost and average energy cost are moderately less than the original IPM data because the PPC simulation does not include any operation and maintenance costs which were included in the IPM.

5.5 Summary

This dissertation compares the performance of direct load control, a traditional form of energy management, with the performance of smart grid enabled energy management functions. To quantify the impact of residential energy management system (REMS) technology on primary energy source utilization (PESU) a probabilistic economic dispatch algorithm is used. The Proposed Aggregate PESU Simulation (PAPS) provides an electric utility centric point of view of residential energy management technology.

This chapter has described the PAPS. First, the Probabilistic Production Costing (PPC) algorithm used in the PAPS was described. Second, the power system input data used was described. Third, the residential energy management aggregation algorithm was described. Forth, the validation of initial PPC algorithm results was described.

The PPC algorithm used in the PAPS computes expected power system results. Given a forecasted electric load and list of available generators, the expected value of each of the following quantities is computed:

- generated energy,
- generated environmental air pollution,
- loss of load probability,
- unserviced energy, and
- average energy cost.

The U.S. Environmental Protection Agency developed the Integrated Planning Model (IPM). Based on the data in the IPM input and output files, the input for PAPS was derived. The power system and load data used in the PAPS was described in this chapter.

Initial results from the Proposed Physically-Based REMS Simulation (PPRS) were used in the PAPS to quantify the effect of the change in electric load due to the residential energy management functions. The time series load computed in the PPRS was used to adjust the load data on the days that demand response is required for reliability based energy management.

Initial PPC algorithm results were compared with the IPM input data used to derive the power system data as validation of the PPC algorithm. The PPC algorithm fuel results had close approximation with the original IPM data. Specifically, the maximum average percent difference for each fuel result was 7.28% and minimum -0.53% compared with the original IPM data. The PPC algorithm generator results statistics had close approximation with the original IPM data, other than the average electricity cost results. Specifically, the maximum average percent difference for each generator result was 3.46% and minimum -1.44%, not including the fuel and average electricity cost results. The PPC algorithm generator fuel cost and average electricity cost were less than the original IPM data because the PPC algorithm used in the PAPS does not include any operation and maintenance costs, which were included in the IPM.

This chapter described the PAPS. Next is a description of the PAPS results.

6 PROPOSED AGGREGATE PRIMARY ENERGY SOURCE UTILIZATION RESULTS

The proposed physically-based residential energy management system (REMS) simulation quantifies the performance of an individual residence using a variety of energy management functions. To quantify the impact of residential energy management technology on primary energy source utilization (PESU) a probabilistic economic dispatch algorithm is used. Specifically, the Probabilistic Production Costing (PPC) algorithm is used [114]. This economic dispatch algorithm computes the PESU based on an algorithm where the availability of each generator and the electric load are considered random variables.

The PPC algorithm results summarized for each simulated energy management function include the generated energy, the generated environmental air pollution (which is the summation of the generated carbon dioxide, mercury, nitrogen oxide, and sulfur dioxide), power system reliability indices (loss of load probability and unserviced energy), and average electricity cost. Further, the PPC algorithm results within the Proposed Aggregate PESU Simulation (PAPS) provide an electric utility centric point of view of residential energy management technology. Specifically, the expected value of each PESU result is computed in the PPC algorithm. The expected PESU results provide quantified results from which electric utility planning decisions can be compared. The ability to compare multiple planning options on an equal basis will guide electric utility technology investment strategies.

The impact of the energy management functions on PESU in four power system areas of the United States is analyzed. The four power system areas of the United States are Versailles Kentucky, Mercury Nevada, Stillwater Oklahoma, and Necedah Wisconsin. These four power system areas were selected to consist of different power system operation areas and different climate zones. Different climate zones were selected to study the impact of ambient temperature on the ability of the various energy management functions to provide automated demand response (DR).

Further, the impact of increasing levels of market penetration of REMS enabled residences is investigated. Each expected PESU result in this chapter is quantified for each energy management function, power system area, various levels of market penetration (10%, 20%, and 40%), and various amounts of electric utility control (number of DR days - from zero to 50 days in steps of 10 days). Notice, zero DR days is the base case (BC) in this chapter. Zero DR days includes no energy management function. The DR days were identified by selecting the days with the highest peak system load for each area.

First is a presentation of a comparison of the BC PAPS results. The BC PAPS results highlight the differences between the power system areas and the four distributed energy resource scenarios: A, B, C, and D. Scenario A consists the full accompaniment of residential appliances (clothes dryer; clothes washer; dishwasher; heating, ventilation, and air conditioning [HVAC]; water heater [WH]; and uncontrolled electric load) with no photovoltaic (PV) generation or plug-in electric vehicle (PEV) load. Scenario B consists of Scenario A plus the PEV load. Scenario C consists of Scenario A plus the PV generation. Scenario D consists of Scenario A plus both the PV generation and PEV load.

After the BC PAPS results is a presentation of each of the PAPS energy management function results (WH direct load control [DLC], HVAC DLC, smart thermostat, smart appliance scheduling, and smart appliance scheduling with a stationary battery). As an example of the structure of the remainder of this chapter a description of the WH DLC energy management function results. The same structure holds for each of the remaining energy management functions.

The WH DLC consists of four distributed energy resource scenarios previously introduced. Where the Scenario A includes the change in electricity load computed in the Proposed Physically-Based REMS Simulation WH DLC for the days corresponding to the highest peak system load. The DR period is set to start one hour before the peak load and last for four hours. This chapter ends with a summary of the PAPS results.

6.1 Base Case

The Proposed Aggregate Primary-Energy-Source-Utilization Simulation (PAPS) base case (BC) simulates the annual power system economic dispatch model for the four power system areas with no demand response (DR) days; thus, no controlled adjustment of the use of residential appliances due to the residential energy management functions. The results in this section depict the increase in each expected PAPS result compared to the expected PAPS Scenario A results. The PAPS Scenario A does not include photovoltaic (PV) generation or plug-in electric (PEV) load. Thus, the increase in the expected PAPS results highlight the effect of the PEV (Scenario B), PV (Scenario C), and combination of PEV and PV (Scenario D). The different PAPS scenario results are included for Versailles Kentucky (ECAK), Mercury Nevada (SNV), Stillwater Oklahoma (SPPS), and Necedah Wisconsin (WUMS) power system areas.

Specifically, the increase in the expected PAPS BC generated energy (GE), the expected PAPS BC generated environmental air pollution (GEAP), the expected PAPS BC loss of load probability (LOLP), the expected PAPS BC unserviced energy (UE), and the expected PAPS BC average energy cost (AEC) is shown in Figure 142, Figure 143, Figure 144, Figure 145, and Figure 146, respectively.

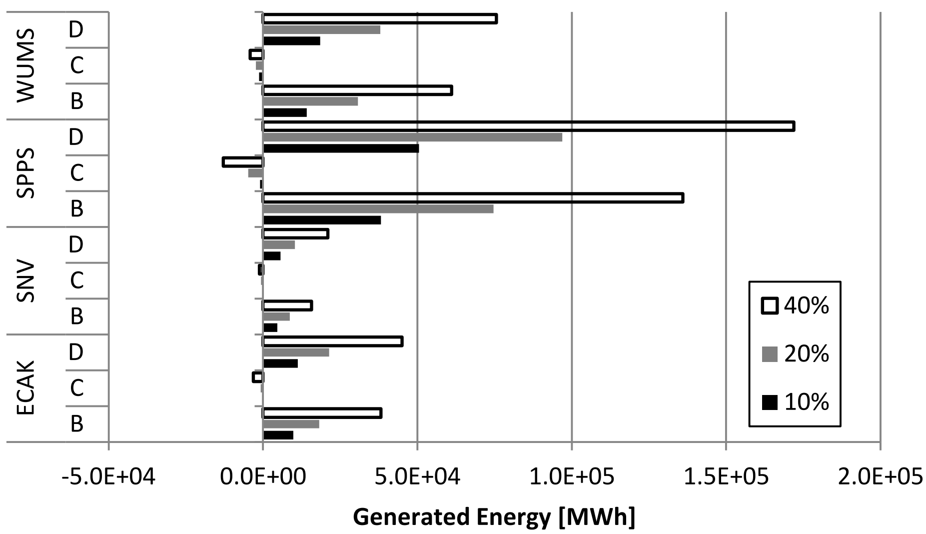

Figure 142: The increase in the expected Proposed Aggregate Primary-Energy-Source-Utilization Simulation [PAPS] base case [BC] generated energy [GE].

The increase in the expected PAPS BC GE shown in Figure 142 illustrates three intuitive findings. First, the ordered list of increase in the expected PAPS BC GE for each power system area is (highest to lowest) SPPS, WUMS, ECAK, and SNV, as expected. Second, the increase in the expected PAPS BC Scenario B and D GE and the decrease in expected PAPS BC Scenario C GE for all power system areas, as expected. Third, a proportional relationship exists between the increase in the expected PAPS BC GE and the REMS market penetration, as expected.

To further illustrate the increase in the expected PAPS BC GE in Figure 142 the PAPS BC ECAK GE is described further. The increase in the expected PAPS BC ECAK

Scenario B GE is 0.017% (9,761 MWh), 0.031% (18,170 MWh), and 0.066% (38,200 MWh) compared to the expected PAPS BC ECAK Scenario A GE for the 10%, 20%, and 40% REMS market penetration, respectively. Also, the decrease in the expected PAPS BC ECAK Scenario C GE is less than 0.001% (200.0 MWh), 0.001% (813.5 MWh), and 0.005% (3,159 MWh) compared to the expected PAPS BC ECAK Scenario A GE for the 10%, 20%, and 40% residential energy management system (REMS) market penetration, respectively. Finally, the increase in the expected PAPS BC ECAK Scenario D GE is 0.019% (11,200 MWh), 0.037% (21,360 MWh), and 0.078% (44,980 MWh) compared to the expected PAPS BC ECAK Scenario A GE for the 10%, 20%, and 40% REMS market penetration, respectively.

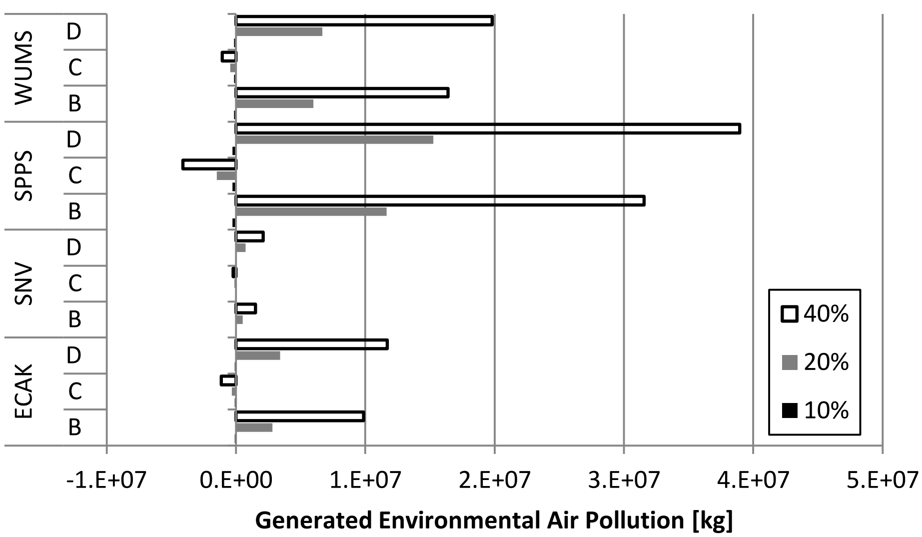

Figure 143: The increase in the expected Proposed Aggregate Primary-Energy-Source-Utilization Simulation [PAPS] base case [BC] generated environmental air pollution [GEAP].

The same relationships described for the increase in the expected PAPS BC GE, shown in Figure 142, are evident in the increase in the expected PAPS BC GEAP, shown in Figure 143. Thus, the PAPS BC GEAP is proportional to the PAPS BC GE.

To further illustrate the increase in expected PAPS BC GEAP in Figure 143 the expected PAPS BC ECAK GEAP is described further. The increase in the expected PAPS BC ECAK Scenario B GEAP is less than 0.010% ($3.492 \cdot 10^6$ kg), 0.018% ($6.420 \cdot 10^6$ kg), and 0.039% ($1.347 \cdot 10^7$ kg) compared to the expected PAPS BC ECAK Scenario A GEAP for the 10%, 20%, and 40% REMS market penetration, respectively. Also, the decrease in the expected PAPS BC ECAK Scenario C GEAP is less than 0.001% ($7.269 \cdot 10^4$ kg), 0.001% ($3.017 \cdot 10^5$ kg), and 0.003% ($1.111 \cdot 10^6$ kg) compared to the expected PAPS BC ECAK Scenario A GEAP for the 10%, 20%, and 40% REMS market penetration, respectively. Finally, the increase in the expected PAPS BC ECAK Scenario D GEAP is 0.011% ($4.015 \cdot 10^6$ kg), 0.022% ($7.537 \cdot 10^6$ kg), and 0.045% ($1.582 \cdot 10^7$ kg) compared to the expected PAPS BC ECAK Scenario A GEAP for the 10%, 20%, and 40% REMS market penetration, respectively. Notice that the PAPS BC ECAK Scenario A EAP is 99.9997% CO_2 ($3.496 \cdot 10^{10}$ kg) and the remainder is MER, NO_x and SO_2 ($1.041 \cdot 10^5$ kg).

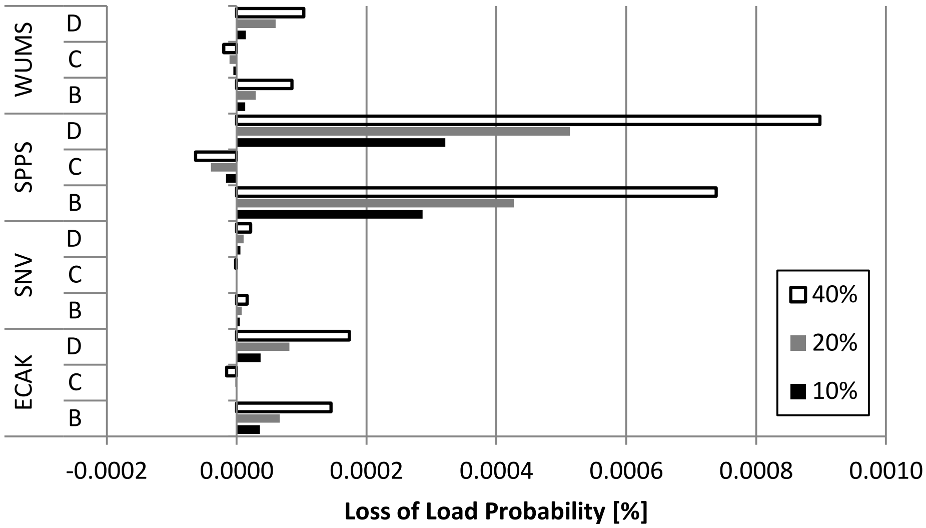

Figure 144: The increase in the expected Proposed Aggregate Primary-Energy-Source-Utilization Simulation [PAPS] base case [BC] loss of load probability [LOLP].

The increase in the expected PAPS BC LOLP shown in Figure 144 illustrates some expected findings. First, the ordered list of increase in the expected PAPS BC LOLP for each power system area is (highest to lowest) SPPS, ECAK, WUMS, and SNV. Second, the increase in the expected PAPS BC Scenario B and D LOLP and the decrease in the expected PAPS BC Scenario C LOLP for all power system areas, as expected. Third, a proportional relationship exists between the increase in the expected PAPS BC LOLP and the REMS market penetration, as expected.

To further illustrate the increase in expected PAPS BC LOLP in Figure 144 the expected PAPS BC ECAK LOLP is described further. The increase in the expected PAPS BC ECAK Scenario B LOLP is 0.284% ($3.568 \cdot 10^{-5}$%), 0.530% (23.210 kg), and 1.155% ($1.453 \cdot 10^{-4}$%) compared to the expected PAPS BC ECAK Scenario A LOLP for the 10%, 20%, and 40% REMS market penetration, respectively. Also, the decrease in the expected PAPS BC ECAK Scenario C LOLP is less than 0.005% ($6.323 \cdot 10^{-7}$%), 0.016% ($2.042 \cdot 10^{-6}$%), and 0.123% ($1.553 \cdot 10^{-5}$%) compared to the expected PAPS BC

ECAK Scenario A LOLP for the 10%, 20%, and 40% REMS market penetration, respectively. Finally, the increase in the expected PAPS BC ECAK Scenario D LOLP is 0.293% ($3.691 \cdot 10^{-5}$%), 0.646% ($8.126 \cdot 10^{-5}$%), and 1.380% ($1.737 \cdot 10^{-4}$%) compared to the expected PAPS BC ECAK Scenario A LOLP for the 10%, 20%, and 40% REMS market penetration, respectively.

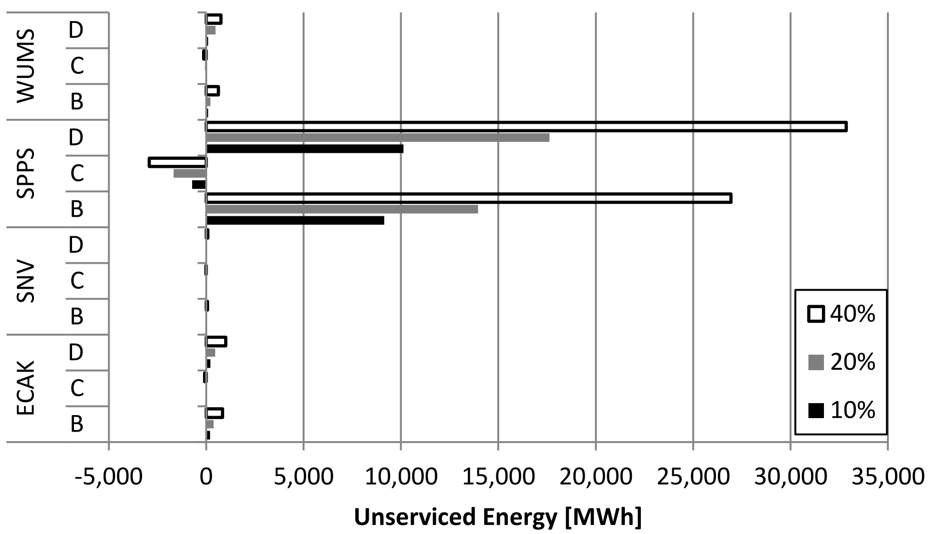

Figure 145: The increase in the expected Proposed Aggregate Primary-Energy-Source-Utilization Simulation [PAPS] base case [BC] unserviced energy [UE].

The same relationships described for the increase in the expected PAPS BC LOLP, shown in Figure 144, are evident in the increase in the expected PAPS BC UE, shown in Figure 145. Thus, the PAPS BC LOLP is proportional to the PAPS BC UE.

To further illustrate the increase in expected PAPS BC UE in Figure 145 the expected PAPS BC ECAK UE is described further. The increase in the expected PAPS BC ECAK Scenario B UE is 0.330% (202.8 MWh), 0.620% (381.3 MWh), and 1.364% (838.7 MWh) compared to the expected PAPS BC ECAK Scenario A UE for the 10%, 20%, and 40% REMS market penetration, respectively. Also, the decrease in the expected PAPS BC ECAK Scenario C UE is 0.004% (2.390 MWh), 0.014% (8.458

MWh), and 0.144% (88.81 MWh) compared to the expected PAPS BC ECAK Scenario A UE for the 10%, 20%, and 40% REMS market penetration, respectively. Finally, the increase in the expected PAPS BC ECAK Scenario D UE is 0.337% (207.1 MWh), 0.759% (467.0 MWh), and 1.636% (1,007 MWh) compared to the expected PAPS BC ECAK Scenario A UE for the 10%, 20%, and 40% REMS market penetration, respectively.

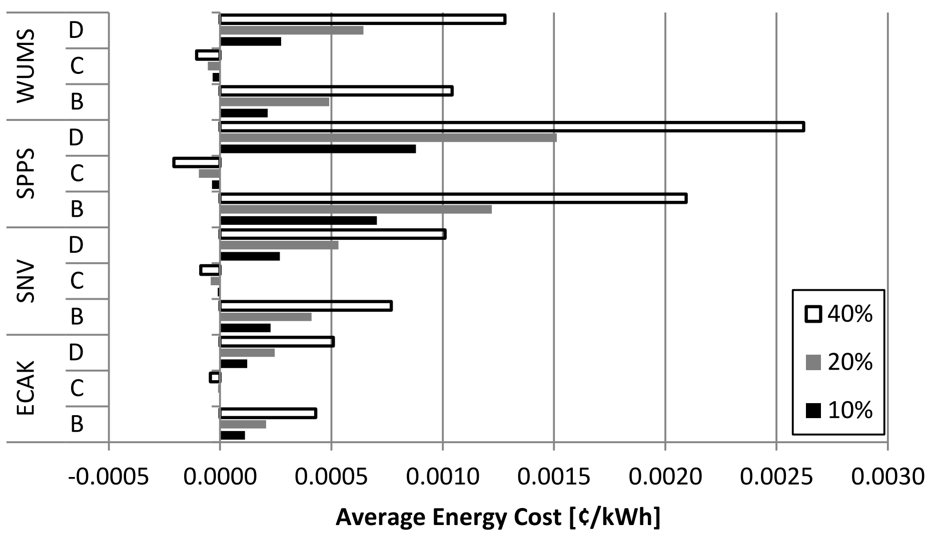

Figure 146: The increase in the expected Proposed Aggregate Primary-Energy-Source-Utilization Simulation [PAPS] base case [BC] average electricity cost [AEC].

The same relationships described for the increase in the expected PAPS BC GE, shown in Figure 142, are evident in the increase in the expected PAPS BC AEC, shown in Figure 146. Thus, the PAPS BC generated AEC is proportional to the PAPS BC GE.

To further illustrate the increase in expected PAPS BC AEC in Figure 146 the expected PAPS BC ECAK AEC is described further. The increase in the expected PAPS BC ECAK Scenario B AEC is 0.012% ($1.116{\cdot}10^{-4}$ ¢/kWh), 0.022% ($2.065{\cdot}10^{-4}$ ¢/kWh), and 0.046% ($4.299{\cdot}10^{-4}$ ¢/kWh) compared to the expected PAPS BC ECAK Scenario A AEC for the 10%, 20%, and 40% REMS market penetration, respectively. The decrease in the expected PAPS BC ECAK Scenario C AEC is less than 0.001% ($2.968 \cdot 10^{-6}$ ¢/kWh), 0.001% ($9.105 \cdot 10^{-6}$ ¢/kWh), and 0.005% ($4.374 \cdot 10^{-6}$ ¢/kWh) compared to the expected PAPS BC ECAK Scenario A AEC for the 10%, 20%, and 40% REMS market penetration, respectively. The increase in the expected PAPS BC ECAK Scenario D AEC is 0.013% ($1.223 \cdot 10^{-4}$ ¢/kWh), 0.026% ($2.453 \cdot 10^{-4}$ ¢/kWh), and 0.054% ($5.085 \cdot 10^{-4}$ ¢/kWh) compared to the expected PAPS BC ECAK Scenario A AEC for the 10%, 20%, and 40% REMS market penetration, respectively.

Next is a presentation of the PAPS water heater direct load control results.

6.2 Water Heater Direct Load Control

The direct load control (DLC) energy management function is provided in two forms: water heater (WH) and heating, ventilation, and air conditioning (HVAC). In both of these forms, the controlled appliance (WH or HVAC) is controlled for an electric utility specified time period (demand response [DR] period - one hour before the daily peak lasting a total of four hours) with limited service during this time period to the controlled appliance only. The WH DLC removes service to the WH for the entire DR period (with all WH energy use rescheduled after the DR period, i.e. 100% payback efficiency).

The results in this section show the percent change of the expected Proposed Aggregate Primary-Energy-Source-Utilization Simulation (PAPS) results for the residential energy management system (REMS) market penetration levels (10%, 20%, and 40%) for each location (Versailles Kentucky [ECAK], Mercury Nevada [SNV], Stillwater Oklahoma [SPPS], and Necedah Wisconsin [WUMS]). The percent change in the expected PAPS results for the various market penetration levels are compared to the corresponding expected PAPS base case (BC) results described in Section 6.1. Further, the slope of the percent change as a function of the DR days is computed for each result. The slope of the percent change is a sensitivity measure of the expected PAPS results to the WH DLC energy management function.

The percent change in the expected PPRS WH DLC Scenario A, Scenario B, Scenario C, and Scenario D generated energy (GE) is shown in Figure 147, Figure 148, Figure 149, Figure 150, respectively.

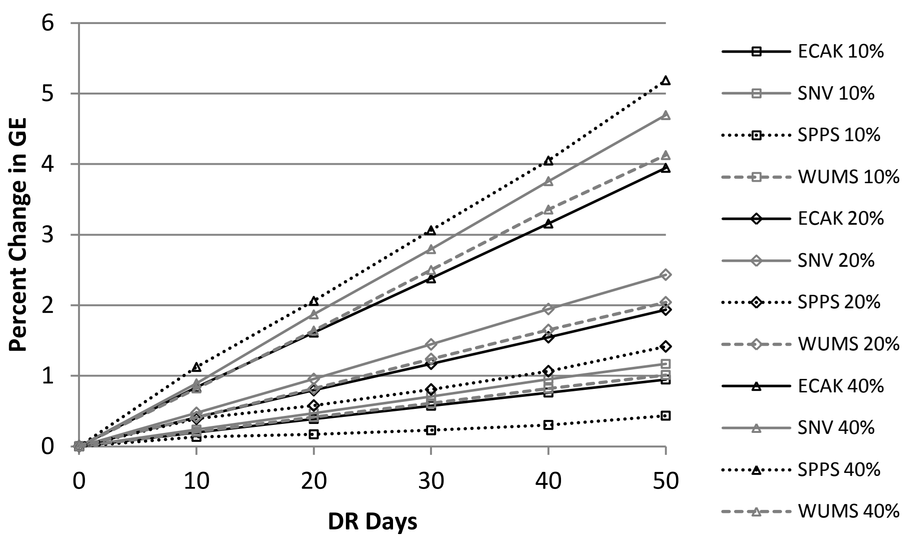

Figure 147: Percent change in the expected Proposed Aggregate Primary-Energy-Source-Utilization Simulation [PAPS] water heater [WH] direct load control [DLC] Scenario A generated energy [GE].

The expected PAPS WH DLC Scenario A GE, shown in Figure 147, quantifies the change in the expected PAPS WH DLC Scenario A GE as a function of the number of DR days (from zero to 50) for three levels of REMS market penetration. Specifically, the slope [%/DR day] of the 10%, 20%, and 40% REMS market penetration percent change in the expected PAPS WH DLC Scenario A GE is 0.019, 0.038, and 0.078 for the ECAK power system area respective REMS market penetration level; 0.023, 0.049, and

0.094 for the SNV power system area respective REMS market penetration level; 0.008, 0.027, and 0.102 for the SPPS power system area respective REMS market penetration level; and 0.020, 0.041, and 0.083 for the WUMS power system area respective REMS market penetration level. Interestingly, the SPPS power system area has lowest sensitivity at 10% market penetration but the highest at 40% market penetration.

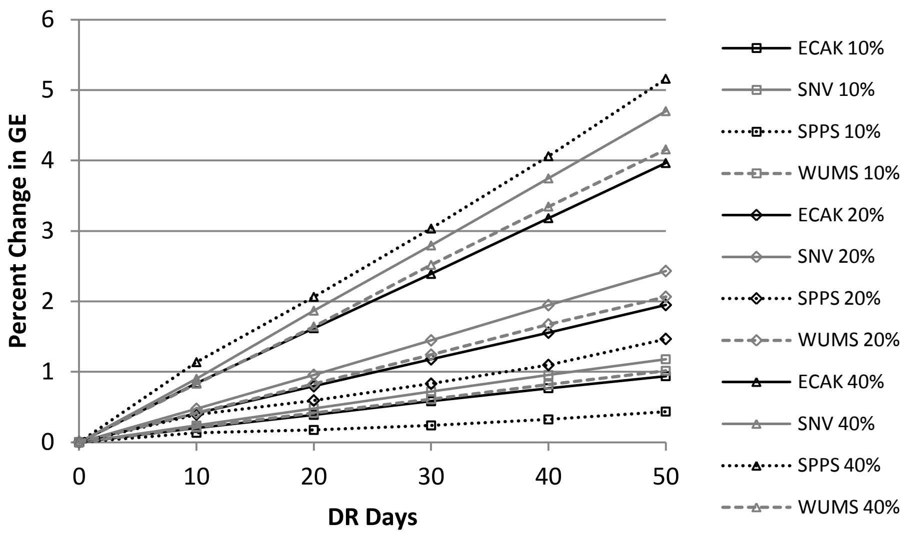

Figure 148: Percent change in the expected Proposed Aggregate Primary-Energy-Source-Utilization Simulation [PAPS] water heater [WH] direct load control [DLC] Scenario B generated energy [GE].

The expected PAPS WH DLC Scenario B GE, shown in Figure 148, quantifies the change in the expected PAPS WH DLC Scenario B GE as a function of the number of DR days (from zero to 50) for three levels of REMS market penetration. Specifically, the slope [%/DR day] of the 10%, 20%, and 40% REMS market penetration percent change in the expected PAPS WH DLC Scenario B GE is 0.019, 0.039, and 0.079 for the ECAK power system area respective REMS market penetration level; 0.024, 0.049, and 0.094 for the SNV power system area respective REMS market penetration level; 0.008, 0.028, and 0.102 for the SPPS power system area respective REMS market penetration level;

and 0.020, 0.041, and 0.083 for the WUMS power system area respective REMS market penetration level.

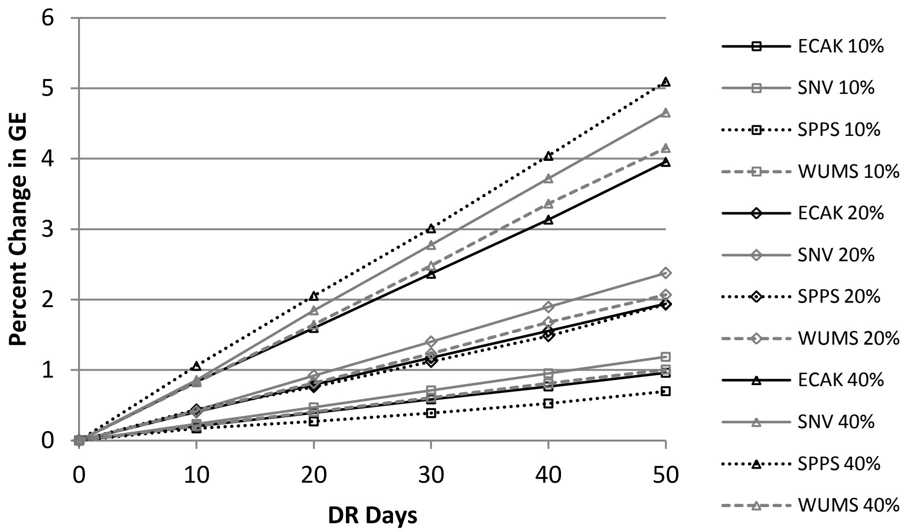

Figure 149: Percent change in the expected Proposed Aggregate Primary-Energy-Source-Utilization Simulation [PAPS] water heater [WH] direct load control [DLC] Scenario C generated energy [GE].

The expected PAPS WH DLC Scenario C GE, shown in Figure 149, quantifies the change in the expected PAPS WH DLC Scenario C GE as a function of the number of DR days (from zero to 50) for three levels of REMS market penetration. Specifically, the slope [%/DR day] of the 10%, 20%, and 40% REMS market penetration percent change in the expected PAPS WH DLC Scenario C GE is 0.019, 0.039, and 0.078 for the ECAK power system area respective REMS market penetration level; 0.024, 0.048, and 0.094 for the SNV power system area respective REMS market penetration level; 0.013, 0.038, and 0.101 for the SPPS power system area respective REMS market penetration level; and 0.020, 0.042, and 0.083 for the WUMS power system area respective REMS market penetration level.

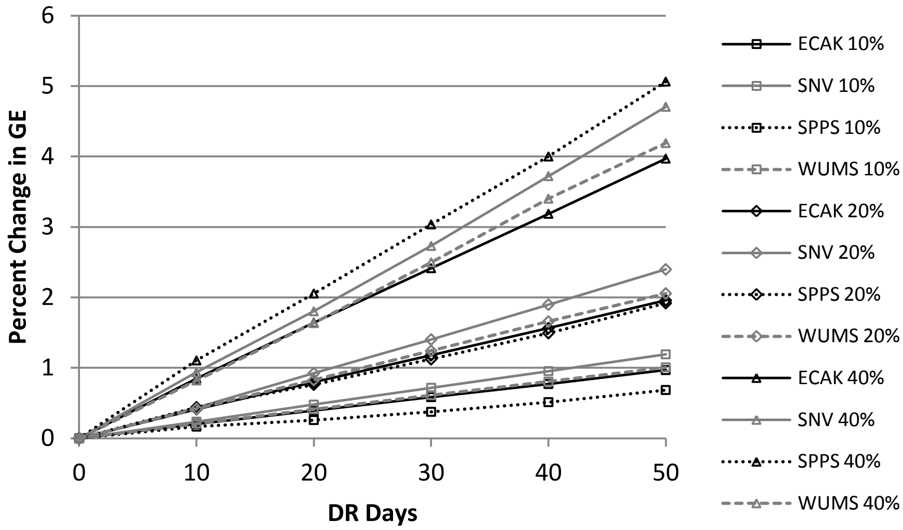

Figure 150: Percent change in the expected Proposed Aggregate Primary-Energy-Source-Utilization Simulation [PAPS] water heater [WH] direct load control [DLC] Scenario D generated energy [GE].

The expected PAPS WH DLC Scenario D GE, shown in Figure 149, quantifies the change in the expected PAPS WH DLC Scenario D GE as a function of the number of DR days (from zero to 50) for three levels of REMS market penetration. Specifically, the slope [%/DR day] of the 10%, 20%, and 40% REMS market penetration percent change in the expected PAPS WH DLC Scenario D GE is 0.019, 0.039, and 0.078 for the ECAK power system area respective REMS market penetration level; 0.024, 0.048, and 0.094 for the SNV power system area respective REMS market penetration level; 0.013, 0.037, and 0.100 for the SPPS power system area respective REMS market penetration level; and 0.020, 0.041, and 0.084 for the WUMS power system area respective REMS market penetration level.

The percent change in the expected PPRS WH DLC Scenario A, Scenario B, Scenario C, and Scenario D generated environmental air pollution (GEAP) is shown in Figure 151, Figure 152, Figure 153, and Figure 154, respectively.

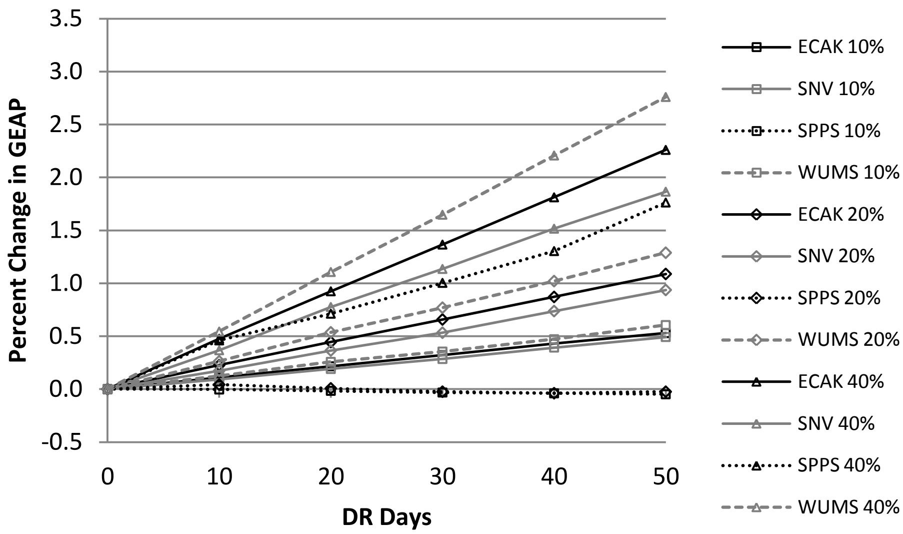

Figure 151: Percent change in the expected Proposed Aggregate Primary-Energy-Source-Utilization Simulation [PAPS] water heater [WH] direct load control [DLC] Scenario A generated environmental air pollution [GEAP].

The expected PAPS WH DLC Scenario A GEAP, shown in Figure 151, quantifies the change in the expected PAPS WH DLC Scenario A GEAP as a function of the number of DR days (from zero to 50) for three levels of REMS market penetration. Specifically, the slope [%/DR day] of the 10%, 20%, and 40% REMS market penetration percent change in the expected PAPS WH DLC Scenario A GEAP is 0.011, 0.022, and 0.045 for the ECAK power system area respective REMS market penetration level; 0.010, 0.019, 0.038 for the SNV power system area respective REMS market penetration level; -0.001, -0.001, and 0.033 for the SPPS power system area respective REMS market penetration level; and 0.012, 0.026, and 0.055 for the WUMS power system area respective REMS market penetration level.

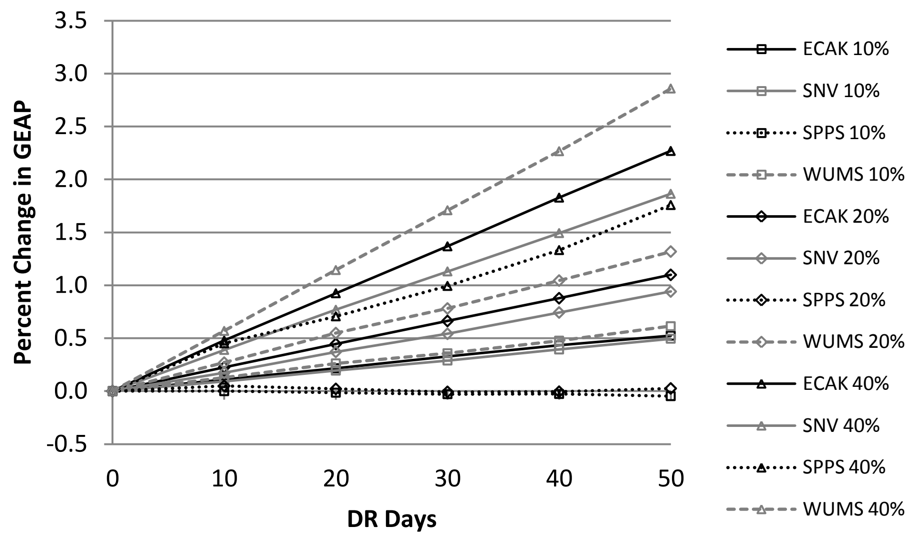

Figure 152: Percent change in the expected Proposed Aggregate Primary-Energy-Source-Utilization Simulation [PAPS] water heater [WH] direct load control [DLC] Scenario B generated environmental air pollution [GEAP].

The expected PAPS WH DLC Scenario B GEAP, shown in Figure 152, quantifies the change in the expected PAPS WH DLC Scenario B GEAP as a function of the number of DR days (from zero to 50) for three levels of REMS market penetration. Specifically, the slope [%/DR day] of the 10%, 20%, and 40% REMS market penetration percent change in the expected PAPS WH DLC Scenario B GEAP is 0.011, 0.022, and 0.045 for the ECAK power system area respective REMS market penetration level; 0.010, 0.019, 0.037 for the SNV power system area respective REMS market penetration level; -0.001, less than 0.001, and 0.033 for the SPPS power system area respective REMS market penetration level; and 0.012, 0.026, and 0.057 for the WUMS power system area respective REMS market penetration level.

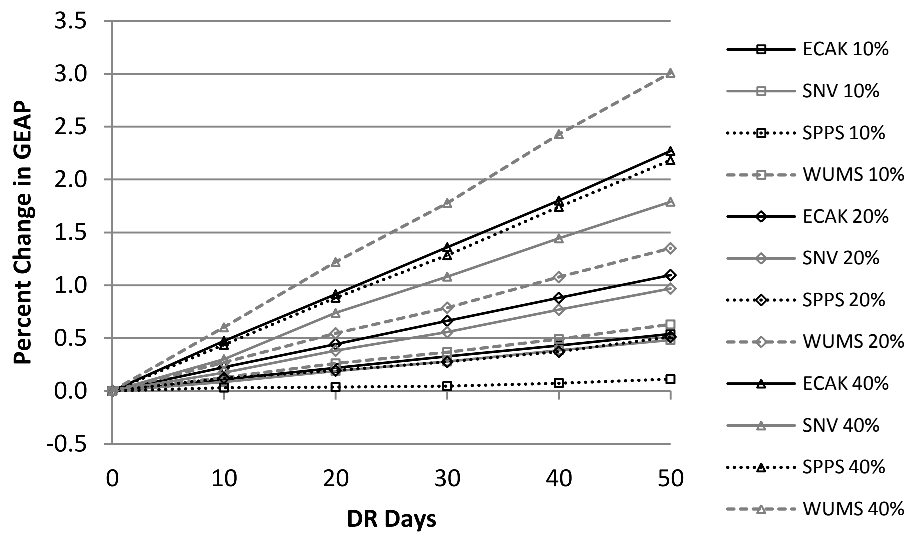

Figure 153: Percent change in the expected Proposed Aggregate Primary-Energy-Source-Utilization Simulation [PAPS] water heater [WH] direct load control [DLC] Scenario C generated environmental air pollution [GEAP].

The expected PAPS WH DLC Scenario C GEAP, shown in Figure 153, quantifies the change in the expected PAPS WH DLC Scenario C GEAP as a function of the number of DR days (from zero to 50) for three levels of REMS market penetration. Specifically, the slope [%/DR day] of the 10%, 20%, and 40% REMS market penetration percent change in the expected PAPS WH DLC Scenario C GEAP is 0.011, 0.022, and 0.045 for the ECAK power system area respective REMS market penetration level; 0.010, 0.019, 0.036 for the SNV power system area respective REMS market penetration level; 0.002, 0.010, and 0.044 for the SPPS power system area respective REMS market penetration level; and 0.012, 0.027, and 0.060 for the WUMS power system area respective REMS market penetration level.

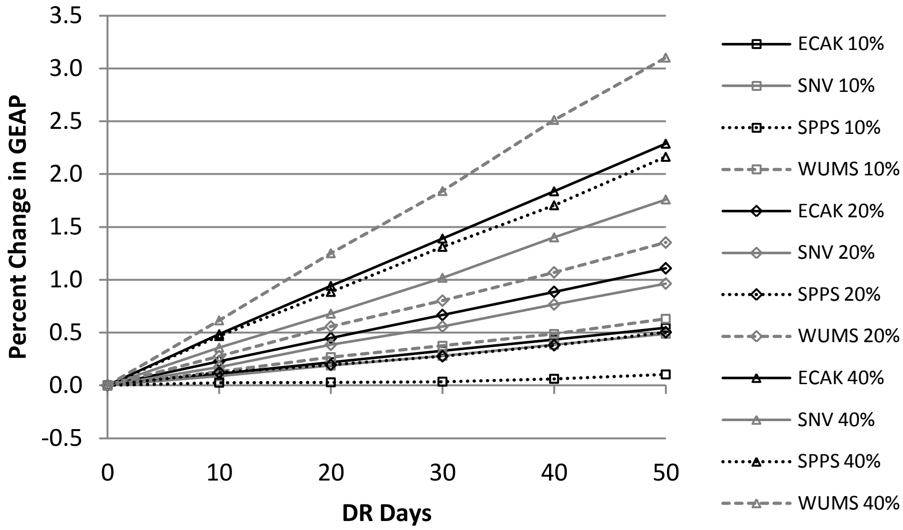

Figure 154: Percent change in the expected Proposed Aggregate Primary-Energy-Source-Utilization Simulation [PAPS] water heater [WH] direct load control [DLC] Scenario D generated environmental air pollution [GEAP].

The expected PAPS WH DLC Scenario D GEAP, shown in Figure 154, quantifies the change in the expected PAPS WH DLC Scenario D GEAP as a function of the number of DR days (from zero to 50) for three levels of REMS market penetration. Specifically, the slope [%/DR day] of the 10%, 20%, and 40% REMS market penetration percent change in the expected PAPS WH DLC Scenario D GEAP is 0.011, 0.022, and 0.046 for the ECAK power system area respective REMS market penetration level; 0.010, 0.019, 0.035 for the SNV power system area respective REMS market penetration level; 0.002, 0.010, and 0.043 for the SPPS power system area respective REMS market penetration level; and 0.012, 0.027, and 0.062 for the WUMS power system area respective REMS market penetration level.

The percent change in the expected PPRS WH DLC Scenario A, Scenario B, Scenario C, and Scenario D loss of load probability (LOLP) is shown in Figure 155, Figure 156, Figure 157, and Figure 158, respectively.

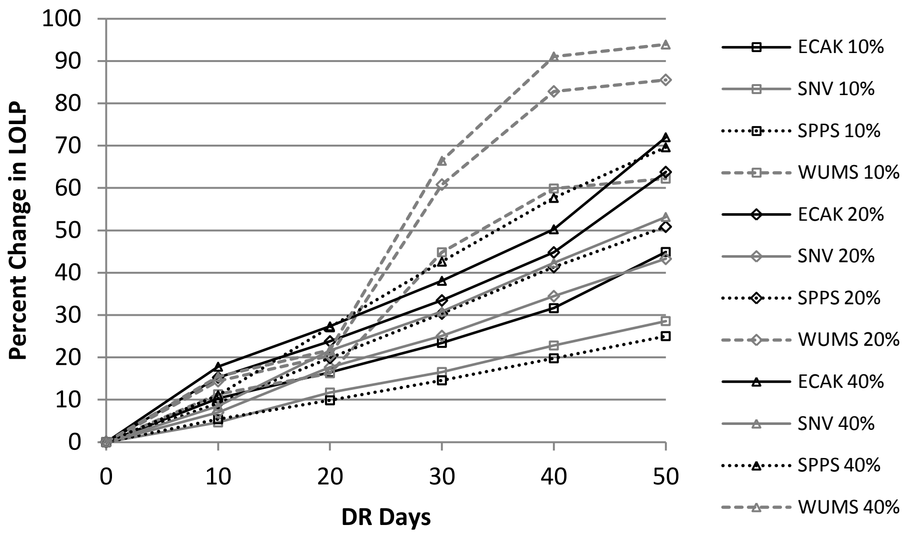

Figure 155: Percent change in the expected Proposed Aggregate Primary-Energy-Source-Utilization Simulation [PAPS] water heater [WH] direct load control [DLC] Scenario A loss of load probability [LOLP].

The expected PAPS WH DLC Scenario A LOLP, shown in Figure 155, quantifies the change in the expected PAPS WH DLC Scenario A LOLP as a function of the number of DR days (from zero to 50) for three levels of REMS market penetration. Specifically, the slope [%/DR day] of the 10%, 20%, and 40% REMS market penetration percent change in the expected PAPS WH DLC Scenario A LOLP is 0.844, 1.192, and 1.337 for the ECAK power system area respective REMS market penetration level; 0.578, 0.875, and 1.075 for the SNV power system area respective REMS market penetration level; 0.494, 1.032, and 1.438 for the SPPS power system area respective REMS market penetration level; and 1.387, 1.924, and 2.117 for the WUMS power system area respective REMS market penetration level.

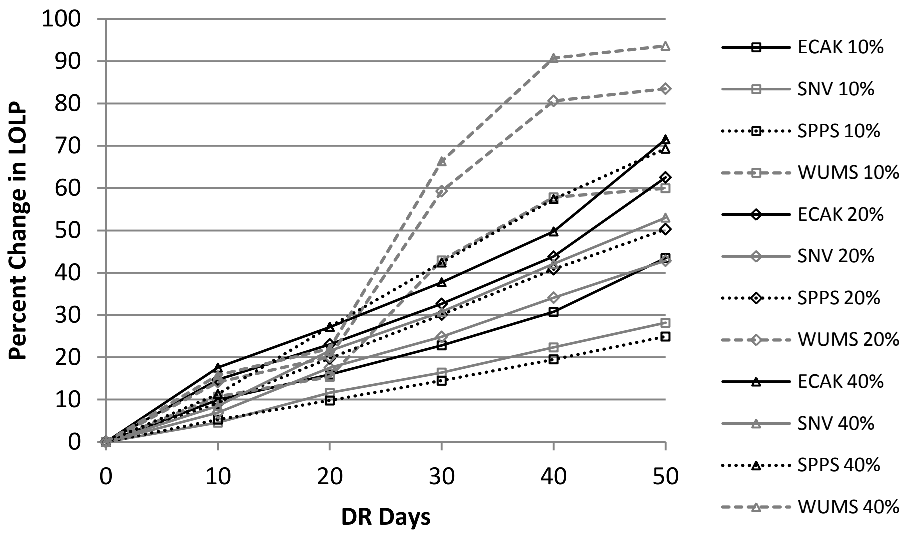

Figure 156: Percent change in the expected Proposed Aggregate Primary-Energy-Source-Utilization Simulation [PAPS] water heater [WH] direct load control [DLC] Scenario B loss of load probability [LOLP].

The expected PAPS WH DLC Scenario B LOLP, shown in Figure 156, quantifies the change in the expected PAPS WH DLC Scenario B LOLP as a function of the number of DR days (from zero to 50) for three levels of REMS market penetration. Specifically, the slope [%/DR day] of the 10%, 20%, and 40% REMS market penetration percent change in the expected PAPS WH DLC Scenario B LOLP is 0.818, 1.170, and 1.328 for the ECAK power system area respective REMS market penetration level; 0.568, 0.866, and 1.072 for the SNV power system area respective REMS market penetration level; 0.491, 1.020, and 1.428 for the SPPS power system area respective REMS market penetration level; and 1.339, 1.875, and 2.107 for the WUMS power system area respective REMS market penetration level.

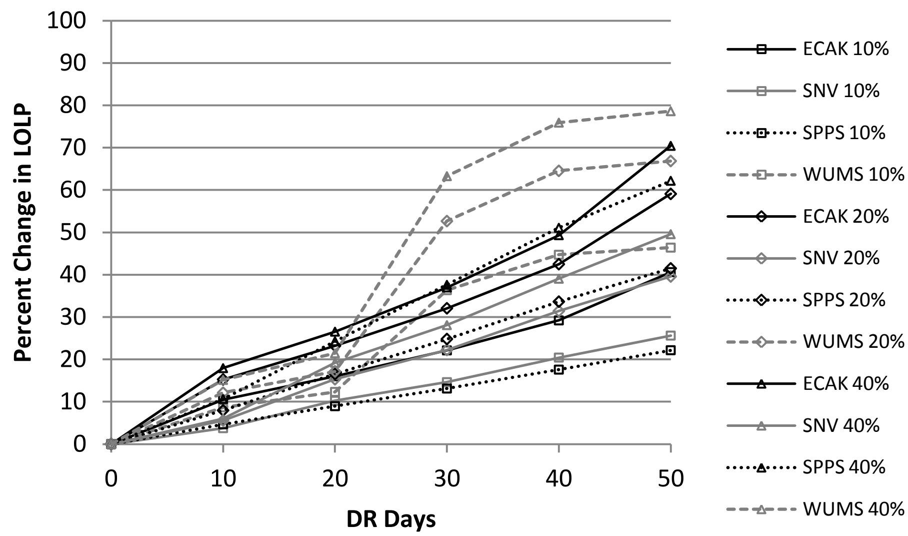

Figure 157: Percent change in the expected Proposed Aggregate Primary-Energy-Source-Utilization Simulation [PAPS] water heater [WH] direct load control [DLC] Scenario C loss of load probability [LOLP].

The expected PAPS WH DLC Scenario C LOLP, shown in Figure 157, quantifies the change in the expected PAPS WH DLC Scenario C LOLP as a function of the number of DR days (from zero to 50) for three levels of REMS market penetration. Specifically, the slope [%/DR day] of the 10%, 20%, and 40% REMS market penetration percent change in the expected PAPS WH DLC Scenario C LOLP is 0.758, 1.103, and 1.305 for the ECAK power system area respective REMS market penetration level; 0.521, 0.807, and 1.016 for the SNV power system area respective REMS market penetration level; 0.439, 0.836, and 1.273 for the SPPS power system area respective REMS market penetration level; and 1.040, 1.506, and 1.763 for the WUMS power system area respective REMS market penetration level.

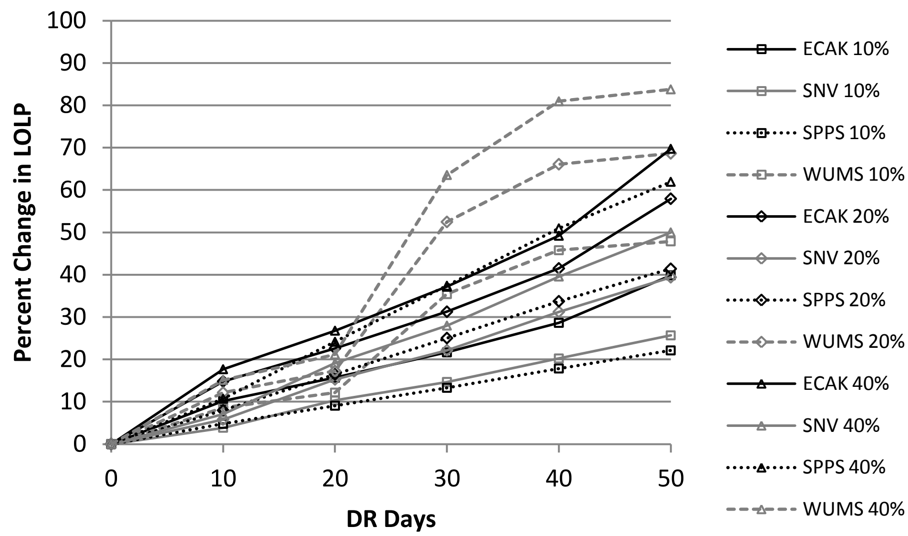

Figure 158: Percent change in the expected Proposed Aggregate Primary-Energy-Source-Utilization Simulation [PAPS] water heater [WH] direct load control [DLC] Scenario D loss of load probability [LOLP].

The expected PAPS WH DLC Scenario D LOLP, shown in Figure 158, quantifies the change in the expected PAPS WH DLC Scenario D LOLP as a function of the number of DR days (from zero to 50) for three levels of REMS market penetration. Specifically, the slope [%/DR day] of the 10%, 20%, and 40% REMS market penetration percent change in the expected PAPS WH DLC Scenario D LOLP is 0.744, 1.081, and 1.296 for the ECAK power system area respective REMS market penetration level; 0.519, 0.800, and 1.018 for the SNV power system area respective REMS market penetration level; 0.440, 0.837, and 1.268 for the SPPS power system area respective REMS market penetration level; and 1.069, 1.544, and 1.882 for the WUMS power system area respective REMS market penetration level.

The percent change in the expected PPRS WH DLC Scenario A, Scenario B, Scenario C, and Scenario D unserviced energy (UE) is shown in Figure 159, Figure 160, Figure 161, and Figure 162, respectively.

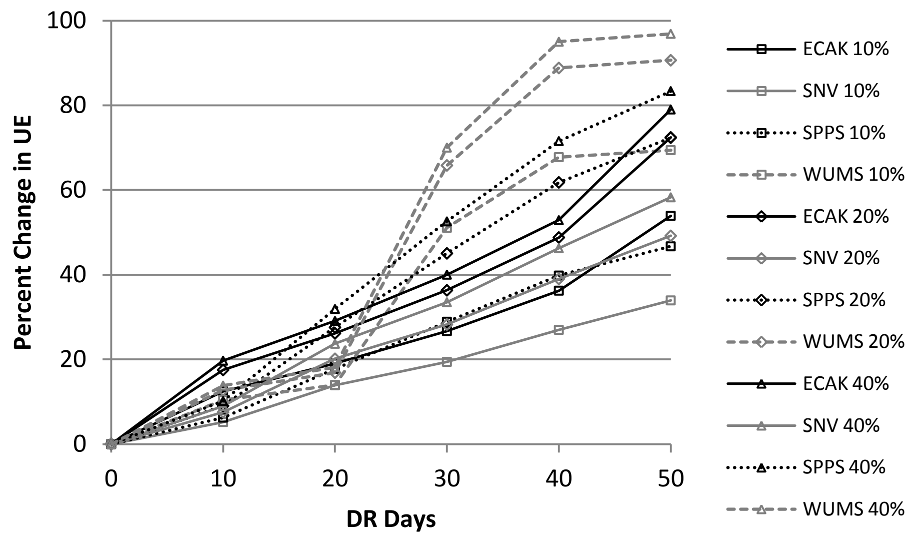

Figure 159: Percent change in the expected Proposed Aggregate Primary-Energy-Source-Utilization Simulation [PAPS] water heater [WH] direct load control [DLC] Scenario A unserviced energy [UE].

The expected PAPS WH DLC Scenario A UE, shown in Figure 159, quantifies the change in the expected PAPS WH DLC Scenario A UE as a function of the number of DR days (from zero to 50) for three levels of REMS market penetration. Specifically, the slope [%/DR day] of the 10%, 20%, and 40% REMS market penetration percent change in the expected PAPS WH DLC Scenario A UE is 0.996, 1.332, and 1.445 for the ECAK power system area respective REMS market penetration level; 0.687, 0.996, and 1.180 for the SNV power system area respective REMS market penetration level; 0.987, 1.536, and 1.776 for the SPPS power system area respective REMS market penetration level; and 1.589, 2.087, and 2.228 for the WUMS power system area respective REMS market penetration level.

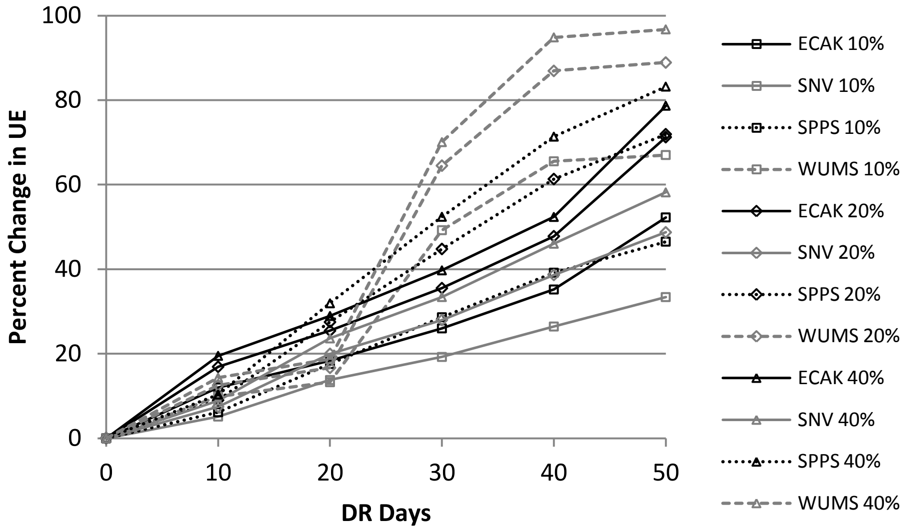

Figure 160: Percent change in the expected Proposed Aggregate Primary-Energy-Source-Utilization Simulation [PAPS] water heater [WH] direct load control [DLC] Scenario B unserviced energy [UE].

The expected PAPS WH DLC Scenario B UE, shown in Figure 160, quantifies the change in the expected PAPS WH DLC Scenario B UE as a function of the number of DR days (from zero to 50) for three levels of REMS market penetration. Specifically, the slope [%/DR day] of the 10%, 20%, and 40% REMS market penetration percent change in the expected PAPS WH DLC Scenario B UE is 0.967, 1.311, and 1.436 for the ECAK power system area respective REMS market penetration level; 0.675, 0.986, and 1.177 for the SNV power system area respective REMS market penetration level; 0.979, 1.525, and 1.770 for the SPPS power system area respective REMS market penetration level; and 1.537, 2.044, and 2.219 for the WUMS power system area respective REMS market penetration level.

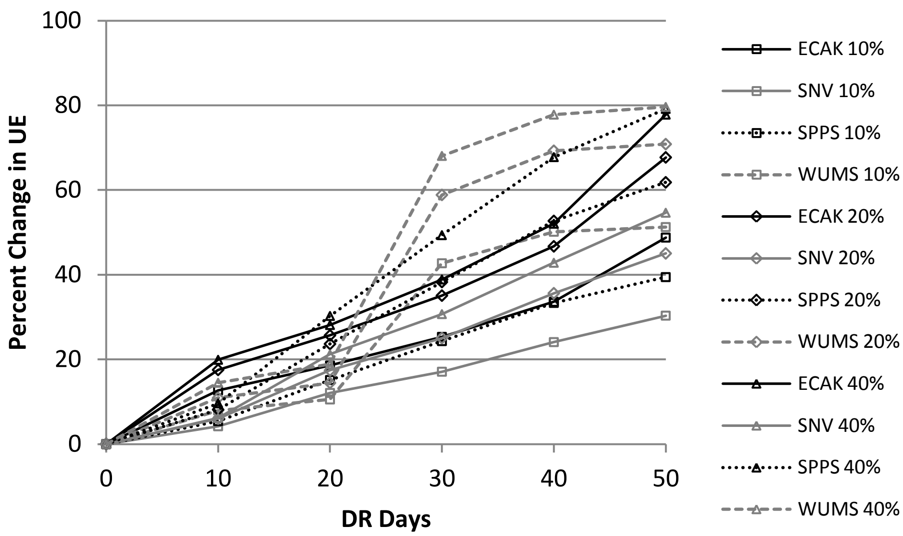

Figure 161: Percent change in the expected Proposed Aggregate Primary-Energy-Source-Utilization Simulation [PAPS] water heater [WH] direct load control [DLC] Scenario C unserviced energy [UE].

The expected PAPS WH DLC Scenario C UE, shown in Figure 161, quantifies the change in the expected PAPS WH DLC Scenario C UE as a function of the number of DR days (from zero to 50) for three levels of REMS market penetration. Specifically, the slope [%/DR day] of the 10%, 20%, and 40% REMS market penetration percent change in the expected PAPS WH DLC Scenario C UE is 0.895, 1.244, and 1.418 for the ECAK power system area respective REMS market penetration level; 0.618, 0.919, and 1.122 for the SNV power system area respective REMS market penetration level; 0.829, 1.307, and 1.684 for the SPPS power system area respective REMS market penetration level; and 1.186, 1.639, and 1.821 for the WUMS power system area respective REMS market penetration level.

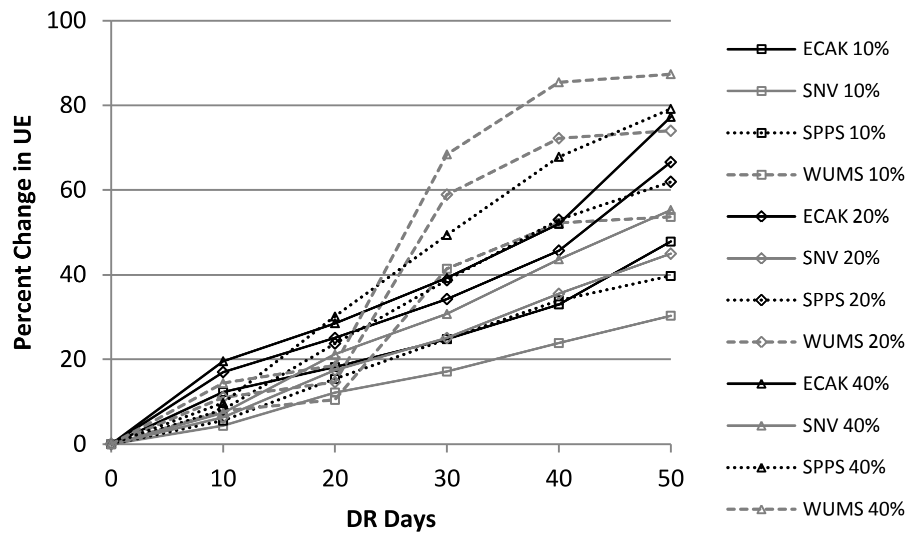

Figure 162: Percent change in the expected Proposed Aggregate Primary-Energy-Source-Utilization Simulation [PAPS] water heater [WH] direct load control [DLC] Scenario D unserviced energy [UE].

The expected PAPS WH DLC Scenario D UE, shown in Figure 162, quantifies the change in the expected PAPS WH DLC Scenario D UE as a function of the number of DR days (from zero to 50) for three levels of REMS market penetration. Specifically, the slope [%/DR day] of the 10%, 20%, and 40% REMS market penetration percent change in the expected PAPS WH DLC Scenario D UE is 0.879, 1.223, and 1.413 for the ECAK power system area respective REMS market penetration level; 0.615, 0.914, and 1.127 for the SNV power system area respective REMS market penetration level; 0.838, 1.312, and 1.684 for the SPPS power system area respective REMS market penetration level; and 1.235, 1.708, and 2.000 for the WUMS power system area respective REMS market penetration level.

The percent change in the expected PPRS WH DLC Scenario A, Scenario B, Scenario C, and Scenario D average electricity cost (AEC) is shown in Figure 163, Figure 164, Figure 165, and Figure 166, respectively.

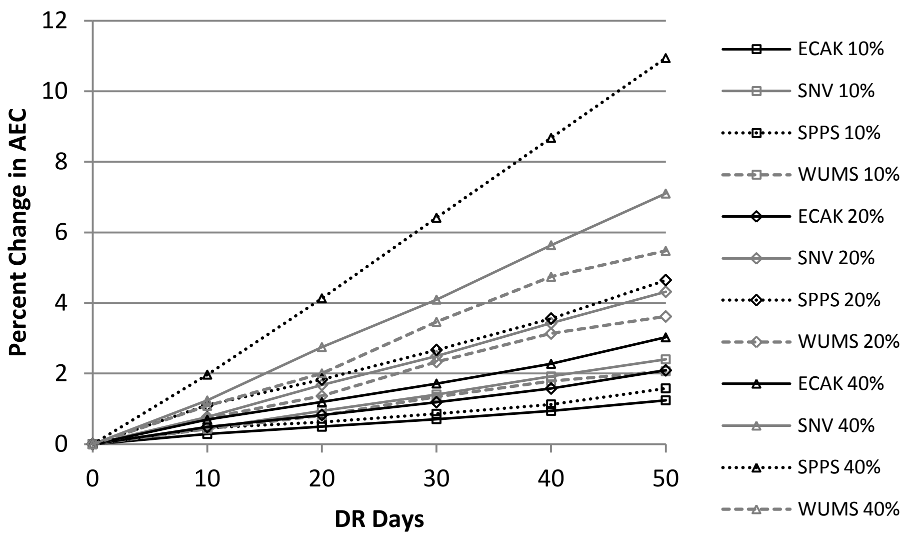

Figure 163: Percent change in the expected Proposed Aggregate Primary-Energy-Source-Utilization Simulation [PAPS] water heater [WH] direct load control [DLC] Scenario A average electricity cost [AEC].

The expected PAPS WH DLC Scenario A AEC, shown in Figure 163, quantifies the change in the expected PAPS WH DLC Scenario A AEC as a function of the number of DR days (from zero to 50) for three levels of REMS market penetration. Specifically, the slope [%/DR day] of the 10%, 20%, and 40% REMS market penetration percent change in the expected PAPS WH DLC Scenario A AEC is 0.024, 0.040, and 0.058 for the ECAK power system area respective REMS market penetration level; 0.048, 0.087, and 0.143 for the SNV power system area respective REMS market penetration level; 0.029, 0.090, and 0.220 for the SPPS power system area respective REMS market penetration level; and 0.043, 0.075, and 0.114 for the WUMS power system area respective REMS market penetration level.

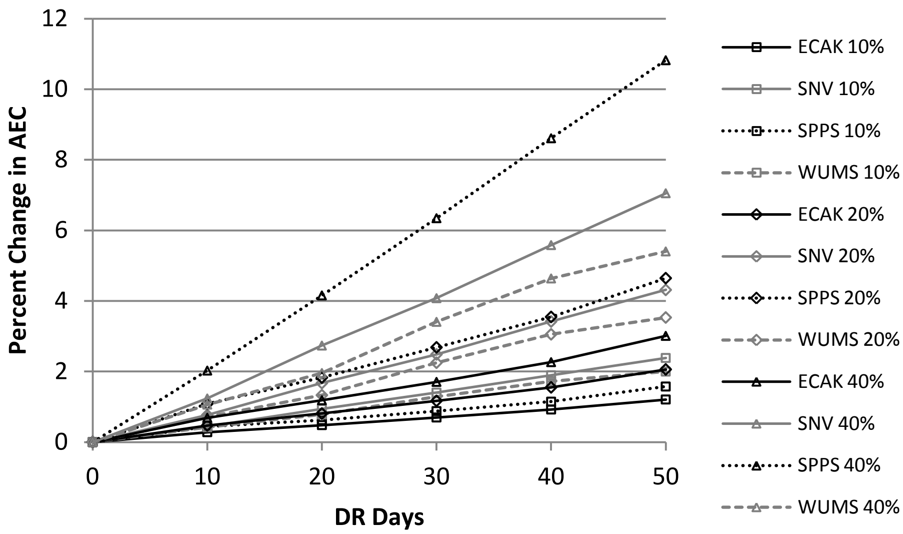

Figure 164: Percent change in the expected Proposed Aggregate Primary-Energy-Source-Utilization Simulation [PAPS] water heater [WH] direct load control [DLC] Scenario B average electricity cost [AEC].

The expected PAPS WH DLC Scenario B AEC, shown in Figure 164, quantifies the change in the expected PAPS WH DLC Scenario B AEC as a function of the number of DR days (from zero to 50) for three levels of REMS market penetration. Specifically, the slope [%/DR day] of the 10%, 20%, and 40% REMS market penetration percent change in the expected PAPS WH DLC Scenario B AEC is 0.023, 0.040, and 0.058 for the ECAK power system area respective REMS market penetration level; 0.048, 0.087, and 0.142 for the SNV power system area respective REMS market penetration level; 0.029, 0.090, and 0.217 for the SPPS power system area respective REMS market penetration level; and 0.041, 0.073, and 0.112 for the WUMS power system area respective REMS market penetration level.

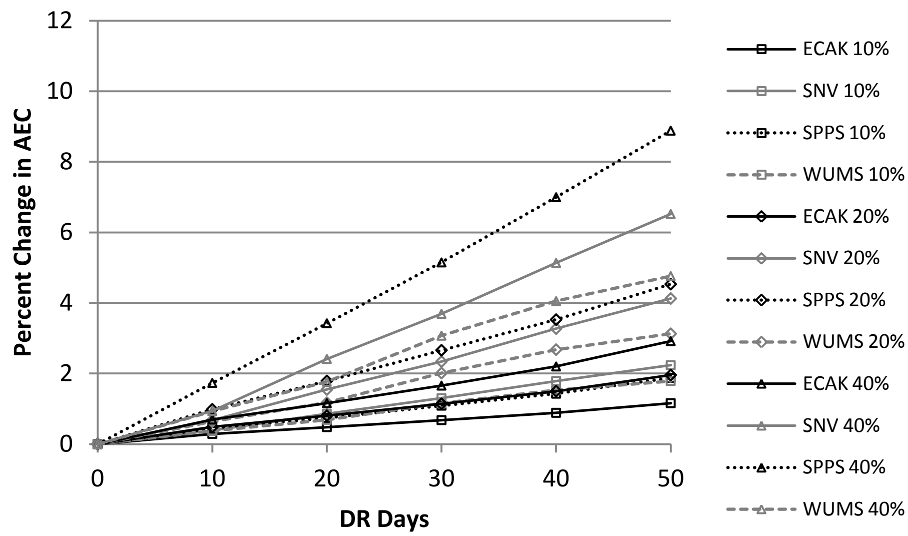

Figure 165: Percent change in the expected Proposed Aggregate Primary-Energy-Source-Utilization Simulation [PAPS] water heater [WH] direct load control [DLC] Scenario C average electricity cost [AEC].

The expected PAPS WH DLC Scenario C AEC, shown in Figure 165, quantifies the change in the expected PAPS WH DLC Scenario C AEC as a function of the number of DR days (from zero to 50) for three levels of REMS market penetration. Specifically, the slope [%/DR day] of the 10%, 20%, and 40% REMS market penetration percent change in the expected PAPS WH DLC Scenario C AEC is 0.022, 0.038, and 0.056 for the ECAK power system area respective REMS market penetration level; 0.045, 0.083, and 0.133 for the SNV power system area respective REMS market penetration level; 0.036, 0.089, and 0.177 for the SPPS power system area respective REMS market penetration level; and 0.037, 0.065, and 0.098 for the WUMS power system area respective REMS market penetration level.

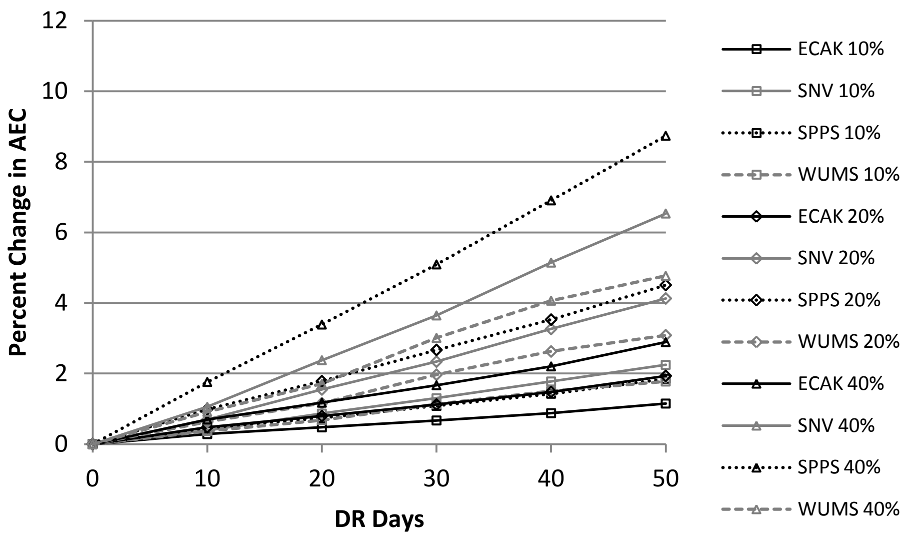

Figure 166: Percent change in the expected Proposed Aggregate Primary-Energy-Source-Utilization Simulation [PAPS] water heater [WH] direct load control [DLC] Scenario D average electricity cost [AEC].

The expected PAPS WH DLC Scenario D AEC, shown in Figure 166, quantifies the change in the expected PAPS WH DLC Scenario D AEC as a function of the number of DR days (from zero to 50) for three levels of REMS market penetration. Specifically, the slope [%/DR day] of the 10%, 20%, and 40% REMS market penetration percent change in the expected PAPS WH DLC Scenario D AEC is 0.022, 0.037, and 0.056 for the ECAK power system area respective REMS market penetration level; 0.045, 0.083, and 0.132 for the SNV power system area respective REMS market penetration level; 0.036, 0.089, and 0.174 for the SPPS power system area respective REMS market penetration level; and 0.036, 0.063, and 0.099 for the WUMS power system area respective REMS market penetration level.

Next is a presentation of the PAPS HVAC DLC results.

6.3 Heating, ventilation, and Air Conditioning Direct Load Control

The direct load control (DLC) is provided in two forms: water heater (WH) and heating, ventilation, and air conditioning (HVAC). In both of these forms, the controlled appliance (WH and HVAC) is controlled for an electric utility specified time period (demand response [DR] period) with limited service during this time period to the controlled appliance only. In the HVAC DLC energy management function the HVAC utilization is rescheduled during the DR period. The HVAC is rescheduled so that within every half-hour during the DR period the HVAC is not allowed to run for n_{off} minutes (e.g. 15 minutes). Within each half-hour increment in the DR period the specific n_{off} minutes are selected randomly to minimize the impact of synchronized payback. This type of grouping scheme is common within DLC demonstration literature [30], [39], and [58].

The results in this section show the percent change of the expected Proposed Aggregate Primary-Energy-Source-Utilization Simulation (PAPS) results for the residential energy management system (REMS) market penetration levels (10%, 20%, and 40%) for each location (Versailles Kentucky [ECAK], Mercury Nevada [SNV], Stillwater Oklahoma [SPPS], and Necedah Wisconsin [WUMS]). The percent change in the expected PAPS results for the various market penetration levels are compared to the corresponding expected PAPS base case (BC) results described in Section 6.1. Further, the slope of the percent change as a function of the DR days is computed for each expected PAPS result. The slope of the percent change is a sensitivity measure of the expected PAPS results to the HVAC DLC energy management function.

The percent change in the expected PPRS HVAC DLC Scenario A, Scenario B, Scenario C, and Scenario D generated energy (GE) is shown in Figure 167, Figure 168, Figure 169, Figure 170, respectively.

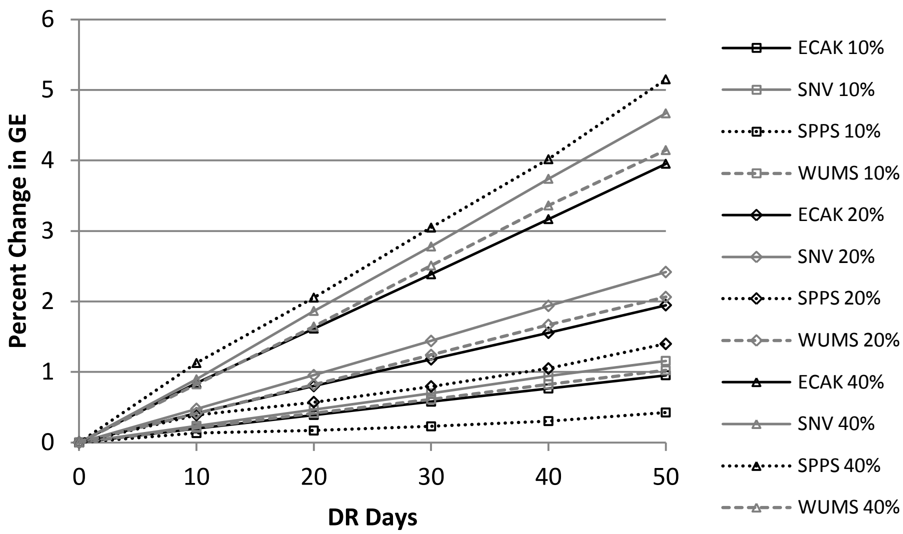

Figure 167: Percent change in the expected Proposed Aggregate Primary-Energy-Source-Utilization Simulation [PAPS] heating, ventilation, and air conditioning [HVAC] direct load control [DLC] Scenario A generated energy [GE].

The expected PAPS HVAC DLC Scenario A GE, shown in Figure 167, quantifies the change in the expected PAPS HVAC DLC Scenario A GE as a function of the number of DR days (from zero to 50) for three levels of REMS market penetration. Specifically, the slope [%/DR day] of the 10%, 20%, and 40% REMS market penetration percent change in the expected PAPS HVAC DLC Scenario A GE is 0.019, 0.039, and 0.079 for the ECAK power system area respective REMS market penetration level; 0.023, 0.048, and 0.094 for the SNV power system area respective REMS market penetration level; 0.008, 0.026, and 0.101 for the SPPS power system area respective REMS market penetration level; and 0.020, 0.041, and 0.083 for the WUMS power system area respective REMS market penetration level.

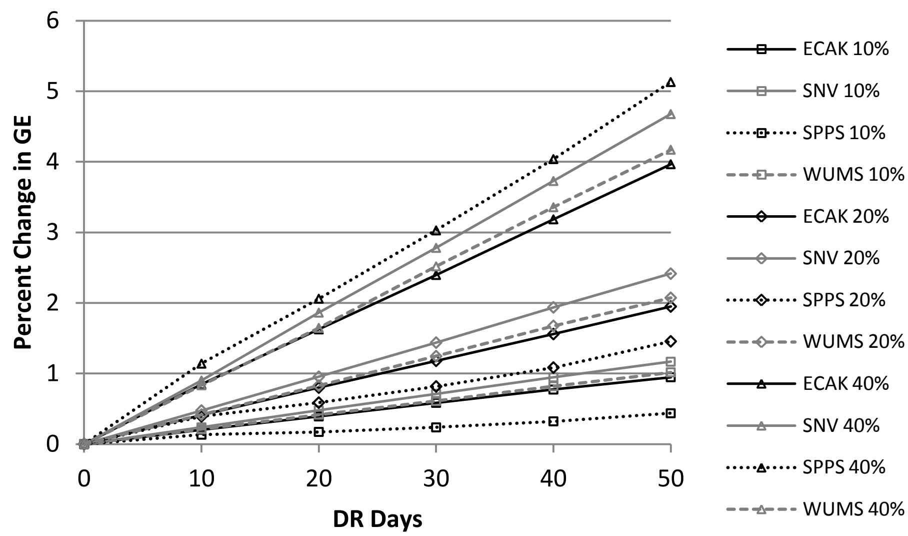

Figure 168: Percent change in the expected Proposed Aggregate Primary-Energy-Source-Utilization Simulation [PAPS] heating, ventilation, and air conditioning [HVAC] direct load control [DLC] Scenario B generated energy [GE].

The expected PAPS HVAC DLC Scenario B GE, shown in Figure 168, quantifies the change in the expected PAPS HVAC DLC Scenario B GE as a function of the number of DR days (from zero to 50) for three levels of REMS market penetration. Notice, the slope [%/DR day] of the 10%, 20%, and 40% REMS market penetration percent change in the expected PAPS HVAC DLC Scenario B GE is 0.019, 0.039, and 0.079 for the ECAK power system area respective REMS market penetration level; 0.023, 0.048, and 0.094 for the SNV power system area respective REMS market penetration level; 0.008, 0.027, and 0.101 for the SPPS power system area respective REMS market penetration level; and 0.020, 0.042, and 0.084 for the WUMS power system area respective REMS market penetration level.

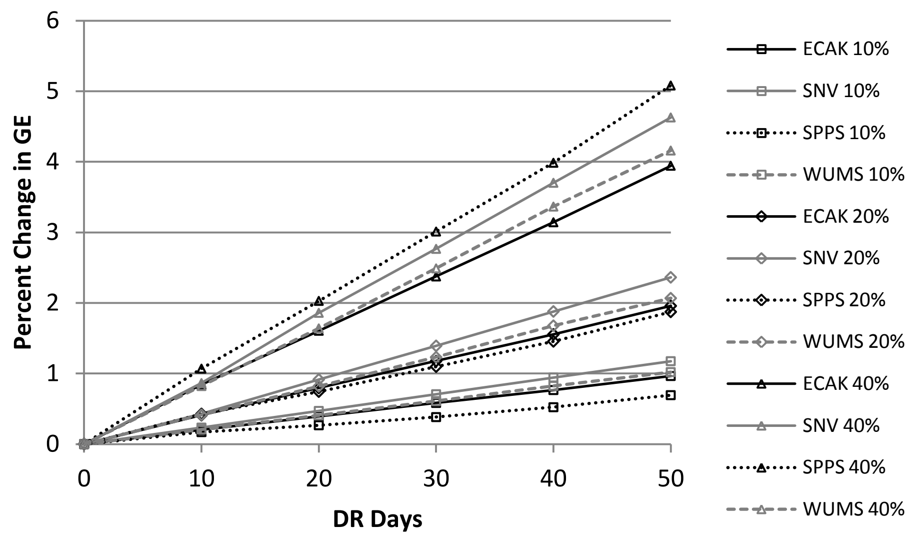

Figure 169: Percent change in the expected Proposed Aggregate Primary-Energy-Source-Utilization Simulation [PAPS] heating, ventilation, and air conditioning [HVAC] direct load control [DLC] Scenario C generated energy [GE].

The expected PAPS HVAC DLC Scenario C GE, shown in Figure 169, quantifies the change in the expected PAPS HVAC DLC Scenario C GE as a function of the number of DR days (from zero to 50) for three levels of REMS market penetration. Specifically, the slope [%/DR day] of the 10%, 20%, and 40% REMS market penetration percent change in the expected PAPS HVAC DLC Scenario C GE is 0.019, 0.039, and 0.078 for the ECAK power system area respective REMS market penetration level; 0.024, 0.048, and 0.093 for the SNV power system area respective REMS market penetration level; 0.013, 0.037, and 0.100 for the SPPS power system area respective REMS market penetration level; and 0.020, 0.042, and 0.084 for the WUMS power system area respective REMS market penetration level.

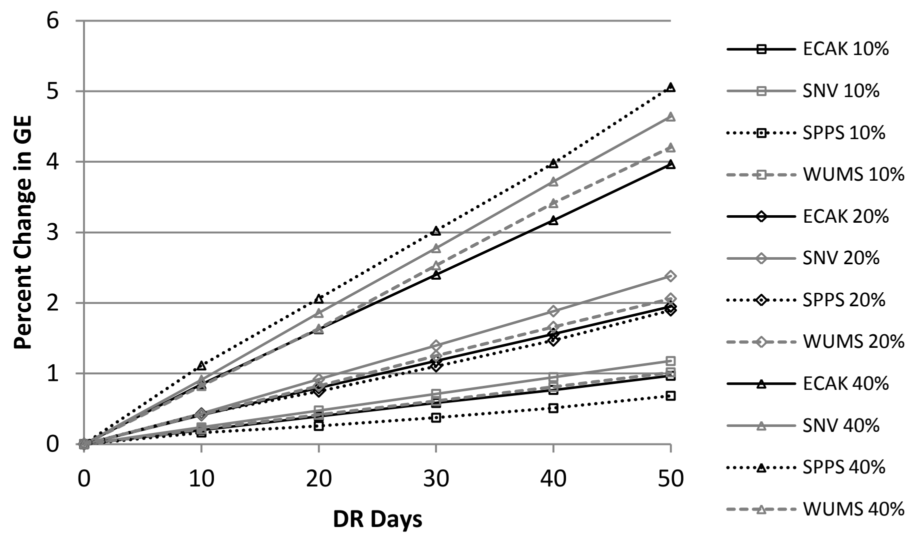

Figure 170: Percent change in the expected Proposed Aggregate Primary-Energy-Source-Utilization Simulation [PAPS] heating, ventilation, and air conditioning [HVAC] direct load control [DLC] Scenario D generated energy [GE].

The expected PAPS HVAC DLC Scenario D GE, shown in Figure 170, quantifies the change in the expected PAPS HVAC DLC Scenario D GE as a function of the number of DR days (from zero to 50) for three levels of REMS market penetration. Specifically, the slope [%/DR day] of the 10%, 20%, and 40% REMS market penetration percent change in the expected PAPS HVAC DLC Scenario D GE is 0.019, 0.039, and 0.079 for the ECAK power system area respective REMS market penetration level; 0.024, 0.048, and 0.093 for the SNV power system area respective REMS market penetration level; 0.013, 0.037, and 0.100 for the SPPS power system area respective REMS market penetration level; and 0.020, 0.041, and 0.085 for the WUMS power system area respective REMS market penetration level.

The percent change in the expected PPRS HVAC DLC Scenario A, Scenario B, Scenario C, and Scenario D generated environmental air pollution (GEAP) is shown in Figure 171, Figure 172, Figure 173, and Figure 174, respectively.

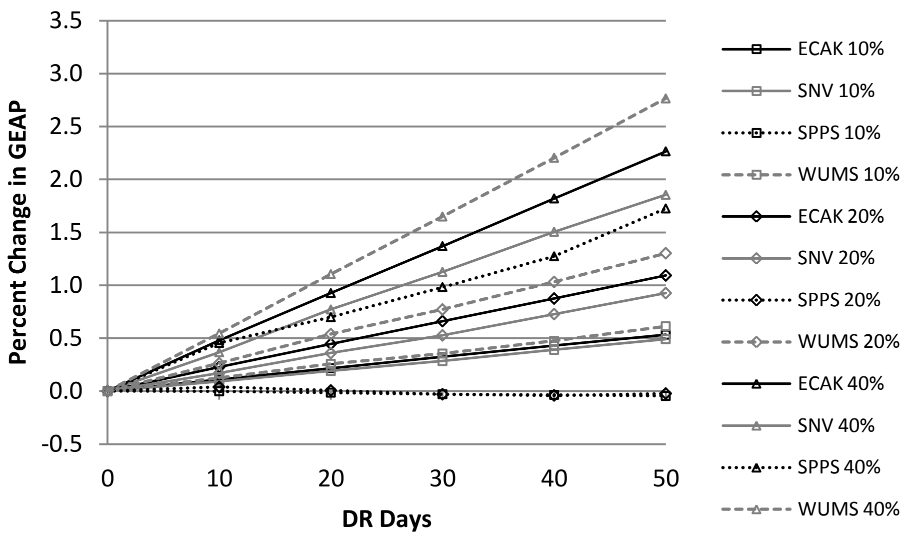

Figure 171: Percent change in the expected Proposed Aggregate Primary-Energy-Source-Utilization Simulation [PAPS] heating, ventilation, and air conditioning [HVAC] direct load control [DLC] Scenario A generated environmental air pollution [GEAP].

The expected PAPS HVAC DLC Scenario A GEAP, shown in Figure 171, quantifies the change in the expected PAPS HVAC DLC Scenario A GEAP as a function of the number of DR days (from zero to 50) for three levels of REMS market penetration. Specifically, the slope [%/DR day] of the 10%, 20%, and 40% REMS market penetration percent change in the expected PAPS HVAC DLC Scenario A GEAP is 0.011, 0.022, and 0.045 for the ECAK power system area respective REMS market penetration level; 0.010, 0.018, and 0.037 for the SNV power system area respective REMS market penetration level; -0.001, -0.001, and 0.032 for the SPPS power system area respective REMS market penetration level; and 0.012, 0.026, and 0.055 for the WUMS power system area respective REMS market penetration level.

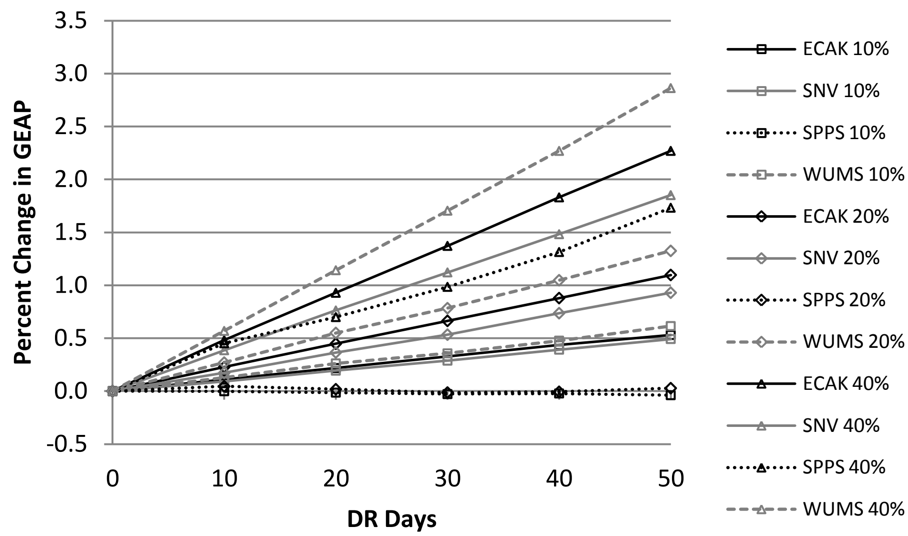

Figure 172: Percent change in the expected Proposed Aggregate Primary-Energy-Source-Utilization Simulation [PAPS] heating, ventilation, and air conditioning [HVAC] direct load control [DLC] Scenario B generated environmental air pollution [GEAP].

The expected PAPS HVAC DLC Scenario B GEAP, shown in Figure 172, quantifies the change in the expected PAPS HVAC DLC Scenario B GEAP as a function of the number of DR days (from zero to 50) for three levels of REMS market penetration. Specifically, the slope [%/DR day] of the 10%, 20%, and 40% REMS market penetration percent change in the expected PAPS HVAC DLC Scenario B GEAP is 0.011, 0.022, and 0.045 for the ECAK power system area respective REMS market penetration level; 0.010, 0.019, and 0.037 for the SNV power system area respective REMS market penetration level; -0.001, less than 0.001, and 0.033 for the SPPS power system area respective REMS market penetration level; and 0.012, 0.026, and 0.057 for the WUMS power system area respective REMS market penetration level.

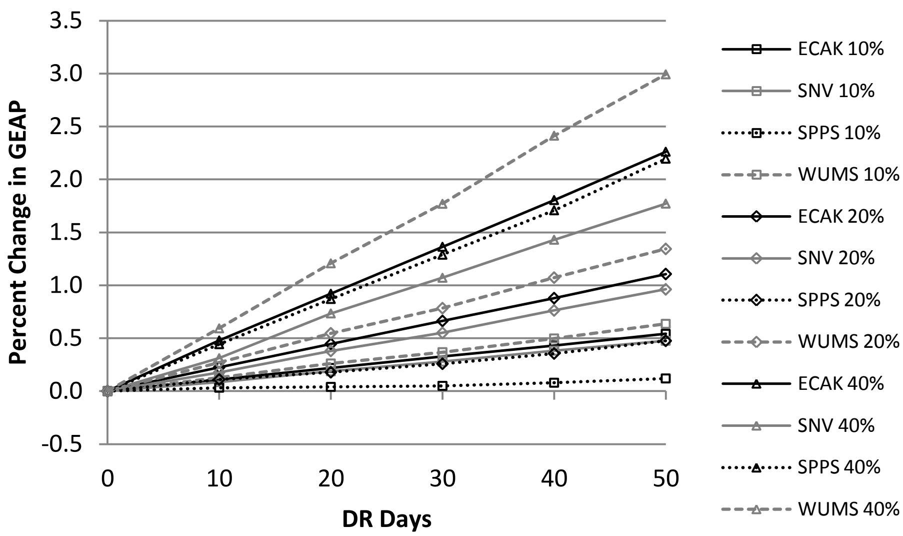

Figure 173: Percent change in the expected Proposed Aggregate Primary-Energy-Source-Utilization Simulation [PAPS] heating, ventilation, and air conditioning [HVAC] direct load control [DLC] Scenario C generated environmental air pollution [GEAP].

The expected PAPS HVAC DLC Scenario C GEAP, shown in Figure 173, quantifies the change in the expected PAPS HVAC DLC Scenario C GEAP as a function of the number of DR days (from zero to 50) for three levels of REMS market penetration. Specifically, the slope [%/DR day] of the 10%, 20%, and 40% REMS market penetration percent change in the expected PAPS HVAC DLC Scenario C GEAP is 0.011, 0.022, and 0.045 for the ECAK power system area respective REMS market penetration level; 0.010, 0.019, and 0.036 for the SNV power system area respective REMS market penetration level; 0.002, 0.009, and 0.043 for the SPPS power system area respective REMS market penetration level; and 0.013, 0.027, and 0.060 for the WUMS power system area respective REMS market penetration level.

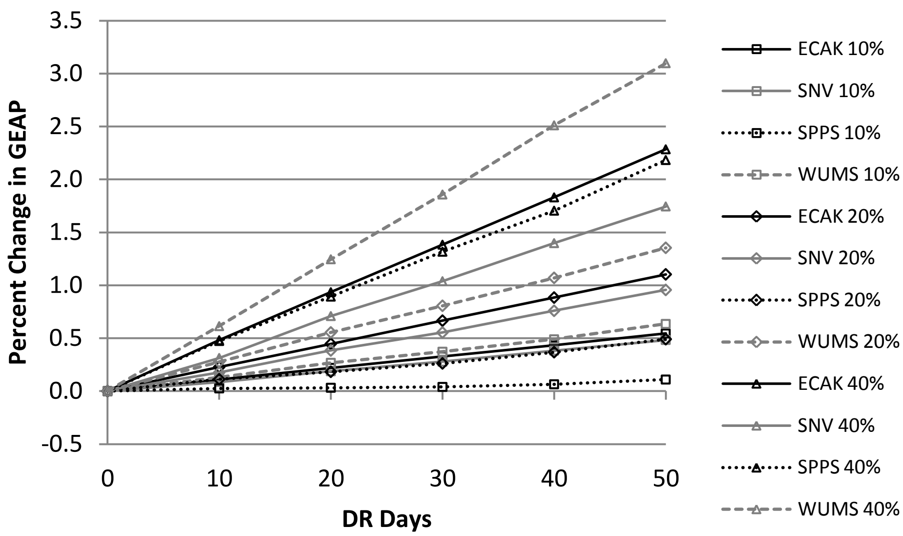

Figure 174: Percent change in the expected Proposed Aggregate Primary-Energy-Source-Utilization Simulation [PAPS] heating, ventilation, and air conditioning [HVAC] direct load control [DLC] Scenario D generated environmental air pollution [GEAP].

The expected PAPS HVAC DLC Scenario D GEAP, shown in Figure 174, quantifies the change in the expected PAPS HVAC DLC Scenario D GEAP as a function of the number of DR days (from zero to 50) for three levels of REMS market penetration. Specifically, the slope [%/DR day] of the 10%, 20%, and 40% REMS market penetration percent change in the expected PAPS HVAC DLC Scenario D GEAP is 0.011, 0.022, and 0.045 for the ECAK power system area respective REMS market penetration level; 0.010, 0.019, and 0.035 for the SNV power system area respective REMS market penetration level; 0.002, 0.009, and 0.043 for the SPPS power system area respective REMS market penetration level; and 0.012, 0.027, and 0.062 for the WUMS power system area respective REMS market penetration level.

The percent change in the expected PPRS HVAC DLC Scenario A, Scenario B, Scenario C, and Scenario D loss of load probability (LOLP) is shown in Figure 175, Figure 176, Figure 177, and Figure 178, respectively.

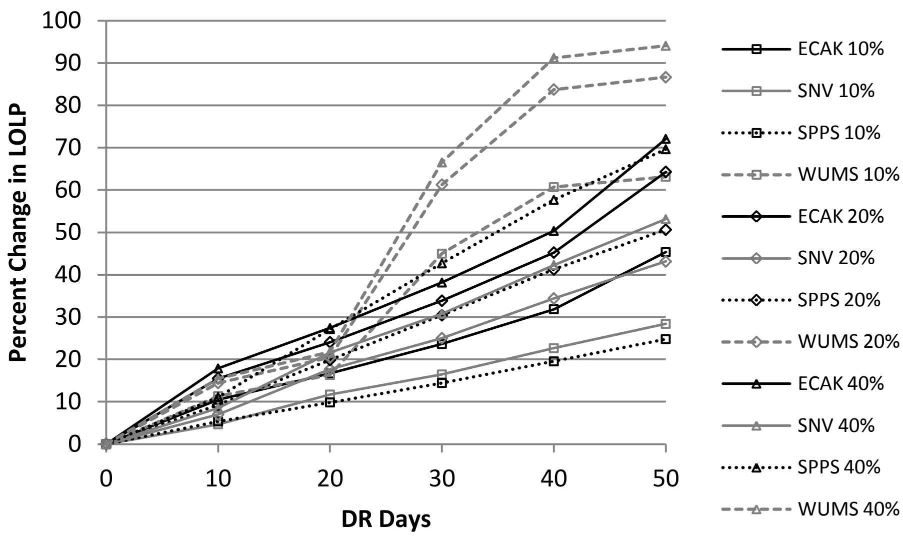

Figure 175: Percent change in the expected Proposed Aggregate Primary-Energy-Source-Utilization Simulation [PAPS] heating, ventilation, and air conditioning [HVAC] direct load control [DLC] Scenario A loss of load probability [LOLP].

The expected PAPS HVAC DLC Scenario A LOLP, shown in Figure 175, quantifies change in the expected PAPS HVAC DLC Scenario A LOLP as a function of the number of DR days (from zero to 50) for three levels of REMS market penetration. Specifically, the slope [%/DR day] of the 10%, 20%, and 40% REMS market penetration percent change in the expected PAPS HVAC DLC Scenario A LOLP is 0.850, 1.201, and 1.339 for the ECAK power system area respective REMS market penetration level; 0.573, 0.872, and 1.074 for the SNV power system area respective REMS market penetration level; 0.489, 1.028, and 1.438 for the SPPS power system area respective REMS market penetration level; and 1.407, 1.948, and 2.121 for the WUMS power system area respective REMS market penetration level.

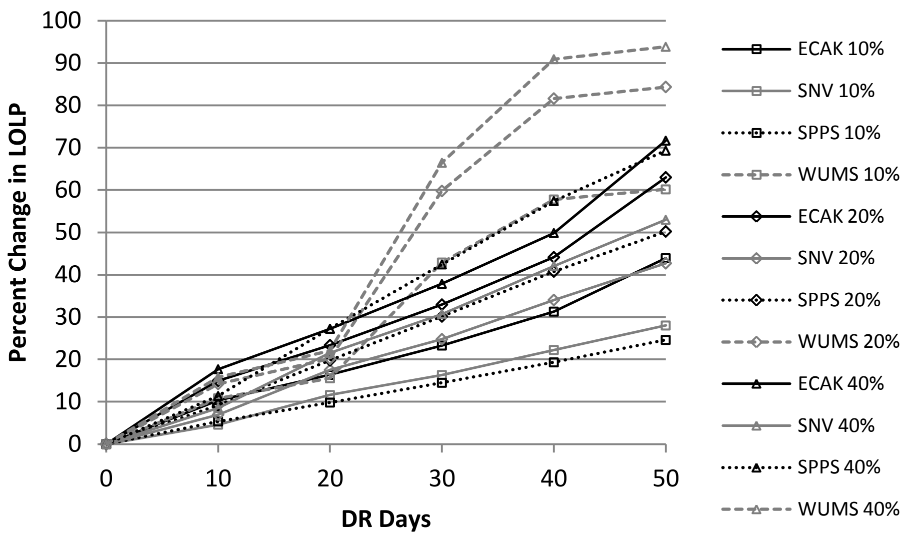

Figure 176: Percent change in the expected Proposed Aggregate Primary-Energy-Source-Utilization Simulation [PAPS] heating, ventilation, and air conditioning [HVAC] direct load control [DLC] Scenario B loss of load probability [LOLP].

The expected PAPS HVAC DLC Scenario B LOLP, shown in Figure 176, quantifies change in the expected PAPS HVAC DLC Scenario B LOLP as a function of the number of DR days (from zero to 50) for three levels of REMS market penetration. Specifically, the slope [%/DR day] of the 10%, 20%, and 40% REMS market penetration percent change in the expected PAPS HVAC DLC Scenario B LOLP is 0.826, 1.177, and 1.330 for the ECAK power system area respective REMS market penetration level; 0.565, 0.863, and 1.071 for the SNV power system area respective REMS market penetration level; 0.484, 1.017, and 1.428 for the SPPS power system area respective REMS market penetration level; and 1.340, 1.896, and 2.111 for the WUMS power system area respective REMS market penetration level.

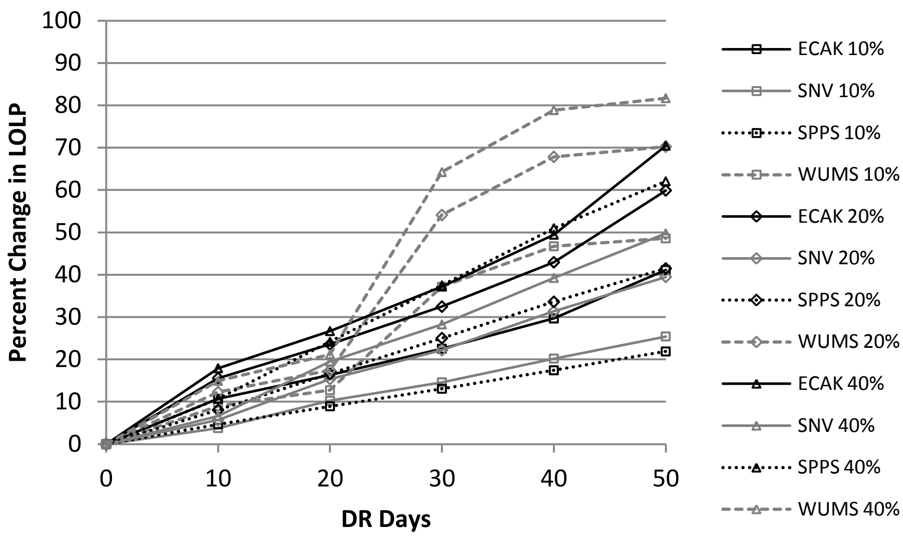

Figure 177: Percent change in the expected Proposed Aggregate Primary-Energy-Source-Utilization Simulation [PAPS] heating, ventilation, and air conditioning [HVAC] direct load control [DLC] Scenario C loss of load probability [LOLP].

The expected PAPS HVAC DLC Scenario C LOLP, shown in Figure 177, quantifies change in the expected PAPS HVAC DLC Scenario C LOLP as a function of the number of DR days (from zero to 50) for three levels of REMS market penetration. Specifically, the slope [%/DR day] of the 10%, 20%, and 40% REMS market penetration percent change in the expected PAPS HVAC DLC Scenario C LOLP is 0.767, 1.116, and 1.307 for the ECAK power system area respective REMS market penetration level; 0.516, 0.803, and 1.015 for the SNV power system area respective REMS market penetration level; 0.433, 0.835, and 1.270 for the SPPS power system area respective REMS market penetration level; and 1.087, 1.585, and 1.838 for the WUMS power system area respective REMS market penetration level.

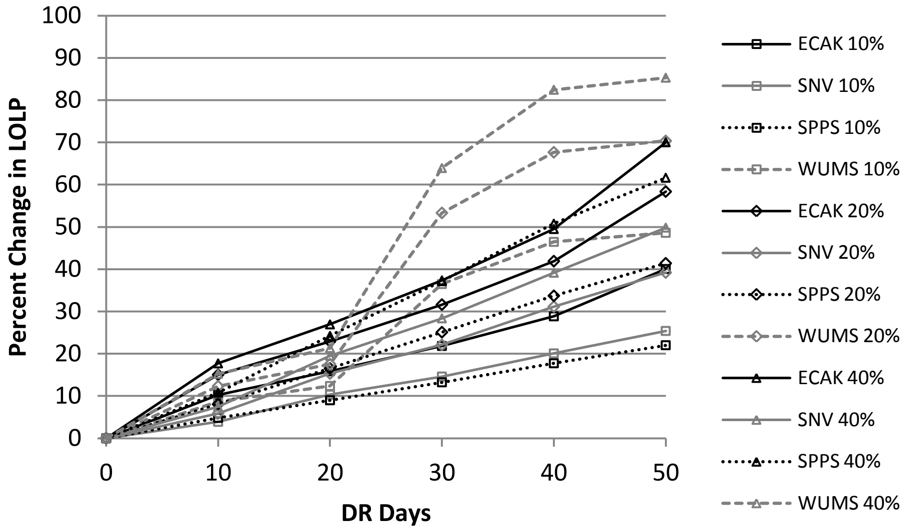

Figure 178: Percent change in the expected Proposed Aggregate Primary-Energy-Source-Utilization Simulation [PAPS] heating, ventilation, and air conditioning [HVAC] direct load control [DLC] Scenario D loss of load probability [LOLP].

The expected PAPS HVAC DLC Scenario D LOLP, shown in Figure 178, quantifies change in the expected PAPS HVAC DLC Scenario D LOLP as a function of the number of DR days (from zero to 50) for three levels of REMS market penetration. Specifically, the slope [%/DR day] of the 10%, 20%, and 40% REMS market penetration percent change in the expected PAPS HVAC DLC Scenario D LOLP is 0.748, 1.089, and 1.303 for the ECAK power system area respective REMS market penetration level; 0.514, 0.796, and 1.009 for the SNV power system area respective REMS market penetration level; 0.437, 0.836, and 1.260 for the SPPS power system area respective REMS market penetration level; and 1.087, 1.582, and 1.916 for the WUMS power system area respective REMS market penetration level.

The percent change in the expected PPRS HVAC DLC Scenario A, Scenario B, Scenario C, and Scenario D unserviced energy (UE) is shown in Figure 179, Figure 180, Figure 181, and Figure 182, respectively.

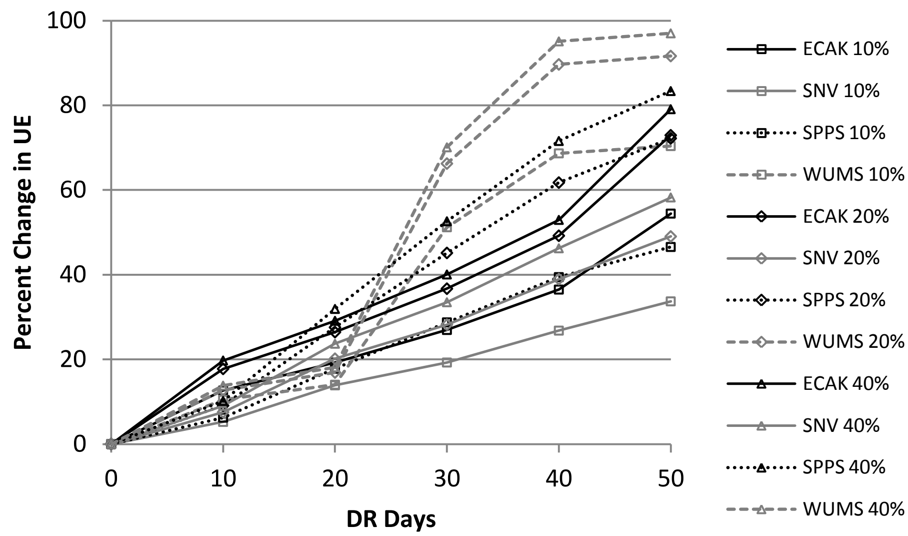

Figure 179: Percent change in the expected Proposed Aggregate Primary-Energy-Source-Utilization Simulation [PAPS] heating, ventilation, and air conditioning [HVAC] direct load control [DLC] Scenario A unserviced energy [UE].

The expected PAPS HVAC DLC Scenario A UE, shown in Figure 179, quantifies the expected PAPS HVAC DLC Scenario A UE as a function of the number of DR days (from zero to 50) for three levels of REMS market penetration. Specifically, the slope [%/DR day] of the 10%, 20%, and 40% REMS market penetration percent change in the expected PAPS HVAC DLC Scenario A UE is 1.004, 1.341, and 1.446 for the ECAK power system area respective REMS market penetration level; 0.682, 0.993, and 1.179 for the SNV power system area respective REMS market penetration level; 0.981, 1.533, and 1.776 for the SPPS power system area respective REMS market penetration level; and 1.610, 2.109, and 2.231 for the WUMS power system area respective REMS market penetration level.

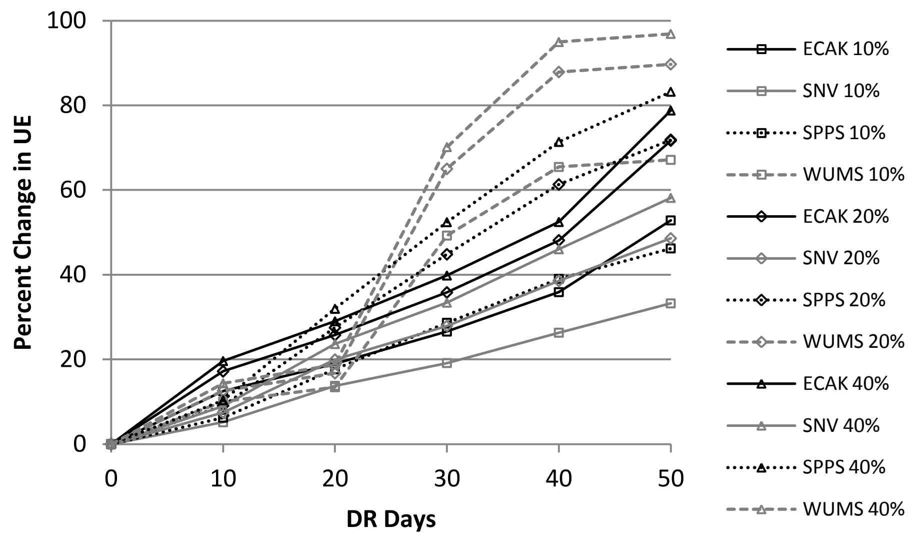

Figure 180: Percent change in the expected Proposed Aggregate Primary-Energy-Source-Utilization Simulation [PAPS] heating, ventilation, and air conditioning [HVAC] direct load control [DLC] Scenario B unserviced energy [UE].

The expected PAPS HVAC DLC Scenario B UE, shown in Figure 180, quantifies the expected PAPS HVAC DLC Scenario B UE as a function of the number of DR days (from zero to 50) for three levels of REMS market penetration. Specifically, the slope [%/DR day] of the 10%, 20%, and 40% REMS market penetration percent change in the expected PAPS HVAC DLC Scenario B UE is 0.997, 1.318, and 1.438 for the ECAK power system area respective REMS market penetration level; 0.671, 0.983, and 1.176 for the SNV power system area respective REMS market penetration level; 0.972, 1.524, and 1.770 for the SPPS power system area respective REMS market penetration level; and 1.536, 2.065, and 2.221 for the WUMS power system area respective REMS market penetration level.

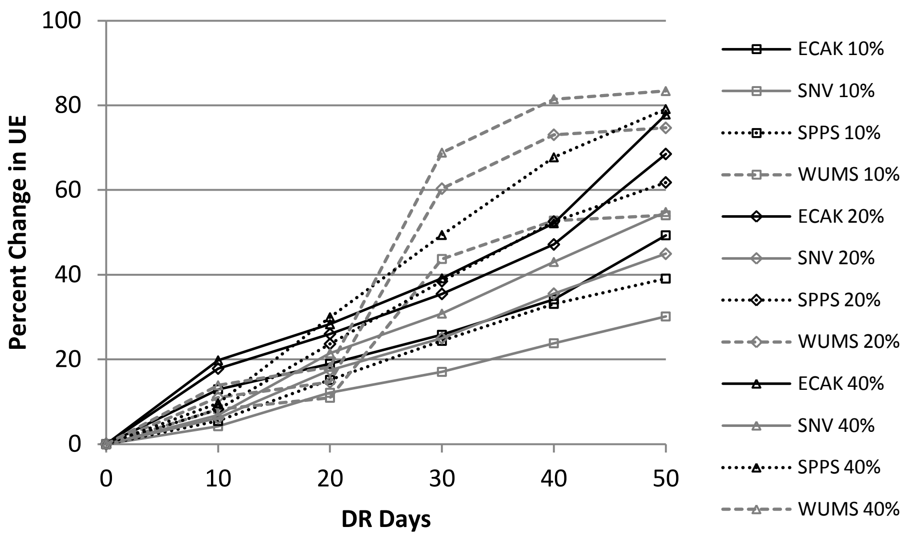

Figure 181: Percent change in the expected Proposed Aggregate Primary-Energy-Source-Utilization Simulation [PAPS] heating, ventilation, and air conditioning [HVAC] direct load control [DLC] Scenario C unserviced energy [UE].

The expected PAPS HVAC DLC Scenario C UE, shown in Figure 181, quantifies the expected PAPS HVAC DLC Scenario C UE as a function of the number of DR days (from zero to 50) for three levels of REMS market penetration. Specifically, the slope [%/DR day] of the 10%, 20%, and 40% REMS market penetration percent change in the expected PAPS HVAC DLC Scenario C UE is 0.906, 1.257, and 1.420 for the ECAK power system area respective REMS market penetration level; 0.612, 0.915, and 1.120 for the SNV power system area respective REMS market penetration level; 0.822, 1.305, and 1.683 for the SPPS power system area respective REMS market penetration level; and 1.247, 1.729, and 1.915 for the WUMS power system area respective REMS market penetration level.

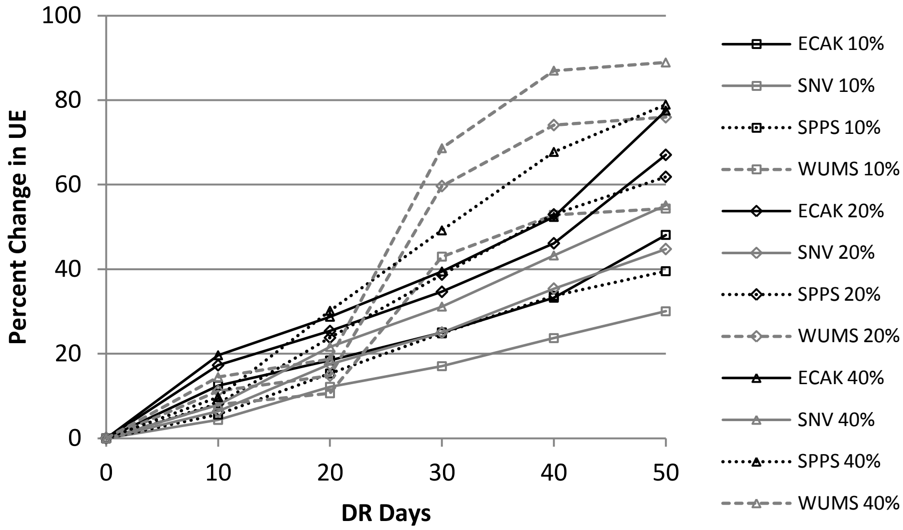

Figure 182: Percent change in the expected Proposed Aggregate Primary-Energy-Source-Utilization Simulation [PAPS] heating, ventilation, and air conditioning [HVAC] direct load control [DLC] Scenario D unserviced energy [UE].

The expected PAPS HVAC DLC Scenario D UE, shown in Figure 182, quantifies the expected PAPS HVAC DLC Scenario D UE as a function of the number of DR days (from zero to 50) for three levels of REMS market penetration. Specifically, the slope [%/DR day] of the 10%, 20%, and 40% REMS market penetration percent change in the expected PAPS HVAC DLC Scenario D UE is 0.884, 1.232, and 1.419 for the ECAK power system area respective REMS market penetration level; 0.609, 0.910, and 1.118 for the SNV power system area respective REMS market penetration level; 0.833, 1.310, and 1.679 for the SPPS power system area respective REMS market penetration level; and 1.253, 1.753, and 2.034 for the WUMS power system area respective REMS market penetration level.

The percent change in the expected PPRS HVAC DLC Scenario A, Scenario B, Scenario C, and Scenario D average electricity cost (AEC) is shown in Figure 183, Figure 184, Figure 185, and Figure 186, respectively.

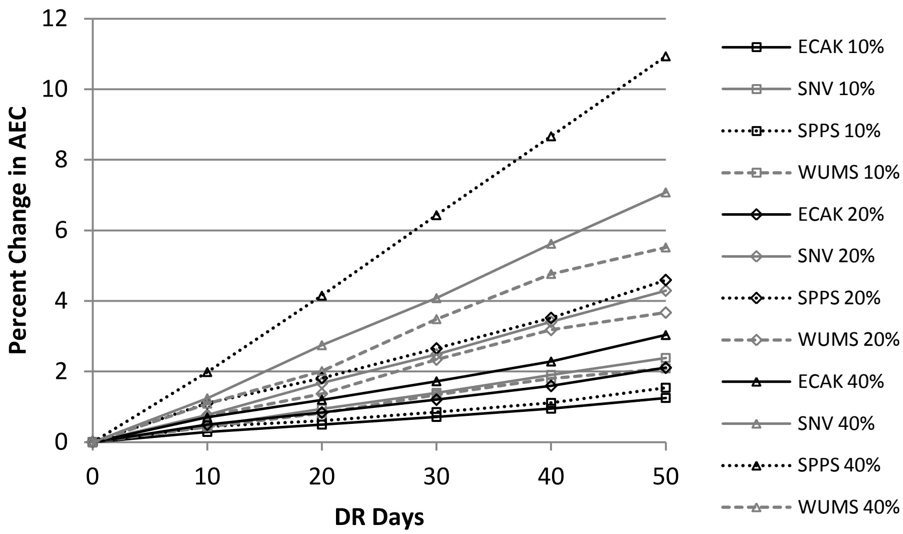

Figure 183: Percent change in the expected Proposed Aggregate Primary-Energy-Source-Utilization Simulation [PAPS] heating, ventilation, and air conditioning [HVAC] direct load control [DLC] Scenario A average electricity cost [AEC].

The expected PAPS HVAC DLC Scenario A AEC, shown in Figure 183, quantifies the change in the expected PAPS HVAC DLC Scenario A AEC as a function of the number of DR days (from zero to 50) for three levels of REMS market penetration. Specifically, the slope [%/DR day] of the 10%, 20%, and 40% REMS market penetration percent change in the expected PAPS HVAC DLC Scenario A AEC is 0.024, 0.041, and 0.058 for the ECAK power system area respective REMS market penetration level; 0.048, 0.086, and 0.142 for the SNV power system area respective REMS market penetration level; 0.028, 0.089, and 0.220 for the SPPS power system area respective REMS market penetration level; and 0.043, 0.076, and 0.115 for the WUMS power system area respective REMS market penetration level.

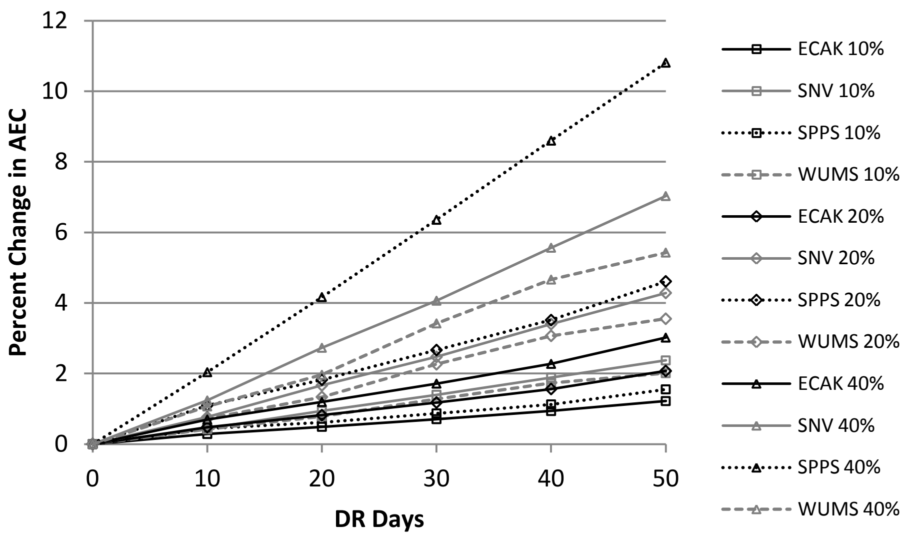

Figure 184: Percent change in the expected Proposed Aggregate Primary-Energy-Source-Utilization Simulation [PAPS] heating, ventilation, and air conditioning [HVAC] direct load control [DLC] Scenario B average electricity cost [AEC].

The expected PAPS HVAC DLC Scenario B AEC, shown in Figure 184, quantifies the change in the expected PAPS HVAC DLC Scenario B AEC as a function of the number of DR days (from zero to 50) for three levels of REMS market penetration. Specifically, the slope [%/DR day] of the 10%, 20%, and 40% REMS market penetration percent change in the expected PAPS HVAC DLC Scenario B AEC is 0.024, 0.040, and 0.058 for the ECAK power system area respective REMS market penetration level; 0.048, 0.086, and 0.141 for the SNV power system area respective REMS market penetration level; 0.029, 0.089, and 0.217 for the SPPS power system area respective REMS market penetration level; and 0.041, 0.074, and 0.112 for the WUMS power system area respective REMS market penetration level.

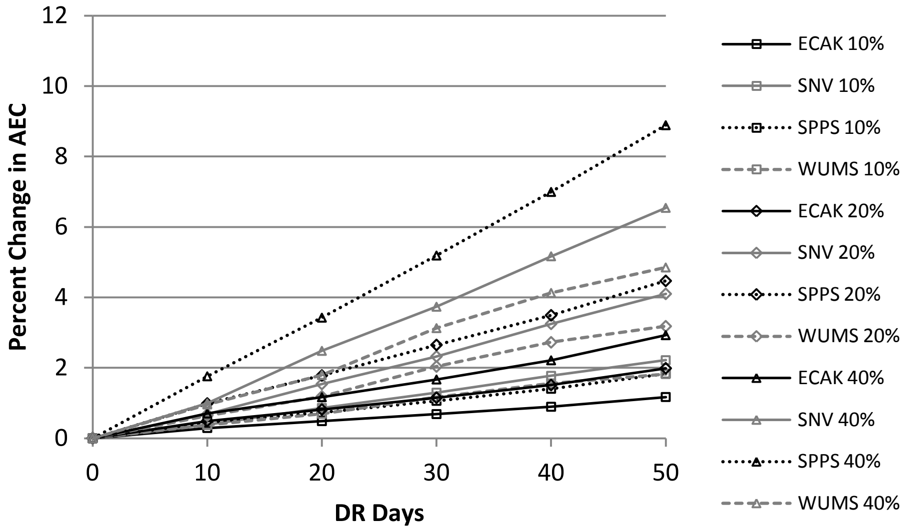

Figure 185: Percent change in the expected Proposed Aggregate Primary-Energy-Source-Utilization Simulation [PAPS] heating, ventilation, and air conditioning [HVAC] direct load control [DLC] Scenario C average electricity cost [AEC].

The expected PAPS HVAC DLC Scenario C AEC, shown in Figure 185, quantifies the change in the expected PAPS HVAC DLC Scenario C AEC as a function of the number of DR days (from zero to 50) for three levels of REMS market penetration. Specifically, the slope [%/DR day] of the 10%, 20%, and 40% REMS market penetration percent change in the expected PAPS HVAC DLC Scenario C AEC is 0.022, 0.038, and 0.056 for the ECAK power system area respective REMS market penetration level; 0.045, 0.083, and 0.133 for the SNV power system area respective REMS market penetration level; 0.035, 0.088, and 0.177 for the SPPS power system area respective REMS market penetration level; and 0.037, 0.066, and 0.100 for the WUMS power system area respective REMS market penetration level.

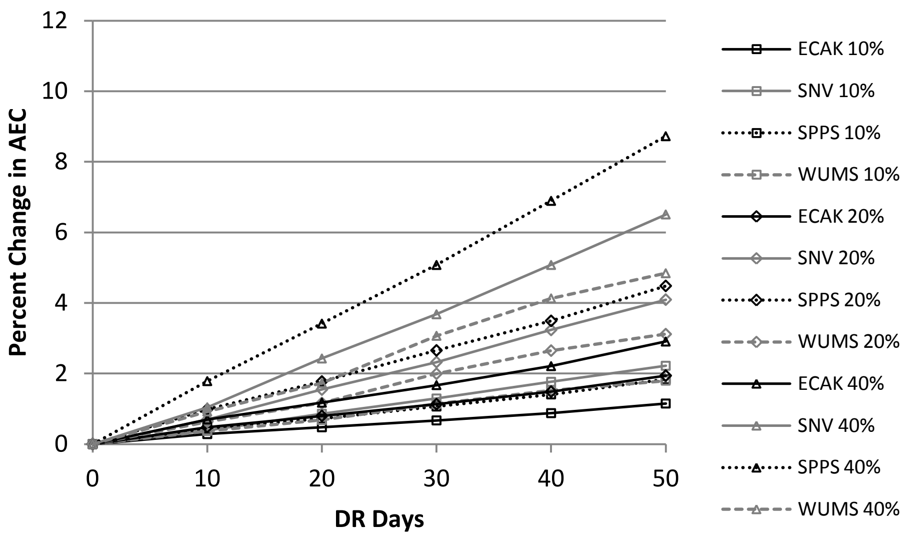

Figure 186: Percent change in the expected Proposed Aggregate Primary-Energy-Source-Utilization Simulation [PAPS] heating, ventilation, and air conditioning [HVAC] direct load control [DLC] Scenario D average electricity cost [AEC].

The expected PAPS HVAC DLC Scenario D AEC, shown in Figure 186, quantifies the change in the expected PAPS HVAC DLC Scenario D AEC as a function of the number of DR days (from zero to 50) for three levels of REMS market penetration. Specifically, the slope [%/DR day] of the 10%, 20%, and 40% REMS market penetration percent change in the expected PAPS HVAC DLC Scenario D AEC is 0.022, 0.037, and 0.056 for the ECAK power system area respective REMS market penetration level; 0.045, 0.083, and 0.131 for the SNV power system area respective REMS market penetration level; 0.035, 0.088, and 0.173 for the SPPS power system area respective REMS market penetration level; and 0.037, 0.064, and 0.100 for the WUMS power system area respective REMS market penetration level.

Next is a presentation of the PAPS smart thermostat results.

6.4 Smart Thermostat

The smart thermostat (ST) energy management function increases (for times that air conditioning is needed) or lowers (for times that heating is needed) the indoor temperature set point during the demand response (DR) period. Specifically, during the summer and warmer days in the transitional months (average temperature greater than or equal to 20 °C) the indoor temperature set point is changed from 20 °C to 26 °C. During the winter and cooler days in the transitional months (average daily temperature less than 20 °C) the indoor temperature set point is changed from 20 °C to 14 °C.

The results in this section show the percent change of the expected Proposed Aggregate Primary-Energy-Source-Utilization Simulation (PAPS) results for the residential energy management system (REMS) market penetration levels (10%, 20%, and 40%) for each location (Versailles Kentucky [ECAK], Mercury Nevada [SNV], Stillwater Oklahoma [SPPS], and Necedah Wisconsin [WUMS]). The percent change in the expected PAPS results for the various market penetration levels are compared to the corresponding expected PAPS base case (BC) results described in Section 6.1. Further, the slope of the percent change as a function of the DR days is computed for each result. The slope of the percent change is a sensitivity measure of the PAPS results to the ST energy management function.

The percent change in the expected PPRS ST Scenario A, Scenario B, Scenario C, and Scenario D generated energy (GE) is shown in Figure 187, Figure 188, Figure 189, Figure 190, respectively.

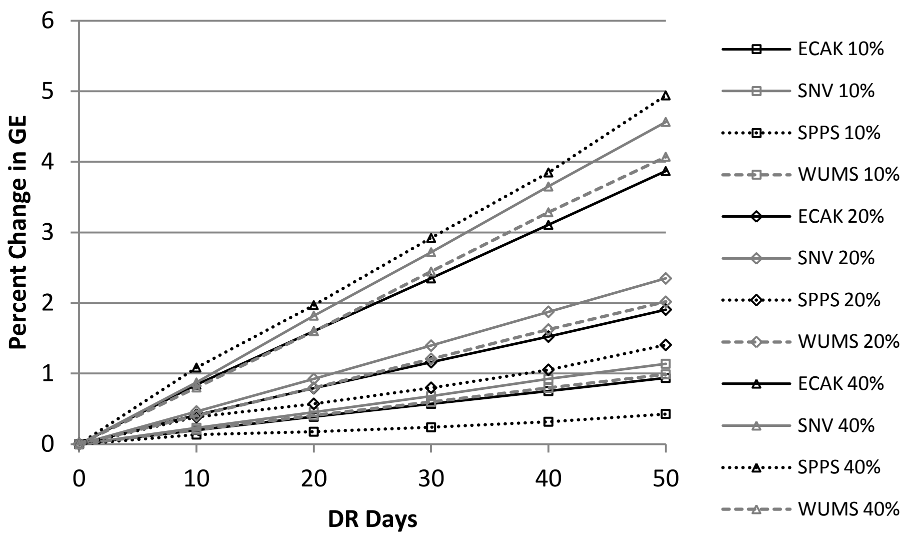

Figure 187: Percent change in the expected Proposed Aggregate Primary-Energy-Source-Utilization Simulation [PAPS] smart thermostat [ST] Scenario A generated energy [GE].

The expected PAPS ST Scenario A GE, shown in Figure 187, quantifies the change in the expected PAPS ST Scenario A GE as a function of the number of DR days (from zero to 50) for three levels of REMS market penetration. Specifically, the slope [%/DR day] of the 10%, 20%, and 40% REMS market penetration percent change in the expected PAPS ST Scenario A GE is 0.019, 0.038, and 0.077 for the ECAK power system area respective REMS market penetration level; 0.023, 0.047, and 0.092 for the SNV power system area respective REMS market penetration level; 0.008, 0.026, and 0.097 for the SPPS power system area respective REMS market penetration level; and 0.020, 0.040, and 0.082 for the WUMS power system area respective REMS market penetration level.

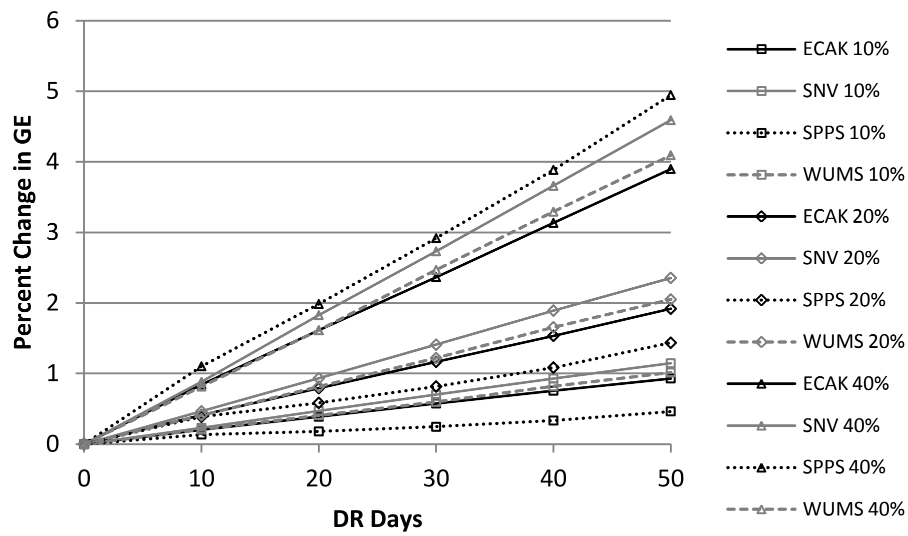

Figure 188: Percent change in the expected Proposed Aggregate Primary-Energy-Source-Utilization Simulation [PAPS] smart thermostat [ST] Scenario B generated energy [GE].

The expected PAPS ST Scenario B GE, shown in Figure 188, quantifies the expected PAPS ST Scenario B GE as a function of the number of DR days (from zero to 50) for three levels of REMS market penetration. Specifically, the slope [%/DR day] of the 10%, 20%, and 40% REMS market penetration percent change in the expected PAPS ST Scenario B GE is 0.019, 0.038, and 0.077 for the ECAK power system area respective REMS market penetration level; 0.023, 0.047, and 0.092 for the SNV power system area respective REMS market penetration level; 0.009, 0.027, and 0.097 for the SPPS power system area respective REMS market penetration level; and 0.020, 0.041, and 0.082 for the WUMS power system area respective REMS market penetration level.

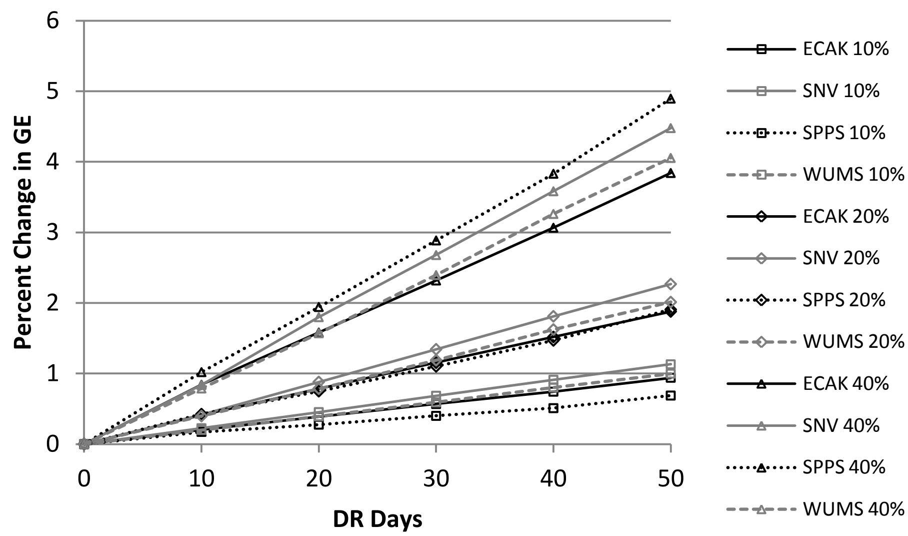

Figure 189: Percent change in the expected Proposed Aggregate Primary-Energy-Source-Utilization Simulation [PAPS] smart thermostat [ST] Scenario C generated energy [GE].

The expected PAPS ST Scenario C GE, shown in Figure 189, quantifies the expected PAPS ST Scenario C GE as a function of the number of DR days (from zero to 50) for three levels of REMS market penetration. Specifically, the slope [%/DR day] of the 10%, 20%, and 40% REMS market penetration percent change in the expected PAPS ST Scenario C GE is 0.019, 0.037, and 0.076 for the ECAK power system area respective REMS market penetration level; 0.023, 0.046, and 0.090 for the SNV power system area respective REMS market penetration level; 0.013, 0.037, and 0.097 for the SPPS power system area respective REMS market penetration level; and 0.020, 0.040, and 0.081 for the WUMS power system area respective REMS market penetration level.

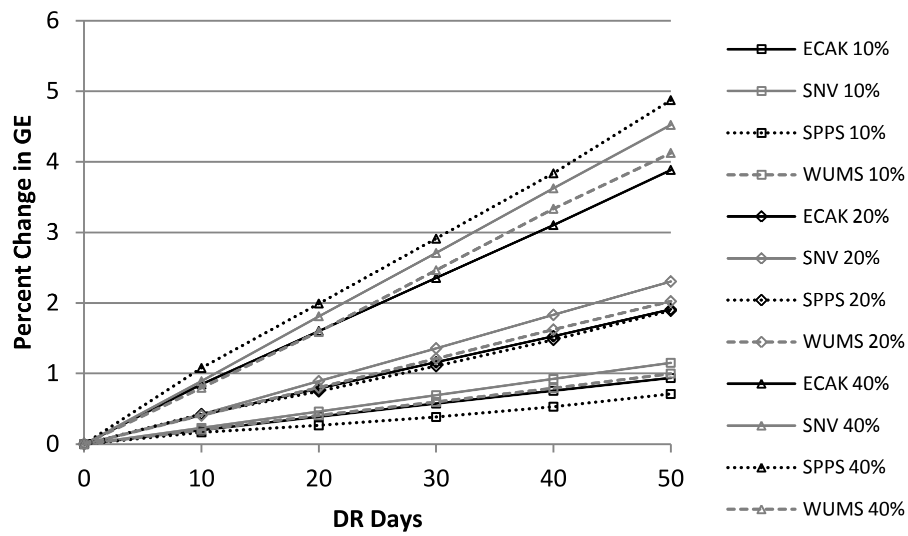

Figure 190: Percent change in the expected Proposed Aggregate Primary-Energy-Source-Utilization Simulation [PAPS] smart thermostat [ST] Scenario D generated energy [GE].

The expected PAPS ST Scenario D GE, shown in Figure 190, quantifies the expected PAPS ST Scenario D GE as a function of the number of DR days (from zero to 50) for three levels of REMS market penetration. Specifically, the slope [%/DR day] of the 10%, 20%, and 40% REMS market penetration percent change in the expected PAPS ST Scenario D GE is 0.019, 0.038, and 0.077 for the ECAK power system area respective REMS market penetration level; 0.023, 0.046, and 0.091 for the SNV power system area respective REMS market penetration level; 0.014, 0.037, and 0.096 for the SPPS power system area respective REMS market penetration level; and 0.020, 0.040, and 0.083 for the WUMS power system area respective REMS market penetration level.

The percent change in the expected PPRS ST Scenario A, Scenario B, Scenario C, and Scenario D generated environmental air pollution (GEAP) is shown in Figure 191, Figure 192, Figure 193, and Figure 194, respectively.

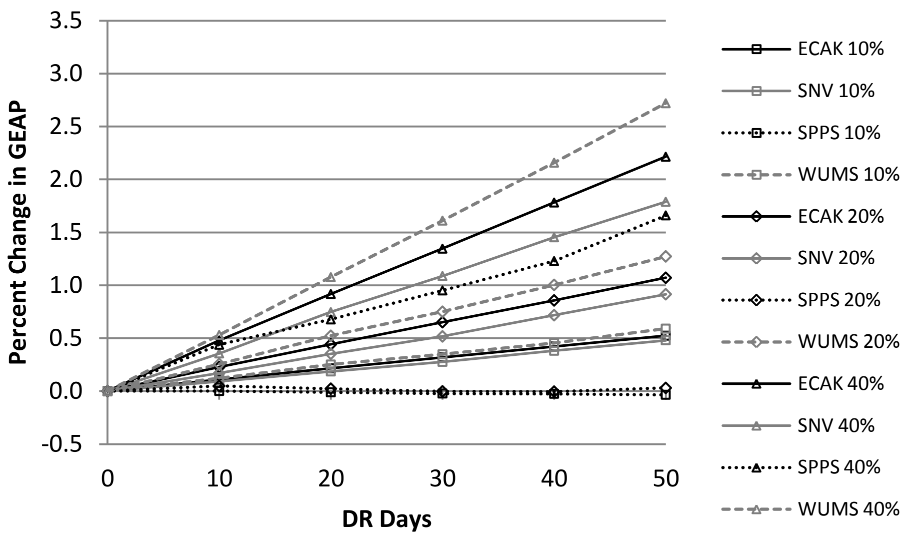

Figure 191: Percent change in the expected Proposed Aggregate Primary-Energy-Source-Utilization Simulation [PAPS] smart thermostat [ST] Scenario A generated environmental air pollution [GEAP].

The expected PAPS ST Scenario A GEAP, shown in Figure 191, quantifies the expected PAPS ST Scenario A GEAP as a function of the number of DR days (from zero to 50) for three levels of REMS market penetration. Specifically, the slope [%/DR day] of the 10%, 20%, and 40% REMS market penetration percent change in the expected PAPS ST Scenario A GEAP is 0.010, 0.021, and 0.044 for the ECAK power system area respective REMS market penetration level; 0.010, 0.018, and 0.036 for the SNV power system area respective REMS market penetration level; -0.001, less than 0.001, and 0.031 for the SPPS power system area respective REMS market penetration level; and 0.012, 0.025, and 0.054 for the WUMS power system area respective REMS market penetration level.

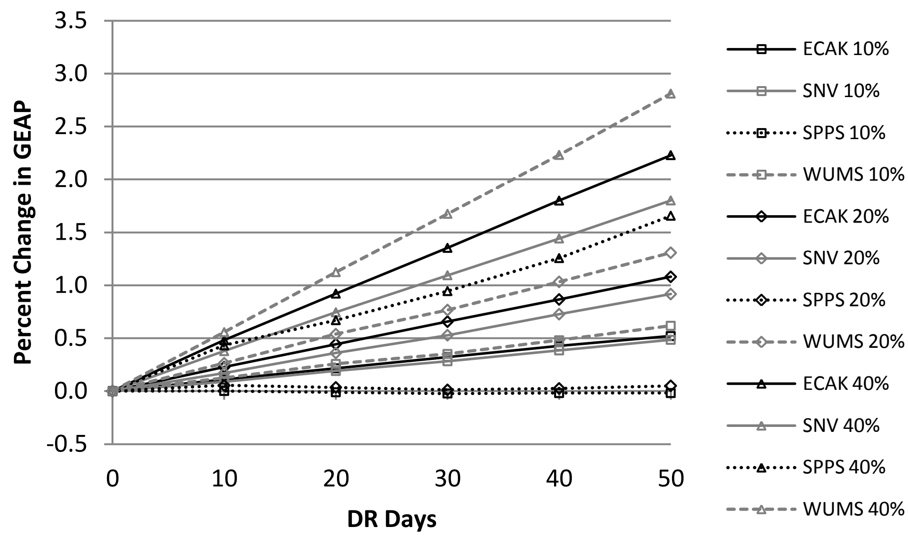

Figure 192: Percent change in the expected Proposed Aggregate Primary-Energy-Source-Utilization Simulation [PAPS] smart thermostat [ST] Scenario B generated environmental air pollution [GEAP].

The expected PAPS ST Scenario B GEAP, shown in Figure 192, quantifies the expected PAPS ST Scenario B GEAP as a function of the number of DR days (from zero to 50) for three levels of REMS market penetration. Specifically, the slope [%/DR day] of the 10%, 20%, and 40% REMS market penetration percent change in the expected PAPS ST Scenario B GEAP is 0.010, 0.022, and 0.044 for the ECAK power system area respective REMS market penetration level; 0.010, 0.018, and 0.036 for the SNV power system area respective REMS market penetration level; less than 0.001, less than 0.001, and 0.032 for the SPPS power system area respective REMS market penetration level; and 0.012, 0.026, and 0.056 for the WUMS power system area respective REMS market penetration level.

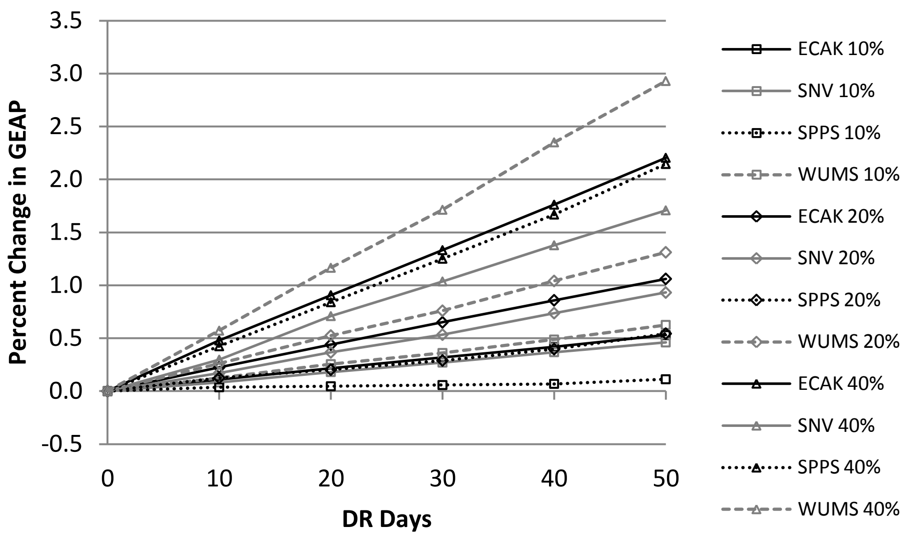

Figure 193: Percent change in the expected Proposed Aggregate Primary-Energy-Source-Utilization Simulation [PAPS] smart thermostat [ST] Scenario C generated environmental air pollution [GEAP].

The expected PAPS ST Scenario C GEAP, shown in Figure 193, quantifies the expected PAPS ST Scenario C GEAP as a function of the number of DR days (from zero to 50) for three levels of REMS market penetration. Specifically, the slope [%/DR day] of the 10%, 20%, and 40% REMS market penetration percent change in the expected PAPS ST Scenario C GEAP is 0.010, 0.021, and 0.044 for the ECAK power system area respective REMS market penetration level; 0.009, 0.019, and 0.035 for the SNV power system area respective REMS market penetration level; 0.002, 0.010, and 0.042 for the SPPS power system area respective REMS market penetration level; and 0.012, 0.026, and 0.059 for the WUMS power system area respective REMS market penetration level.

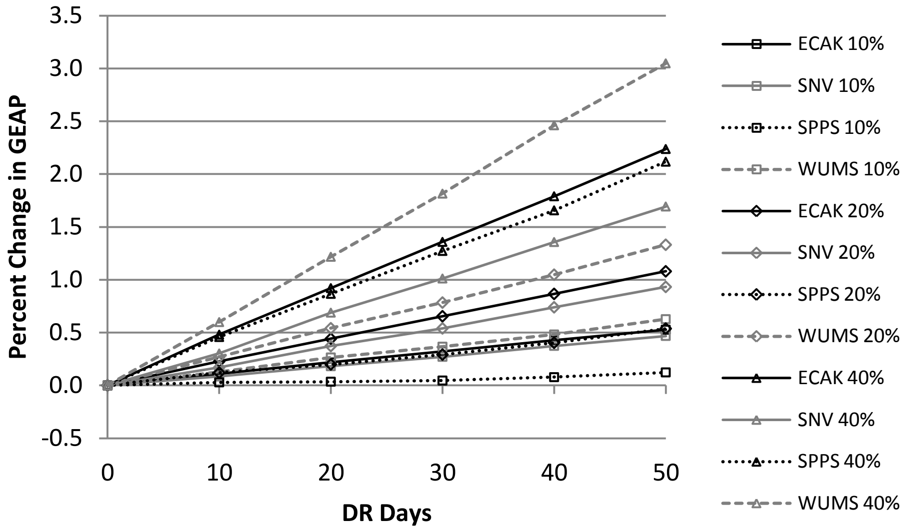

Figure 194: Percent change in the expected Proposed Aggregate Primary-Energy-Source-Utilization Simulation [PAPS] smart thermostat [ST] Scenario D generated environmental air pollution [GEAP].

The expected PAPS ST Scenario D GEAP, shown in Figure 194, quantifies the expected PAPS ST Scenario D GEAP as a function of the number of DR days (from zero to 50) for three levels of REMS market penetration. Specifically, the slope [%/DR day] of the 10%, 20%, and 40% REMS market penetration percent change in the expected PAPS ST Scenario D GEAP is 0.011, 0.022, and 0.044 for the ECAK power system area respective REMS market penetration level; 0.009, 0.019, and 0.034 for the SNV power system area respective REMS market penetration level; 0.002, 0.010, and 0.042 for the SPPS power system area respective REMS market penetration level; and 0.012, 0.026, and 0.061 for the WUMS power system area respective REMS market penetration level.

The percent change in the expected PPRS ST Scenario A, Scenario B, Scenario C, and Scenario D loss of load probability (LOLP) is shown in Figure 195, Figure 196, Figure 197, and Figure 198, respectively.

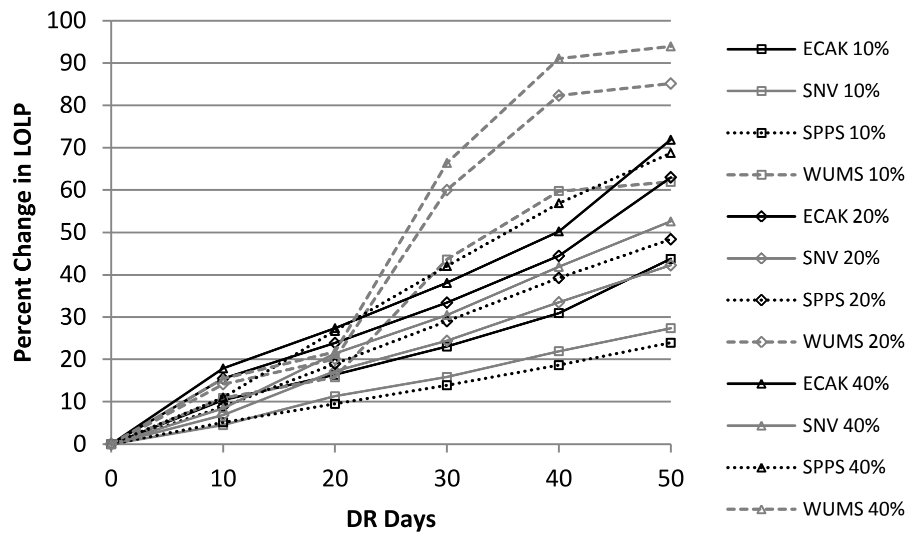

Figure 195: Percent change in the expected Proposed Aggregate Primary-Energy-Source-Utilization Simulation [PAPS] smart thermostat [ST] Scenario A loss of load probability [LOLP].

The expected PAPS ST Scenario A LOLP, shown in Figure 195, quantifies the expected PAPS ST Scenario A LOLP as a function of the number of DR days (from zero to 50) for three levels of REMS market penetration. Specifically, the slope [%/DR day] of the 10%, 20%, and 40% REMS market penetration percent change in the expected PAPS ST Scenario A LOLP is 0.820, 1.176, and 1.335 for the ECAK power system area respective REMS market penetration level; 0.553, 0.852, and 1.064 for the SNV power system area respective REMS market penetration level; 0.470, 0.980, and 1.419 for the SPPS power system area respective REMS market penetration level; and 1.383, 1.915, and 2.118 for the WUMS power system area respective REMS market penetration level.

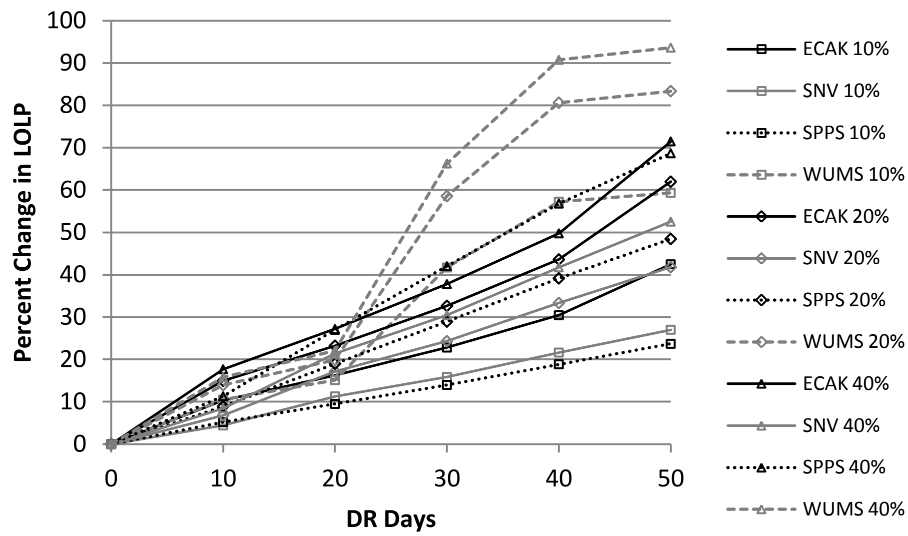

Figure 196: Percent change in the expected Proposed Aggregate Primary-Energy-Source-Utilization Simulation [PAPS] smart thermostat [ST] Scenario B loss of load probability [LOLP].

The expected PAPS ST Scenario B LOLP, shown in Figure 196, quantifies the expected PAPS ST Scenario B LOLP as a function of the number of DR days (from zero to 50) for three levels of REMS market penetration. Specifically, the slope [%/DR day] of the 10%, 20%, and 40% REMS market penetration percent change in the expected PAPS ST Scenario B LOLP is 0.797, 1.157, and 1.326 for the ECAK power system area respective REMS market penetration level; 0.546, 0.845, and 1.062 for the SNV power system area respective REMS market penetration level; 0.468, 0.980, and 1.414 for the SPPS power system area respective REMS market penetration level; and 1.324, 1.873, and 2.107 for the WUMS power system area respective REMS market penetration level.

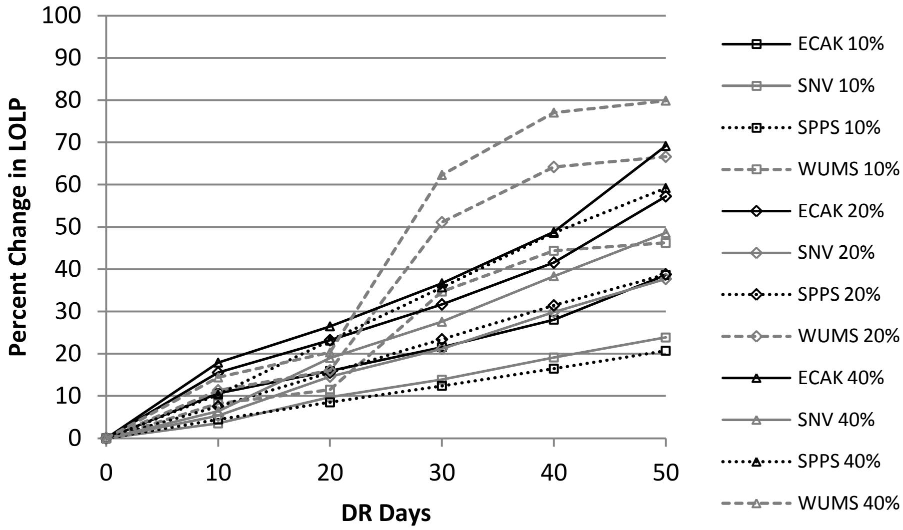

Figure 197: Percent change in the expected Proposed Aggregate Primary-Energy-Source-Utilization Simulation [PAPS] smart thermostat [ST] Scenario C loss of load probability [LOLP].

The expected PAPS ST Scenario C LOLP, shown in Figure 197, quantifies the expected PAPS ST Scenario C LOLP as a function of the number of DR days (from zero to 50) for three levels of REMS market penetration. Specifically, the slope [%/DR day] of the 10%, 20%, and 40% REMS market penetration percent change in the expected PAPS ST Scenario C LOLP is 0.717, 1.065, and 1.282 for the ECAK power system area respective REMS market penetration level; 0.486, 0.767, and 0.992 for the SNV power system area respective REMS market penetration level; 0.410, 0.781, and 1.209 for the SPPS power system area respective REMS market penetration level; and 1.037, 1.505, and 1.798 for the WUMS power system area respective REMS market penetration level.

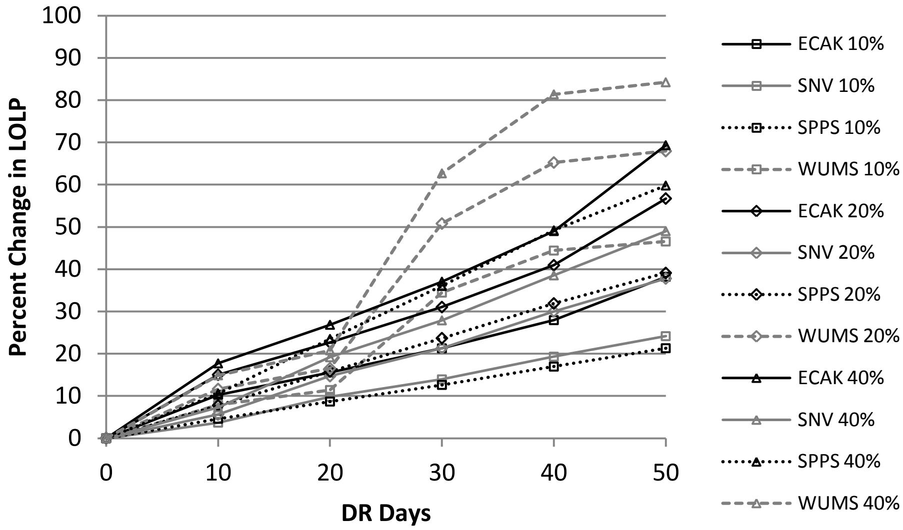

Figure 198: Percent change in the expected Proposed Aggregate Primary-Energy-Source-Utilization Simulation [PAPS] smart thermostat [ST] Scenario D loss of load probability [LOLP].

The expected PAPS ST Scenario D LOLP, shown in Figure 198, quantifies the expected PAPS ST Scenario D LOLP as a function of the number of DR days (from zero to 50) for three levels of REMS market penetration. Specifically, the slope [%/DR day] of the 10%, 20%, and 40% REMS market penetration percent change in the expected PAPS ST Scenario D LOLP is 0.713, 1.056, and 1.288 for the ECAK power system area respective REMS market penetration level; 0.491, 0.768, and 0.993 for the SNV power system area respective REMS market penetration level; 0.421, 0.788, and 1.221 for the SPPS power system area respective REMS market penetration level; and 1.043, 1.528, and 1.893 for the WUMS power system area respective REMS market penetration level.

The percent change in the expected PPRS ST Scenario A, Scenario B, Scenario C, and Scenario D unserviced energy (UE) is shown in Figure 199, Figure 200, Figure 201, and Figure 202, respectively.

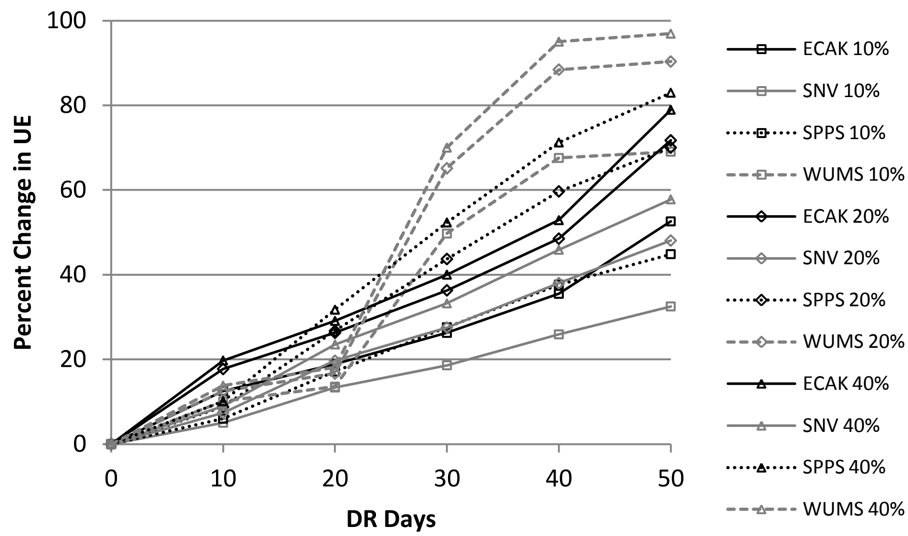

Figure 199: Percent change in the expected Proposed Aggregate Primary-Energy-Source-Utilization Simulation [PAPS] smart thermostat [ST] Scenario A unserviced energy [UE].

The expected PAPS ST Scenario A UE, shown in Figure 199, quantifies the expected PAPS ST Scenario A UE as a function of the number of DR days (from zero to 50) for three levels of REMS market penetration. Specifically, the slope [%/DR day] of the 10%, 20%, and 40% REMS market penetration percent change in the expected PAPS ST Scenario A UE is 0.969, 1.317, and 1.443 for the ECAK power system area respective REMS market penetration level; 0.658, 0.971, and 1.170 for the SNV power system area respective REMS market penetration level; 0.942, 1.485, and 1.768 for the SPPS power system area respective REMS market penetration level; and 1.583, 2.079, and 2.229 for the WUMS power system area respective REMS market penetration level.

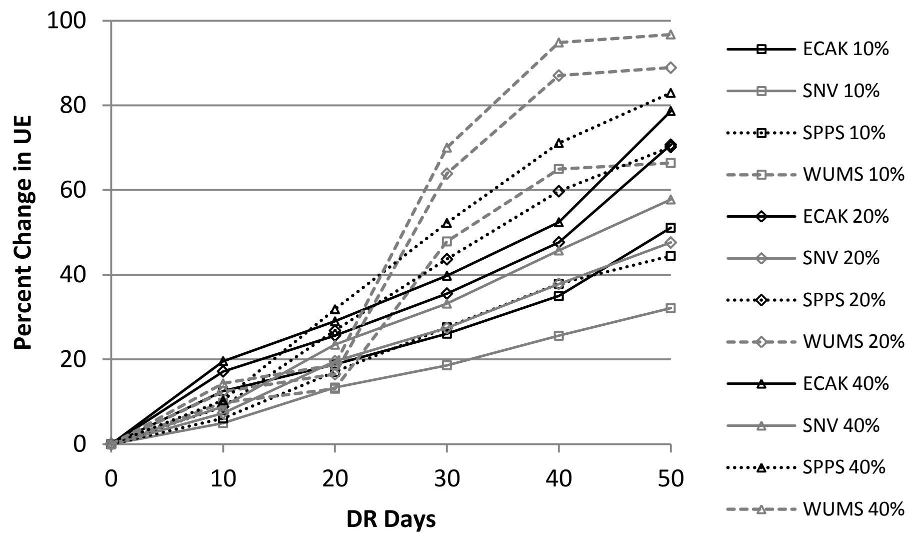

Figure 200: Percent change in the expected Proposed Aggregate Primary-Energy-Source-Utilization Simulation [PAPS] smart thermostat [ST] Scenario B unserviced energy [UE].

The expected PAPS ST Scenario B UE, shown in Figure 200, quantifies the expected PAPS ST Scenario B UE as a function of the number of DR days (from zero to 50) for three levels of REMS market penetration. Specifically, the slope [%/DR day] of the 10%, 20%, and 40% REMS market penetration percent change in the expected PAPS ST Scenario B UE is 0.943, 1.299, and 1.436 for the ECAK power system area respective REMS market penetration level; 0.650, 0.964, and 1.169 for the SNV power system area respective REMS market penetration level; 0.937, 1.486, and 1.764 for the SPPS power system area respective REMS market penetration level; and 1.521, 2.045, and 2.219 for the WUMS power system area respective REMS market penetration level.

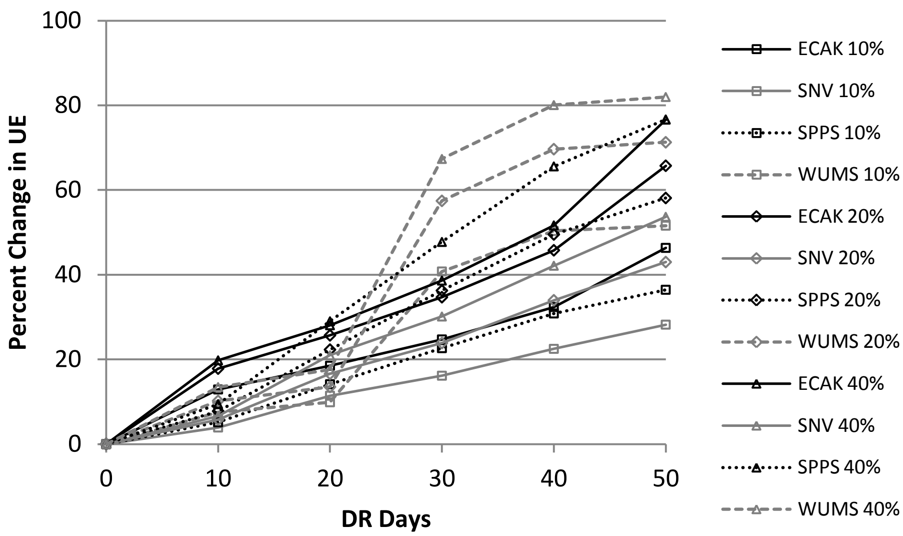

Figure 201: Percent change in the expected Proposed Aggregate Primary-Energy-Source-Utilization Simulation [PAPS] smart thermostat [ST] Scenario C unserviced energy [UE].

The expected PAPS ST Scenario C UE, shown in Figure 201, quantifies the expected PAPS ST Scenario C UE as a function of the number of DR days (from zero to 50) for three levels of REMS market penetration. Specifically, the slope [%/DR day] of the 10%, 20%, and 40% REMS market penetration percent change in the expected PAPS ST Scenario C UE is 0.847, 1.204, and 1.398 for the ECAK power system area respective REMS market penetration level; 0.576, 0.876, and 1.097 for the SNV power system area respective REMS market penetration level; 0.765, 1.228, and 1.630 for the SPPS power system area respective REMS market penetration level; and 1.192, 1.653, and 1.884 for the WUMS power system area respective REMS market penetration level.

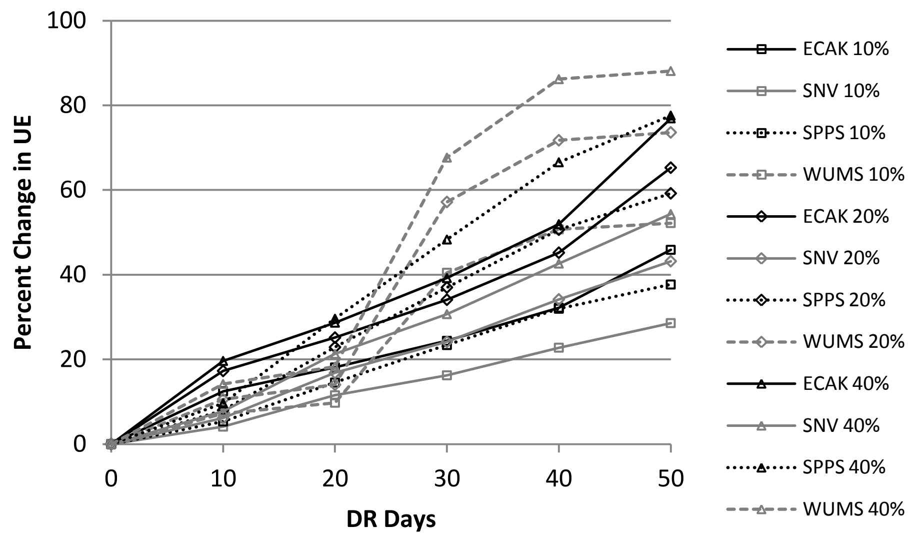

Figure 202: Percent change in the expected Proposed Aggregate Primary-Energy-Source-Utilization Simulation [PAPS] smart thermostat [ST] Scenario D unserviced energy [UE].

The expected PAPS ST Scenario D UE, shown in Figure 202, quantifies the expected PAPS ST Scenario D UE as a function of the number of DR days (from zero to 50) for three levels of REMS market penetration. Specifically, the slope [%/DR day] of the 10%, 20%, and 40% REMS market penetration percent change in the expected PAPS ST Scenario D UE is 0.843, 1.197, and 1.406 for the ECAK power system area respective REMS market penetration level; 0.581, 0.878, and 1.102 for the SNV power system area respective REMS market penetration level; 0.792, 1.252, and 1.650 for the SPPS power system area respective REMS market penetration level; and 1.206, 1.699, and 2.017 for the WUMS power system area respective REMS market penetration level.

The percent change in the expected PPRS ST Scenario A, Scenario B, Scenario C, and Scenario D average electricity cost (AEC) is shown in Figure 203, Figure 204, Figure 205, and Figure 206, respectively.

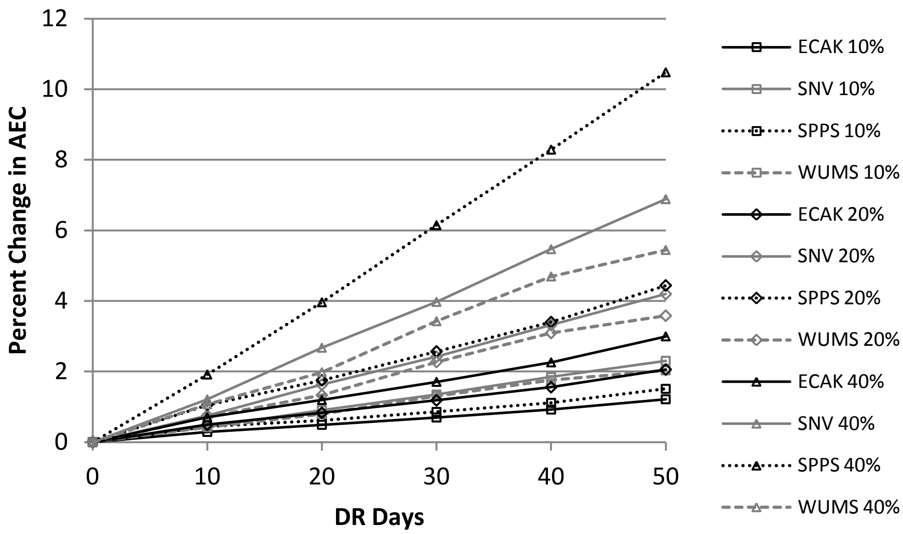

Figure 203: Percent change in the expected Proposed Aggregate Primary-Energy-Source-Utilization Simulation [PAPS] smart thermostat [ST] Scenario A average electricity cost [AEC].

The expected PAPS ST Scenario A AEC, shown in Figure 203, quantifies the change in the expected PAPS ST Scenario A AEC as a function of the number of DR days (from zero to 50) for three levels of REMS market penetration. Specifically, the slope [%/DR day] of the 10%, 20%, and 40% REMS market penetration percent change in the expected PAPS ST Scenario A AEC is 0.023, 0.039, and 0.058 for the ECAK power system area respective REMS market penetration level; 0.046, 0.084, and 0.139 for the SNV power system area respective REMS market penetration level; 0.028, 0.086, and 0.211 for the SPPS power system area respective REMS market penetration level; and 0.042, 0.074, and 0.113 for the WUMS power system area respective REMS market penetration level.

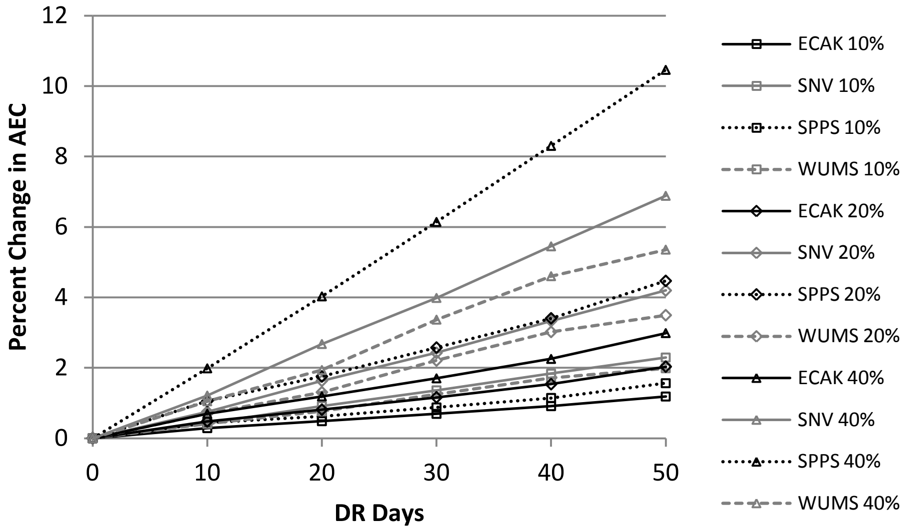

Figure 204: Percent change in the expected Proposed Aggregate Primary-Energy-Source-Utilization Simulation [PAPS] smart thermostat [ST] Scenario B average electricity cost [AEC].

The expected PAPS ST Scenario B AEC, shown in Figure 204, quantifies the change in the expected PAPS ST Scenario B AEC as a function of the number of DR days (from zero to 50) for three levels of REMS market penetration. Specifically, the slope [%/DR day] of the 10%, 20%, and 40% REMS market penetration percent change in the expected PAPS ST Scenario B AEC is 0.023, 0.039, and 0.057 for the ECAK power system area respective REMS market penetration level; 0.046, 0.084, and 0.138 for the SNV power system area respective REMS market penetration level; 0.029, 0.086, and 0.210 for the SPPS power system area respective REMS market penetration level; and 0.041, 0.072, and 0.111 for the WUMS power system area respective REMS market penetration level.

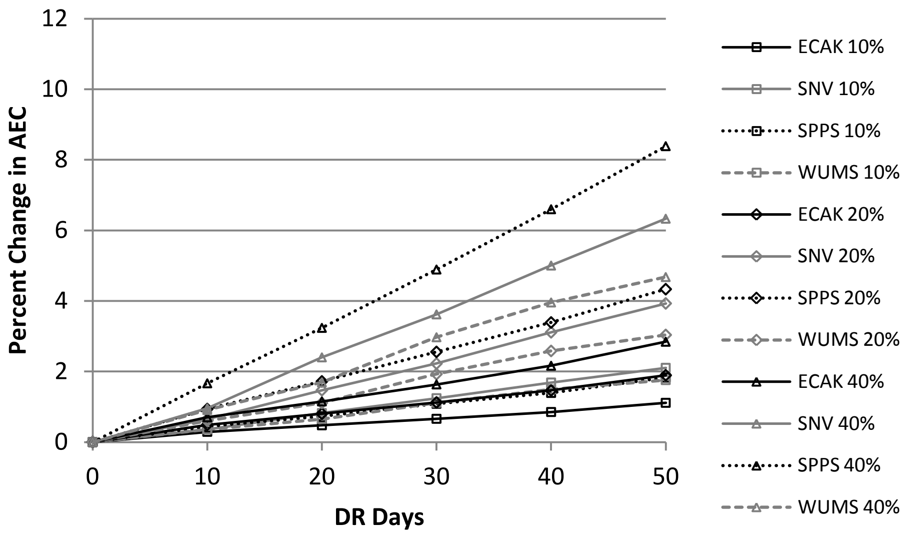

Figure 205: Percent change in the expected Proposed Aggregate Primary-Energy-Source-Utilization Simulation [PAPS] smart thermostat [ST] Scenario C average electricity cost [AEC].

The expected PAPS ST Scenario C AEC, shown in Figure 205, quantifies the change in the expected PAPS ST Scenario C AEC as a function of the number of DR days (from zero to 50) for three levels of REMS market penetration. Specifically, the slope [%/DR day] of the 10%, 20%, and 40% REMS market penetration percent change in the expected PAPS ST Scenario C AEC is 0.021, 0.036, and 0.055 for the ECAK power system area respective REMS market penetration level; 0.043, 0.079, and 0.129 for the SNV power system area respective REMS market penetration level; 0.035, 0.085, and 0.167 for the SPPS power system area respective REMS market penetration level; and 0.036, 0.063, and 0.097 for the WUMS power system area respective REMS market penetration level.

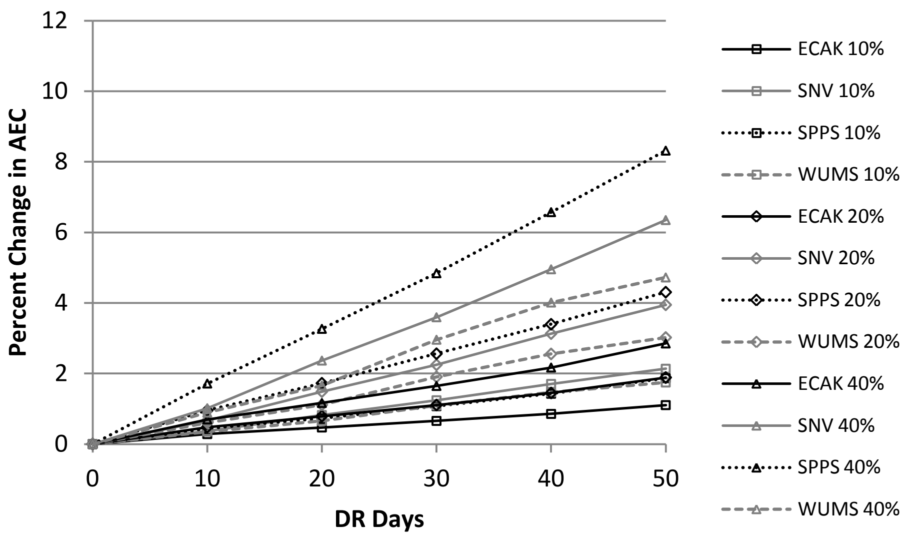

Figure 206: Percent change in the expected Proposed Aggregate Primary-Energy-Source-Utilization Simulation [PAPS] smart thermostat [ST] Scenario D average electricity cost [AEC].

The expected PAPS ST Scenario D AEC, shown in Figure 206, quantifies the change in the expected PAPS ST Scenario D AEC as a function of the number of DR days (from zero to 50) for three levels of REMS market penetration. Specifically, the slope [%/DR day] of the 10%, 20%, and 40% REMS market penetration percent change in the expected PAPS ST Scenario D AEC is 0.021, 0.036, and 0.055 for the ECAK power system area respective REMS market penetration level; 0.043, 0.080, and 0.128 for the SNV power system area respective REMS market penetration level; 0.036, 0.085, and 0.165 for the SPPS power system area respective REMS market penetration level; and 0.036, 0.062, and 0.098 for the WUMS power system area respective REMS market penetration level.

Next is a presentation of the PAPS smart appliance scheduling results.

6.5 Smart Appliance Scheduling

The smart appliance scheduling (SAS) energy management function delays the use of the smart appliances (clothes washer, clothes dryer, dishwasher, plug-in electric vehicle [PEV], and refrigerator) prior to and during the demand response (DR) period. The SAS energy management function allows the smart appliances to be delayed if the appliance is scheduled to start just before or during the DR period. One caveat of this rule is for the refrigerator. The refrigerator is delayed for a maximum of one hour (60 minutes), because the internal temperature of the refrigerator must remain cold during the DR period. It is assumed that the internal temperature of the refrigerator will not rise to unsafe levels in a single hour [107]. All the other smart appliances are delayed if they are started such that they will run into the DR period. All of the delayed appliances are rescheduled in a priority-based sequential sequence (e.g. clothes washer, clothes dryer, dishwasher, and PEV). A sequential sequence is needed so that a new daily peak is not created when all delayed appliances are restarted (i.e. synchronized payback) after the DR period.

The results in this section show the percent change of the expected PAPS results for the REMS market penetration levels (10%, 20%, and 40%) for each location (Versailles Kentucky [ECAK], Mercury Nevada [SNV], Stillwater Oklahoma [SPPS], and Necedah Wisconsin [WUMS]). The percent change in the expected PAPS results for the various market penetration levels are compared to the corresponding expected PAPS base case (BC) results described in Section 6.1. Further, the slope of the percent change as a function of the DR days is computed for each result. The slope of the percent change is a sensitivity measure of the PAPS results to the SAS energy management function.

The percent change in the expected PPRS SAS Scenario A, Scenario B, Scenario C, and Scenario D generated energy (GE) is shown in Figure 207, Figure 208, Figure 209, Figure 210, respectively.

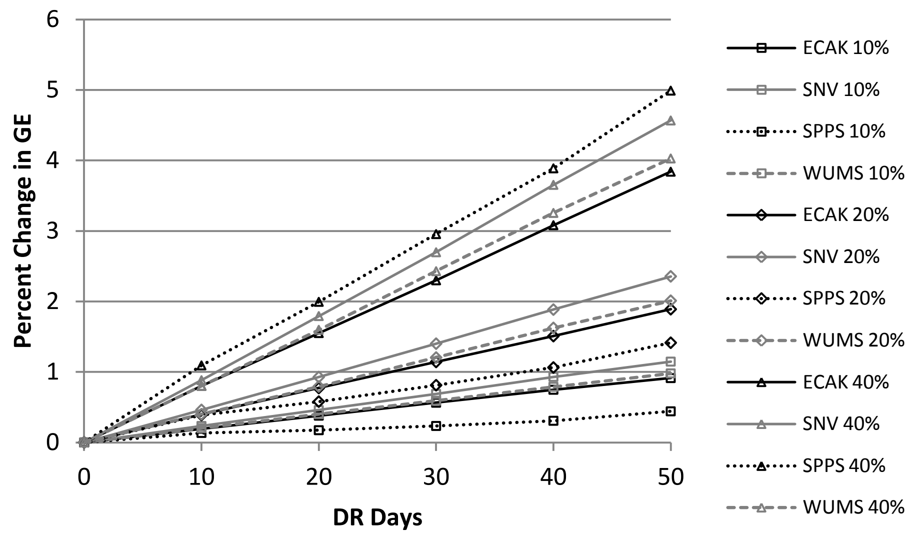

Figure 207: Percent change in the expected Proposed Aggregate Primary-Energy-Source-Utilization Simulation [PAPS] smart appliance scheduling [SAS] Scenario A generated energy [GE].

The expected PAPS SAS Scenario A GE, shown in Figure 207, quantifies the change in the expected PAPS SAS Scenario A GE as a function of the number of DR days (from zero to 50) for three levels of REMS market penetration (10%, 20%, and 40%). Specifically, the slope [%/DR day] of the 10%, 20%, and 40% REMS market penetration percent change in the expected PAPS SAS Scenario A GE is 0.018, 0.038, and 0.077 for the ECAK power system area respective REMS market penetration level; 0.023, 0.047, and 0.092 for the SNV power system area respective REMS market penetration level; 0.008, 0.027, and 0.098 for the SPPS power system area respective REMS market penetration level; and 0.020, 0.040, and 0.081 for the WUMS power system area respective REMS market penetration level.

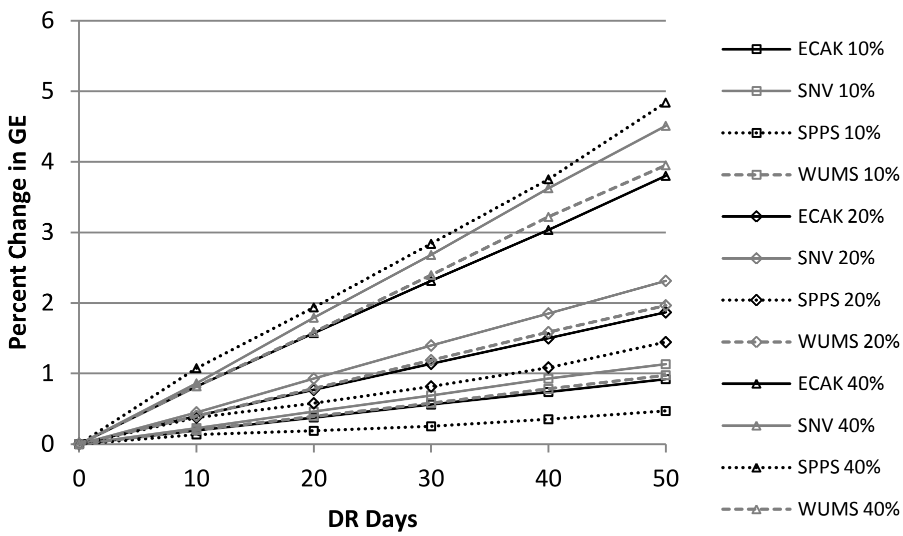

Figure 208: Percent change in the expected Proposed Aggregate Primary-Energy-Source-Utilization Simulation [PAPS] smart appliance scheduling [SAS] Scenario B generated energy [GE].

The expected PAPS SAS Scenario B GE, shown in Figure 208, quantifies the expected PAPS SAS Scenario B GE as a function of the number of DR days (from zero to 50) for three levels of REMS market penetration. Specifically, the slope [%/DR day] of the 10%, 20%, and 40% REMS market penetration percent change in the expected PAPS SAS Scenario B GE is 0.018, 0.037, and 0.075 for the ECAK power system area respective REMS market penetration level; 0.023, 0.046, and 0.091 for the SNV power system area respective REMS market penetration level; 0.009, 0.027, and 0.095 for the SPPS power system area respective REMS market penetration level; and 0.019, 0.039, and 0.079 for the WUMS power system area respective REMS market penetration level.

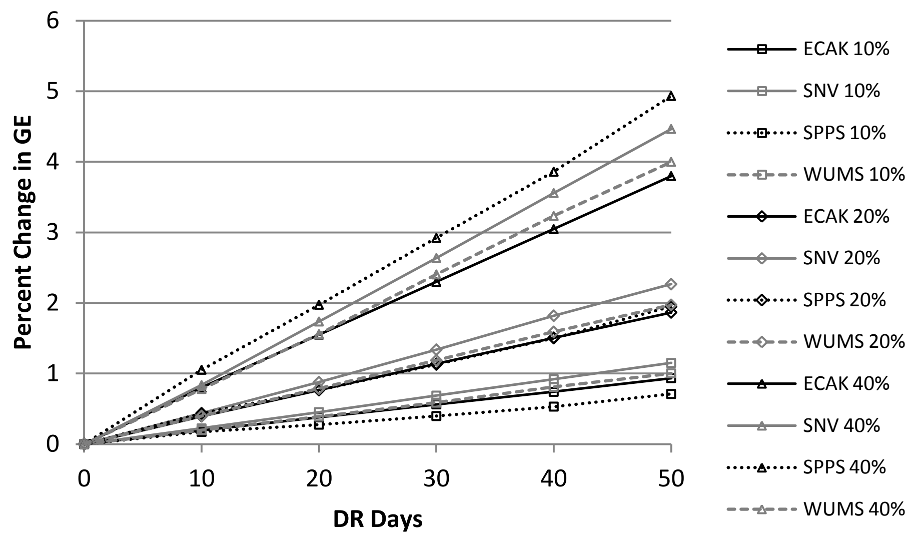

Figure 209: Percent change in the expected Proposed Aggregate Primary-Energy-Source-Utilization Simulation [PAPS] smart appliance scheduling [SAS] Scenario C generated energy [GE].

The expected PAPS SAS Scenario C GE, shown in Figure 209, quantifies the expected PAPS SAS Scenario C GE as a function of the number of DR days (from zero to 50) for three levels of REMS market penetration. Specifically, the slope [%/DR day] of the 10%, 20%, and 40% REMS market penetration percent change in the expected PAPS SAS Scenario C GE is 0.019, 0.037, and 0.076 for the ECAK power system area respective REMS market penetration level; 0.023, 0.046, and 0.090 for the SNV power system area respective REMS market penetration level; 0.014, 0.038, and 0.097 for the SPPS power system area respective REMS market penetration level; and 0.020, 0.040, and 0.081 for the WUMS power system area respective REMS market penetration level.

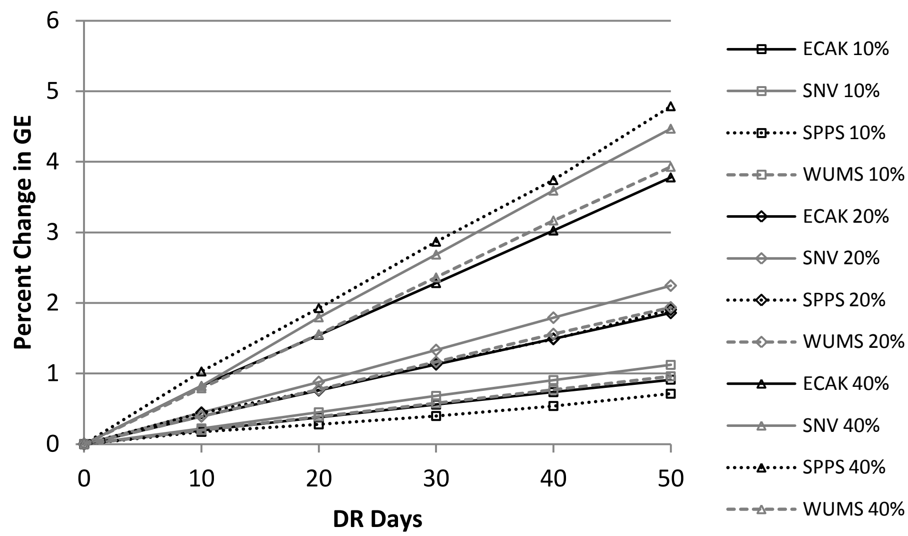

Figure 210: Percent change in the expected Proposed Aggregate Primary-Energy-Source-Utilization Simulation [PAPS] smart appliance scheduling [SAS] Scenario D generated energy [GE].

The expected PAPS SAS Scenario D GE, shown in Figure 210, quantifies the expected PAPS SAS Scenario D GE as a function of the number of DR days (from zero to 50) for three levels of REMS market penetration. Specifically, the slope [%/DR day] of the 10%, 20%, and 40% REMS market penetration percent change in the expected PAPS SAS Scenario D GE is 0.018, 0.037, and 0.075 for the ECAK power system area respective REMS market penetration level; 0.023, 0.045, and 0.090 for the SNV power system area respective REMS market penetration level; 0.014, 0.037, and 0.094 for the SPPS power system area respective REMS market penetration level; and 0.019, 0.039, and 0.079 for the WUMS power system area respective REMS market penetration level.

The percent change in the expected PPRS SAS Scenario A, Scenario B, Scenario C, and Scenario D generated environmental air pollution (GEAP) is shown in Figure 211, Figure 212, Figure 213, and Figure 214, respectively.

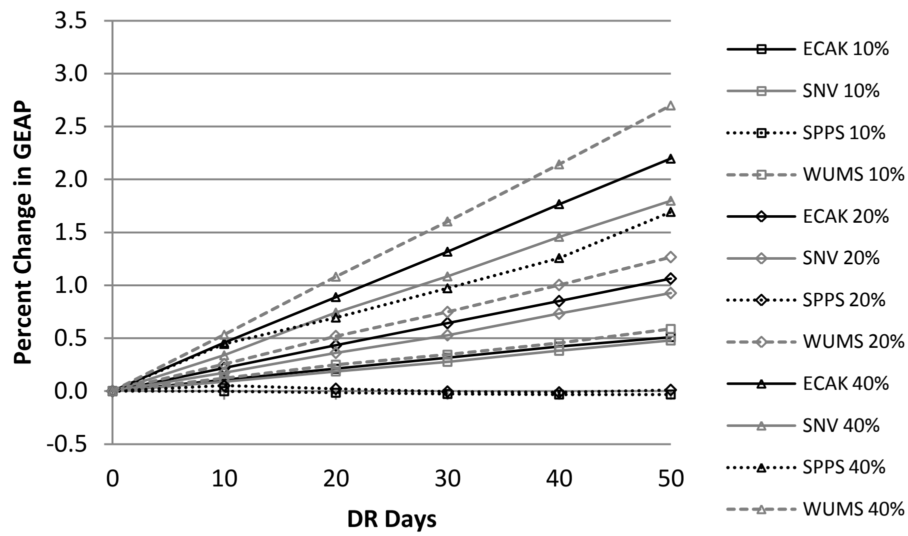

Figure 211: Percent change in the expected Proposed Aggregate Primary-Energy-Source-Utilization Simulation [PAPS] smart appliance scheduling [SAS] Scenario A generated environmental air pollution [GEAP].

The expected PAPS SAS Scenario A GEAP, shown in Figure 211, quantifies the change in the expected PAPS SAS Scenario A GEAP as a function of the number of DR days (from zero to 50) for three levels of REMS market penetration. Specifically, the slope [%/DR day] of the 10%, 20%, and 40% REMS market penetration percent change in the expected PAPS SAS Scenario A GEAP is 0.010, 0.021, and 0.044 for the ECAK power system area respective REMS market penetration level; 0.010, 0.018, and 0.036 for the SNV power system area respective REMS market penetration level; -0.001, less than 0.001, 0.032 for the SPPS power system area respective REMS market penetration level; and 0.012, 0.025, and 0.054 for the WUMS power system area respective REMS market penetration level.

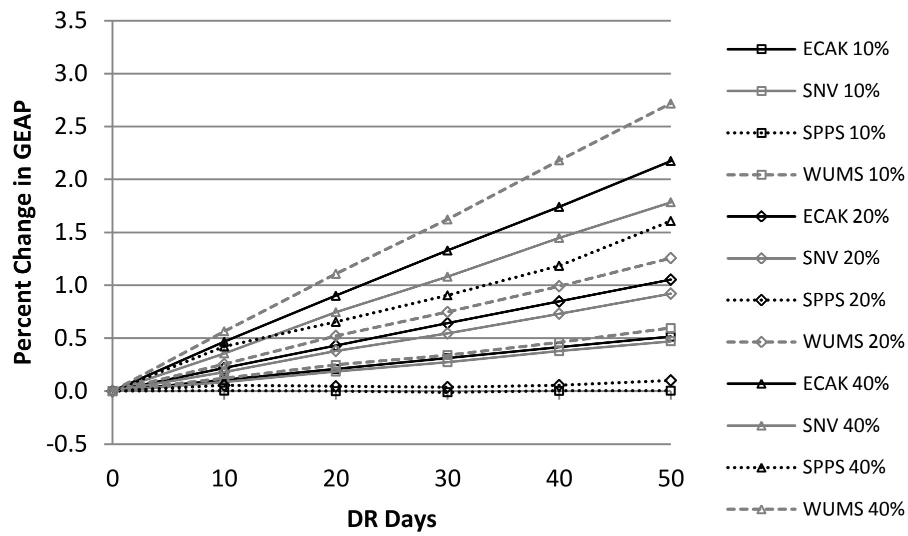

Figure 212: Percent change in the expected Proposed Aggregate Primary-Energy-Source-Utilization Simulation [PAPS] smart appliance scheduling [SAS] Scenario B generated environmental air pollution [GEAP].

The expected PAPS SAS Scenario B GEAP, shown in Figure 212, quantifies the change in the expected PAPS SAS Scenario B GEAP as a function of the number of DR days (from zero to 50) for three levels of REMS market penetration. Specifically, the slope [%/DR day] of the 10%, 20%, and 40% REMS market penetration percent change in the expected PAPS SAS Scenario B GEAP is 0.010, 0.021, and 0.043 for the ECAK power system area respective REMS market penetration level; 0.009, 0.018, and 0.036 for the SNV power system area respective REMS market penetration level; less than 0.001, 0.001, 0.030 for the SPPS power system area respective REMS market penetration level; and 0.012, 0.025, and 0.054 for the WUMS power system area respective REMS market penetration level.

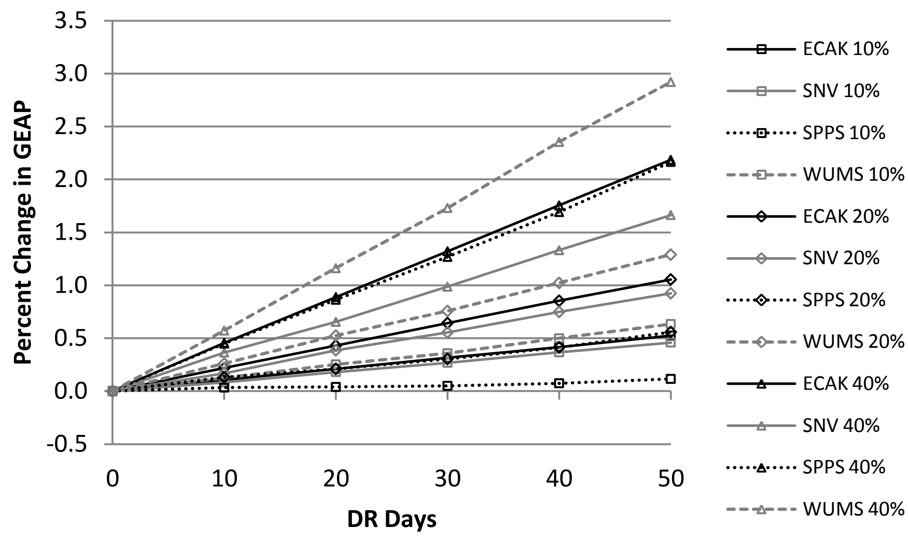

Figure 213: Percent change in the expected Proposed Aggregate Primary-Energy-Source-Utilization Simulation [PAPS] smart appliance scheduling [SAS] Scenario C generated environmental air pollution [GEAP].

The expected PAPS SAS Scenario C GEAP, shown in Figure 213, quantifies the change in the expected PAPS SAS Scenario C GEAP as a function of the number of DR days (from zero to 50) for three levels of REMS market penetration. Specifically, the slope [%/DR day] of the 10%, 20%, and 40% REMS market penetration percent change in the expected PAPS SAS Scenario C GEAP is 0.010, 0.021, and 0.044 for the ECAK power system area respective REMS market penetration level; 0.009, 0.019, and 0.033 for the SNV power system area respective REMS market penetration level; 0.002, 0.011, 0.043 for the SPPS power system area respective REMS market penetration level; and 0.013, 0.026, and 0.059 for the WUMS power system area respective REMS market penetration level.

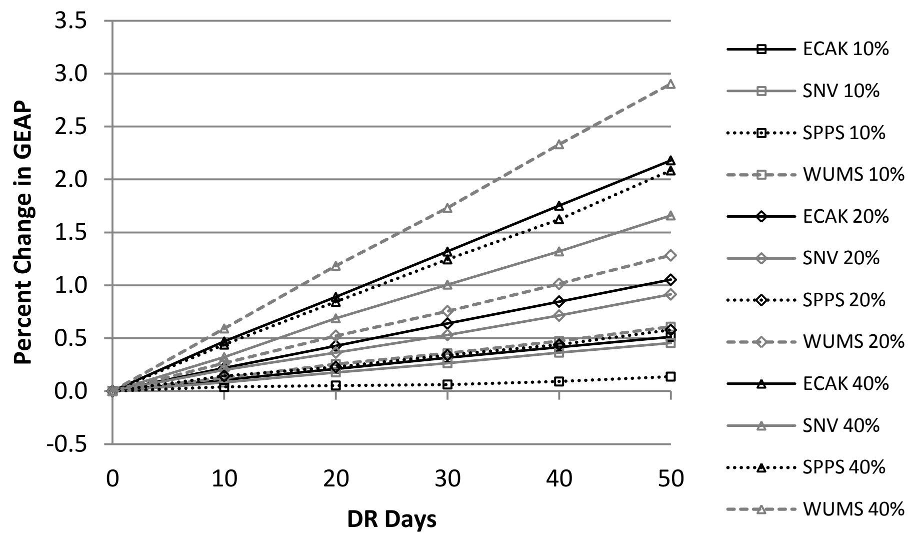

Figure 214: Percent change in the expected Proposed Aggregate Primary-Energy-Source-Utilization Simulation [PAPS] smart appliance scheduling [SAS] Scenario D generated environmental air pollution [GEAP].

The expected PAPS SAS Scenario D GEAP, shown in Figure 214, quantifies the change in the expected PAPS SAS Scenario D GEAP as a function of the number of DR days (from zero to 50) for three levels of REMS market penetration. Specifically, the slope [%/DR day] of the 10%, 20%, and 40% REMS market penetration percent change in the expected PAPS SAS Scenario D GEAP is 0.010, 0.021, and 0.043 for the ECAK power system area respective REMS market penetration level; 0.009, 0.018, and 0.033 for the SNV power system area respective REMS market penetration level; 0.002, 0.011, 0.041 for the SPPS power system area respective REMS market penetration level; and 0.012, 0.025, and 0.058 for the WUMS power system area respective REMS market penetration level.

The percent change in the expected PPRS SAS Scenario A, Scenario B, Scenario C, and Scenario D loss of load probability (LOLP) is shown in Figure 215, Figure 216, Figure 217, and Figure 218, respectively.

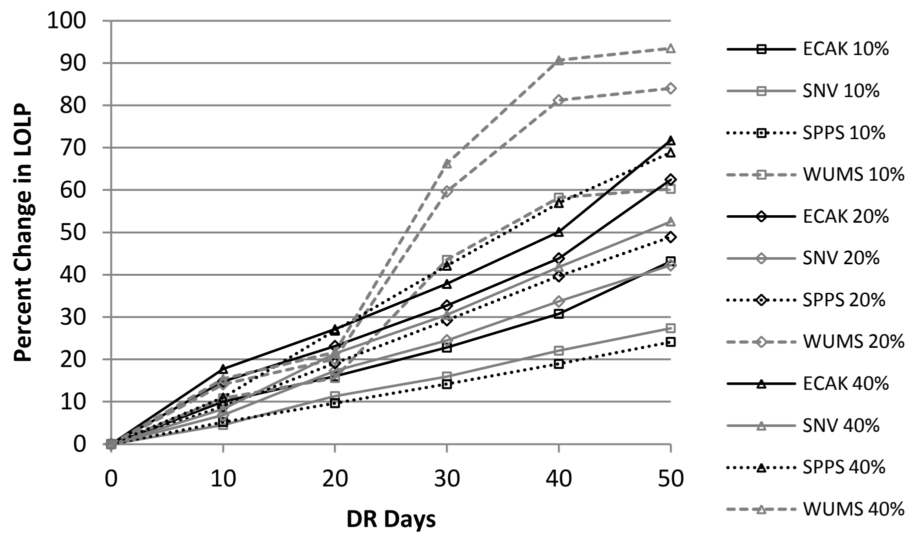

Figure 215: Percent change in the expected Proposed Aggregate Primary-Energy-Source-Utilization Simulation [PAPS] smart appliance scheduling [SAS] Scenario A loss of load probability [LOLP].

The expected PAPS SAS Scenario A LOLP, shown in Figure 215, quantifies the change in the expected PAPS SAS Scenario A LOLP as a function of the number of DR days (from zero to 50) for three levels of REMS market penetration. Specifically, the slope [%/DR day] of the 10%, 20%, and 40% REMS market penetration percent change in the expected PAPS SAS Scenario A LOLP is 0.813, 1.169, and 1.333 for the ECAK power system area respective REMS market penetration level; 0.554, 0.854, and 1.064 for the SNV power system area respective REMS market penetration level; 0.475, 0.991, and 1.421 for the SPPS power system area respective REMS market penetration level; and 1.347, 1.888, and 2.108 for the WUMS power system area respective REMS market penetration level.

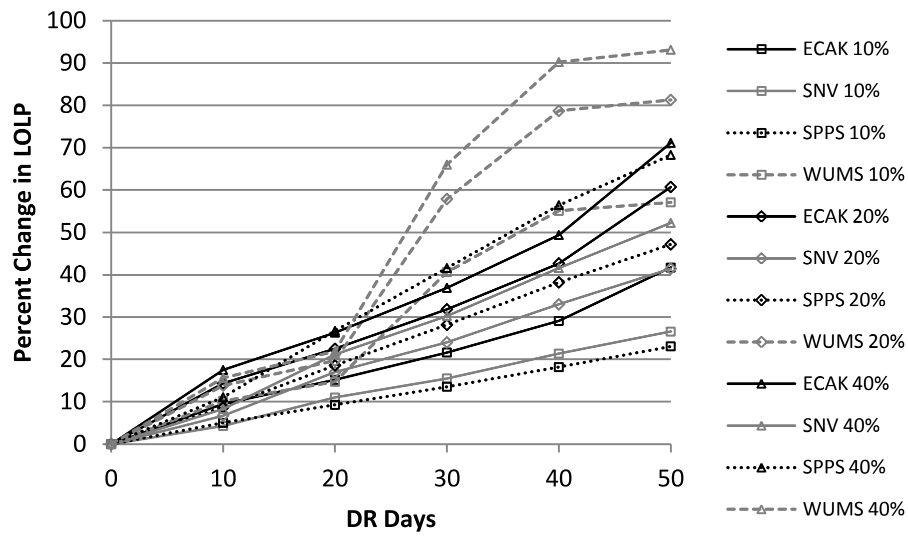

Figure 216: Percent change in the expected Proposed Aggregate Primary-Energy-Source-Utilization Simulation [PAPS] smart appliance scheduling [SAS] Scenario B loss of load probability [LOLP].

The expected PAPS SAS Scenario B LOLP, shown in Figure 216, quantifies the change in the expected PAPS SAS Scenario B LOLP as a function of the number of DR days (from zero to 50) for three levels of REMS market penetration. Specifically, the slope [%/DR day] of the 10%, 20%, and 40% REMS market penetration percent change in the expected PAPS SAS Scenario B LOLP is 0.782, 1.137, and 1.319 for the ECAK power system area respective REMS market penetration level; 0.539, 0.837, and 1.057 for the SNV power system area respective REMS market penetration level; 0.454, 0.954, and 1.406 for the SPPS power system area respective REMS market penetration level; and 1.274, 1.826, and 2.096 for the WUMS power system area respective REMS market penetration level.

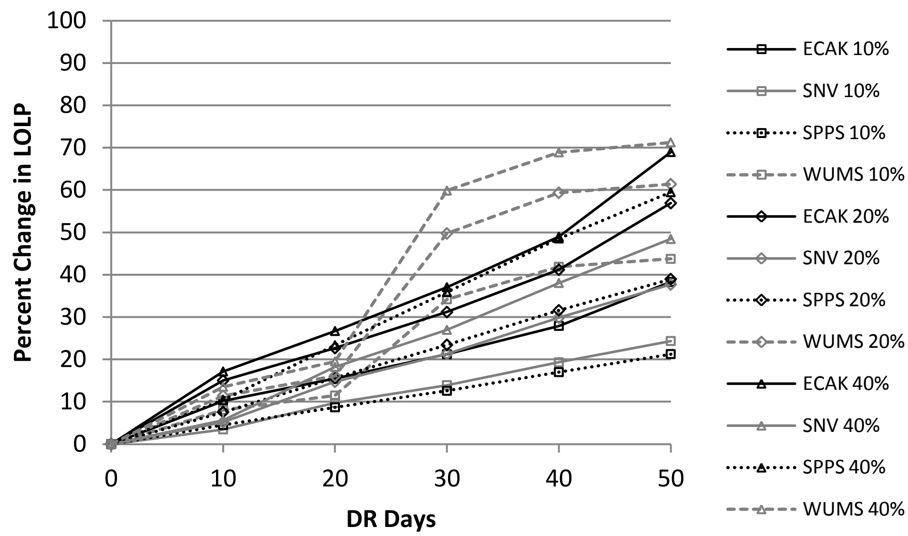

Figure 217: Percent change in the expected Proposed Aggregate Primary-Energy-Source-Utilization Simulation [PAPS] smart appliance scheduling [SAS] Scenario C loss of load probability [LOLP].

The expected PAPS SAS Scenario C LOLP, shown in Figure 217, quantifies the change in the expected PAPS SAS Scenario C LOLP as a function of the number of DR days (from zero to 50) for three levels of REMS market penetration. Specifically, the slope [%/DR day] of the 10%, 20%, and 40% REMS market penetration percent change in the expected PAPS SAS Scenario C LOLP is 0.716, 1.061, and 1.287 for the ECAK power system area respective REMS market penetration level; 0.496, 0.769, and 0.995 for the SNV power system area respective REMS market penetration level; 0.422, 0.785, and 1.212 for the SPPS power system area respective REMS market penetration level; and 0.979, 1.384, and 1.608 for the WUMS power system area respective REMS market penetration level.

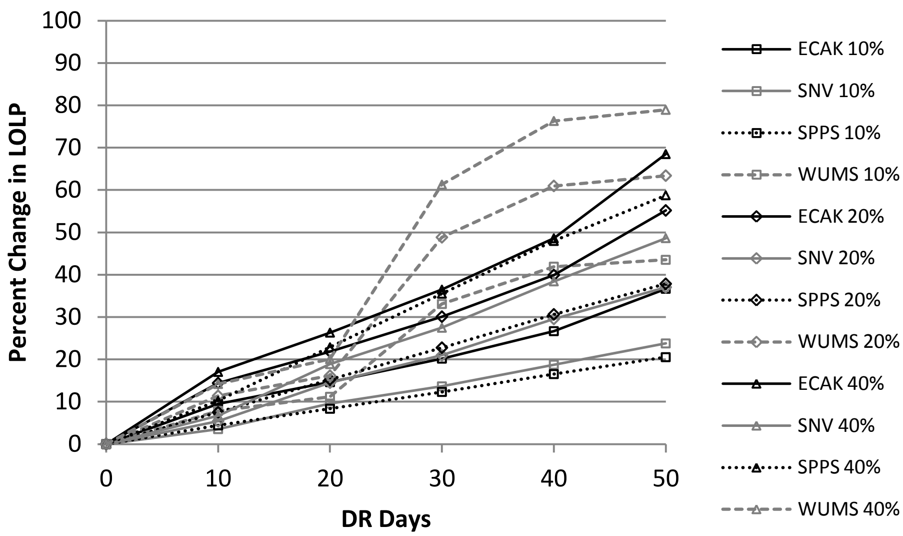

Figure 218: Percent change in the expected Proposed Aggregate Primary-Energy-Source-Utilization Simulation [PAPS] smart appliance scheduling [SAS] Scenario D loss of load probability [LOLP].

The expected PAPS SAS Scenario D LOLP, shown in Figure 218, quantifies the change in the expected PAPS SAS Scenario D LOLP as a function of the number of DR days (from zero to 50) for three levels of REMS market penetration. Specifically, the slope [%/DR day] of the 10%, 20%, and 40% REMS market penetration percent change in the expected PAPS SAS Scenario D LOLP is 0.687, 1.030, and 1.278 for the ECAK power system area respective REMS market penetration level; 0.4826, 0.755, and 0.991 for the SNV power system area respective REMS market penetration level; 0.408, 0.761, and 1.199 for the SPPS power system area respective REMS market penetration level; and 0.976, 1.424, and 1.778 for the WUMS power system area respective REMS market penetration level.

The percent change in the expected PPRS SAS Scenario A, Scenario B, Scenario C, and Scenario D unserviced energy (UE) is shown in Figure 219, Figure 220, Figure 221, and Figure 222, respectively.

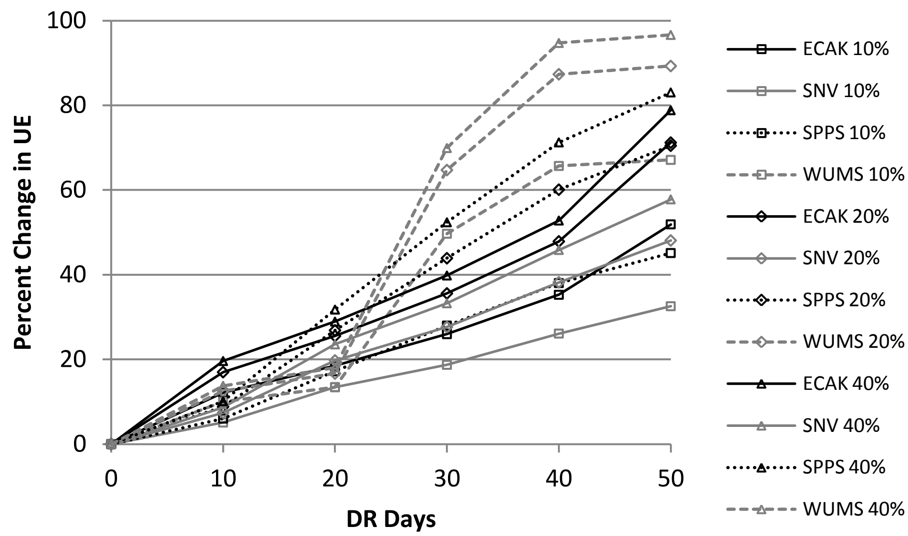

Figure 219: Percent change in the expected Proposed Aggregate Primary-Energy-Source-Utilization Simulation [PAPS] smart appliance scheduling [SAS] Scenario A unserviced energy [UE].

The expected PAPS SAS Scenario A UE, shown in Figure 219, quantifies the expected PAPS SAS Scenario A UE as a function of the number of DR days (from zero to 50) for three levels of REMS market penetration. Specifically, the slope [%/DR day] of the 10%, 20%, and 40% REMS market penetration percent change in the expected PAPS SAS Scenario A UE is 0.961, 1.310, and 1.442 for the ECAK power system area respective REMS market penetration level; 0.660, 0.974, and 1.172 for the SNV power system area respective REMS market penetration level; 0.950, 1.495, and 1.769 for the SPPS power system area respective REMS market penetration level; and 1.540, 2.054, and 2.222 for the WUMS power system area respective REMS market penetration level.

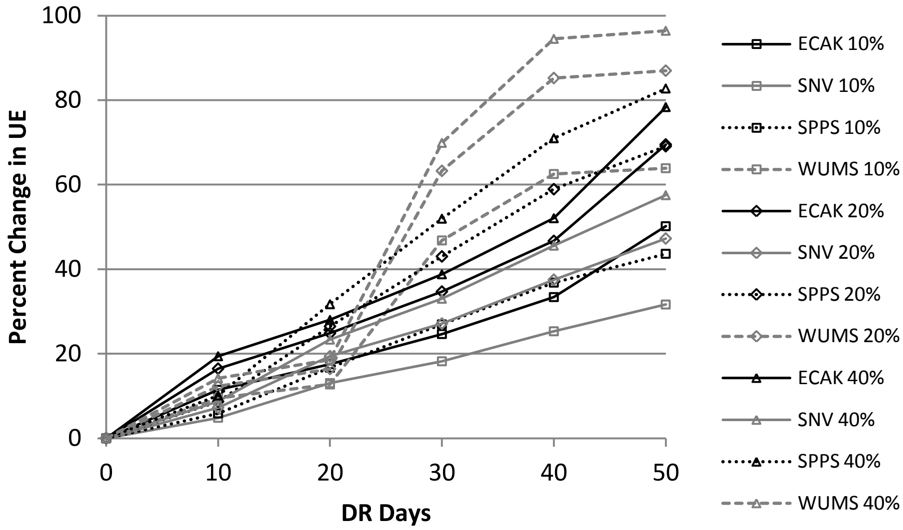

Figure 220: Percent change in the expected Proposed Aggregate Primary-Energy-Source-Utilization Simulation [PAPS] smart appliance scheduling [SAS] Scenario B unserviced energy [UE].

The expected PAPS SAS Scenario B UE, shown in Figure 220, quantifies the expected PAPS SAS Scenario B UE as a function of the number of DR days (from zero to 50) for three levels of REMS market penetration. Specifically, the slope [%/DR day] of the 10%, 20%, and 40% REMS market penetration percent change in the expected PAPS SAS Scenario B UE is 0.925, 1.280, and 1.430 for the ECAK power system area respective REMS market penetration level; 0.642, 0.957, and 1.165 for the SNV power system area respective REMS market penetration level; 0.918, 1.465, and 1.762 for the SPPS power system area respective REMS market penetration level; and 1.465, 2.001, and 2.212 for the WUMS power system area respective REMS market penetration level.

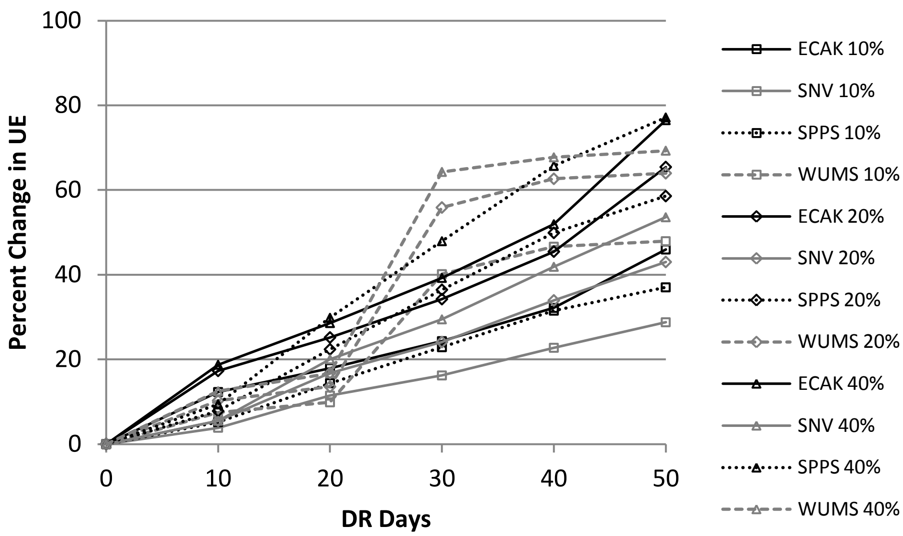

Figure 221: Percent change in the expected Proposed Aggregate Primary-Energy-Source-Utilization Simulation [PAPS] smart appliance scheduling [SAS] Scenario C unserviced energy [UE].

The expected PAPS SAS Scenario C UE, shown in Figure 221, quantifies the expected PAPS SAS Scenario C UE as a function of the number of DR days (from zero to 50) for three levels of REMS market penetration. Specifically, the slope [%/DR day] of the 10%, 20%, and 40% REMS market penetration percent change in the expected PAPS SAS Scenario C UE is 0.845, 1.202, and 1.408 for the ECAK power system area respective REMS market penetration level; 0.586, 0.879, and 1.104 for the SNV power system area respective REMS market penetration level; 0.779, 1.238, and 1.636 for the SPPS power system area respective REMS market penetration level; and 1.107, 1.484, and 1.599 for the WUMS power system area respective REMS market penetration level.

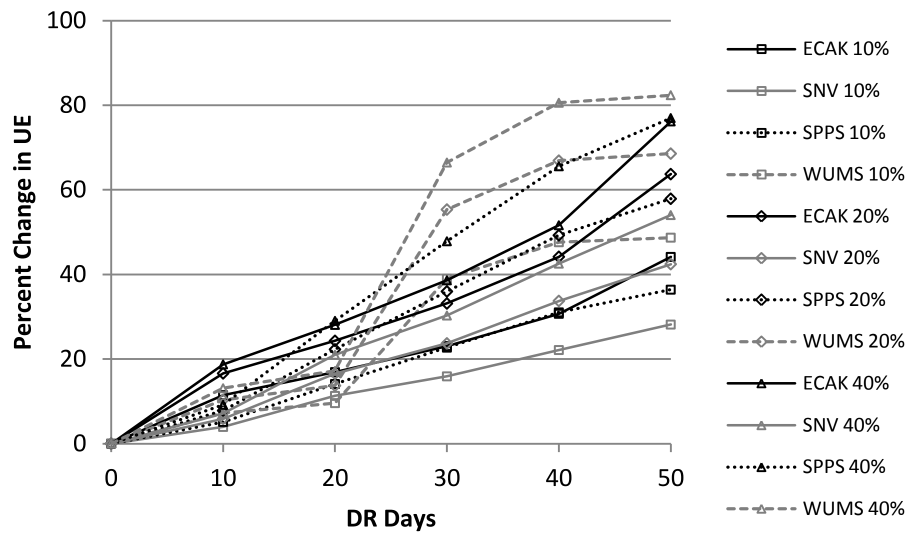

Figure 222: Percent change in the expected Proposed Aggregate Primary-Energy-Source-Utilization Simulation [PAPS] smart appliance scheduling [SAS] Scenario D unserviced energy [UE].

The expected PAPS SAS Scenario D UE, shown in Figure 222, quantifies the expected PAPS SAS Scenario D UE as a function of the number of DR days (from zero to 50) for three levels of REMS market penetration. Specifically, the slope [%/DR day] of the 10%, 20%, and 40% REMS market penetration percent change in the expected PAPS SAS Scenario D UE is 0.813, 1.172, and 1.400 for the ECAK power system area respective REMS market penetration level; 0.571, 0.865, and 1.102 for the SNV power system area respective REMS market penetration level; 0.766, 1.221, and 1.637 for the SPPS power system area respective REMS market penetration level; and 1.126, 1.583, and 1.896 for the WUMS power system area respective REMS market penetration level.

The percent change in the expected PPRS SAS Scenario A, Scenario B, Scenario C, and Scenario D average electricity cost (AEC) is shown in Figure 223, Figure 224, Figure 225, and Figure 226, respectively.

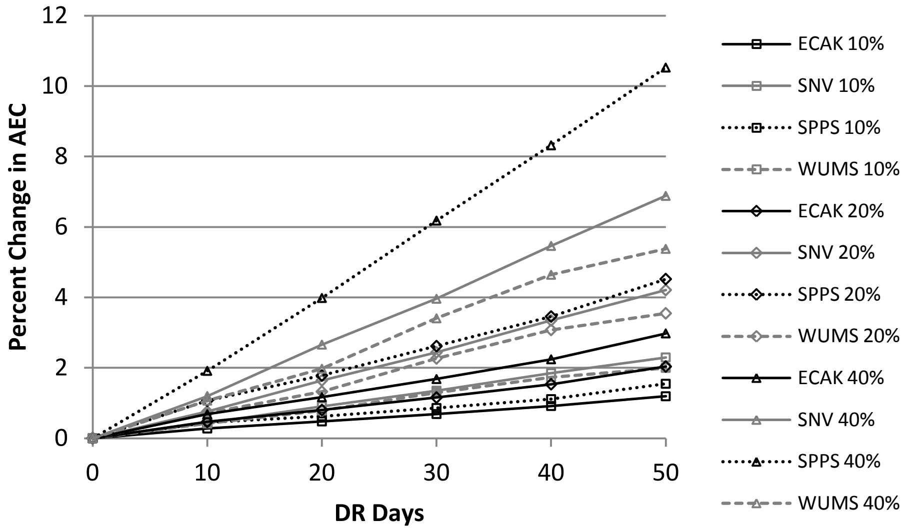

Figure 223: Percent change in the expected Proposed Aggregate Primary-Energy-Source-Utilization Simulation [PAPS] smart appliance scheduling [SAS] Scenario A average electricity cost [AEC].

The expected PAPS SAS Scenario A AEC, shown in Figure 223, quantifies the change in the expected PAPS SAS Scenario A AEC as a function of the number of DR days (from zero to 50) for three levels of REMS market penetration. Specifically, the slope [%/DR day] of the 10%, 20%, and 40% REMS market penetration percent change in the expected PAPS SAS Scenario A AEC is 0.023, 0.039, and 0.057 for the ECAK power system area respective REMS market penetration level; 0.046, 0.085, and 0.139 for the SNV power system area respective REMS market penetration level; 0.028, 0.087, and 0.212 for the SPPS power system area respective REMS market penetration level; and 0.041, 0.074, and 0.112 for the WUMS power system area respective REMS market penetration level.

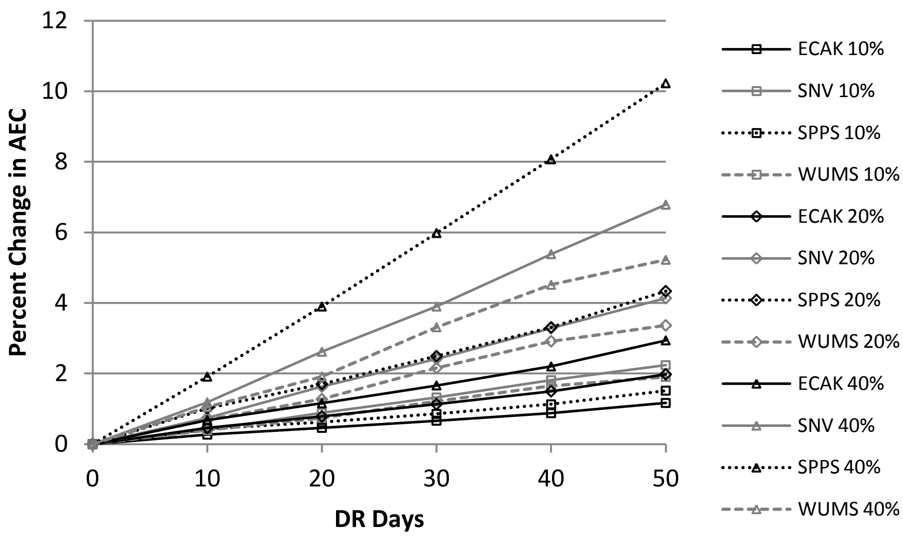

Figure 224: Percent change in the expected Proposed Aggregate Primary-Energy-Source-Utilization Simulation [PAPS] smart appliance scheduling [SAS] Scenario B average electricity cost [AEC].

The expected PAPS SAS Scenario B AEC, shown in Figure 224, quantifies the change in the expected PAPS SAS Scenario B AEC as a function of the number of DR days (from zero to 50) for three levels of REMS market penetration. Specifically, the slope [%/DR day] of the 10%, 20%, and 40% REMS market penetration percent change in the expected PAPS SAS Scenario B AEC is 0.022, 0.038, and 0.056 for the ECAK power system area respective REMS market penetration level; 0.045, 0.083, and 0.137 for the SNV power system area respective REMS market penetration level; 0.028, 0.084, and 0.205 for the SPPS power system area respective REMS market penetration level; and 0.039, 0.070, and 0.108 for the WUMS power system area respective REMS market penetration level.

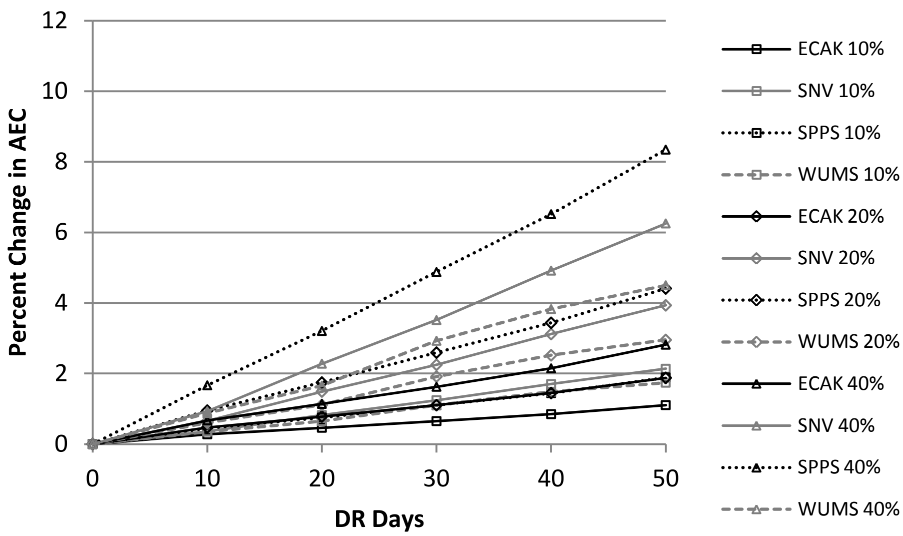

Figure 225: Percent change in the expected Proposed Aggregate Primary-Energy-Source-Utilization Simulation [PAPS] smart appliance scheduling [SAS] Scenario C average electricity cost [AEC].

The expected PAPS SAS Scenario C AEC, shown in Figure 225, quantifies the change in the expected PAPS SAS Scenario C AEC as a function of the number of DR days (from zero to 50) for three levels of REMS market penetration. Specifically, the slope [%/DR day] of the 10%, 20%, and 40% REMS market penetration percent change in the expected PAPS SAS Scenario C AEC is 0.021, 0.036, and 0.054 for the ECAK power system area respective REMS market penetration level; 0.043, 0.079, and 0.127 for the SNV power system area respective REMS market penetration level; 0.036, 0.087, and 0.166 for the SPPS power system area respective REMS market penetration level; and 0.036, 0.061, and 0.093 for the WUMS power system area respective REMS market penetration level.

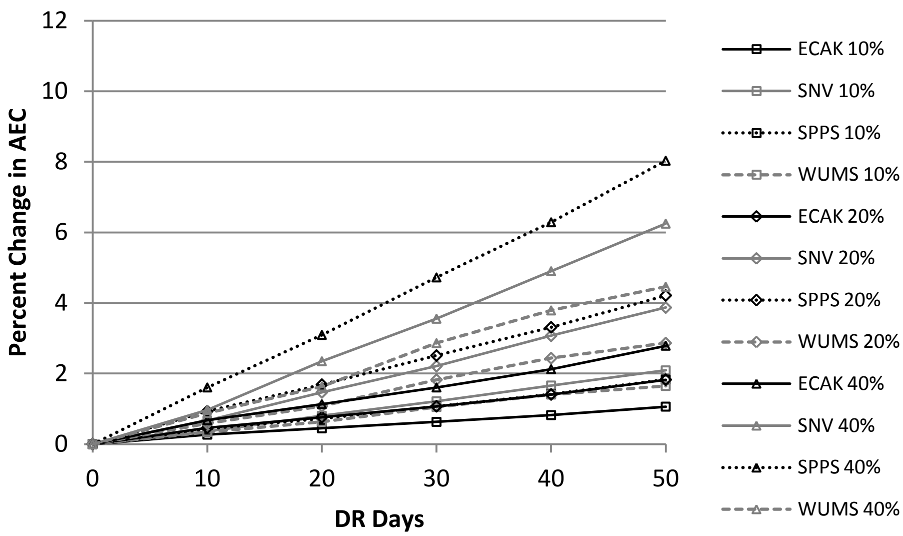

Figure 226: Percent change in the expected Proposed Aggregate Primary-Energy-Source-Utilization Simulation [PAPS] smart appliance scheduling [SAS] Scenario D average electricity cost [AEC].

The expected PAPS SAS Scenario D AEC, shown in Figure 226, quantifies the change in the expected PAPS SAS Scenario D AEC as a function of the number of DR days (from zero to 50) for three levels of REMS market penetration. Specifically, the slope [%/DR day] of the 10%, 20%, and 40% REMS market penetration percent change in the expected PAPS SAS Scenario D AEC is 0.020, 0.035, and 0.054 for the ECAK power system area respective REMS market penetration level; 0.042, 0.078, and 0.126 for the SNV power system area respective REMS market penetration level; 0.035, 0.083, and 0.159 for the SPPS power system area respective REMS market penetration level; and 0.034, 0.059, and 0.092 for the WUMS power system area respective REMS market penetration level.

Next is a presentation of the PAPS smart appliance scheduling with a stationary battery results.

6.6 Smart Appliance Scheduling with a Stationary Battery

The smart appliance scheduling with a stationary battery (SASB) energy management function adds a stationary battery dispatching function to the smart appliance scheduling (SAS) energy management function. In the SASB energy management function, a battery dispatching function is added to the appliance rescheduling in the SAS energy management function. The stationary battery is only dispatched during demand response (DR). The stationary battery output is limited to 120 V and 15 A (1.8 kW). The stationary battery capacity is 4.8 kWh. The stationary battery is scheduled to recharge at 4a. Notice, the stationary battery charging is stopped early if the battery charging will continue in the DR period; resulting in a partially charge stationary battery.

The results in this section show the percent change of the expected Proposed Aggregate Primary-Energy-Source-Utilization Simulation (PAPS) results for the residential energy management system (REMS) market penetration levels (10%, 20%, and 40%) for each location (Versailles Kentucky [ECAK], Mercury Nevada [SNV], Stillwater Oklahoma [SPPS], and Necedah Wisconsin [WUMS]). The percent change in the expected PAPS results for the various market penetration levels are compared to the corresponding expected PAPS base case (BC) results described in Section 6.1. Further, the slope of the percent change as a function of the DR days is computed for each result. The slope of the percent change is a sensitivity measure of the PAPS results to the SASB energy management function.

The percent change in the expected PPRS SASB Scenario A, Scenario B, Scenario C, and Scenario D generated energy (GE) is shown in Figure 227, Figure 228, Figure 229, and Figure 230, respectively.

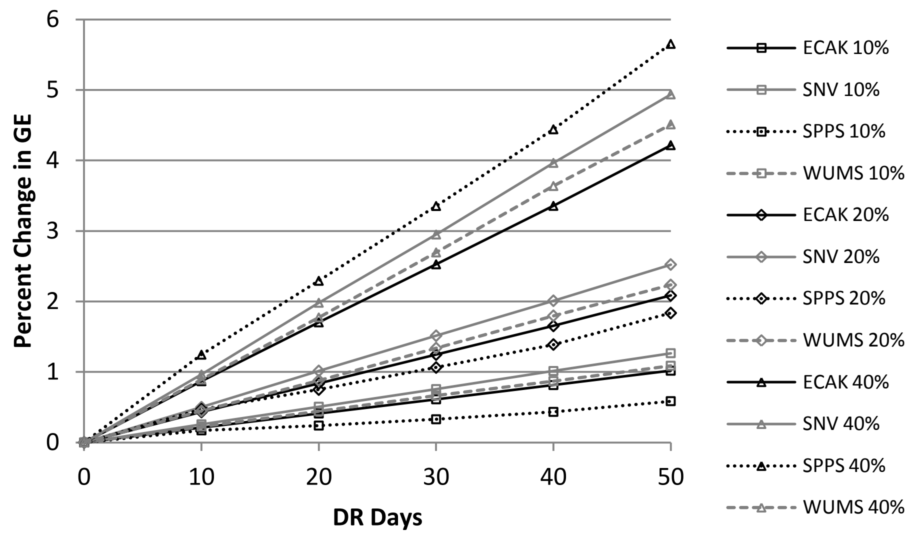

Figure 227: Percent change in the expected Proposed Aggregate Primary-Energy-Source-Utilization Simulation [PAPS] smart appliance scheduling with a stationary battery [SASB] Scenario A generated energy [GE].

The expected PAPS SASB Scenario A GE, shown in Figure 227, quantifies the change in the expected PAPS SASB Scenario A GE as a function of the number of DR days (from zero to 50) for three levels of REMS market penetration. Specifically, the slope [%/DR day] of the 10%, 20%, and 40% REMS market penetration percent change in the expected PAPS SASB Scenario A GE is 0.020, 0.041, and 0.084 for the ECAK power system area respective REMS market penetration level; 0.025, 0.050, and 0.099 for the SNV power system area respective REMS market penetration level; 0.011, 0.035, and 0.111 for the SPPS power system area respective REMS market penetration level; and 0.022, 0.045, and 0.091 for the WUMS power system area respective REMS market penetration level.

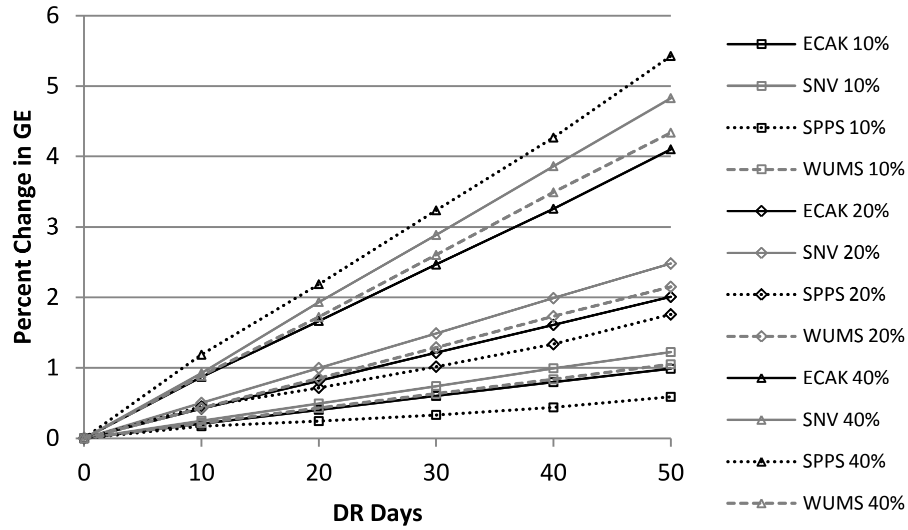

Figure 228: Percent change in the expected Proposed Aggregate Primary-Energy-Source-Utilization Simulation [PAPS] smart appliance scheduling with a stationary battery [SASB] Scenario B generated energy [GE].

The expected PAPS SASB Scenario B GE, shown in Figure 228, quantifies the expected PAPS SASB Scenario B GE as a function of the number of DR days (from zero to 50) for three levels of REMS market penetration. Specifically, the slope [%/DR day] of the 10%, 20%, and 40% REMS market penetration percent change in the expected PAPS SASB Scenario B GE is 0.020, 0.040, and 0.081 for the ECAK power system area respective REMS market penetration level; 0.025, 0.050, and 0.097 for the SNV power system area respective REMS market penetration level; 0.011, 0.034, and 0.107 for the SPPS power system area respective REMS market penetration level; and 0.021, 0.043, and 0.087 for the WUMS power system area respective REMS market penetration level.

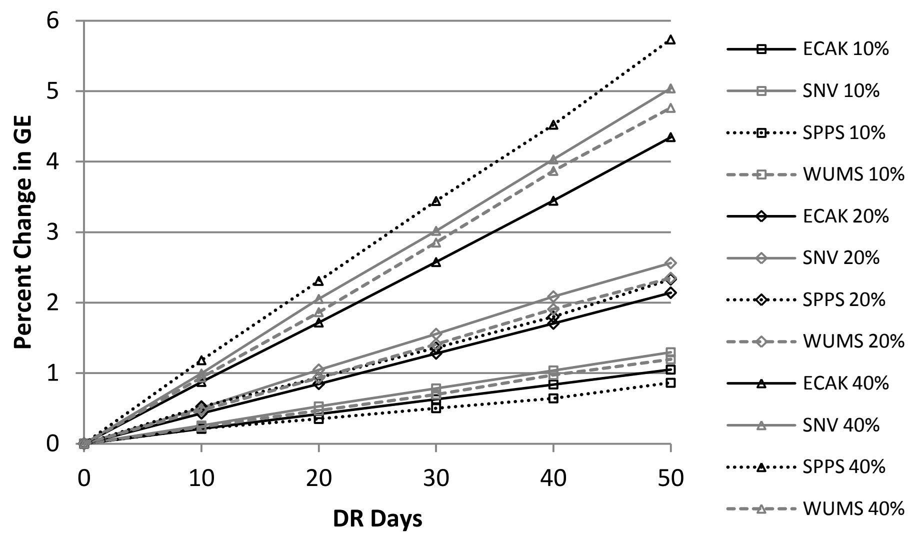

Figure 229: Percent change in the expected Proposed Aggregate Primary-Energy-Source-Utilization Simulation [PAPS] smart appliance scheduling with a stationary battery [SASB] Scenario C generated energy [GE].

The expected PAPS SASB Scenario C GE, shown in Figure 229, quantifies the expected PAPS SASB Scenario C GE as a function of the number of DR days (from zero to 50) for three levels of REMS market penetration. Specifically, the slope [%/DR day] of the 10%, 20%, and 40% REMS market penetration percent change in the expected PAPS SASB Scenario C GE is 0.021, 0.043, and 0.087 for the ECAK power system area respective REMS market penetration level; 0.026, 0.052, and 0.101 for the SNV power system area respective REMS market penetration level; 0.016, 0.045, and 0.114 for the SPPS power system area respective REMS market penetration level; and 0.024, 0.047, and 0.096 for the WUMS power system area respective REMS market penetration level.

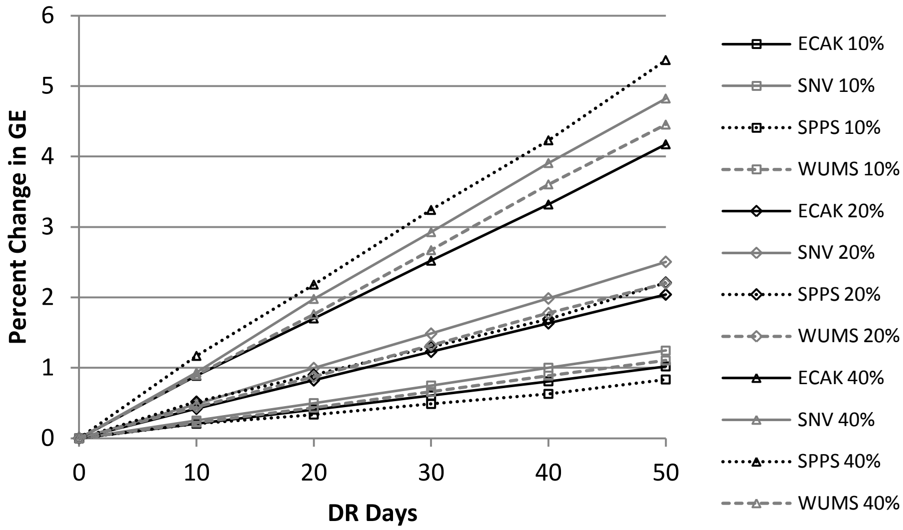

Figure 230: Percent change in the expected Proposed Aggregate Primary-Energy-Source-Utilization Simulation [PAPS] smart appliance scheduling with a stationary battery [SASB] Scenario D generated energy [GE].

The expected PAPS SASB Scenario D GE, shown in Figure 230, quantifies the expected PAPS SASB Scenario D GE as a function of the number of DR days (from zero to 50) for three levels of REMS market penetration. Specifically, the slope [%/DR day] of the 10%, 20%, and 40% REMS market penetration percent change in the expected PAPS SASB Scenario D GE is 0.020, 0.041, and 0.083 for the ECAK power system area respective REMS market penetration level; 0.025, 0.050, and 0.097 for the SNV power system area respective REMS market penetration level; 0.016, 0.043, and 0.106 for the SPPS power system area respective REMS market penetration level; and 0.022, 0.044, and 0.089 for the WUMS power system area respective REMS market penetration level.

The percent change in the expected PPRS SASB Scenario A, Scenario B, Scenario C, and Scenario D generated environmental air pollution (GEAP) is shown in Figure 231, Figure 232, Figure 233, and Figure 234, respectively.

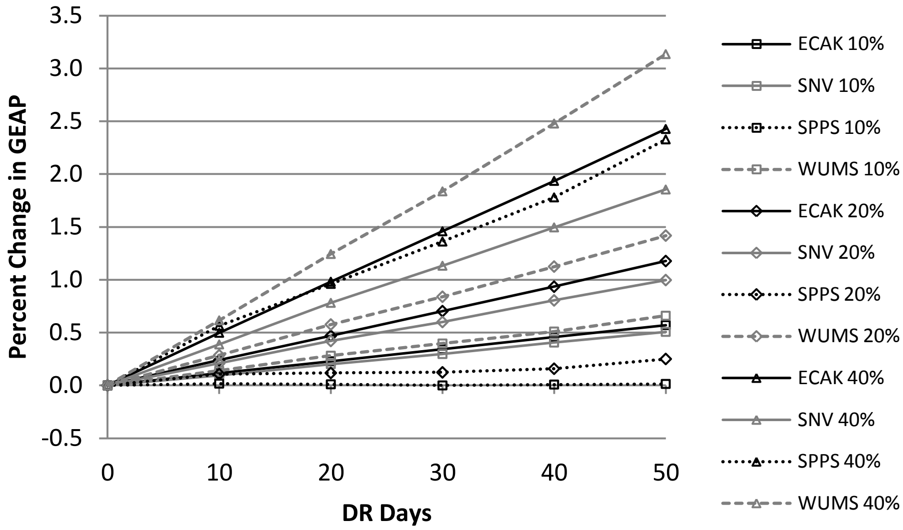

Figure 231: Percent change in the expected Proposed Aggregate Primary-Energy-Source-Utilization Simulation [PAPS] smart appliance scheduling with a stationary battery [SASB] Scenario A generated environmental air pollution [GEAP].

The expected PAPS SASB Scenario A GEAP, shown in Figure 231, quantifies the change in the expected PAPS SASB Scenario A GEAP as a function of the number of DR days (from zero to 50) for three levels of REMS market penetration. Specifically, the slope [%/DR day] of the 10%, 20%, and 40% REMS market penetration percent change in the expected PAPS SASB Scenario A GEAP is 0.011, 0.023, and 0.048 for the ECAK power system area respective REMS market penetration level; 0.010, 0.020, and 0.037 for the SNV power system area respective REMS market penetration level; less than 0.001, 0.004, 0.045 for the SPPS power system area respective REMS market penetration level; and 0.013, 0.028, and 0.062 for the WUMS power system area respective REMS market penetration level.

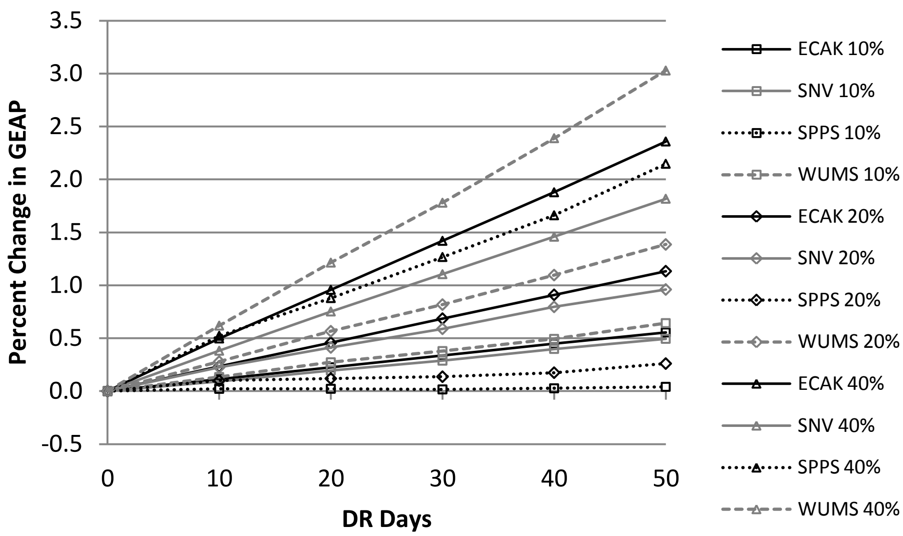

Figure 232: Percent change in the expected Proposed Aggregate Primary-Energy-Source-Utilization Simulation [PAPS] smart appliance scheduling with a stationary battery [SASB] Scenario B generated environmental air pollution [GEAP].

The expected PAPS SASB Scenario B GEAP, shown in Figure 232, quantifies the change in the expected PAPS SASB Scenario B GEAP as a function of the number of DR days (from zero to 50) for three levels of REMS market penetration. Specifically, the slope [%/DR day] of the 10%, 20%, and 40% REMS market penetration percent change in the expected PAPS SASB Scenario B GEAP is 0.011, 0.023, and 0.047 for the ECAK power system area respective REMS market penetration level; 0.010, 0.019, and 0.036 for the SNV power system area respective REMS market penetration level; 0.001, 0.004, 0.042 for the SPPS power system area respective REMS market penetration level; and 0.013, 0.028, and 0.060 for the WUMS power system area respective REMS market penetration level.

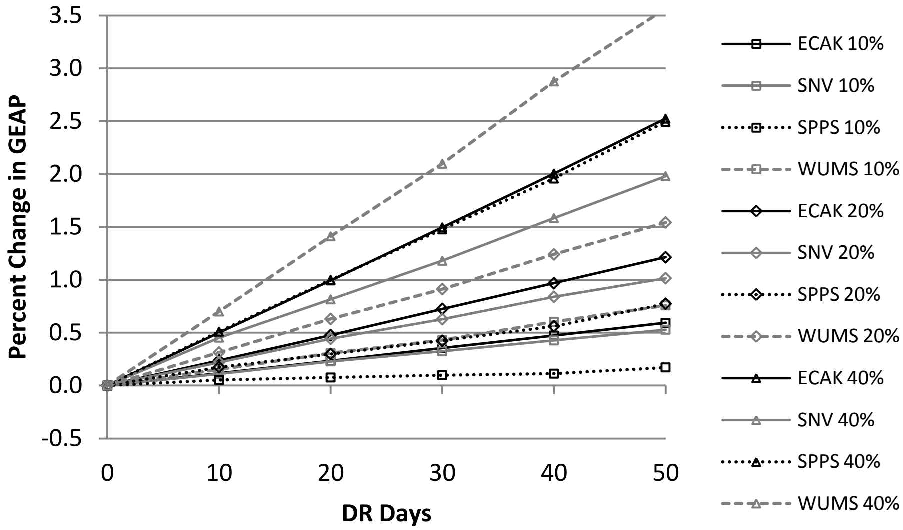

Figure 233: Percent change in the expected Proposed Aggregate Primary-Energy-Source-Utilization Simulation [PAPS] smart appliance scheduling with a stationary battery [SASB] Scenario C generated environmental air pollution [GEAP].

The expected PAPS SASB Scenario C GEAP, shown in Figure 233, quantifies the change in the expected PAPS SASB Scenario C GEAP as a function of the number of DR days (from zero to 50) for three levels of REMS market penetration. Specifically, the slope [%/DR day] of the 10%, 20%, and 40% REMS market penetration percent change in the expected PAPS SASB Scenario C GEAP is 0.012, 0.024, and 0.050 for the ECAK power system area respective REMS market penetration level; 0.011, 0.020, and 0.039 for the SNV power system area respective REMS market penetration level; 0.003, 0.015, 0.049 for the SPPS power system area respective REMS market penetration level; and 0.015, 0.031, and 0.072 for the WUMS power system area respective REMS market penetration level.

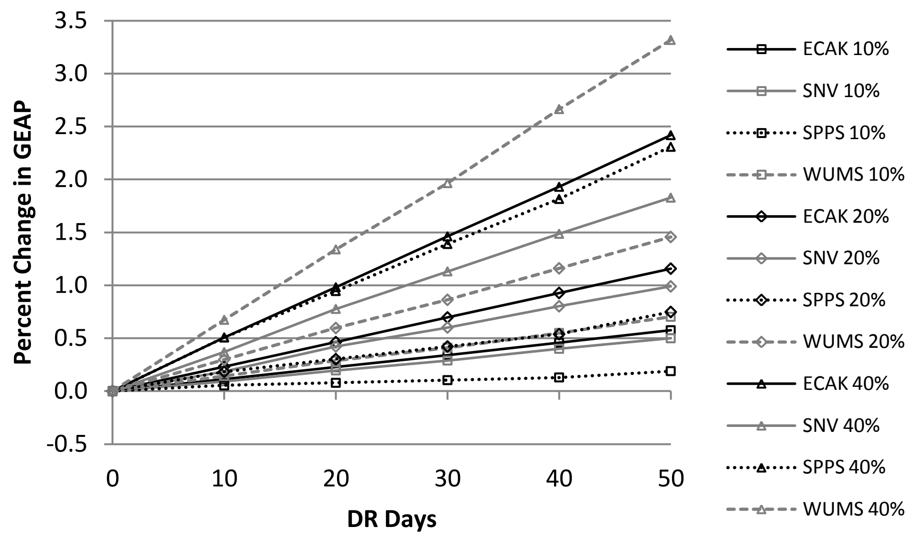

Figure 234: Percent change in the expected Proposed Aggregate Primary-Energy-Source-Utilization Simulation [PAPS] smart appliance scheduling with a stationary battery [SASB] Scenario D generated environmental air pollution [GEAP].

The expected PAPS SASB Scenario D GEAP, shown in Figure 234, quantifies the change in the expected PAPS SASB Scenario D GEAP as a function of the number of DR days (from zero to 50) for three levels of REMS market penetration. Specifically, the slope [%/DR day] of the 10%, 20%, and 40% REMS market penetration percent change in the expected PAPS SASB Scenario D GEAP is 0.011, 0.023, and 0.048 for the ECAK power system area respective REMS market penetration level; 0.010, 0.020, and 0.037 for the SNV power system area respective REMS market penetration level; 0.003, 0.014, 0.045 for the SPPS power system area respective REMS market penetration level; and 0.014, 0.029, and 0.066 for the WUMS power system area respective REMS market penetration level.

The percent change in the expected PPRS SASB Scenario A, Scenario B, Scenario C, and Scenario D loss of load probability (LOLP) is shown in Figure 235, Figure 236, Figure 237, and Figure 238, respectively.

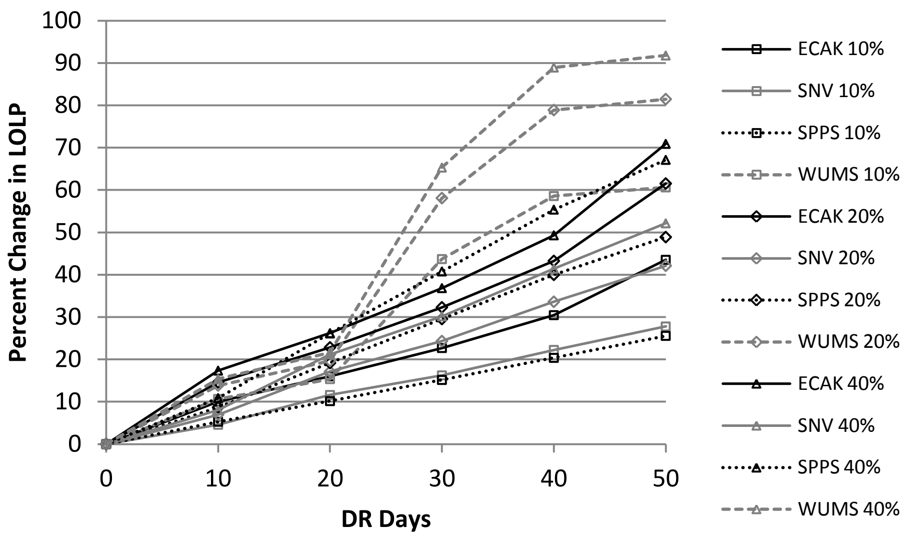

Figure 235: Percent change in the expected Proposed Aggregate Primary-Energy-Source-Utilization Simulation [PAPS] smart appliance scheduling with a stationary battery [SASB] Scenario A loss of load probability [LOLP].

The expected PAPS SASB Scenario A LOLP, shown in Figure 235, quantifies the change in the expected PAPS SASB Scenario A LOLP as a function of the number of DR days (from zero to 50) for three levels of REMS market penetration. Specifically, the slope [%/DR day] of the 10%, 20%, and 40% REMS market penetration percent change in the expected PAPS SASB Scenario A LOLP is 0.816, 1.152, and 1.317 for the ECAK power system area respective REMS market penetration level; 0.561, 0.851, and 1.056 for the SNV power system area respective REMS market penetration level; 0.509, 0.996, and 1.382 for the SPPS power system area respective REMS market penetration level; and 1.358, 1.831, and 2.066 for the WUMS power system area respective REMS market penetration level.

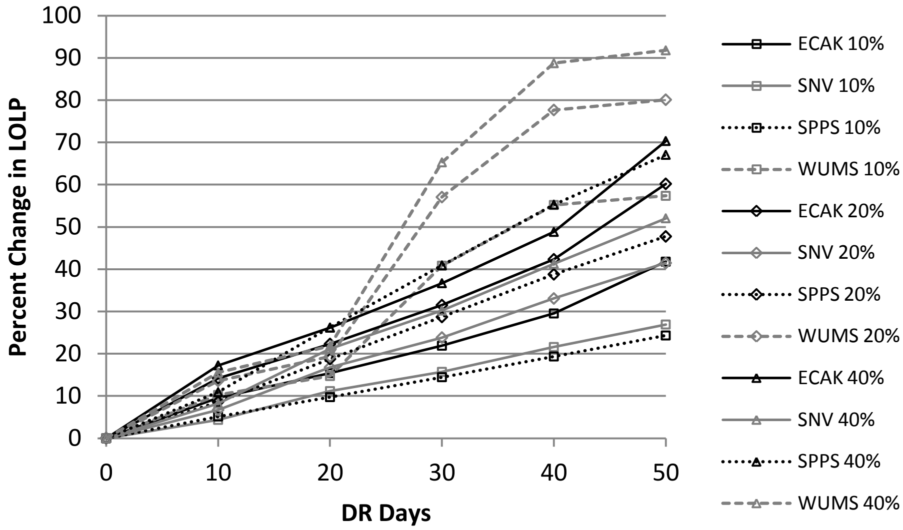

Figure 236: Percent change in the expected Proposed Aggregate Primary-Energy-Source-Utilization Simulation [PAPS] smart appliance scheduling with a stationary battery [SASB] Scenario B loss of load probability [LOLP].

The expected PAPS SASB Scenario B LOLP, shown in Figure 236, quantifies the change in the expected PAPS SASB Scenario B LOLP as a function of the number of DR days (from zero to 50) for three levels of REMS market penetration. Specifically, the slope [%/DR day] of the 10%, 20%, and 40% REMS market penetration percent change in the expected PAPS SASB Scenario B LOLP is 0.786, 1.127, and 1.305 for the ECAK power system area respective REMS market penetration level; 0.545, 0.839, and 1.053 for the SNV power system area respective REMS market penetration level; 0.483, 0.969, and 1.380 for the SPPS power system area respective REMS market penetration level; and 1.279, 1.801, and 2.063 for the WUMS power system area respective REMS market penetration level.

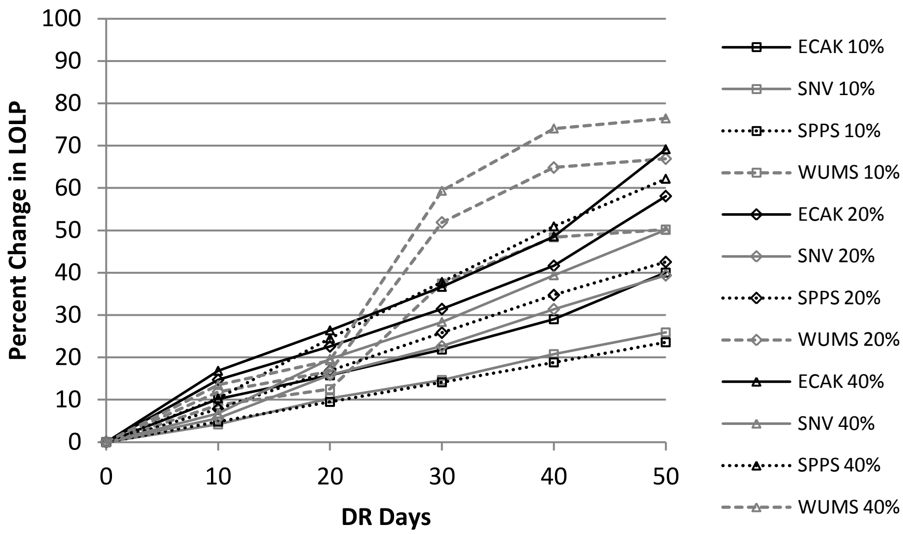

Figure 237: Percent change in the expected Proposed Aggregate Primary-Energy-Source-Utilization Simulation [PAPS] smart appliance scheduling with a stationary battery [SASB] Scenario C loss of load probability [LOLP].

The expected PAPS SASB Scenario C LOLP, shown in Figure 237, quantifies the change in the expected PAPS SASB Scenario C LOLP as a function of the number of DR days (from zero to 50) for three levels of REMS market penetration. Specifically, the slope [%/DR day] of the 10%, 20%, and 40% REMS market penetration percent change in the expected PAPS SASB Scenario C LOLP is 0.750, 1.086, and 1.289 for the ECAK power system area respective REMS market penetration level; 0.525, 0.802, and 1.020 for the SNV power system area respective REMS market penetration level; 0.470, 0.864, and 1.275 for the SPPS power system area respective REMS market penetration level; and 1.128, 1.510, and 1.726 for the WUMS power system area respective REMS market penetration level.

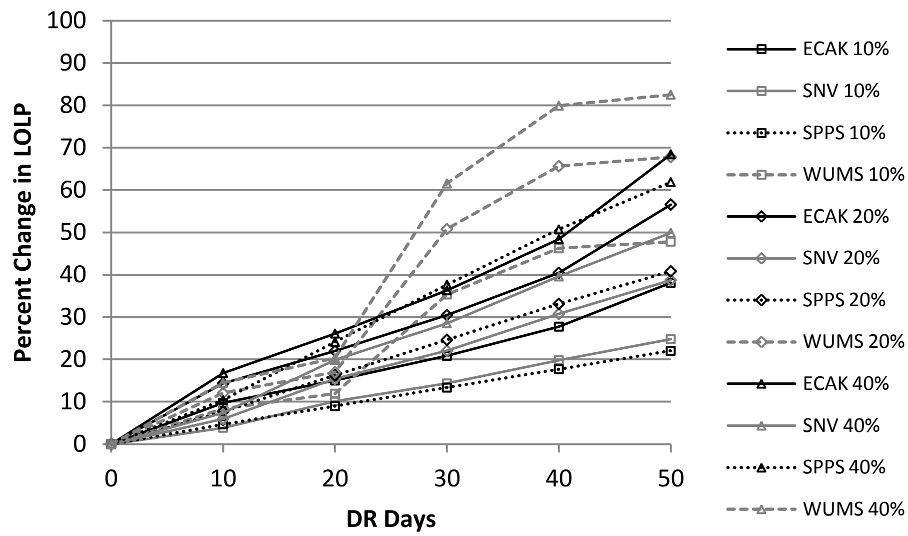

Figure 238: Percent change in the expected Proposed Aggregate Primary-Energy-Source-Utilization Simulation [PAPS] smart appliance scheduling with a stationary battery [SASB] Scenario D loss of load probability [LOLP].

The expected PAPS SASB Scenario D LOLP, shown in Figure 238, quantifies the change in the expected PAPS SASB Scenario D LOLP as a function of the number of DR days (from zero to 50) for three levels of REMS market penetration. Specifically, the slope [%/DR day] of the 10%, 20%, and 40% REMS market penetration percent change in the expected PAPS SASB Scenario D LOLP is 0.715, 1.056, and 1.278 for the ECAK power system area respective REMS market penetration level; 0.503, 0.784, and 1.017 for the SNV power system area respective REMS market penetration level; 0.439, 0.824, and 1.268 for the SPPS power system area respective REMS market penetration level; and 1.074, 1.524, and 1.857 for the WUMS power system area respective REMS market penetration level.

The percent change in the expected PPRS SASB Scenario A, Scenario B, Scenario C, and Scenario D unserviced energy (UE) is shown in Figure 239, Figure 240, Figure 241, and Figure 242, respectively.

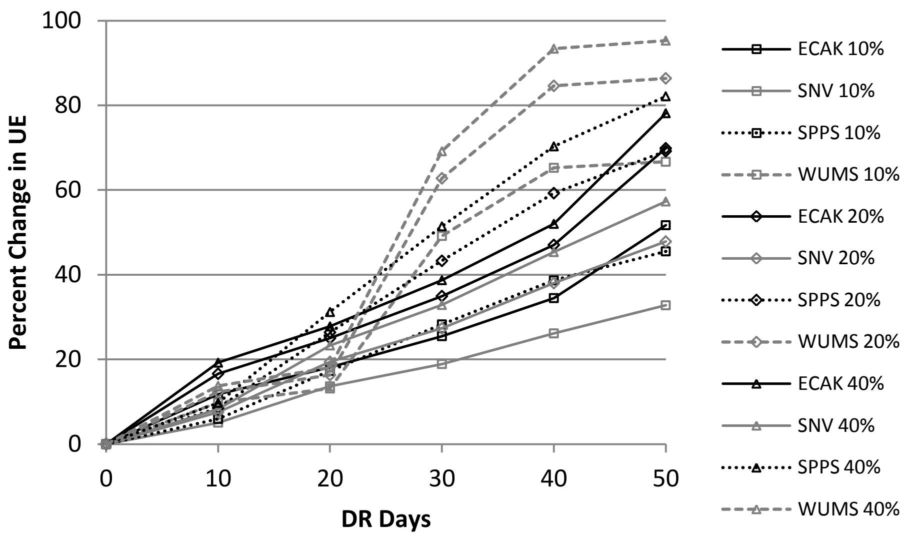

Figure 239: Percent change in the expected Proposed Aggregate Primary-Energy-Source-Utilization Simulation [PAPS] smart appliance scheduling with a stationary battery [SASB] Scenario A unserviced energy [UE].

The expected PAPS SASB Scenario A UE, shown in Figure 239, quantifies the expected PAPS SASB Scenario A UE as a function of the number of DR days (from zero to 50) for three levels of REMS market penetration. Specifically, the slope [%/DR day] of the 10%, 20%, and 40% REMS market penetration percent change in the expected PAPS SASB Scenario A UE is 0.954, 1.287, and 1.428 for the ECAK power system area respective REMS market penetration level; 0.664, 0.967, and 1.164 for the SNV power system area respective REMS market penetration level; 0.962, 1.471, and 1.750 for the SPPS power system area respective REMS market penetration level; and 1.531, 1.986, and 2.190 for the WUMS power system area respective REMS market penetration level.

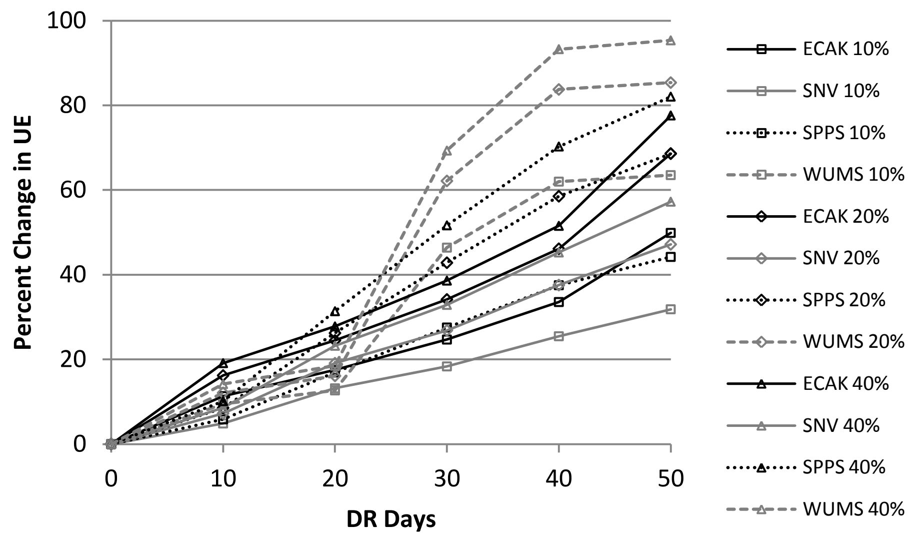

Figure 240: Percent change in the expected Proposed Aggregate Primary-Energy-Source-Utilization Simulation [PAPS] smart appliance scheduling with a stationary battery [SASB] Scenario B unserviced energy [UE].

The expected PAPS SASB Scenario B UE, shown in Figure 240, quantifies the expected PAPS SASB Scenario B UE as a function of the number of DR days (from zero to 50) for three levels of REMS market penetration. Specifically, the slope [%/DR day] of the 10%, 20%, and 40% REMS market penetration percent change in the expected PAPS SASB Scenario B UE is 0.923, 1.264, and 1.417 for the ECAK power system area respective REMS market penetration level; 0.646, 0.956, and 1.160 for the SNV power system area respective REMS market penetration level; 0.933, 1.456, and 1.746 for the SPPS power system area respective REMS market penetration level; and 1.454, 1.965, and 2.185 for the WUMS power system area respective REMS market penetration level.

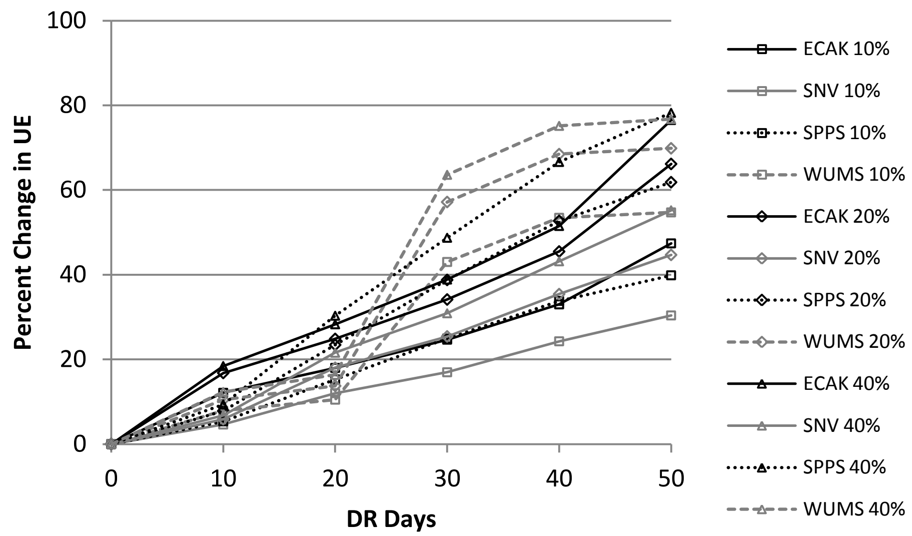

Figure 241: Percent change in the expected Proposed Aggregate Primary-Energy-Source-Utilization Simulation [PAPS] smart appliance scheduling with a stationary battery [SASB] Scenario C unserviced energy [UE].

The expected PAPS SASB Scenario C UE, shown in Figure 241, quantifies the expected PAPS SASB Scenario C UE as a function of the number of DR days (from zero to 50) for three levels of REMS market penetration. Specifically, the slope [%/DR day] of the 10%, 20%, and 40% REMS market penetration percent change in the expected PAPS SASB Scenario C UE is 0.875, 1.218, and 1.407 for the ECAK power system area respective REMS market penetration level; 0.617, 0.913, and 1.127 for the SNV power system area respective REMS market penetration level; 0.841, 1.312, and 1.661 for the SPPS power system area respective REMS market penetration level; and 1.256, 1.619, and 1.770 for the WUMS power system area respective REMS market penetration level.

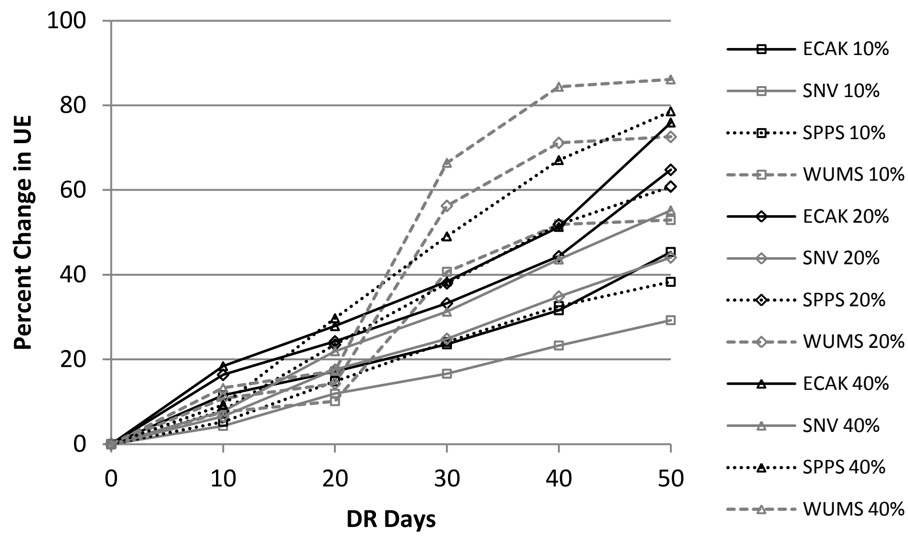

Figure 242: Percent change in the expected Proposed Aggregate Primary-Energy-Source-Utilization Simulation [PAPS] smart appliance scheduling with a stationary battery [SASB] Scenario D unserviced energy [UE].

The expected PAPS SASB Scenario D UE, shown in Figure 242, quantifies the expected PAPS SASB Scenario D UE as a function of the number of DR days (from zero to 50) for three levels of REMS market penetration. Specifically, the slope [%/DR day] of the 10%, 20%, and 40% REMS market penetration percent change in the expected PAPS SASB Scenario D UE is 0.838, 1.191, and 1.397 for the ECAK power system area respective REMS market penetration level; 0.594, 0.893, and 1.122 for the SNV power system area respective REMS market penetration level; 0.808, 1.287, and 1.674 for the SPPS power system area respective REMS market penetration level; and 1.222, 1.673, and 1.980 for the WUMS power system area respective REMS market penetration level.

The percent change in the expected PPRS SASB Scenario A, Scenario B, Scenario C, and Scenario D average energy cost (AEC) is shown in Figure 243, Figure 244, Figure 245, and Figure 246, respectively.

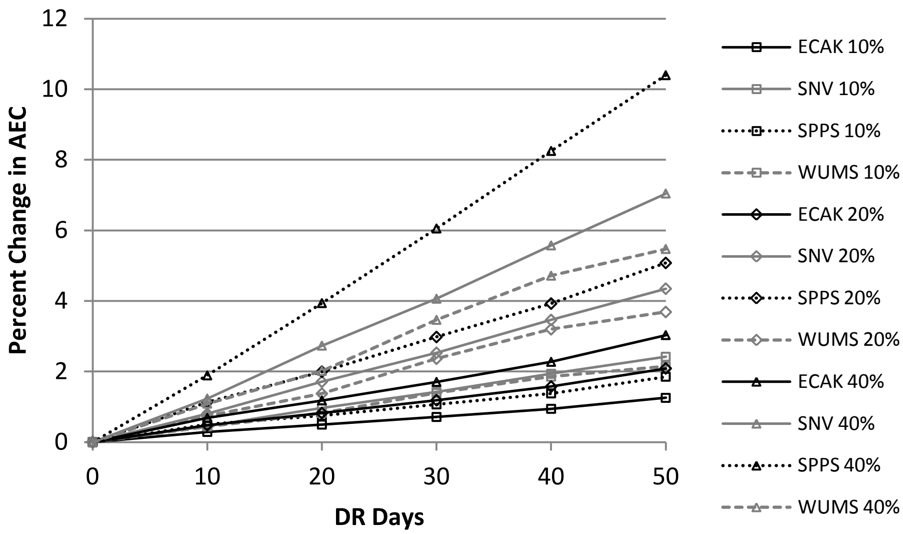

Figure 243: Percent change in the expected Proposed Aggregate Primary-Energy-Source-Utilization Simulation [PAPS] smart appliance scheduling with a stationary battery [SASB] Scenario A average electricity cost [AEC].

The expected PAPS SASB Scenario A AEC, shown in Figure 243, quantifies the change in the expected PAPS SASB Scenario A AEC as a function of the number of DR days (from zero to 50) for three levels of REMS market penetration. Specifically, the slope [%/DR day] of the 10%, 20%, and 40% REMS market penetration percent change in the expected PAPS SASB Scenario A AEC is 0.024, 0.040, and 0.058 for the ECAK power system area respective REMS market penetration level; 0.049, 0.087, and 0.142 for the SNV power system area respective REMS market penetration level; 0.035, 0.099, and 0.209 for the SPPS power system area respective REMS market penetration level; and 0.044, 0.077, and 0.113 for the WUMS power system area respective REMS market penetration level.

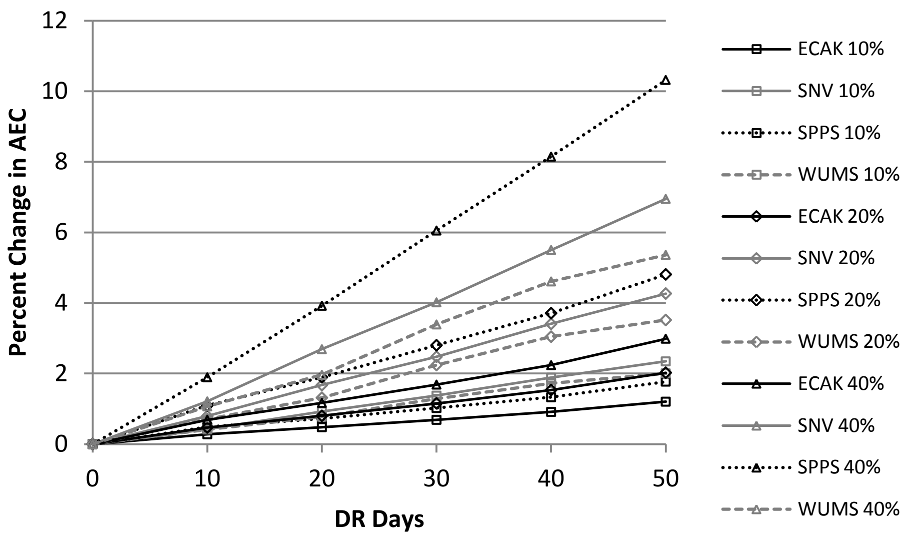

Figure 244: Percent change in the expected Proposed Aggregate Primary-Energy-Source-Utilization Simulation [PAPS] smart appliance scheduling with a stationary battery [SASB] Scenario B average electricity cost [AEC].

The expected PAPS SASB Scenario B AEC, shown in Figure 244, quantifies the change in the expected PAPS SASB Scenario B AEC as a function of the number of DR days (from zero to 50) for three levels of REMS market penetration. Specifically, the slope [%/DR day] of the 10%, 20%, and 40% REMS market penetration percent change in the expected PAPS SASB Scenario B AEC is 0.023, 0.039, and 0.057 for the ECAK power system area respective REMS market penetration level; 0.047, 0.086, and 0.140 for the SNV power system area respective REMS market penetration level; 0.033, 0.094, and 0.207 for the SPPS power system area respective REMS market penetration level; and 0.041, 0.073, and 0.111 for the WUMS power system area respective REMS market penetration level.

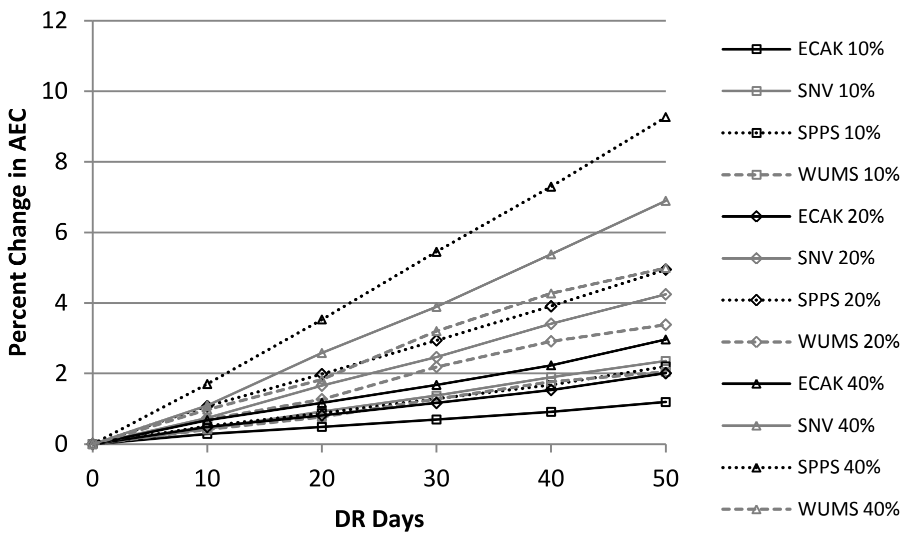

Figure 245: Percent change in the expected Proposed Aggregate Primary-Energy-Source-Utilization Simulation [PAPS] smart appliance scheduling with a stationary battery [SASB] Scenario C average electricity cost [AEC].

The expected PAPS SASB Scenario C AEC, shown in Figure 245, quantifies the change in the expected PAPS SASB Scenario C AEC as a function of the number of DR days (from zero to 50) for three levels of REMS market penetration. Specifically, the slope [%/DR day] of the 10%, 20%, and 40% REMS market penetration percent change in the expected PAPS SASB Scenario C AEC is 0.023, 0.039, and 0.057 for the ECAK power system area respective REMS market penetration level; 0.047, 0.086, and 0.139 for the SNV power system area respective REMS market penetration level; 0.043, 0.098, and 0.186 for the SPPS power system area respective REMS market penetration level; and 0.042, 0.073, and 0.103 for the WUMS power system area respective REMS market penetration level.

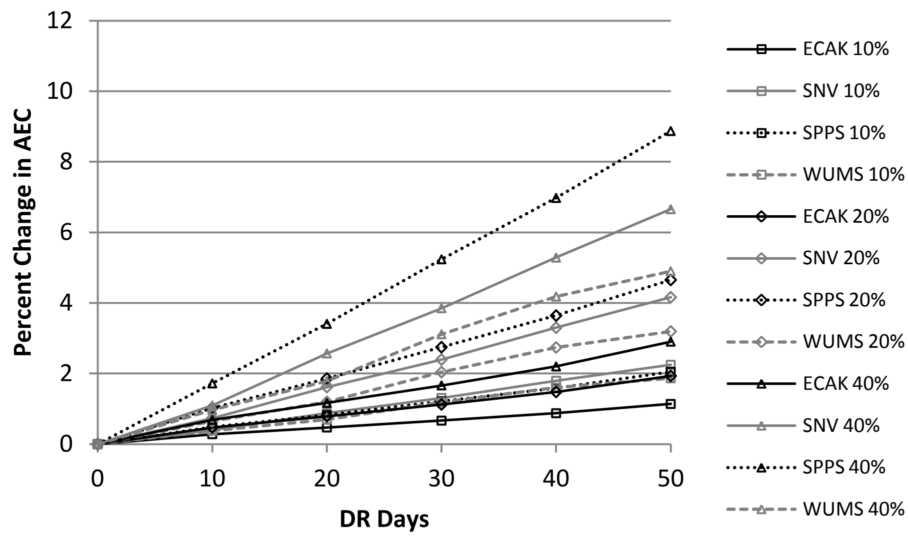

Figure 246: Percent change in the expected Proposed Aggregate Primary-Energy-Source-Utilization Simulation [PAPS] smart appliance scheduling with a stationary battery [SASB] Scenario D average electricity cost [AEC].

The expected PAPS SASB Scenario D AEC, shown in Figure 246, quantifies the change in the expected PAPS SASB Scenario D AEC as a function of the number of DR days (from zero to 50) for three levels of REMS market penetration. Specifically, the slope [%/DR day] of the 10%, 20%, and 40% REMS market penetration percent change in the expected PAPS SASB Scenario D AEC is 0.022, 0.037, and 0.056 for the ECAK power system area respective REMS market penetration level; 0.045, 0.084, and 0.135 for the SNV power system area respective REMS market penetration level; 0.040, 0.091, and 0.177 for the SPPS power system area respective REMS market penetration level; and 0.038, 0.066, and 0.101 for the WUMS power system area respective REMS market penetration level.

This chapter has described the PAPS results. First, the PAPS BC results were presented. Second, the PAPS water heater direct load control (DLC) results were presented. Third, the PAPS heating, ventilation, and air conditioning DLC results were presented. Fourth, the PAPS smart thermostat results were presented. Fifth, the PAPS

SAS results were presented. Sixth, the PAPS SASB results were presented. Next is a summary of the, key findings from the PAPS results.

6.7 Summary

To quantify the impact of residential energy management technology on primary energy source utilization (PESU) a probabilistic economic dispatch algorithm (Probabilistic Production Costing - PPC [114]) was used. This economic dispatch algorithm computes the PESU based on the changes in electric load with and without the energy management functions computed in the proposed physically-based residential energy management system (REMS) simulation.

The PESU results were computed for each residential energy management function: water heater (WH) direct load control (DLC); heating ventilating, and air conditioning (HVAC) DLC; smart thermostat (ST); smart appliance scheduling (SAS); and smart appliance scheduling with a stationary battery (SASB). The PESU results consist of generated energy (GE), generated environmental air pollution (GEAP - which is the summation of generated carbon dioxide, mercury, nitrogen oxide, and sulfur dioxide), loss of load probability (LOLP), unserviced energy (UE), and average electricity cost (AEC). The PESU results were computed for each power system are Versailles Kentucky (ECAK), Mercury Nevada (SNV), Stillwater Oklahoma (SPPS), and Necedah Wisconsin (WUMS). Specifically, the expected value of each PESU result is computed in the PPC algorithm. These results provide quantified results from which electric utility planning decisions can be compared. The ability to compare multiple planning options on an equal basis will guide electric utility technology investment strategies.

To summarize the large amount of data presented in this chapter each expected PESU result is combined to provide a cumulative PESU slope for each energy management function and each power system area. First, the percent change of the expected PESU result, as a function of the demand response (DR) days, is linearized. Second, the derivative of the linearized PESU result is computed. Taking the derivative reduces the dimension of the expected PESU results, eliminating the number of DR days variable. The slope of each linear function is multiplied by the residual squared error of each linear approximation to account for the quality of each linear approximation. Finally, the scaled slope result is summed over each result, resulting in a cumulative PESU slope.

The cumulative PESU slope indicates which power system area is most affected by the distributed energy resource scenarios and energy management functions. The cumulative PESU slope indicates which distributed energy resource scenario and location causes the most significant change in the combined PESU results as the number of DR days increase. Thus, a low cumulative PESU slope indicates a not as significant change in cumulative PESU results as more DR days are added than a relatively higher cumulative PESU slope. First, the summation of the cumulative PESU slope over all the power system areas is described. Second, the individual power system area cumulative PESU slope is described. The cumulative PESU slope is shown for each distributed energy resource scenario and each energy management function.

The figures in this section include bar charts with negative and positive error bars. The bars in each figure are the 20% market penetration cumulative PESU slope. The negative error bars in each figure are the 10% market penetration cumulative PESU slope. And, the positive error bars in each figure are the 40% market penetration cumulative PESU slope.

The summation of the cumulative PESU slope over all the power system areas is shown in Figure 247.

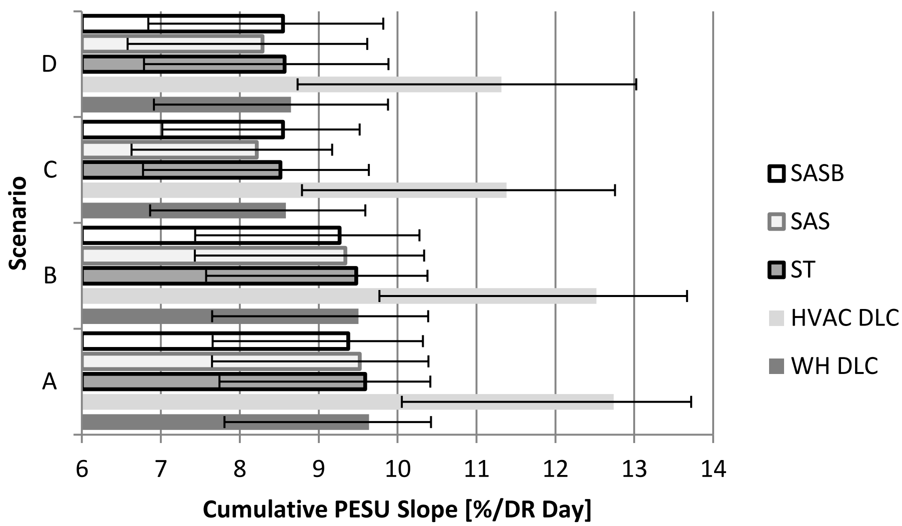

Figure 247: Cumulative primary energy source utilization [PESU] slope for all power system areas.

The summation of the cumulative PESU slope for all power system areas is shown in Figure 247. These results indicate the HVAC DLC energy management function has the largest cumulative PESU slope in each distributed energy resource scenario. Specifically, on average the HVAC DLC energy management function causes the largest reduction in GE, GEAP, LOLP, UE, and AEC. This result holds for each location and for all considered combinations of distributed energy resources.

Further, the improvement in cumulative PESU slope increases faster between the 10% and 20% market penetration than between the 20% and 40% market penetration. This general shape of improved system performance is expected. The increase in reduction in PESU results will level out as the market penetration increases.

The ECAK power system area cumulative PESU slope is shown in Figure 248.

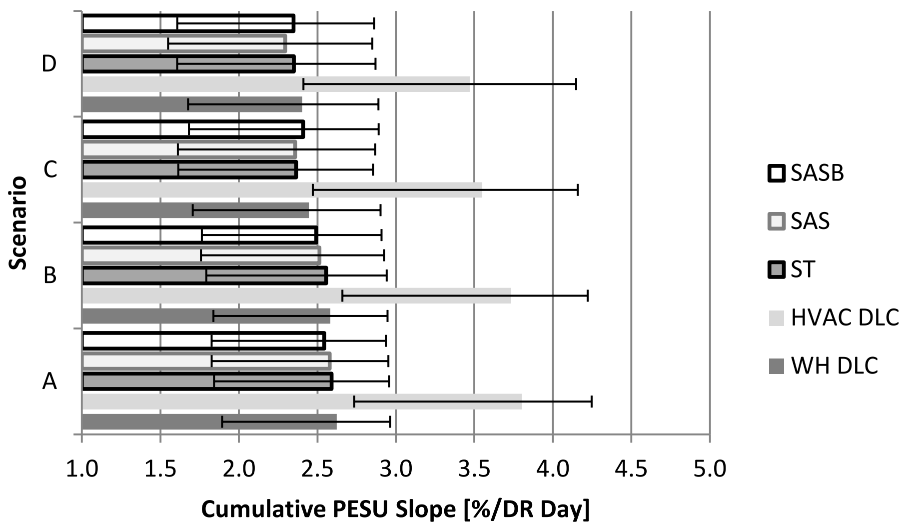

Figure 248: Cumulative primary energy source utilization [PESU] slope for the Versailles Kentucky [ECAK] power system area.

The cumulative PESU slope for the ECAK power system area is shown in Figure 248. The same trends in the ECAK power system area cumulative PESU slope results are shown in Figure 248 as in the summation of the cumulative PESU slope over all the power system areas in Figure 247.

The SNV power system area cumulative PESU slope is shown in Figure 249.

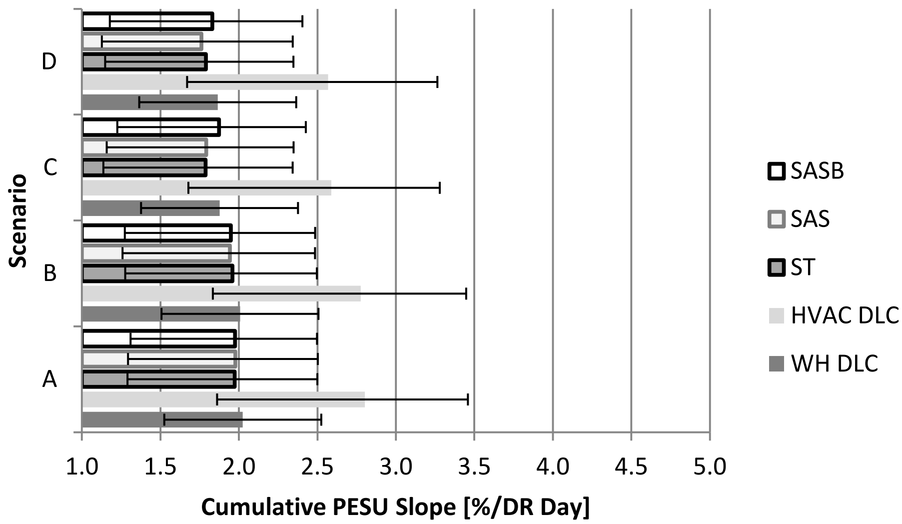

Figure 249: Cumulative primary energy source utilization [PESU] slope for the Mercury Nevada [SNV] power system area.

The cumulative PESU slope for the SNV power system area is shown in Figure 249. Similar trends in the SNV power system area cumulative PESU slope results are shown in Figure 249 as in the summation of the cumulative PESU slope over all the power system areas in Figure 247. The same energy management function provides the most improved system performance. However, the magnitude of the superiority is smaller in the SNV power system area. This results is surprising because the SNV power system area had the highest ambient temperature than the other power system areas. The smaller sensitivity may be caused by the small size of the SNV power system area.

The SPPS power system area cumulative PESU slope is shown in Figure 250.

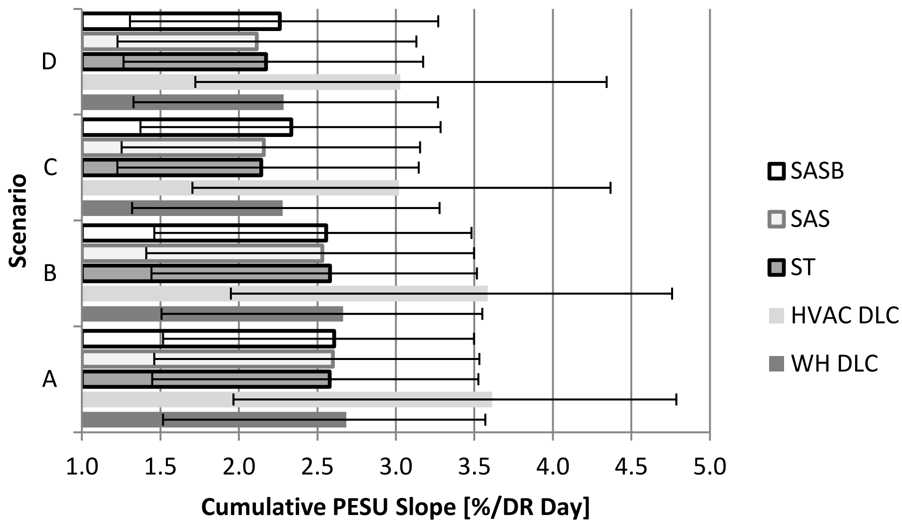

Figure 250: Cumulative primary energy source utilization [PESU] slope for the Stillwater Oklahoma [SPPS] power system area.

The cumulative PESU slope for the SPPS power system area is shown in Figure 250. Similar trends in the SPPS power system area cumulative PESU slope results are shown in Figure 250 as in the summation of the cumulative PESU slope over all the power system areas in Figure 247. The same energy management function provides the most improved system performance. However, the magnitude of superiority is smaller in the SPPS power system area. Further, the increase between the 10% and 20% market penetration cumulative PESU slope is approximately the same as between the 20% and 40% market penetration cumulative PESU slope. This suggest a larger market penetration of residences in the SPPS power system area than the other power system areas would provide the optimal market penetration level.

The WUMS power system area cumulative PESU slope is shown in Figure 251.

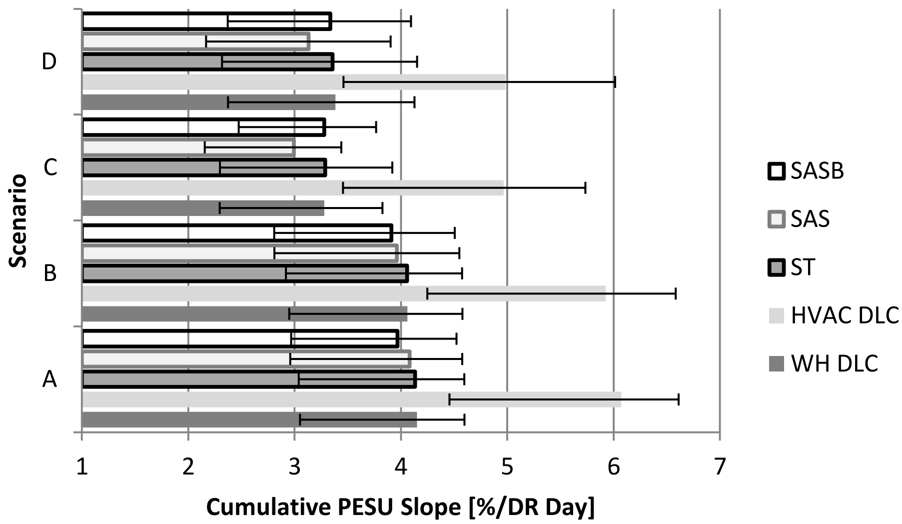

Figure 251: Cumulative primary energy source utilization [PESU] slope for the Necedah Wisconsin [WUMS] power system area.

The cumulative PESU slope for the WUMS power system area is shown in Figure 251. The same trends in the ECAK power system area cumulative PESU slope results are shown in Figure 251 as in the summation of the cumulative PESU slope over all the power system areas in Figure 247.

This chapter described the PAPS simulation results. Next is a summary of the conclusions made in this dissertation.

7 CONCLUSIONS

The potential impact of smart grid technology includes cleaner, cheaper, and more reliable electricity generation. There exists the opportunity for residential electric load to provide some portion of the benefits from smart grid technology. Demand-side management through price responsive load or demand response has the potential to provide significant system level benefits via increased controllability of residential electric load. However, the impact of random events (e.g. loss of a generator) can greatly change the magnitude of the potential benefits. To achieve the increased controllability of residential load requires investment in additional infrastructure. There will be a tradeoff between the amount of added infrastructure and the amount of benefits from smart grid technology.

This dissertation compares the performance of direct load control (DLC), a traditional form of energy management, with the performance of smart grid enabled energy management functions. The various energy management functions are compared by their ability to provide automated demand response (DR).

First, simulations of five energy management functions were used to test various levels of a residential energy management system (REMS). Second, the results from these simulations were used in a primary energy source utilization (PESU) analysis. The PESU uses a production costing economic dispatch algorithm to compute the primary fuels used to satisfy electric load given power system generating constraints.

Two levels of system simulation provide quantified performance of residential energy management functions from both the residence owner and electric utility perspectives. The first level of system simulation was the Proposed Physically-Based

REMS Simulation (PPRS). The second level of system simulation was the Proposed Aggregate PESU Simulation (PAPS). The proposed system simulations provided a test bed for energy management functions, quantifying the effects of the changes in electric load using PESU. Further, the use of photovoltaic (PV) and plug-in electric vehicle (PEV) distributed energy resources were considered in conjunction with the residential energy management functions.

The traditional energy management functions were two forms of DLC. Both water heater (WH) and heating, ventilation, and air conditioning (HVAC) DLC were considered. The DLC energy management functions consisted of the direct electric utility control of a specific appliance (e.g. WH and HVAC). The smart grid enabled energy management functions were smart thermostat (ST), smart appliance scheduling (SAS), and smart appliance scheduling with a stationary battery (SASB). The ST energy management function adjusts the temperature set point of the HVAC system during DR. The SAS energy management function delays the use of residential smart appliances (clothes dryer, clothes washer, dishwasher, HVAC, refrigerator, and WH) during DR. The SASB energy management function adds a stationary battery dispatching function to the SAS energy management function. The stationary battery adds an additional level of flexibility to reduce the residential electric load during DR.

The PPRS peak power and DR energy (energy use during the DR period) were calculated for each power system area and for two extreme weather seasons: winter and summer. These days were selected to highlight the performance of the PPRS in the coldest and hottest ambient temperatures for each area. The performance of each energy management function was compared to the PPRS base case (BC) where no controlled modification of the residential appliances occurred. Similarly, the performance of each distributed energy resource was compared to the PPRS with no distributed energy resource scenario.

The impact of the energy management functions was computed in terms of the peak power. The average winter PPRS WH DLC peak power provided the most significant savings of 1.6% (0.1 kW) across all the power system areas compared to the average winter PPRS BC peak power. The average summer PPRS SASB peak power provided the most significant savings of 0.7% (0.1 kW) across all the power system areas compared to the average summer PPRS BC peak power.

The impact of the distributed energy resources was computed in terms of the peak power. In the average winter and summer PPRS peak power for all energy management functions, the PEV caused an increase of 7.6% (0.7 kW) and 5.9% (0.7 kW) compared to the average winter and summer PPRS with no distributed energy resource scenario peak power. In the average winter and summer PPRS peak power for all energy management functions, the PV caused a decrease of 2.5% (0.2 kW) and 4.8% (0.5 kW) compared to the average winter and summer PPRS with no distributed energy resource scenario peak power. In the average winter and summer PPRS peak power for all energy management functions, the combination of PEV and PV caused an increase of 5.1% (0.4 kW) and 2.0% (0.2 kW) compared to the average winter and summer PPRS with no distributed energy resource scenario peak power.

The impact of the energy management functions was computed in terms of the DR energy. The DR energy is the PPRS energy during the DR period, from 4p to 7p. The average winter PPRS SASB DR energy provided the most significant savings of

94.8% (6.3 kWh) across all the power system areas compared to the average winter PPRS BC DR energy. The average summer PPRS SASB DR energy for all power system areas provided the most significant savings of 70.6% (7.5 kWh) across all the power system areas compared to the average summer PPRS BC DR energy.

The impact of the distributed energy resources was computed in terms of the DR energy. In the average winter and summer PPRS DR energy for all energy management functions, the PEV caused an increase of 24.8% (1.4 kWh) and 16.0% (1.4 kWh) compared to the average winter and summer PPRS with no distributed energy resource scenario DR energy. In the average winter and summer PPRS DR energy for all energy management functions, the PV caused a decrease of 14.9% (0.5 kWh) and 34.9% (2.6 kWh) compared to the average winter and summer PPRS with no distributed energy resource scenario DR energy. In the average winter and summer PPRS Scenario DR energy for all energy management functions, the combination of PEV and PV caused an increase of 10.5% (0.9 kWh) and decrease of 18.7% (1.2 kW) compared to the average winter and summer PPRS with no distributed energy resource scenario DR energy.

The PAPS provided an electric utility centric point of view of residential energy management technology. To quantify the impact of residential energy management in a power system point of view, a probabilistic economic dispatch algorithm was used. This economic dispatch algorithm computed the PESU using an algorithm where the availability of each generator and the electric load were considered random variables. The PAPS results summarized for each energy management function included the expected generated energy (GE), the generated environmental air pollution (GEAP), power system reliability indices (loss of load probability [LOLP] and unserviced energy [UE]), and average electricity cost (AEC).

To summarize the large amount of PAPS data, each expected PESU result was combined to provide a cumulative PESU slope for each energy management function and each power system area. First, the percent change of the expected PESU result, as a function of the DR days, was linearized. Second, the derivative of the linearized PESU result was computed. Taking the derivative reduced the dimension of the expected PESU results, eliminating the number of DR days variable. The slope of each linear function was multiplied by the residual squared error of each linear approximation to account for the quality of each linear approximation. Finally, the scaled slope result was summed over each result, ending in a cumulative PESU slope.

The cumulative PESU slope indicates which distributed energy resource scenario and location causes the most significant decrease in the combined PESU results as the number of DR days increase. Thus, a low cumulative PESU slope indicates not as significant a change in cumulative PESU results as more DR days are added than a relatively higher cumulative PESU slope.

The PAPS cumulative PESU slope indicated the HVAC DLC energy management function had the largest cumulative PESU slope in each power system area and distributed energy resource scenario. Specifically, on average the HVAC DLC energy management function that caused the largest reduction in GE, GEAP, LOLP, UE, and AEC. This result holds for each location and for all combinations of distributed energy resources.

The quantified impact of multiple residential energy management functions have been compared with various levels of distributed energy resources for four areas of the United States. The potential benefits of 10% market penetration of the HVAC DLC results in cleaner (CO_2 production reduced from $4.0262 \cdot 10^{10}$ kg to $4.0139 \cdot 10^{10}$ kg), cheaper (AEC reduced from 1,275 $/MWh to 1,253 $/MWh), and more reliable (LOLP reduced from 4.24% to 3.06%) electricity generation. The potential benefits of increased levels of market penetration increase significantly up to a point then the potential benefits level off. The point of inflection of the potential benefits depends on the power system considered. Additional research is needed to determine the optimal combination of distributed energy resources, energy storage, and energy management functions for different locations and climate regions. The work in this dissertation has established a framework to quantify the impacts of automated residential energy management technology using primary energy source utilization.

The remainder of this chapter includes published contributions, lessons learned, and future work. The contributions describes the published work. The lessons learned are thoughts for further work in this research area The future work includes specifics for future investigations.

7.1 Original Contributions

This dissertation describes three original contributions: (1) the development of a discrete-event simulation of the energy use in a residential premises, (2) the side by side analysis of multiple energy management functions, and (3) the investigation of residential energy storage in conjunction with energy management functions, distributed energy resources for multiple regions of the U.S. for the residence owner and utility provider.

These original contributions are the culmination of six related publications:

Conference Papers

- Curtis Roe, Dr. Sunil Chhaya, and Dr. Robert Entriken, "Comparison of HVAC Direct Load Control and Smart Thermostat Energy Management Performance," Center for Research in Regulated Industries - Annual Western Conference, 2012.
- Curtis Roe, Dr. Jerome Meisel, Dr. A.P. Meliopoulos, Farantatos Evangelos, and Dr. Thomas Overbye, "Power System Level Impacts of PHEVs," 42nd Hawaii International Conference on System Sciences (HICSS), 2009.

Conference Papers with Presentations

- Curtis Roe, Dr. Sunil Chhaya, and Dr. Robert Entriken, "Premises Energy Management Simulation Platform," Center for Research in Regulated Industries - Annual Western Conference, 2011.
- Curtis Roe, Dr. Sakis Meliopoulos, Dr. Robert Entriken, and Dr. Sunil Chhaya, "Simulated Demand Response of a Residential Energy Management System," IEEE Energy Tech Conference, 2011.Curtis Roe, Dr. A.P. Meliopoulos, Dr. Jerome Meisel, and Dr. Thomas Overbye, "Power System Level Impacts of Plug-In Hybrid Electric Vehicles Using Simulation Data," IEEE Conference on Global Sustainable Energy Infrastructure (Energy 2030), 2008.

Technical Reports

- Premises Energy Management: A Matlab Platform for Discrete Event Simulation. EPRI, Palo Alto, CA: 2011. 1022642.
- Dr. Sakis Meliopoulos, Dr. Jerome Meisel, and Dr. Tom Overbye "Power System Level Impacts of Plug-In Hybrid Vehicles," Power System Engineering Research Center (PSERC), PSERC Document 09-12, 2009.

7.2 Lessons Learned

Three lessons learned are provided in this section. The lessons learned provide suggestions that may be helpful to students studying related material or students using simulation analysis. The four lessons include: parallelizing simulation code, adding simulation iterations, and considering initial conditions.

The Proposed Physically-Based Residential-Energy-Management-System Simulation (PPRS) and the Proposed Aggregate Primary-Energy-Source-Utilization

Simulation (PAPS) are structured so that the execution of the simulations could be easily parallelized. No information is shared between the repeated PPRS iterations. This is also similar, with the different PAPS locations. Thus, each iteration and location could be performed independently. Specifically, little reworking of the code used in this dissertation would be needed to use the Mathworks Parallel Computing Toolbox™ to improve the execution time of these simulations using parallel simulation techniques.

Additional simulation iterations could have facilitated additional statistical analysis. The output analysis of the PPRS included descriptive statistics only. Significant additional work could be provided using inference statistics. In future research, this next step could be facilitated by structuring the simulation code so additional iterations could be performed adding to the sample data already generated. Initial hypothesis testing, testing the null hypothesis of normal daily energy had no conclusion. It is the author's conjecture that additional simulation iterations would have provided conclusive hypothesis testing.

Finally, the initial conditions of the simulation should be addressed. The PPRS assumed all smart appliances were off at the start of each simulation. This is a limiting assumption of the existing research.

7.3 Future Work

The Proposed Physically-Based Residential-Energy-Management-System Simulation (PPRS) and the Proposed Aggregate Primary-Energy-Source-Utilization Simulation (PAPS) have been applied in the current research. Additional considerations that are a direct follow up to this could include analysis of time-of-use electricity rate structures, optimal heating, ventilation, and air conditioning (HVAC) direct load control (DLC) scheduling, and optimized battery dispatching.

The economics of time-of-use electricity rate structures will make economic analysis of residential energy management technology possible. This is an additional dimension left out of the current research. Near term public policy decisions could be aided through additional economic analysis using the probabilistic modeling developed throughout this dissertation.

In the HVAC DLC, the HVAC is rescheduled so that within every half-hour during the demand response (DR) period the HVAC is not allowed to run for n_{off} minutes (e.g. 15 minutes). Within each half-hour increment in the DR period the specific n_{off} minutes are selected randomly to minimize the impact of synchronized payback. An investigation of the optimal off period and DR length could lead to improved system performance.

Finally, the utilization of energy storage is a technology that holds much promise. The specific use case and development of viable technology is still work in progress. The current research showed that the heuristic scheduling provided little benefit of storage to the residence owner and even less benefits to the electric utility. Thus, more intelligent energy storage dispatching could be investigated.

APPENDIX A POWER SYSTEM DATA DERIVATION

The U.S. Environmental Protection Agency developed the Integrated Planning Model (IPM) [117]. Based on the IPM input and output files, the input for the Probabilistic Production Costing (PPC) algorithm was derived. This appendix describes the derivation methodology. The PPC input data is introduced in Chapter 5 and tabulated in Appendix B. First the input data in the IPM input and output files used is defined. Second the derived values are defined.

Input data from the IPM input and output files 'Base Case 2006.RPE' and 'Base Case 2006.TAC' was used to derive the PPC input. Data used from the 'Base Case 2006.RPE' file was capacity $C(g)$ [MW], generated energy $G(g)$ [GWh], fuel input energy $F(g)$ [TBtu], carbon dioxide (CO_2) generated $E_C(g)$ [MMtons], mercury (MER) generated $E_M(g)$ [tons], nitrogen oxide (NO_x) generated $E_N(g)$ [Mtons], sulfur dioxide (SO_2) generated $E_S(g)$ [MTons], and fuel cost $\kappa(g)$ [Mill/kWh]. Each of the input data is defined for generator g. Notice, only generators with capacity above 7.5 MW were used. The input data is summarized in Table 38.

Table 38: Integrated Planning Model [IPM] input and output files data used to derive the Probabilistic Production Costing (PPC) algorithm input.

Value	Symbol	Units
Capacity	$C(g)$	MW
Generated Energy	$G(g)$	GWh
Fuel Input Energy	$F(g)$	TBtu
CO_2 Generated	$E_C(g)$	MMtons
MER Generated	$E_M(g)$	tons
NO_x Generated	$E_N(g)$	Mtons
SO_2 Generated	$E_S(g)$	Mtons
Fuel Cost	$\kappa(g)$	Mill/kWh

The units in Table 38 and conversion factors are defined next. The units of the fuel input energy [TBtu] is equivalent to 251,995,769,600 kcal (let 251,995,769,600 be defined as Υ). The units of the CO_2 generated [MMtons] is million metric tons, which is equivalent to 10^9 kg. The units of the MER generated [tons] is U.S. short ton, which is equivalent to 907.18474 kg. The units of the NO_x generated and SO_2 generated [Mtons] is metric tons, which is equivalent to 10^3 kg. The units of the fuel cost [Mill/kWh] is mill per kWh, which is equivalent to $/MWh (Mill is $/1000).

The values derived from the input and output IPM files are used as input to the PPC algorithm for each of the power system areas. The derived values were computed using the data defined in Table 38. The derived values include average environmental air pollution (EAP) rate $R_e(g)$ [kg/MWh], (where e is a generic place holder for the specific EAP: CO_2, MER, NO_x, and SO_2] forced outage rate $F_{OR}(g)$, fuel cost per unit energy $K(f)$ [$/kcal], minimum capacity $C_{min}(g)$ [MW], maximum capacity $C_{max}(g)$ [MW], constant heat rate coefficient $\alpha(g)$ [kcal/h], linear heat rate coefficient $\beta(g)$ [kcal/MWh], quadratic heat rate coefficient $\gamma(g)$ [kcal/(MW)^{2}h], constant emission rate coefficient $a_e(g)$ [kg/h], and linear emission rate coefficient $b_e(g)$ [kg/MWh]. All of the derived values are defined for generator g, except the cost per unit energy $K(f)$ which is defined for fuel type f. The derived values are summarized in Table 39.

Table 39: Derived Probabilistic Production Costing [PPC] input.

Value	Symbol	Units
Average EAP Rate	$R_e(g)$	kg/MWh
Forced Outage Rate	$F_{OR}(g)$	
Fuel Cost per Fuel Energy	$K(f)$	\$/kcal
Minimum Capacity	$C_{\min}(g)$	MW
Maximum Capacity	$C_{\max}(g)$	MW
Constant Heat Rate Coefficient	$\alpha(g)$	kcal/h
Linear Heat Rate Coefficient	$\beta(g)$	kcal/MWh
Quadratic Heat Rate Coefficient	$\gamma(g)$	kcal/(MW)^{2}h
Constant Emission Rate Coefficient	$a_e(g)$	kg/h
Linear Emission Rate Coefficient	$b_e(g)$	kg/MWh

The environmental air pollution average rates are computed dividing the generated EAP by the generated energy. The average CO_2 rate $R_C(g)$ is defined in Equation 22.

$$R_C(g) = E_C(g) \cdot 10^9 / (G(g) \cdot 10^3) \qquad (22)$$

The average MER rate $R_M(g)$ is defined in Equation 23.

$$R_M(g) = E_M(g) \cdot 907.18474 \, / (G(g) \cdot 10^3) \qquad (23)$$

The average NO_x rate R_N is defined in Equation 24.

$$R_N(g) = E_N(g) \cdot 10^3 / (G(g) \cdot 10^3) \qquad (24)$$

The average SO_2 rate R_S is defined in Equation 25.

$$R_S(g) = E_S(g) \cdot 10^3 / (G(g) \cdot 10^3) \qquad (25)$$

The forced outage rate $F_{OR}(g)$ is defined in Equation 26. The linear relationship between $F_{OR}(g)$ and $\tilde{c}(g)$ [MW] was approximated based on forced outage rate data from [118] shown in Figure 252.

$$F_{OR}(g) = 0.0002 \cdot \tilde{c}(g) + 0.0333 \qquad (26)$$

In Equation 25, $\tilde{c}(g)$ is the normalized generator capacity, defined in Equation 27. Notice, 400 MW is the largest generator capacity in [118].

$$\tilde{c}(g) = \frac{C(g)}{\max_{g} C(g)} \cdot 400 \tag{27}$$

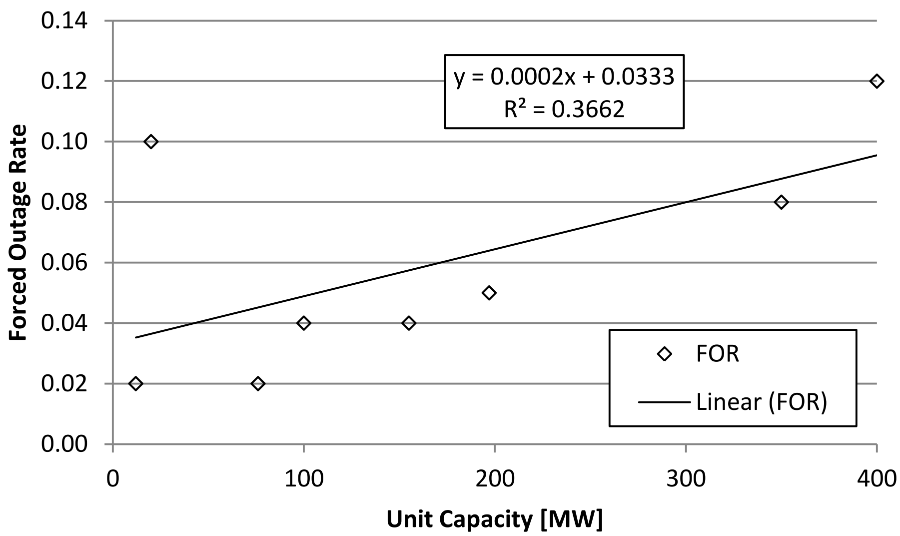

Figure 252: Linear forced outage rate approximation.

The normalized generator capacity is used, as opposed to the generator capacity; so that the functional approximations are evaluated on the range the functions were defined.

The fuel cost per unit energy $K(f)$ is defined in Equation 28.

$$K(f) = \frac{1}{|\mathcal{G}(f)|} \sum_{g \in \mathcal{G}(f)} \frac{\kappa(g)}{(F(g) \cdot \Upsilon)} \tag{28}$$

The fuel cost per unit energy defined in Equation 28 is the average fuel cost for each generator that uses the same fuel. Thus, the set $\mathcal{G}(f)$ is all of the generators that use fuel f and $|\mathcal{G}(f)|$ is the number of generators in the set $\mathcal{G}(f)$.

The minimum capacity $C_{min}(g)$ is defined in Equation 29.

$$C_{min}(g) = 0.35 \cdot C(g) \tag{29}$$

The multiplier 0.35 in Equation 29 was selected based on the average ratio of minimum capacity (C_{min}) to maximum capacity (C_{max}) from the data in [118] shown in Table 40.

Table 40: Maximum and minimum generator capacity.

Generator	C_{max} [MW]	C_{min} [MW]	Ratio of C_{min} to C_{max} [%]
1	12	2.4	20
2	20	16	80
3	76	15.2	20
4	100	25	25
5	155	54.25	35
6	197	68.95	35
7	350	140	40
8	400	100	25
Average			**35**

The maximum capacity $C_{max}(g)$ is defined in Equation 30.

$$C_{max}(g) = C(g) \tag{30}$$

A quadratic heat rate function is used to relate the required fuel for a given power level output, this general equation is defined in Equation 31.

$$h(P, g) = \alpha(g) + \beta(g) \cdot P + \gamma(g) \cdot P^2 \tag{31}$$

In Equation 31, $h(P, g)$ [kcal/h] is the required heat rate, $\alpha(g)$ is the constant heat rate coefficient, $\beta(g)$ is the linear heat rate coefficient, and $\gamma(g)$ is the quadratic heat rate coefficient, and P [MW] is the generator power output. The heat rate coefficients are computed based on heat rate coefficient data in [118]. The functional approximation for $\alpha(g)$ is defined in Equation 32 and shown in Figure 253.

$$\beta(g) = 2.1680 \cdot 10^5 \cdot \tilde{c}(g) + 3.5743 \cdot 10^6 \tag{32}$$

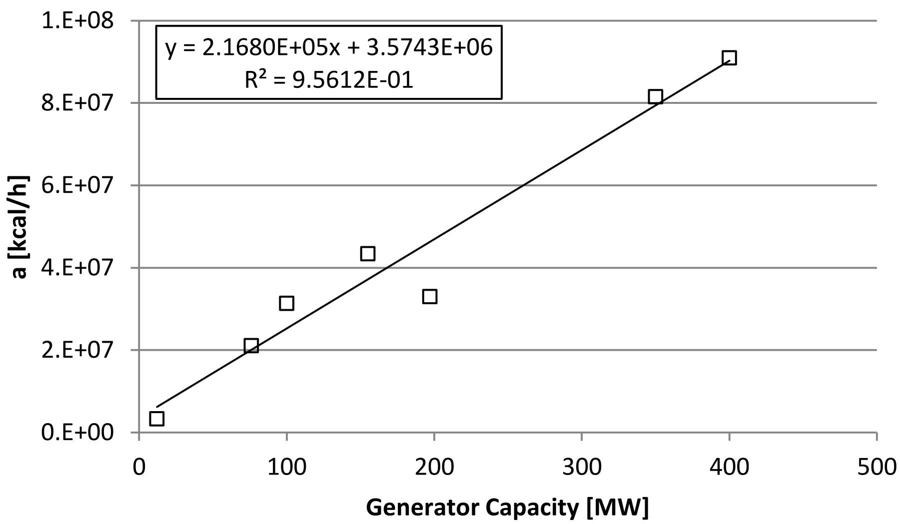

Figure 253: Constant heat rate coefficient linear approximation.

The functional approximation for $\beta(g)$ is defined in Equation 33 and shown in Figure 254.

$$\beta(g) = -9.3542 \cdot 10^2 \cdot \tilde{c}(g) + 2.3614 \cdot 10^6 \tag{33}$$

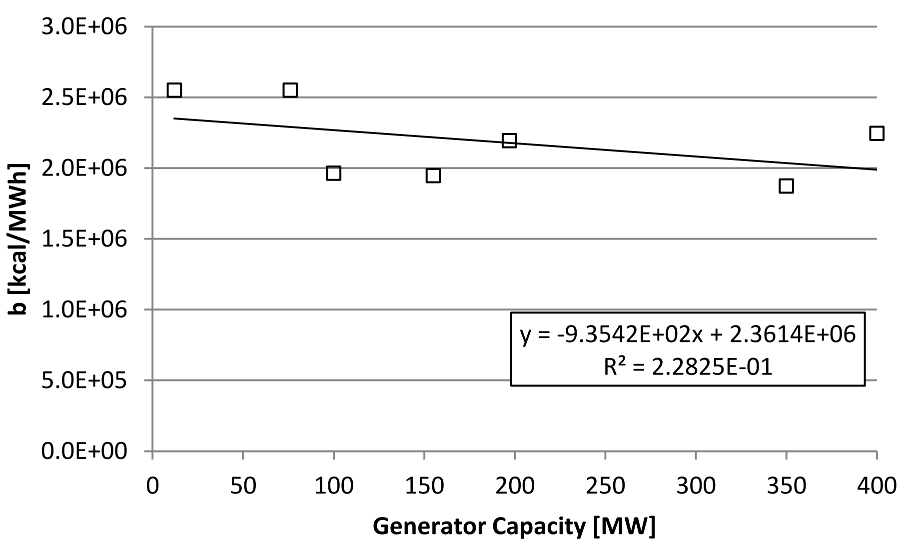

Figure 254: Linear heat rate coefficient linear approximation.

The functional approximation for $\gamma(g)$ is defined in Equation 34 and shown in Figure 255. Notice, the 4th order polynomial approximation was used so that negative quadratic heat rate coefficient values were avoided.

$$\gamma(g) = 5.4935 \cdot 10^{-6} \cdot \tilde{c}\,(g)^4 - 5.8872 \cdot 10^{-3} \cdot \tilde{c}(g)^3 + 2.2012 \cdot \tilde{c}(g)^2 - 3.3613 \cdot 10^2 \cdot \tilde{c}(g) + 1.8613 \cdot 10^4 \tag{34}$$

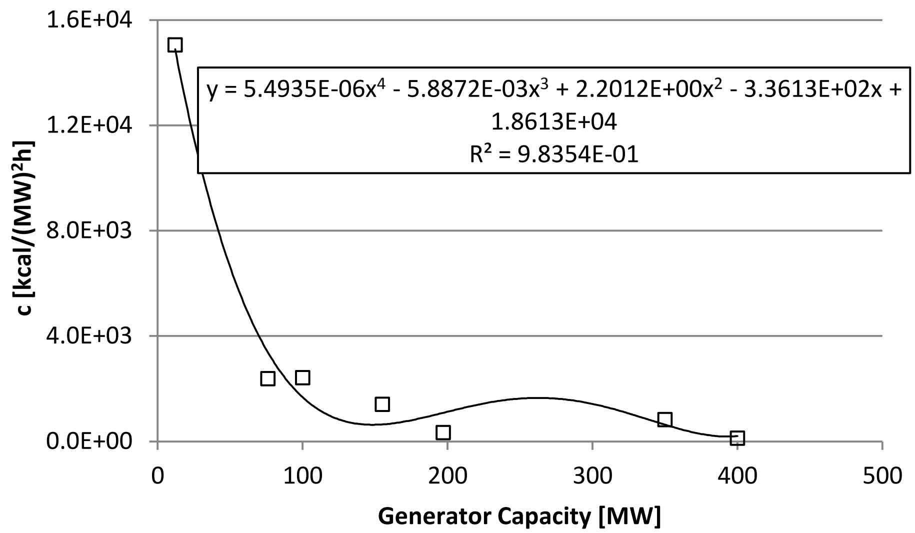

Figure 255: Quadratic heat rate coefficient polynomial approximation.

A linear emission rate function is used to relate the generated EAP for a given power level output, this general equation is defined in Equation 35.

$$e(P, g) = a_e(g) + b_e(g) \cdot P \tag{35}$$

In Equation 35, $e(P, g)$ [kg/h] is the emission rate, $a_e(g)$ [kg/h] is the constant emission rate coefficient, $b_e(g)$ [kg/MWh] is the constant emission rate coefficient, and P [MW] is the generator power output. Again, e is a generic place holder for the specific EAP $e \in \{CO_2, MER, NO_x, SO_2\}$.

A linear least square method is used to calculate the emission rate coefficients a_e and b_e for each generator. The general equations used for each generator and each EAP includes $\vec{Y}(g)$ defined in Equation 36, $\boldsymbol{A}(g)$ defined in Equation 37, and $\vec{X}(g)$ defined in Equation 38. The emission rate coefficients are computed assuming the EAP rate will increase 20% from minimum output to maximum generator output. The linear least square result used to compute $\vec{X}$ is shown in Equation 39.

$$\vec{Y}(g) = \begin{bmatrix} 0.9 \cdot R_e(g) \cdot C_{ave}(g) \\ R_e(g) \cdot C_{ave}(g) \\ 1.1 \cdot R_e(g) \cdot C_{ave}(g) \end{bmatrix} \tag{36}$$

$$\boldsymbol{A}(g) = \begin{bmatrix} 1 & C_{min}(g) \\ 1 & C_{ave}(g) \\ 1 & C_{max}(g) \end{bmatrix} \tag{37}$$

$$\vec{X}(g) = \begin{bmatrix} a_e(g) \\ b_e(g) \end{bmatrix} \tag{38}$$

$$\vec{X}(g) = \left(\boldsymbol{A}(g)^T \cdot \boldsymbol{A}(g)\right)^{-1} \cdot \boldsymbol{A}(g)^T \cdot \vec{Y}(g) \tag{39}$$

In Equation 36, $R_e(g)$ is a general average emission rate for EAP e and the average generator capacity $C_{ave}(g)$ is defined in Equation 40.

$$C_{ave}(g) = \frac{C_{min}(g) + C_{max}(g)}{2} \tag{40}$$

This appendix has described methodology used to derive the PPC input data derivation based on the IPM input and output files. The PPC input data is described in Chapter 5 and tabulated in Appendix B.

APPENDIX B POWER SYSTEM DATA TABLES

Each of the power system operating regions used a large set of generators. Each generator data consists of maximum capacity (C_{Max}), minimum capacity (C_{Min}), forced outage rate (FOR), three heat rate coefficients (α, β, and γ), fuel number, and two emission rate coefficients (a_e and b_e where the subscript is used to denote environmental air pollutant [EAP] e) for each EAP (carbon dioxide [CO_2], mercury [MER], nitrogen oxide [NO_x], and sulfur dioxide [SO_2]).

The Versailles Kentucky (ECAK) power system area consists of 36 generators. The ECAK power system area generator C_{Max}, C_{Min}, FOR, heat rate coefficients, and fuel type (i.e. generator data) are shown in Table 41. The ECAK power system area emission rate coefficients are shown in Table 42.

The Mercury Nevada (SNV) power system area consists of 21 generators. The SNV power system area generator C_{Max}, C_{Min}, FOR, heat rate coefficients, and fuel type (i.e. generator data) are shown in Table 43. The SNV power system area emission rate coefficients are shown in Table 44.

The Stillwater Oklahoma (SPPS) power system area consists of 65 generators. The SPPS power system area generator C_{Max}, C_{Min}, FOR, heat rate coefficients, and fuel type (i.e. generator data) are shown in Table 45. The SPPS power system area emission rate coefficients are shown in Table 46.

The Necedah Wisconsin (WUMS) power system area consists of 77 generators. The WUMS power system area generator C_{Max}, C_{Min}, FOR, heat rate coefficients, and fuel type (i.e. generator data) are shown in Table 47. The WUMS power system area emission rate coefficients are shown in Table 48.

Table 41: Listing of the Versailles Kentucky [ECAK] generator data.

Generator	C_{Max} [MW]	C_{Min} [MW]	FOR [%]	α [kcal/h]	β [kcal/MWh]	γ [kcal/(MW)^{2}h]	Fuel
1	420.00	147.00	0.06	3.68E+07	2.22E+06	6.39E+02	1
2	868.00	303.80	0.09	7.23E+07	2.06E+06	1.19E+03	1
3	145.00	50.75	0.04	1.51E+07	2.31E+06	6.15E+03	1
4	509.00	178.15	0.06	4.39E+07	2.19E+06	9.36E+02	1
5	312.00	109.20	0.05	2.83E+07	2.25E+06	1.11E+03	1
6	484.00	169.40	0.06	4.19E+07	2.20E+06	8.23E+02	1
7	986.00	345.10	0.10	8.17E+07	2.02E+06	4.75E+02	1
8	270.00	94.50	0.04	2.50E+07	2.27E+06	1.74E+03	2
9	240.00	84.00	0.04	2.26E+07	2.28E+06	2.42E+03	3
10	323.00	113.05	0.05	2.92E+07	2.25E+06	9.92E+02	3
11	303.00	106.05	0.05	2.76E+07	2.26E+06	1.22E+03	3
12	301.00	105.35	0.05	2.74E+07	2.26E+06	1.24E+03	3
13	464.00	162.40	0.06	4.03E+07	2.20E+06	7.45E+02	3
14	455.00	159.25	0.06	3.96E+07	2.21E+06	7.15E+02	3
15	167.00	58.45	0.04	1.68E+07	2.30E+06	5.04E+03	3
16	429.00	150.15	0.06	3.75E+07	2.21E+06	6.51E+02	3
17	429.00	150.15	0.06	3.75E+07	2.21E+06	6.51E+02	3
18	525.00	183.75	0.06	4.52E+07	2.18E+06	1.01E+03	4
19	325.00	113.75	0.05	2.93E+07	2.25E+06	9.73E+02	5
20	46.00	16.10	0.03	7.22E+06	2.35E+06	1.36E+04	6
21	150.00	52.50	0.04	1.55E+07	2.31E+06	5.88E+03	6
22	116.00	40.60	0.03	1.28E+07	2.32E+06	7.89E+03	6
23	225.00	78.75	0.04	2.14E+07	2.28E+06	2.84E+03	6
24	71.00	24.85	0.03	9.20E+06	2.34E+06	1.13E+04	6
25	484.00	169.40	0.06	4.19E+07	2.20E+06	8.23E+02	6
26	65.00	22.75	0.03	8.72E+06	2.34E+06	1.18E+04	6
27	10.00	3.50	0.03	4.37E+06	2.36E+06	1.74E+04	6
28	536.00	187.60	0.06	4.60E+07	2.18E+06	1.07E+03	7
29	330.00	115.50	0.05	2.97E+07	2.25E+06	9.28E+02	8
30	23.00	8.05	0.03	5.40E+06	2.35E+06	1.59E+04	8
31	34.00	11.90	0.03	6.27E+06	2.35E+06	1.48E+04	8
32	323.00	113.05	0.05	2.92E+07	2.25E+06	9.92E+02	8
33	1,095.00	383.25	0.10	9.03E+07	1.99E+06	2.06E+02	8
34	36.00	12.60	0.03	6.43E+06	2.35E+06	1.46E+04	8
35	160.00	56.00	0.04	1.62E+07	2.31E+06	5.38E+03	8
36	101.00	35.35	0.03	1.16E+07	2.33E+06	8.92E+03	9

Table 42: Listing of the Versailles Kentucky [ECAK] generator emission rate data.

Gen.	a_{CO2} [kg/h]	b_{CO2} [kg/MWh]	a_{MER} [kg/h]	b_{MER} [kg/MWh]	a_{NOx} [kg/h]	b_{NOx} [kg/MWh]	a_{SO2} [kg/h]	b_{SO2} [kg/MWh]
1	224,692	208	0.001	0	0.073	0	0.546	0.001
2	461,288	206	0.002	0	0.150	0	1.922	0.001
3	78,606	211	0	0	0.065	0	0.099	0
4	256,054	195	0.001	0	0.083	0	0.242	0
5	173,652	216	0.001	0	0.057	0	0.197	0
6	248,071	199	0.001	0	0.080	0	0.307	0
7	524,044	206	0.002	0	0.171	0	0.827	0
8	149,010	214	0.002	0	0.146	0	0.188	0
9	125,708	203	0.002	0	0.211	0	0.235	0
10	177,886	214	0.002	0	0.375	0	0.340	0
11	158,051	203	0.002	0	0.269	0	0.374	0
12	158,826	205	0.002	0	0.266	0	0.376	0
13	248,226	208	0.003	0	0.456	0	0.235	0
14	240,161	205	0.003	0	0.421	0	0.379	0
15	82,591	192	0.001	0	0.133	0	0.098	0
16	219,404	199	0.003	0	0.378	0	0.260	0
17	219,336	199	0.003	0	0.378	0	0.346	0
18	271,448	201	0.004	0	0.088	0	0.321	0
19	160,289	192	0.003	0	0.052	0	0.908	0.001
20	26,948	228	0.001	0	0.079	0.001	0.211	0.002
21	84,976	220	0.001	0	0.191	0	0.481	0.001
22	56,364	189	0.001	0	0.141	0	0.319	0.001
23	115,264	199	0.002	0	0.286	0	0.653	0.001
24	38,267	209	0.001	0	0.087	0	0.217	0.001
25	241,356	194	0.005	0	0.361	0	1.367	0.001
26	44,512	266	0.001	0	0.121	0.001	0.347	0.002
27	7,131	277	0	0	0.027	0.001	0.224	0.009
28	232,855	169	0.003	0	0.075	0	0.066	0
29	93,286	110	0	0	0.045	0	0	0
30	7,380	125	0	0	0.030	0	0	0
31	10,391	119	0	0	0.044	0.001	0	0
32	96,533	116	0	0	0.066	0	0	0
33	396,707	141	0	0	0.151	0	0	0
34	9,627	104	0	0	0.070	0.001	0	0
35	47,818	116	0	0	0.035	0	0	0
36	54,230	209	0	0	0.018	0	0.086	0

Table 43: Listing of the Mercury Nevada [SNV] generator data.

Generator	C_{Max} [MW]	C_{Min} [MW]	FOR [%]	α [kcal/h]	β [kcal/MWh]	γ [kcal/(MW)^{2}h]	Fuel
1	110.00	38.50	0.03	1.15E+07	2.33E+06	8.97E+03	1
2	110.00	38.50	0.03	1.15E+07	2.33E+06	8.97E+03	1
3	110.00	38.50	0.03	1.15E+07	2.33E+06	8.97E+03	1
4	225.00	78.75	0.04	1.98E+07	2.29E+06	3.48E+03	1
5	790.00	276.50	0.08	6.07E+07	2.12E+06	1.65E+03	2
6	790.00	276.50	0.08	6.07E+07	2.12E+06	1.65E+03	2
7	790.00	276.50	0.08	6.07E+07	2.12E+06	1.65E+03	2
8	181.00	63.35	0.04	1.67E+07	2.30E+06	5.13E+03	3
9	1,092.00	382.20	0.10	8.25E+07	2.02E+06	4.20E+02	4
10	450.00	157.50	0.05	3.61E+07	2.22E+06	6.32E+02	4
11	560.00	196.00	0.06	4.40E+07	2.19E+06	9.46E+02	4
12	1,200.00	420.00	0.10	9.03E+07	1.99E+06	2.06E+02	4
13	469.00	164.15	0.06	3.75E+07	2.22E+06	6.50E+02	4
14	77.00	26.95	0.03	9.14E+06	2.34E+06	1.13E+04	5
15	141.00	49.35	0.03	1.38E+07	2.32E+06	7.09E+03	5
16	50.00	17.50	0.03	7.19E+06	2.35E+06	1.36E+04	5
17	9.00	3.15	0.03	4.22E+06	2.36E+06	1.76E+04	6
18	41.00	14.35	0.03	6.54E+06	2.35E+06	1.44E+04	6
19	170.00	59.50	0.04	1.59E+07	2.31E+06	5.62E+03	6
20	220.00	77.00	0.04	1.95E+07	2.29E+06	3.64E+03	6
21	101.00	35.35	0.03	1.09E+07	2.33E+06	9.57E+03	6

Table 44: Listing of the Mercury Nevada [SNV] generator emission rate data.

Gen.	a_{CO2} [kg/h]	b_{CO2} [kg/MWh]	a_{MER} [kg/h]	b_{MER} [kg/MWh]	a_{NOx} [kg/h]	b_{NOx} [kg/MWh]	a_{SO2} [kg/h]	b_{SO2} [kg/MWh]
1	54,254	192	0.001	0	0.110	0	0.018	0
2	55,755	197	0.001	0	0.117	0	0.018	0
3	57,256	202	0.001	0	0.095	0	0.019	0
4	113,472	196	0.000	0	0.215	0	0.037	0
5	441,228	217	0.004	0	0.957	0	0.215	0
6	441,271	217	0.007	0	0.957	0	0.344	0
7	441,041	217	0.007	0	0.961	0	0.343	0
8	102,063	219	0.002	0	0.104	0	0.578	0.001
9	234,358	83	0	0	0.046	0	0	0
10	140,387	121	0	0	0.017	0	0	0
11	115,700	80	0	0	0.064	0	0	0
12	239,653	78	0	0	0.025	0	0	0
13	120,314	100	0	0	0.193	0	0	0
14	22,174	112	0	0	0.016	0	0	0
15	45,245	125	0	0	0.121	0	0	0
16	13,370	104	0	0	0.067	0.001	0	0
17	1,925	83	0	0	0.000	0	0	0
18	8,970	85	0	0	0.001	0	0	0
19	41,883	96	0	0	0.030	0	0	0
20	45,427	80	0	0	0.033	0	0	0
21	33,760	130	0	0	0.024	0	0	0

Table 45: Listing of the Stillwater Oklahoma [SPPS] generator data.

Generator	C_{Max} [MW]	C_{Min} [MW]	FOR [%]	α [kcal/h]	β [kcal/MWh]	γ [kcal/(MW)^{2}h]	Fuel
1	675.00	236.25	0.05	2.83E+07	2.25E+06	1.10E+03	1
2	520.00	182.00	0.04	2.26E+07	2.28E+06	2.41E+03	2
3	528.00	184.80	0.04	2.29E+07	2.28E+06	2.31E+03	3
4	26.00	9.10	0.03	4.53E+06	2.36E+06	1.72E+04	3
5	528.00	184.80	0.04	2.29E+07	2.28E+06	2.31E+03	3
6	1056.00	369.60	0.06	4.23E+07	2.19E+06	8.43E+02	3
7	346.00	121.10	0.04	1.63E+07	2.31E+06	5.37E+03	3
8	720.00	252.00	0.05	3.00E+07	2.25E+06	9.02E+02	3
9	1080.00	378.00	0.06	4.31E+07	2.19E+06	8.92E+02	3
10	523.00	183.05	0.04	2.27E+07	2.28E+06	2.37E+03	3
11	450.00	157.50	0.04	2.01E+07	2.29E+06	3.38E+03	3
12	505.00	176.75	0.04	2.21E+07	2.28E+06	2.59E+03	3
13	514.00	179.90	0.04	2.24E+07	2.28E+06	2.48E+03	3
14	501.00	175.35	0.04	2.19E+07	2.28E+06	2.64E+03	3
15	514.00	179.90	0.04	2.24E+07	2.28E+06	2.48E+03	3
16	450.00	157.50	0.04	2.01E+07	2.29E+06	3.38E+03	3
17	502.00	175.70	0.04	2.20E+07	2.28E+06	2.63E+03	3
18	940.00	329.00	0.06	3.80E+07	2.21E+06	6.62E+02	3
19	320.00	112.00	0.04	1.53E+07	2.31E+06	5.99E+03	4
20	660.00	231.00	0.05	2.78E+07	2.26E+06	1.19E+03	5
21	457.00	159.95	0.04	2.03E+07	2.29E+06	3.27E+03	6
22	243.00	85.05	0.03	1.25E+07	2.32E+06	8.13E+03	6
23	480.00	168.00	0.04	2.12E+07	2.29E+06	2.93E+03	6
24	1832.00	641.20	0.09	7.07E+07	2.07E+06	1.30E+03	7
25	1274.00	445.90	0.07	5.03E+07	2.16E+06	1.33E+03	7
26	19.00	6.65	0.03	4.27E+06	2.36E+06	1.76E+04	7
27	310.00	108.50	0.04	1.49E+07	2.31E+06	6.24E+03	7
28	2367.00	828.45	0.10	9.03E+07	1.99E+06	2.06E+02	7
29	318.00	111.30	0.04	1.52E+07	2.31E+06	6.04E+03	7
30	222.00	77.70	0.03	1.17E+07	2.33E+06	8.80E+03	7
31	22.00	7.70	0.03	4.38E+06	2.36E+06	1.74E+04	7
32	22.00	7.70	0.03	4.38E+06	2.36E+06	1.74E+04	7
33	485.00	169.75	0.04	2.13E+07	2.28E+06	2.86E+03	7
34	40.00	14.00	0.03	5.04E+06	2.36E+06	1.64E+04	7
35	486.00	170.10	0.04	2.14E+07	2.28E+06	2.84E+03	7
36	540.00	189.00	0.04	2.34E+07	2.28E+06	2.18E+03	7
37	171.00	59.85	0.03	9.84E+06	2.33E+06	1.06E+04	7
38	16.00	5.60	0.03	4.16E+06	2.36E+06	1.77E+04	7
39	494.00	172.90	0.04	2.17E+07	2.28E+06	2.73E+03	7
40	153.00	53.55	0.03	9.18E+06	2.34E+06	1.13E+04	8

Generator	C_{Max} [MW]	C_{Min} [MW]	FOR [%]	α [kcal/h]	β [kcal/MWh]	γ [kcal/(MW)^{2}h]	Fuel
41	18.00	6.30	0.03	4.23E+06	2.36E+06	1.76E+04	8
42	480.00	168.00	0.04	2.12E+07	2.29E+06	2.93E+03	8
43	13.00	4.55	0.03	4.05E+06	2.36E+06	1.79E+04	8
44	285.00	99.75	0.03	1.40E+07	2.32E+06	6.90E+03	8
45	43.00	15.05	0.03	5.15E+06	2.35E+06	1.63E+04	8
46	134.00	46.90	0.03	8.48E+06	2.34E+06	1.21E+04	8
47	443.00	155.05	0.04	1.98E+07	2.29E+06	3.49E+03	8
48	11.00	3.85	0.03	3.98E+06	2.36E+06	1.80E+04	8
49	16.00	5.60	0.03	4.16E+06	2.36E+06	1.77E+04	8
50	41.00	14.35	0.03	5.08E+06	2.35E+06	1.64E+04	8
51	26.00	9.10	0.03	4.53E+06	2.36E+06	1.72E+04	8
52	25.00	8.75	0.03	4.49E+06	2.36E+06	1.72E+04	8
53	64.00	22.40	0.03	5.92E+06	2.35E+06	1.52E+04	8
54	22.00	7.70	0.03	4.38E+06	2.36E+06	1.74E+04	8
55	17.00	5.95	0.03	4.20E+06	2.36E+06	1.77E+04	8
56	27.00	9.45	0.03	4.56E+06	2.36E+06	1.71E+04	8
57	168.00	58.80	0.03	9.73E+06	2.33E+06	1.07E+04	8
58	53.00	18.55	0.03	5.52E+06	2.35E+06	1.58E+04	9
59	34.00	11.90	0.03	4.82E+06	2.36E+06	1.68E+04	9
60	20.00	7.00	0.03	4.31E+06	2.36E+06	1.75E+04	9
61	221.00	77.35	0.03	1.17E+07	2.33E+06	8.83E+03	9
62	1,290.00	451.50	0.07	5.08E+07	2.16E+06	1.36E+03	10
63	402.00	140.70	0.04	1.83E+07	2.30E+06	4.21E+03	10
64	650.00	227.50	0.05	2.74E+07	2.26E+06	1.25E+03	11
65	650.00	227.50	0.05	2.74E+07	2.26E+06	1.25E+03	11

Table 46: Listing of the Stillwater Oklahoma [SPPS] emission rate data.

Gen.	a_{CO2} [kg/h]	b_{CO2} [kg/MWh]	a_{MER} [kg/h]	b_{MER} [kg/MWh]	a_{NOx} [kg/h]	b_{NOx} [kg/MWh]	a_{SO2} [kg/h]	b_{SO2} [kg/MWh]
1	370,158	213	0.014	0	0.328	0	1.448	0.001
2	283,269	212	0.006	0	0.535	0	0.362	0
3	277,792	204	0.008	0	0.295	0	1.367	0.001
4	12,408	185	0	0	0.046	0.001	0.047	0.001
5	291,405	214	0.007	0	0.259	0	0.885	0.001
6	560,607	206	0.014	0	0.537	0	1.702	0.001
7	178,946	201	0.005	0	0.131	0	0.543	0.001
8	373,155	201	0.003	0	0.277	0	1.133	0.001
9	550,220	198	0.004	0	0.406	0	1.670	0.001
10	286,257	213	0.007	0	0.330	0	0.869	0.001
11	238,116	205	0.006	0	0.482	0	0.723	0.001
12	262,725	202	0.008	0	0.569	0	1.292	0.001
13	273,654	207	0.008	0	0.476	0	1.347	0.001
14	275,438	214	0.008	0	0.405	0	1.355	0.001
15	287,995	218	0.009	0	0.487	0	1.417	0.001
16	238,552	206	0.007	0	0.483	0	1.174	0.001
17	265,780	206	0.008	0	0.495	0	1.308	0.001
18	604,501	250	0.018	0	1.050	0	2.974	0.001
19	184,511	224	0.006	0	0.154	0	0.076	0
20	315,814	186	0.002	0	0.093	0	0.562	0
21	135,371	115	0	0	0.273	0	0	0
22	71,179	114	0	0	0.079	0	0	0
23	142,205	115	0	0	0.615	0	0	0
24	378,457	80	0	0	0.153	0	0	0
25	263,226	80	0	0	0.099	0	0	0
26	4,516	92	0	0	0.006	0	0	0
27	61,035	76	0	0	0.045	0	0	0
28	484,458	79	0	0	0.698	0	0	0
29	87,243	107	0	0	0.296	0	0	0
30	49,990	87	0	0	0.019	0	0	0
31	4,452	79	0	0	0.002	0	0	0
32	4,452	79	0	0	0.002	0	0	0
33	100,084	80	0	0	0.021	0	0	0
34	8,200	80	0	0	0.004	0	0	0
35	100,463	80	0	0	0.040	0	0	0
36	107,857	78	0	0	0.011	0	0	0
37	35,422	80	0	0	0.027	0	0	0
38	4,278	104	0	0	0.013	0	0	0
39	137,072	108	0	0	0.470	0	0	0
40	44,632	113	0	0	0.030	0	0	0

Gen.	a_{CO2} [kg/h]	b_{CO2} [kg/MWh]	a_{MER} [kg/h]	b_{MER} [kg/MWh]	a_{NOx} [kg/h]	b_{NOx} [kg/MWh]	a_{SO2} [kg/h]	b_{SO2} [kg/MWh]
41	4,278	92	0	0	0.081	0.002	0	0
42	145,785	118	0	0	0.111	0	0	0
43	2,980	89	0	0	0.001	0	0	0
44	101,613	138	0	0	0.149	0	0	0
45	11,498	104	0	0	0.052	0	0	0
46	38,506	112	0	0	0.061	0	0	0
47	163,753	144	0	0	0.401	0	0	0
48	2,941	104	0	0	0.084	0.003	0	0
49	0	0	0	0	0.017	0	0	0
50	21,927	208	0	0	0.110	0.001	0	0
51	13,905	208	0	0	0.264	0.004	0	0
52	13,370	208	0	0	0.040	0.001	0	0
53	34,228	208	0	0	0.120	0.001	0	0
54	11,766	208	0	0	0.024	0	0	0
55	6,061	138	0	0	0.076	0.002	0	0
56	14,440	208	0	0	0.087	0.001	0	0
57	51,342	119	0	0	0.039	0	0	0
58	18,897	138	0	0	0.028	0	0	0
59	12,122	138	0	0	0.018	0	0	0
60	6,418	125	0	0	0.001	0	0	0
61	70,277	123	0	0	0.026	0	0	0
62	266,498	80	0	0	0.203	0	0	0
63	83,065	80	0	0	0.020	0	0	0
64	355,828	213	0.014	0	0.111	0	0.668	0
65	355,875	213	0.014	0	0.111	0	0.870	0.001

Table 47: Listing of the Necedah Wisconsin [WUMS] generator data.

Generator	C_{Max} [MW]	C_{Min} [MW]	FOR [%]	α [kcal/h]	β [kcal/MWh]	γ [kcal/(MW)^{2}h]	Fuel
1	617.00	215.95	0.06	4.71E+07	2.17E+06	1.14E+03	1
2	617.00	215.95	0.06	4.71E+07	2.17E+06	1.14E+03	1
3	1,230.00	430.50	0.10	9.03E+07	1.99E+06	2.06E+02	1
4	519.00	181.65	0.06	4.02E+07	2.20E+06	7.38E+02	2
5	44.00	15.40	0.03	6.68E+06	2.35E+06	1.42E+04	3
6	13.00	4.55	0.03	4.49E+06	2.36E+06	1.72E+04	4
7	16.00	5.60	0.03	4.70E+06	2.36E+06	1.69E+04	4
8	13.00	4.55	0.03	4.49E+06	2.36E+06	1.72E+04	4
9	36.00	12.60	0.03	6.11E+06	2.35E+06	1.50E+04	4
10	263.00	92.05	0.04	2.21E+07	2.28E+06	2.58E+03	4
11	21.00	7.35	0.03	5.05E+06	2.36E+06	1.64E+04	4
12	25.00	8.75	0.03	5.34E+06	2.35E+06	1.60E+04	4
13	176.00	61.60	0.04	1.60E+07	2.31E+06	5.54E+03	4
14	264.00	92.40	0.04	2.22E+07	2.28E+06	2.55E+03	4
15	70.00	24.50	0.03	8.51E+06	2.34E+06	1.20E+04	4
16	70.00	24.50	0.03	8.51E+06	2.34E+06	1.20E+04	4
17	70.00	24.50	0.03	8.51E+06	2.34E+06	1.20E+04	4
18	70.00	24.50	0.03	8.51E+06	2.34E+06	1.20E+04	4
19	70.00	24.50	0.03	8.51E+06	2.34E+06	1.20E+04	4
20	70.00	24.50	0.03	8.51E+06	2.34E+06	1.20E+04	4
21	70.00	24.50	0.03	8.51E+06	2.34E+06	1.20E+04	4
22	70.00	24.50	0.03	8.51E+06	2.34E+06	1.20E+04	4
23	26.00	9.10	0.03	5.41E+06	2.35E+06	1.59E+04	4
24	25.00	8.75	0.03	5.34E+06	2.35E+06	1.60E+04	4
25	25.00	8.75	0.03	5.34E+06	2.35E+06	1.60E+04	4
26	257.00	89.95	0.04	2.17E+07	2.28E+06	2.73E+03	4
27	148.00	51.80	0.03	1.40E+07	2.32E+06	6.91E+03	4
28	108.00	37.80	0.03	1.12E+07	2.33E+06	9.28E+03	4
29	111.00	38.85	0.03	1.14E+07	2.33E+06	9.08E+03	4
30	132.00	46.20	0.03	1.29E+07	2.32E+06	7.79E+03	4
31	338.00	118.30	0.05	2.74E+07	2.26E+06	1.24E+03	4
32	23.00	8.05	0.03	5.20E+06	2.35E+06	1.62E+04	4
33	21.00	7.35	0.03	5.05E+06	2.36E+06	1.64E+04	4
34	21.00	7.35	0.03	5.05E+06	2.36E+06	1.64E+04	4
35	558.00	195.30	0.06	4.29E+07	2.19E+06	8.79E+02	4
36	551.00	192.85	0.06	4.24E+07	2.19E+06	8.51E+02	4
37	22.00	7.70	0.03	5.13E+06	2.35E+06	1.63E+04	4
38	75.00	26.25	0.03	8.86E+06	2.34E+06	1.16E+04	4
39	97.00	33.95	0.03	1.04E+07	2.33E+06	1.00E+04	4
40	261.00	91.35	0.04	2.20E+07	2.28E+06	2.63E+03	4

Generator	C_{Max} [MW]	C_{Min} [MW]	FOR [%]	α [kcal/h]	β [kcal/MWh]	γ [kcal/(MW)^{2}h]	Fuel
41	264.00	92.40	0.04	2.22E+07	2.28E+06	2.55E+03	4
42	298.00	104.30	0.04	2.46E+07	2.27E+06	1.84E+03	4
43	312.00	109.20	0.05	2.56E+07	2.27E+06	1.60E+03	4
44	334.00	116.90	0.05	2.71E+07	2.26E+06	1.29E+03	4
45	422.00	147.70	0.05	3.33E+07	2.23E+06	6.73E+02	4
46	21.00	7.35	0.03	5.05E+06	2.36E+06	1.64E+04	5
47	30.00	10.50	0.03	5.69E+06	2.35E+06	1.55E+04	5
48	512.00	179.20	0.06	3.97E+07	2.21E+06	7.18E+02	6
49	514.00	179.90	0.06	3.98E+07	2.21E+06	7.23E+02	6
50	560.00	196.00	0.06	4.31E+07	2.19E+06	8.87E+02	6
51	545.00	190.75	0.06	4.20E+07	2.20E+06	8.28E+02	7
52	545.00	190.75	0.06	4.20E+07	2.20E+06	8.28E+02	7
53	598.00	209.30	0.06	4.57E+07	2.18E+06	1.05E+03	7
54	74.00	25.90	0.03	8.79E+06	2.34E+06	1.17E+04	8
55	25.00	8.75	0.03	5.34E+06	2.35E+06	1.60E+04	8
56	521.00	182.35	0.06	4.03E+07	2.20E+06	7.44E+02	8
57	1,065.00	372.75	0.09	7.87E+07	2.04E+06	6.99E+02	8
58	850.00	297.50	0.08	6.35E+07	2.10E+06	1.62E+03	8
59	100.00	35.00	0.03	1.06E+07	2.33E+06	9.81E+03	8
60	100.00	35.00	0.03	1.06E+07	2.33E+06	9.81E+03	8
61	100.00	35.00	0.03	1.06E+07	2.33E+06	9.81E+03	8
62	100.00	35.00	0.03	1.06E+07	2.33E+06	9.81E+03	8
63	93.00	32.55	0.03	1.01E+07	2.33E+06	1.03E+04	8
64	20.00	7.00	0.03	4.98E+06	2.36E+06	1.65E+04	8
65	150.00	52.50	0.03	1.41E+07	2.32E+06	6.80E+03	9
66	251.00	87.85	0.04	2.13E+07	2.29E+06	2.88E+03	9
67	33.00	11.55	0.03	5.90E+06	2.35E+06	1.53E+04	10
68	66.00	23.10	0.03	8.23E+06	2.34E+06	1.24E+04	11
69	25.00	8.75	0.03	5.34E+06	2.35E+06	1.60E+04	11
70	25.00	8.75	0.03	5.34E+06	2.35E+06	1.60E+04	11
71	23.00	8.05	0.03	5.20E+06	2.35E+06	1.62E+04	11
72	23.00	8.05	0.03	5.20E+06	2.35E+06	1.62E+04	11
73	25.00	8.75	0.03	5.34E+06	2.35E+06	1.60E+04	11
74	25.00	8.75	0.03	5.34E+06	2.35E+06	1.60E+04	11
75	25.00	8.75	0.03	5.34E+06	2.35E+06	1.60E+04	11
76	25.00	8.75	0.03	5.34E+06	2.35E+06	1.60E+04	11
77	74.00	25.90	0.03	8.79E+06	2.34E+06	1.17E+04	11

Table 48: Listing of the Necedah Wisconsin [WUMS] emission rate data.

Gen.	a_{CO2} [kg/h]	b_{CO2} [kg/MWh]	a_{MER} [kg/h]	b_{MER} [kg/MWh]	a_{NOx} [kg/h]	b_{NOx} [kg/MWh]	a_{SO2} [kg/h]	b_{SO2} [kg/MWh]
1	340,218	214	0.009	0	0.107	0	0.107	0
2	342,683	216	0.009	0	0.108	0	0.108	0
3	550,687	174	0.005	0	0.173	0	0.173	0
4	232,287	174	0.005	0	0.073	0	0.109	0
5	29,801	263	0	0	0.023	0	0.014	0
6	7,662	229	0	0	0.024	0.001	0.038	0.001
7	9,484	230	0	0	0.028	0.001	0.046	0.001
8	9,506	284	0	0	0.058	0.002	0.047	0.001
9	26,757	289	0.001	0	0.048	0.001	0.081	0.001
10	155,400	229	0.004	0	0.176	0	0.472	0.001
11	14,216	263	0	0	0.051	0.001	0.073	0.001
12	17,723	275	0	0	0.03	0	0.139	0.002
13	97,978	216	0	0	0.202	0	0.371	0.001
14	164,151	241	0.001	0	0.338	0	0.531	0.001
15	46,674	259	0	0	0.08	0	0.176	0.001
16	46,628	259	0	0	0.08	0	0.578	0.003
17	46,276	257	0	0	0.08	0	0.175	0.001
18	46,987	261	0	0	0.081	0	0.581	0.003
19	45,490	252	0	0	0.079	0	0.173	0.001
20	45,642	253	0	0	0.078	0	0.565	0.003
21	45,827	254	0	0	0.079	0	0.173	0.001
22	45,918	255	0	0	0.079	0	0.568	0.003
23	18,745	280	0.002	0	0.069	0.001	0.28	0.004
24	17,610	274	0.001	0	0.036	0.001	0.361	0.006
25	18,180	282	0.001	0	0.035	0.001	0.09	0.001
26	164,659	249	0.004	0	0.222	0	0.5	0.001
27	90,333	237	0.002	0	0.146	0	0.274	0.001
28	59,442	214	0.002	0	0.12	0	0.181	0.001
29	59,937	210	0.002	0	0.12	0	0.182	0.001
30	69,858	206	0.002	0	0.083	0	0.212	0.001
31	177,076	203	0.001	0	0.253	0	0.538	0.001
32	16,532	279	0.001	0	0.061	0.001	0.205	0.003
33	15,509	287	0	0	0.024	0	0.076	0.001
34	11,663	216	0	0	0.018	0	0.057	0.001
35	302,199	210	0.008	0	0.231	0	0.917	0.001
36	293,831	207	0.008	0	0.185	0	0.892	0.001
37	15,541	274	0	0	0.045	0.001	0.369	0.007
38	40,111	208	0	0	0.08	0	0.08	0
39	52,052	208	0	0	0.09	0	0.197	0.001
40	131,485	196	0.003	0	0.118	0	0.399	0.001

Gen.	a_{CO2} [kg/h]	b_{CO2} [kg/MWh]	a_{MER} [kg/h]	b_{MER} [kg/MWh]	a_{NOx} [kg/h]	b_{NOx} [kg/MWh]	a_{SO2} [kg/h]	b_{SO2} [kg/MWh]
41	133,664	197	0.003	0	0.12	0	0.406	0.001
42	149,503	195	0.004	0	0.101	0	0.454	0.001
43	153,102	191	0.004	0	0.1	0	0.465	0.001
44	169,390	197	0.004	0	0.273	0	0.514	0.001
45	218,355	201	0.006	0	0.249	0	0.663	0.001
46	12,455	230	0	0	0.018	0	0.037	0.001
47	14,340	186	0.001	0	0.004	0	0.025	0
48	0	0	0	0	0	0	0	0
49	0	0	0	0	0	0	0	0
50	0	0	0	0	0	0	0	0
51	166,769	119	0	0	0.038	0	0	0
52	167,013	119	0	0	0.018	0	0	0
53	123,784	80	0	0	0.02	0	0	0
54	19,788	104	0	0	0	0	0	0
55	13,370	208	0	0	0.053	0.001	0	0
56	157,049	117	0	0	0.046	0	0	0
57	427,178	156	0	0	0.356	0	0	0
58	257,313	118	0	0	0.193	0	0	0
59	35,654	138	0	0	0.018	0	0	0
60	35,654	138	0	0	0.036	0	0	0
61	35,654	138	0	0	0.036	0	0	0
62	35,654	138	0	0	0.036	0	0	0
63	33,158	138	0	0	0.017	0	0	0
64	0	0	0	0	0.021	0	0	0
65	29,783	77	0	0	0.003	0	0	0
66	55,274	86	0	0	0.01	0	0	0
67	16,724	197	0	0	0.005	0	0.051	0.001
68	48,608	286	0.001	0	0.125	0.001	0.147	0.001
69	16,570	257	0	0	0.019	0	0.063	0.001
70	16,185	251	0	0	0.018	0	0.202	0.003
71	15,068	254	0	0	0.017	0	0.057	0.001
72	15,304	258	0	0	0.017	0	0.19	0.003
73	16,246	252	0	0	0.018	0	0.062	0.001
74	16,169	251	0	0	0.018	0	0.202	0.003
75	16,364	254	0	0	0.018	0	0.062	0.001
76	16,277	253	0	0	0.018	0	0.202	0.003
77	42,643	224	0.001	0	0.065	0	0.13	0.001

REFERENCES

[1] IEEE Future Directions. (2011, November 1). *Smart Grid Conceptual Model* [Online]. Available: http://smartgrid.ieee.org

[2] F. C. Schweppe et al., "Homeostatic utility control," *IEEE Trans. Power App. Sys.*, vol. PAS-99, pp. 1151-1163, May/Jun. 1980.

[3] A. H. Rosenfeld et al., "Smart meters and spot pricing: Experiments and potential," *IEEE Technology Soc. Mag.*, vol. 5, pp. 23-28, Mar. 1986.

[4] J. C. Laurent, G. Desaulniers, R. P. Malhamé, and F. Soumis, "A column generation method for optimal load management via control of electric water heaters," *IEEE Trans. Power Syst.*, vol.10, pp. 1389–1400, Aug. 1995.

[5] D.-C. Wei and N. Chen, "Air conditioner direct load control by multi-pass dynamic programming," *IEEE Trans. Power Syst.*, vol. 10, pp. 307–313, Feb. 1995.

[6] A. I. Cohen and C. C. Wang, "An optimization method for load management scheduling," *IEEE Trans. Power Syst.*, vol. 3, pp. 612–618, May 1988.

[7] Q. Wu, P. Wang, and L. Goel, "Direct load control (DLC) considering nodal interrupted energy assessment rate (NIEAR) in restructured power systems," *IEEE Trans. Power Syst.*, vol. 25, pp. 1449–1456, Aug. 2010.

[8] Y. Y. Hsu and C. C. Su, "Dispatch of direct load control using dynamic programming," *IEEE Trans. Power Syst.*, vol. 6, pp. 1056–1061, Aug. 1991.

[9] A. Gomes, C. H. Antunes, and A.G. Martins, "A multiple objective approach to direct load control using an interactive evolutionary algorithm," *IEEE Trans. Power Syst.*, vol. 22, pp. 1004–1011, Aug. 2007.

[10] A. J. Gaul, E. Handschin, W. Hoffmann, and C. Lehmkoster, "Establishing a rule base for a hybrid ES/XPS approach to load management," *IEEE Trans. Power Syst.*, vol. 13, pp. 86–93, Feb. 1998.

[11] L. Goel, Q. Wu and P. Wang, "Fuzzy logic-based direct load control of air conditioning loads considering nodal reliability characteristics in restructured power systems," *Electric Power Systems Research*, vol. 80, num. 1, pp. 98–107, Jan. 2010.

[12] H. Salehfar and A. Wehbe, "Direct control of residential water heater loads to reduce power system distribution losses," in *IEEE Power Engineering Society Winter Meeting*, Columbus, OH, US, Jan. 2001, pp. 1455–1460.

[13] A. Wehbe and H. Salehfar, "Direct load control for reducing losses in the main and laterals of distribution systems," in *IEEE Power Engineering Society Summer Meeting*, Chicago, IL, US, July 2002, pp. 1593–1598.

[14] N. Ruiz, I. Cobelo, and J. Oyarzabal, "A direct load control model for virtual power plant management," *IEEE Trans. Power Syst.*, vol. 24, pp. 959–966, May 2009.

[15] C. N. Kurucz, D. Brandt, and S. Sim, "A linear programming model for reducing system peak through customer load control programs," *IEEE Trans. Power Syst.*, vol. 11, pp. 1817–1824, Nov. 1996.

[16] H. Jorge, C. H. Antunes, and A. G. Martins, "A multiple objective decision support model for the selection of remote load control strategies," *IEEE Trans. Power Syst.*, vol. 15, pp. 865–872, May 2000.

[17] K.-H. Ng and G. B. Sheblé, "Direct load control-A profit-based load management using linear programming," *IEEE Trans. Power Syst.*, vol. 13, pp. 688–694, May 1998.

[18] A. Molina et al., "Approach to multivariable predictive control applications in residential HVAC direct load control," in *IEEE Power Engineering Society Summer Meeting*, Seattle, WA, US, July 2000, pp. 1811–1816.

[19] B. Rautenbach and I. E. Lane, "The multi-objective controller: A novel approach to domestic hot water load control," *IEEE Trans. Power Syst.*, vol. 11, pp. 1832–1837, Nov. 1996.

[20] S. C. Lee, S. J. Kim, and S. H. Kim, "Demand side management with air conditioner loads based on the queuing system model," IEEE Trans. Power Syst., vol. 26, pp. 661–668, May 2011.

[21] M. Stadler, W. Krause, M. Sonnenschein, and U. Vogel, "Modelling and evaluation of control schemes for enhancing load shift of electricity demand for cooling devices," *Environmental Modelling & Software*, vol. 24, num. 2, pp. 285-295, Feb. 2009.

[22] M. W. Davis, T. J. Krupa, and M. J. Diedzic, "The economics of direct control of residential loads on the design and operation of the distribution system Part II Load characteristics" *IEEE Trans. Power App. Syst.*, vol. PAS-102, pp. 654–665, Mar. 1983.

[23] M. W. Davis, T. J. Krupa, and M. J. Diedzic, "The economics of direct control of residential loads on the design and operation of the distribution system Part III The economics of load management," *IEEE Trans. Power App. Syst.*, vol. PAS-102, pp. 666–674, Mar. 1983.

[24] G. S. Fiske, E. T. K. Law, and D. Q. Seeto, "The economic analysis of load management: The case of residential AC cycling," *IEEE Trans. Power App. Syst.*, vol. PAS-100, pp. 4725–4732, Dec. 1984.

[25] R. Bhatnagar, J. Latimer, L. J. Hamant, A.A. Garcia, G. Gregg, and E. Chan, "On-line load control dispatch at Florida Power & Light," *IEEE Trans. Power Syst.*, vol. 3, pp. 1237–1243, Aug. 1988.

[26] R. Peri, M. L. Chan, R. W. Osborne, and W. A. Weber, "A coordinated load management system for Allegheny Electric Cooperative, Inc." *IEEE Trans. Power Syst.*, vol. 2, pp. 707–712, Aug. 1987.

[27] E. J. Davis, "Impacts of several major load management projects," *IEEE Trans. Power App. Syst.*, vol. PAS-101, pp. 3885–3891, Oct. 1982.

[28] R. Bhatnagar and S. Rahman, "Direct load control: Relationships between electric utility experiences/assessments and system characteristics," *IEEE Trans. Power App. Syst.*, vol. PAS-104, pp. 2168–2175, Aug. 1985.

[29] P. A. Gnadt et al., *Automating Electric Utility Distribution Systems: The Athens Automation and Control Experiment*. Englewood Cliffs, NJ: Prentice Hall, 1990.

[30] N. E. Ryan, J. T. Powers, S. D. Braithwait, and B. A. Smith, "Generalizing direct load control program analysis: Implementation of the duty cycle approach," *IEEE Trans. Power Syst.*, vol. 4, pp. 293–299, Feb. 1989.

[31] W. Kempton, C. Reynolds, M. Fels, and D. Hull, "Utility control of residential cooling: Residential-perceived effects and potential program improvements," *Energy and Buildings*, vol. 18, num. 3, pp. 201–219, 1992.

[32] S. H. Lee and C. L. Wilkins, "A practical approach to appliance load control analysis: A water heater case study," *IEEE Trans. Power App. Syst.*, vol. PAS-102, pp. 1007–1013, Apr. 1983.

[33] B. F. Hastings, "Ten years of operating experience with a remote controlled water heater load management system at Detroit Edison," *IEEE Trans. Power App. Syst.*, vol. PAS-99, pp. 1437–1441, July/Aug. 1980.

[34] D. V. Stocker, "Load management study of simulated control of residential central air conditioners on the Detroit Edison Company System," *IEEE Trans. Power Syst.*, vol. PAS-99, pp. 1616–1624, July/Aug. 1980.

[35] R. Bhatnagar, J. Latimer, L. J. Hamant, A.A. Garcia, G. Gregg, and E. Chan, "On-line load control dispatch at Florida Power & Light," *IEEE Trans. Power Syst.*, vol. 3, pp. 1237–1243, Aug. 1988.

[36] A. S. Davis, "Florida Power Corporation's load management system," *IEEE Comput. Appl. Power*, vol. 3, num. 2, pp. 11–15, 1990.

[37] J. R. Stitt, "Implementation of a large-scale direct load control system-Some critical factors," *IEEE Trans. Power App. Syst.*, vol. PAS-104, pp. 1663–1669, July 1985.

[38] H. G. Weller III, "Managing the instantaneous load shape impacts caused by the operation of a large-scale direct load control system," *IEEE Trans. Power Syst.*, vol. 3, pp. 197–199, Feb. 1988.

[39] J. J. Bzura, "Radio control of air conditioning in Rhode Island," *IEEE Trans. Power Syst.*, vol. 5, pp. 448–451, May 1990.

[40] J. J. Bzura, "Radio control of water heaters in Rhode Island," *IEEE Trans. Power Syst.*, vol. 4, pp. 26–29, Feb. 1989.

[41] M. Delson, M. L. Chan, G. C. Ferrell, and B. Flattery, "A statewide load control system at North Carolina Electric Membership Corporation," *IEEE Trans. Power App. Syst.*, vol. PAS-104, pp. 1270–1275, June 1985.

[42] D. E. Nordell, "Forced duty cycling of air conditioning units for load management," *IEEE Power Eng. Rev.*, vol. PER-7, num. 11, pp. 55–56, May 1987.

[43] E. H. P. Chan, M. G. Delson, J. L. Green, and C. L. Nash, "A coordinated statewide load management and SCADA system," *IEEE Trans. Power App. Syst.*, vol. PAS-102, pp. 3496–3501, Nov. 1983.

[44] G. C. Heffner and R. P. Thompson, "A review of 1983 dispatchable load management operations at Pacific Gas and Electric Co.," *IEEE Trans. Power App. Syst.*, vol. PAS-103, pp. 1608–1613, July 1984.

[45] D. L. Becker, "Load management direct control: Fact or simulation," *IEEE Trans. Power Syst.*, vol. 1, pp. 82–88, Feb. 1986.

[46] J. Flitter, L. Markel, and P. Grimsrud, "A load management feasibility study for South Carolina Electric & Gas Co.," *IEEE Trans. Power App. Syst.*, vol. PAS-101, pp. 3877–3884, Oct. 1982.

[47] J. R. Espinosa, "Implementation and integration of air conditioner cycling at Southern California Edison," *IEEE Trans. Power Syst.*, vol. 2, pp. 792–798, Aug. 1987.

[48] G. F. Strickler and S. K. Noel1, "Residential air conditioner cycling-A case study," *IEEE Trans. Power Syst.*, vol. 3, pp. 207–212, Feb. 1988.

[49] C.-M. Chu et al., "A direct load control of air-conditioning loads with thermal comfort control," in *IEEE Power Engineering Society General Meeting*, San Francisco, CA, US, Jun. 2005, pp. 664–669.

[50] C.-M. Chu et al. "Mitigating DLC constraints of air-conditioning loads using a group-DLC method," in *Power Engineering Society General Meeting*, Tampa, FL, US, June 2007, pp. 1–6.

[51] C. S. Chen and J. T. Leu, "Interruptible load control for Taiwan power Company," *IEEE Trans. Power Syst.*, vol. 5, pp. 460–465, May 1990.

[52] J.-N. Sheen, C.-S. Chen, and J.K. Yang, "Time-of-use pricing for load management programs in Taiwan power company," *IEEE Trans. Power Syst.*, vol. 9, pp. 388–396, Feb. 1994.

[53] J.-N. Sheen, C.-S. Chen, and J.K. Yang, "Response of large industrial customers to electricity pricing by voluntary time-of-use in Taiwan," *IEE Proceedings Generation, Transmission and Distribution*, vol. 142, no. 2, pp. 157–166, Mar. 1995.

[54] R. F. Bischke and R. A. Sella, "Design and controlled use of water heater load management," *IEEE Trans. Power App. Syst.*, vol. PAS-104, pp. 1290–1293, June 1985.

[55] R. A. Abdoo, G. Lokken, and R. F. Bischke, "Load management implementation decisions, opportunities and operation," *IEEE Trans. Power App. Syst.*, vol. PAS-101, pp. 3902–3906, Oct. 1982.

[56] A. M. Breipohl and F. N. Lee, "Operational cost savings of direct load control," IEEE Trans. Power App. Syst., vol. PAS-103, pp. 988–993, May 1984.

[57] K. Bhattacharyya and M.L. Crow, "A fuzzy logic based approach to direct load control," *IEEE Trans. Power Syst.*, vol. 11, pp. 708–714, May 1996.

[58] S. Nadel and H. Geller, "Utility DSM. What have we learned? Where are we going?" *Energy Policy*, vol. 24, num. 4, pp. 289-302, Apr. 1996.

[59] J. Abreu et al., "An approach to discover the potential for demand response in the domestic sector," in *Innovative Technologies for an Efficient and Reliable Electricity Supply*, Waltham, MA, US, Sept. 2010, pp. 240–245.

[60] Federal Energy Regulatory Commission. (2010, July 1). *Top Initiatives*[Online]. Available: www.ferc.gov

[61] U.S. Department of Energy, "Benefits of Demand Response in Electricity Markets and Recommendations for Achieving Them," A Report to the United States Congress Pursuant to Section 1252 of the Energy Policy Act of 2005, 2006.

[62] G. C. Heffner and C. A. Goldman, "Demand responsive programs - An emerging resource for competitive electricity markets?," in *The Proceedings of the International Energy Program Evaluation Conference*, Salt Lake City, Utah, U.S., Dec. 2001.

[63] D. J. Hammerstrom et al., "Pacific Northwest GridWise™ Testbed Demonstration Projects; Part 1. Olympic Peninsula Project", Pacific Northwest National Laboratory, Richland, WA, U.S., PNNL-17617, 2007.

[64] D. P. Chassin et al., "The pacific northwest demand response market demonstration," in *IEEE Power and Energy Society General Meeting*, Pittsburgh, Pennsylvania, U.S., 2008, pp. 1-6.

[65] G. Conte et al., "A simulation environment for the analysis of home automation systems," in *Mediterranean Conference on Control & Automation*, 2007 © IEEE. doi: 10.1109/MED.2007.4433913

[66] A. Amato et al., "A smart distributed measurement data management system for DSM," in *IEEE Instrumentation and Measurement Technology Conference Proceedings*, Warsaw, Poland, May 2007, pp. 1–5.

[67] S. Abras et al., "An anticipation mechanism for power management in a smart home using multi-agent systems," in *3rd International Conference*

on Information and Communication Technologies: From Theory to Applications, 2008 © IEEE. doi: 10.1109/ICTTA.2008.4530305.

[68] A.-H. Mohsenian-Rad, V. W. S. Wong, J. Jatskevich, R. Schober, and A. Leon-Garcia, "Autonomous demand-side management based on game-theoretic energy consumption scheduling for the future Smart Grid," *IEEE Trans. Smart Grid*, vol. 1, Dec. 2010.

[69] A.-H. Mohsenian-Rad et al., "Optimal and autonomous incentive-based energy consumption scheduling algorithm for smart grid," in *Innovative Smart Grid Technologies*, 2010 © ISGT. doi 10.1109/ISGT.2010.5434752.

[70] *Advanced Metering Infrastructure (AMI)/Home Area Network (HAN)* Economic Benefits Analysis for Utilities. EPRI, Palo Alto, CA: 2009. 1018985.

[71] R. Teng and T. Yamazaki, "Bit-Watt home system with hybrid power supply," in *2nd International Conference on Computer and Automation Engineering*, Singapore, Feb. 2010, pp. 59-63.

[72] A. A. Moholkar, "Computer aided home energy management system," M.S. thesis, Dept. Comput. Sci. Elect. Eng., West Virginia University, Morgantown, West Virginia, U.S. 2005.

[73] G. L. van Harmelen, et al., "System impact of decentralised AI controllers operating on domestic devices in the intelligent home," in *Instrumentation and Measurement Technology Conference*, Hamamatsu, Japan, May 1994, pp. 1111–1114.

[74] S. Park et al., "Concurrent simulation platform for energy-aware smart metering systems," *IEEE Trans. Consum. Electron.*, vol. 56, pp. 1918-1926, Aug. 2010.

[75] M. Newborough and P. Augood, "Demand-side management opportunities for the UK domestic sector," *IEE Proceedings Generation, Transmission and Distribution*, vol. 146, num. 3, pp. 283–293, May 1999.

[76] N. Gudi et al., "Demand response simulation implementing heuristic optimization for home energy management," in *North American Power Symposium*, 2010 © NAPS. doi: 10.1109/NAPS.2010.5619967.

[77] C. H. Antunes et al., "A two-phase decision support approach for the selection of load control actions," in *IEEE International Engineering Management Conference*, Estoril, Portugal, June 2008, pp. 1–6.

[78] X. Guan et al., "Energy-efficient buildings facilitated by microgrid," *IEEE Trans. Smart Grid*, vol. 1, pp. 243-252. Dec. 2010.

[79] A. Molderink, et al., “Domestic energy management methodology for optimizing efficiency in smart grids,” in *IEEE Conf. Power Technology*, Bucharest, Romania, 2009, pp. 1–7.

[80] A. Molderink et al., "Simulating the effect on the energy efficiency of smart grid technologies," in *Winter Simulation Conference*, Austin, TX, US, Dec. 2009, pp. 1530–1541.

[81] A. Molderink, et al., “A three-step methodology to improve domestic energy efficiency," in *Innovative Smart Grid Technologies*, Gaithersburg, MD, 2010, pp. 1–8.

[82] A. Molderink et al., "Management and control of domestic smart grid technology," *IEEE Trans. Smart Grid*, vol. 1, pp 109-119, Sept. 2010.

[83] V. Bakker et al., "Demand side load management using a three step optimization methodology," in *IEEE International Conference on Smart Grid Communications*, Brussels, Belgium, Oct. 2010, pp. 431–436.

[84] V. Bakker, et al., "On simulating the effect on the energy efficiency of smart grid technologies," in *Winter Simulation Conference*, Baltimore, MD, US, Dec. 2010, pp. 393–404.

[85] A.-H. Mohsenian-Rad and A. Leon-Garcia, "Optimal residential load control with price prediction in real-time electricity pricing environments," *IEEE Trans. Smart Grid*, vol. 1, Sept. 2010.

[86] D. O'Neill et al., "Residential demand response using reinforcement learning," in *IEEE International Conference on Smart Grid Communications*, Brussels, Belgium, 2010, pp. 409-414.

[87] M. A. Pedrasa et al., "Scheduling of demand side resources using binary particle swarm optimization," *IEEE Trans. Power Syst.*, vol. 24, pp. 1173–1181, Aug. 2009.

[88] A. J. Roscoe and G. Ault, "Supporting high penetrations of renewable generation via implementation of real-time electricity pricing and demand response," *IET Renewable Power Generation*, vol. 4, iss. 4, pp. 369-382, Apr. 2010.

[89] N. Lu and S. Katipamula, "Control strategies of thermostatically controlled appliances in a competitive electricity market," in *Power Engineering Society General Meeting*, San Francisco, CA, US June 2005, pp. 202–207.

[90] P. Asmus and B. Davis, "Virtual Power Plants Demand Response, Supply-Side, Mixed Asset, and Wholesale Auction VPPs: Market Analysis and Forecasts," Pike Research Cleantech Market Intelligence, Boulder, Colorado, U.S., 2010.

[91] J. P. Fox and C. Wheelock, "Building Energy Management Systems Enabling Systems for Energy Efficiency, Demand Response, Energy Management, and Facility Automation in Commercial Buildings," Pike Research Cleantech Market Intelligence, Boulder, Colorado, U.S., 2010.

[92] J. Walton and G. Gohn, "Smart Appliances Household Appliances on the Smart Grid: Energy Management and Demand Response Applications,

Communications Technologies, Standards, and Key Industry Players," Pike Research Cleantech Market Intelligence, Boulder, Colorado, U.S., 2010.

[93] K. Parks et al., "Costs and emissions associated with plug-in hybrid electric vehicle charging in the Xcel Energy Colorado service territory," National Renewable Energy Laboratory, Golden, Colorado, U.S., Tech. Rep. NREL/TP-640-41410, 2007.

[94] C. A. Roe, "Power system level impacts of plug-in electric vehicles," M. S. thesis, Dept. Elect. Comput. Eng., The Georgia Institute of Technology, Atlanta, Georgia, U.S., 2007.

[95] G. Keith et al., "Modeling demand response and air emissions in New England," Synapse Energy Economics, Cambridge, Massachusetts, U.S., 2003.

[96] M. A. Kuliasha, "A dynamic model of power system operation incorporating load control," in *Decision and Control including the Symposium on Adaptive Processes*, San Diego, CA, US, Dec. 1981, pp. 458–463.

[97] J. Chen, F. N. Lee, A. M. Breipohl, and R. Adapa, "Scheduling direct load control to minimize system operation cost," *IEEE Trans. Power Syst.*, vol. 10, pp. 1994–2001, Nov. 1995.

[98] K. D. Le, R. F. Boyle, M. D. Hunter, and K. D. Jones, "A procedure for coordinating direct-load-control strategies to minimize system production costs," *IEEE Trans. Power App. Syst.*, vol. PAS-102, pp. 1843–1849, June 1983.

[99] *Premise Energy Management*. EPRI, Palo Alto, CA: 2010, 1022462.

[100] R. G. Pratt, C. C. Conner, B. A. Cooke, and E. E. Richman, "Metered end-use consumption and load shapes from the ELCAP residential sample of existing homes in the Pacific Northwest," *Energy and Buildings*, vol. 19, num. 3, pp. 179-193, 1993.

[101] L. Devroye, *Non-Uniform Random Variate Generation*. New York, New York: Springer-Verlag, 1986.

[102] U.S. Department of Transportation. (2011, November 1). *National Household Travel Survey: Our Nation's Travel* [Online]. Available: http://nhts.ornl.gov

[103] NOAA Satellite and Information Service. (2010). *USCRN/USRCRN FTP HOURLY02 STREAM* [Online]. Available FTP: ftp://ftp.ncdc.noaa.gov/pub/data/uscrn/products/hourly02 Directory: 2010 File: CRNH0202-2010-KY_Versailles_3_NNW.txt

[104] NOAA Satellite and Information Service. (2010). *USCRN/USRCRN FTP HOURLY02 STREAM* [Online]. Available FTP:

ftp://ftp.ncdc.noaa.gov/pub/data/uscrn/products/hourly02 Directory: 2010 File: CRNH0202-2010-NV_Mercury_3_SSW.txt

[105] NOAA Satellite and Information Service. (2010). *USCRN/USRCRN FTP HOURLY02 STREAM* [Online]. Available FTP: ftp://ftp.ncdc.noaa.gov/pub/data/uscrn/products/hourly02 Directory: 2010 File: CRNH0202-2010-OK_Stillwater_2_W.txt

[106] NOAA Satellite and Information Service. (2010). *USCRN/USRCRN FTP HOURLY02 STREAM* [Online]. Available FTP: ftp://ftp.ncdc.noaa.gov/pub/data/uscrn/products/hourly02 Directory: 2010 File: CRNH0202-2010-WI_Necedah_5_WNW.txt

[107] J. T. Gajjar and Z. Tajularas, "Feasibility study of residential level demand-side management in Malaysia," in *IEEE Region 10 International Conference on Global Connectivity in Energy, Computer, Communication and Control*, New Delhi, India, Dec. 1998, pp. 514–517.

[108] Otter Tail Power Company. (2011, January 1). *Appliance Energy Usage* [Online]. Available: www.otpco.com

[109] U.S. Energy Information Administration. (2011, November 1). *End-Use Consumption of Electricity 2001* [Online]. Available: www.eia.gov

[110] R. G. Pratt, C. C. Conner, B. A. Cooke, and E. E. Richman, "Metered end-use consumption and load shapes from the ELCAP residential sample of existing homes in the Pacific Northwest," *Energy and Buildings*, vol. 19, num. 3, pp. 179–193, 1993.

[111] A. M. Law, *Simulation Modeling & Analysis*. New York, New York: McGraw-Hill Companies, 2007.

[112] M. Frigge, D. C. Hoaglin, and Boris Iglewicz, "Some implementations of the boxplot," *The American Statistician*, vol. 43, num. 1, pp. 50–54, 1989.

[113] U.S. Food and Drug Administration. (2012, March 1). *Food Code 2009* [Online]. Available: www.fda.gov

[114] A. P. Meliopoulos, "Computer aided instruction of energy source utilization problems," *IEEE Trans. on Education*, vol. E-24, no. 3, pp. 204-209, Aug. 1981.

[115] U.S. Energy Information Administration. (2011, November 1). *Annual Energy Review* [Online]. Available: www.eia.gov

[116] S. M. Ross, *Introduction to Probability Models*. Burlington, Massachusetts: Academic Press, 2007.

[117] U.S. Environmental Protection Agency. (2011, October 1). *EPA's IPM Base Case 2006 (v3.0)* [Online]. Available: www.epa.gov

[118] Reliability Test System Task Force of the Application of Probability Methods Subcommittee, "IEEE reliability test system," *IEEE Trans. Power App. Syst.*, vol. PAS-98, no. 6, pp. 1843–1849, Nov. 1979.

[119] U.S. Energy Information Administration. (2011, November 1). *Electric Power Annual 2010 - State Data Tables* [Online]. Available: www.eia.gov

VITA

Curtis A Roe

Curtis Roe was born in Wausau, Wisconsin. He attended public schools in Wausau and received a B.S. in Electrical Engineering from the University of Wisconsin-Madison in 2005. He then moved to Atlanta Georgia to pursue studies at the Georgia Institute of Technology in the fall of 2007, receiving a M.S. in Electrical Engineering in 2009. He then continued to pursue a doctorate in Electrical Engineering at Georgia Tech. When he is not working on his research, he enjoys being active outdoors and spending time with his family.